Identification Of Novel Mechanisms Of Glucolipotoxicity In Type 2 Diabetes

Marta Bagnati

Primary Supervisor: Prof. Graham Hitman

Secondary Supervisor: Dr. Mark Turner

Tertiary Supervisor: Dr. Tania Maffucci

Thesis submitted for the degree of Doctor of Philosophy

Centre For Diabetes, Blizard Institute

Barts and the London School of Medicine and Dentistry,

Queen Mary University of London

January 2015

I, Marta Bagnati, confirm that the research included within this thesis is my own work or that where it has been carried out in collaboration with, or supported by others, that is duly acknowledged below and my contribution indicated. Previously published material is also acknowledged below.

I attest that I have exercised reasonable care to ensure that the work is original, and does not to the best of my knowledge break any UK law, infringe any third party's copyright or other Intellectual Property Right, or contain any confidential material.

I accept that the College has the right to use plagiarism detection software to check the electronic version of the thesis.

I confirm that this thesis has not been previously submitted for the award of a degree by this or any other university.

Signature:

Date:

Abstract

Type 2 Diabetes, a metabolic disorder associated with chronic hyperglycaemia and hyperlipidaemia, is characterised by an impairment of insulin secretion and production and β-cell death. This β-cell dysfunction is determined by different factors, among which inflammatory processes, characterised by increased expression of pro-inflammatory cytokines and chemokines. Although some molecular mechanisms have been proposed to be involved in this β-cell dysfunction, they fail to explain the whole process.

In this thesis, a combined approach of microarray, RNAseq, RT-qPCR and western blot will be used to elucidate the pathways affected under glucolipotoxicity, in order to discover novel molecules involved in the pathogenesis of T2D.

We found that INS-1 cells exposed to 27 mM glucose, 200 µM oleic acid, 200 µM palmitic acid, show an overexpression of CD40, a TNF receptor involved in inflammation (more than 300% $p<0.01$), both at RNA and protein level. These data were validated in cultured human islets ($p<0.05$) and in islets of mice fed a high fat diet ($p<0.05$). We showed also that siRNA downregulation of CD40 is associated with increase in insulin secretion ($p<0.05$), revealing a potential new role of this receptor in β-cells. In addition, RNAseq analysis revealed a wide list of molecules differentially expressed in glucolipotoxicity, in particular molecules involved in inflammation, insulin/IGF pathway, fatty acids-cholesterol metabolism and biosynthesis. We focused our attention on potential novel targets, including the thyroid pathway, unknown microRNAs and novel genes, in order to discover new pathways involved in the impairment of insulin secretion in T2D.

This work will open the way to future studies aiming to characterise these molecules and to understand their role in the insulin secretion process. Interesting candidates can then be used in the future as potential targets for the development of new and specific therapeutic strategies.

Aknowledgements

I would like to thank my supervisors, Professor Graham Hitman and Dr. Mark Turner, who gave me the opportunity to work in their lab. With their guidance and support, I could be able to complete my PhD project and grow professionally and personally. I'm very grateful also to Dr. Tania Maffucci, who helped and supported me in the day to day work in the lab. Her advice has always been very precious and helped me solving problems and difficulties.

I also want to thank Dr. William Ogunkolade for his assistance and help and Dr. Rob Lowe for the bioinformatic support.

I would like to thank my group, the collaborators that provided me reagents and materials and all the people in Centre for Diabetes. Particular thanks to Irene, who always provided me support for administrative issues.

Special thanks to my family and Sergio, who encouraged and supported me during stressfull and difficult times and who always believed in me. Thanks to all my friends, in Italy and in London, who were always there when I needed.

Final thanks to my running club, and to the running itself, that made me stronger and more determined to solve difficulties.

Contents

List of Tables

List of Figures

Abbreviations

AAV	Adeno-associated Virus
ACC	Acetyl-CoA Carboxylase
ACS	Acetyl-CoA Synthetase
ADAR	Adenosine Deaminase Acting on RNA
ADP	Adenosine Diphosphate
AGE	Advanced Glycosylated End Product
AMP	Adenosine Monophosphate
AMPK	AMP Kinase
ATF	Activating Transcription Factor
ATP	Adenosine Triphosphate
BCA	Bicinchoninic Acid
BSA	Bovine Serum Albumin
C	Control
CaMK	Ca^{2+}/calmodulin-dependent protein kinase
cAMP	Cyclic AMP
CAPN-10	Calpain 10
CD40L	CD40 Ligand
cDNA	Complementary DNA
cGMP	Cyclic GMP
cIAPs	Cellular Inhibitors of Apoptosis
CPT-1	Carnitine palmitoyltransferase 1
Ct	Cycle Threshold
DD	Death Domain
DEVD	Asp-Glu-Val-Asp
DG	Diglyceride
DGCR8	DiGeorge Syndrome Critical Region Gene 8
DMSO	Dimethyl sulfoxide
DNA	Deoxyribonucleic Acid
EAE	Experimental Autoimmune Encephalomyelitis
eIF-4E	Eukaryotic Translation Initiation Factor 4E
ELISA	Enzyme-Linked ImmunoSorbent Assay
ER	Endoplasmic Reticulum
ERK	Extracellular Regulated Kinase
EST	Expressed Sequence Tags
EXP5	Exportin 5
exRNA	Extracellular RNA
FACS	Fluorescence Activated Cell Sorting
FADD	Fas-Associated protein with Death Domain
FasL	Fas Ligand
FBS	Foetal Bovine Serum
FFAs	Free Fatty Acids
GCK	Glucokinase
GDP	Guanosine Diphosphate
GH	Growth Hormone
GIP	Glucose-dependent Insulinotropic Peptide
GLP-1	Glucagon Like Peptide 1
GPR	G protein coupled Receptor
GSK-3	Glycogen Synthase Kinase 3
GSIS	Glucose Stimulated Insulin Secretion
GTP	Guanosine Triphosphate
GWAS	Genome Wide Association Studies
HF	High Fat

HG	High Glucose
HGHF	High Glucose High Fat
HIPK3	Homeodomain Interacting Protein Kinase 3
HPT	Hypothalamus Pituitary Thyroid
HRP	Horseradish Peroxidase
IAPP	Islet Amyloid Polypeptide
ICAM	Intercellular Adhesion Molecule
IFN-γ	Interferon γ
IGF	Insulin-like Growth Factor
Ig	Immunoglobulin
IKKB	Inhibitor of Nuclear Factor Kappa-B Kinase
IL	Interleukin
IMP	IGF-II mRNA Binding Protein
iNOS	Inducible Nitric Oxide Synthase
IR	InfraRed
IRAK	Interleukin-1 Receptor-Associated Kinase
IRF-1	Interferon Regulatory Factor 1
IRS	Insulin Receptor Substrate
JAK	Janus Kinase
JNK	c-Jun N-terminal Kinase
kDa	kiloDalton
LC-CoA	Long Chain Acyl-CoA
LOC	Locus
LT-α	Lymphotoxin-α
LT-βR	Lymphotoxin-β Receptor
MAPK	Mitogen Activated Protein Kinase
MAQC	Microarray Quality Control
MEKK1	Mitogen-activated Protein kinase kinase kinase 1
mRNA	Messenger RNA
miRNA	Micro RNA
mTOR	Mammalian Target of Rapamycin
MTT	3-(4,5-Dimethylthiazol-2-yl)-2,5-diphenyltetrazolium bromide
NADPH	Nicotinamide Adenine Dinucleotide Phosphate
ncRNA	Non Coding RNA
NES	Nuclear Export Signal
NF-κB	Nuclear Factor Kappa-light-chain-enhancer of activated B cells
NIK	NF-κB Inducing Kinase
NLS	Nuclear Localisation Signal
NO	Nitric Oxide
NOD	Nonobese Diabetic
PA	Phosphatidic Acid
PACT	Protein Activator of PKR
PBMC	Peripheral Blood Mononuclear Cell
PBS	Phosphate Buffer Saline
PCR	Polymerase Chain Reaction
PDK1	Phosphoinositide Dependent Protein Kinase-1
PDX-1	Pancreatic and duodenal homeobox 1
PI	Propidium Iodide
PI3K	Phosphatidylinositol-4,5-bisphosphate 3-kinase
piRNA	Piwi-interacting RNA
PKA	Protein Kinase A
PKB	Protein Kinase B
PKC	Protein Kinase C
PL	Phospholipids
PLC	Phospholipase C
PPAR	Peroxisome Proliferator-Activated Receptors

PTP	Protein Tyrosine Phosphatases
qPCR	Quantitative PCR
QTL	Quantitative Trait Locus
RANKL	Receptor Activator of Nuclear factor Kappa-B Ligand
RCF	Relative Centrifugal Force
RGD	Rat Genome Database
RIN	RNA Integrity Number
RIP-1	Receptor-Interacting Protein 1
RISC	RNA-Induced Silencing Complex
RNA	Ribonucleic Acid
Rpm	Revolutions per minute
rRNA	Ribosomal RNA
ROS	Reactive Oxygen Species
RT-PCR	Reverse Transcriptase PCR
SAGE	Serial Analysis of Gene Expression
SAPE	Streptavidin-Phycoerythrin
SAPK	Stress-Activated Protein Kinase
SBS	Sequencing by Synthesis
SH2	Src Homology 2
siRNA	Short Interfering RNA
SLE	Systemic Lupus Erythematosus
SNAP-25	Synaptosomal-Associated Protein 25
SNARE	soluble NH_2-ethylmaleimide-sensitive fusion protein attachment protein receptor proteins
SNP	Single Nucleotide Polymorphism
snRNA	Small Nuclear RNA
snoRNA	Small Nucleolar RNA
SREBPs	Sterol Regulatory Element-Binding Proteins
SRIH	Somatostatin
STAT	Signal Transducer and Activator of Transcription
STZ	Streptozotocin
T1D	Type 1 Diabetes
T2D	Type 2 Diabetes
T3	Triiodothyronine
T4	Thyroxine
TAG	Triacylglycerol
TBE	Tris/Borate/EDTA
TCA	Tricarboxylic Acid
TG	Thyroglobulin
TM	Transmembrane
TNF	Tumor Necrosis Factor
TNFR	Tumor Necrosis Factor Receptor
TPO	Thyroid Peroxidase
TRADD	Tumor Necrosis Factor Receptor Type 1-Associated Death Domain
TRAF	Tumor Necrosis Factor Associated Factor
TRAIL	TNF-Related Apoptosis-Inducing Ligand
TRBP	Trans-Activation-Responsive RNA-Binding Protein
tRNA	Transfer RNA
TSH	Tyroid Stimulating Hormone
TRH	Thyrotropin Releasing Hormone
TXNIP	Thioredoxin Interacting Protein
UCP2	Mitochondrial Uncoupling Protein 2
UKPDS	UK Prospective Diabetes Study
UPR	Unfolded Protein Response
VAMP	Synaptobrevin
VDCC	Voltage Dependent Calcium Channel

Pubblications arising from this thesis

- Bagnati, M. et al., (2015) "Emerging evidence for the role of TNFR5/CD40 in pancreatic β-cell proinflammatory response to glucolipotoxicity." *Under submission*

Chapter 1

Introduction

1.1 Pancreatic β-cell physiology

Pancreatic β-cells are located in the islets of Langherans in the pancreas, making up 65-80% of the total cells in the islets. The primary function of β-cells is to produce and store the hormone insulin, which is responsible for the regulation of the blood glucose concentration. This tight control is governed by the balance between glucose absorption from the intestine, production by the liver and uptake and metabolism by peripheral tissues.

A dysregulation of the mechanisms responsible of the maintenance of glucose homeostasis and function leads to pathologic conditions, in particular diabetes mellitus.

1.1.1 Insulin biosynthesis

The secreted insulin consists of 51 amino acids with a molecular weight of 5.8 kDa. However, the insulin gene encodes a 110 amino acid precursor known as preproinsulin (Figure 1.1).

Preproinsulin contains a hydrophobic amino-terminal signal sequence that is required in order for the precursor hormone to pass through the membrane of the endoplasmic reticulum for post-translational processing. Upon entering the ER, the preproinsulin signal sequence is proteolitically removed, generating proinsulin. Proinsulin then undergoes folding and formation of three disulphide bonds, a process requiring a diverse range of endoplasmic reticulum (ER) chaperone proteins.

Subsequent to maturation of the 3 dimensional conformation, the folded proinsulin is transported from the ER to the Golgi apparatus where proinsulin enters immature secretory granules and is cleaved to yield the A chain (21 amino acids) and B chain (30 aminoacids) of insulin and C-peptide (Figure 1.1). Insulin and C-peptide are then stored in the secretory granules together with islet amyloid polypeptide (IAPP or amylin) and other less abundant β-cell secretory products [1].

Following their generation at the trans Golgi network and subsequent maturation, each dense-core granule ultimately needs to be transported to the cell surface, a process that

is activated by elevated glucose concentrations via Ca^{2+} dependent mechanisms [2] through the motor protein kinesin-1.

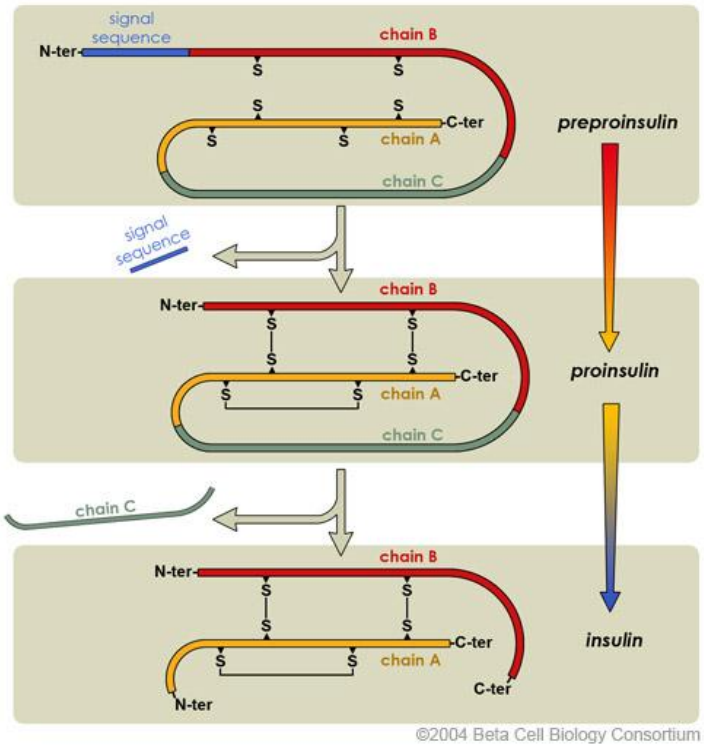

Figure 1.1 Insulin biosynthesis. Insulin is translated as a 110 amino acids peptide called preproinsulin. Preproinsulin contains a hydrophobic amino-terminal signal sequence required for entering the ER. In the ER, the preproinsulin signal sequence is proteolitically removed, generating proinsulin. Subsequent to maturation of the three dimensional conformation, the folded proinsulin is transported from the ER to the Golgi apparatus where proinsulin enters immature secretory vesicles and is cleaved to yield the A chain and B chain of insulin and C-peptide. Figure adapted from Beta Cell Biology Consortium website.

1.1.2 Insulin secretion

The β-cell responds to many nutrients in the blood circulation, including glucose, other monosaccharides, amino acids and fatty acids.

Glucose is the main driver of insulin secretion and of proinsulin and insulin transcription and it is the most abundant sugar in our diet. It circulates in the blood and it is able to enter β-cells through transporters called GLUT. There are different isoforms of this receptor, with GLUT2 being the β-cell transporter responsible for constitutive glucose

uptake. Also hepatic glucose uptake is GLUT2 mediated. Skeletal muscle and adipocyte glucose uptake is mediated by GLUT4 transporters, which reside in intracellular storage pools and translocate to the surface in response to stimuli [3].

Once glucose is internalised in the cell, it is phosphorylated by the enzyme glucokinase (GCK), to glucose 6-phosphate. This enzyme is a glucose sensor in the pancreatic β-cell [4]. After this process, glucose 6-phosphate then enters the glycolytic pathways eventually leading to ATP synthesis. Elevated ATP/ADP ratio induces closure of cell-surface ATP-sensitive K^+ (KATP) channels, leading to cell membrane depolarisation. This depolarisation triggers the opening of cell-surface voltage-dependent Ca^{2+} channels (VDCC), facilitating extracellular Ca^{2+} influx into the β-cell. A rise in free cytosolic Ca^{2+} triggers the exocytosis of insulin granules (Figure 1.2).

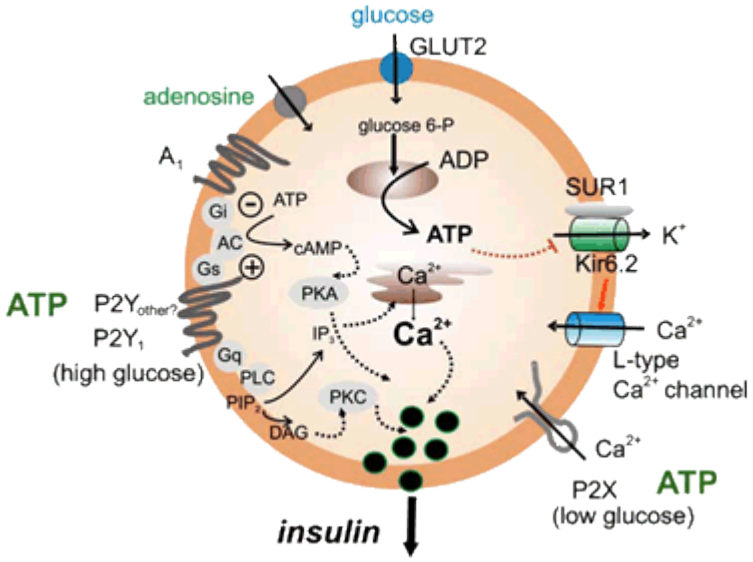

Figure 1.2 Glucose stimulates insulin secretion. Glucose enters the β-cell through the transporter GLUT2 and it is metabolised to ATP. An elevated ATP/ADP ratio triggers the closure of ATP sensitive K^+ channels and membrane depolarisation; this depolarisation opens voltage-dependent Ca^{2+} with the consequent Ca^{2+} influx that triggers insulin granules exocytosis. Figure from reference [5].

The initial (or first phase) exocytotic response can be replicated by any stimuli that increase intracellular Ca^{2+}, causing the release of the insulin granules that are already associated to the plasma membrane. Sustained (or second phase) secretion, which is dependent on vesicles mobilisation and priming, can only be elicited by metabolisable

fuel secretagogues (i.e. pyruvate, glyceraldehyde, amino acids) [6]. In rat β-cell, glucose stimulates an increase in the number of insulin granules associated with the plasma membrane [7] and vesicles movement in the cytoplasm likely occurs along microtubules, mediated by the ATP dependent motor activity of the conventional kinesin KIF5B [8]. Disruption of the microtubule network impairs granules movement and the exocytotic response [9].

Fusion of exocytotic granules with the plasma membrane is mediated by SNARE proteins (soluble NH_2-ethylmaleimide-sensitive fusion protein attachment protein receptor proteins). These include the plasma membrane proteins Syntaxin-1 and SNAP-25 (synaptosome-associated protein of 25 kDa) and the vesicular protein VAMP2 (synaptobrevin). Interaction of the coiled coil domains of these proteins to form a SNARE "pin" appears to provide both membrane selectivity and the thermodynamic driving force for membrane fusion [10]. Ca^{2+} sensitivity is conferred on the process by additional proteins such as members of the synaptogamin family, which are able to interact with the SNARE complex and with membrane phospholipids [11]. Cumulative evidence emphasizes the crucial role of synaptogamin VII and IX as mediators of glucose-induced insulin secretion [12]. In addition, calpain-10 (CAPN10), a member of calcium-dependant non-lysosomal cysteine proteases, has been shown to interact with SNARE proteins and be implicated in calcium mediated insulin exocytosis, through SNAP-25 proteolisis [13]. It has been proposed that under non-stimulating conditions granules are docked adjacent to L-Type calcium channels through their SNARE complex interaction, with intact SNAP-25 inhibiting fusion. The influx of calcium generated by secretagogue stimulation activates calpain-10, which cleaves SNAP-25 and leads to conformational changes within the SNARE complex, facilitating membrane fusion (Figure 1.3) [13-14].

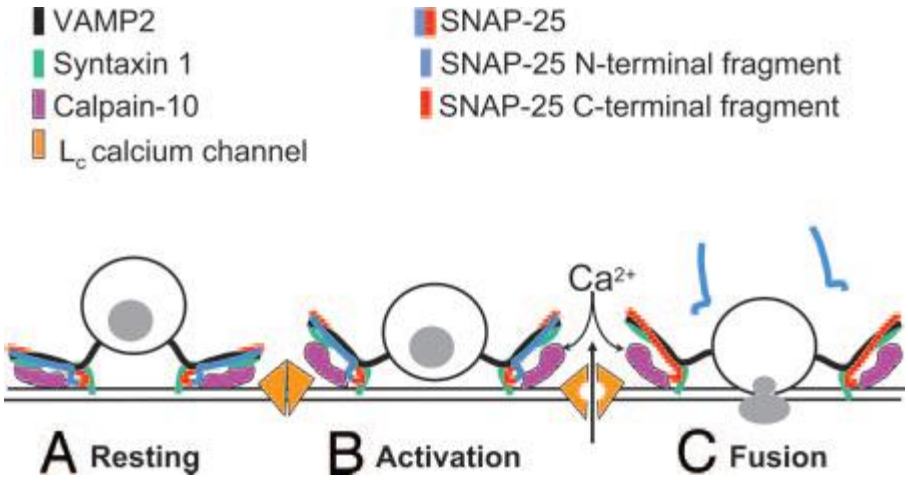

Figure 1.3 Proposed mechanism of insulin granules exocytosis. Under nonstimulating conditions granules are docked adjacent to L-Type calcium channels through their SNARE complex interaction, with intact SNAP-25 inhibiting fusion. The influx of calcium generated by secretagogue stimulation activates calpain-10, which cleaves SNAP-25 and leads to conformational changes within the SNARE complex, facilitating membrane fusion. Figure adapted from reference [13].

Prior to Ca^{2+}-triggered and SNARE-mediated exocytosis, a docked insulin granule must be firstly primed for release, a chemical ATP-dependent modification. Intra-vesicular acidification by a V-type H^+ ATPase plays an important role in insulin granule priming [15].

The β-cell responds to the increase in blood glucose by stimulating the rate of glucose metabolism and insulin secretion, as well as insulin biosynthesis.

The mammalian insulin gene is exclusively expressed in the β-cell of the endocrine pancreas. Its promoter is regulated by the binding of some specific transcription factors (PDX-1, MafA, BETA2, E2A, STAT5) (see Figure 1.4) [16]. Insulin gene regulation results not only from specific binding combinations of these activators, but also from their relative nuclear concentrations.

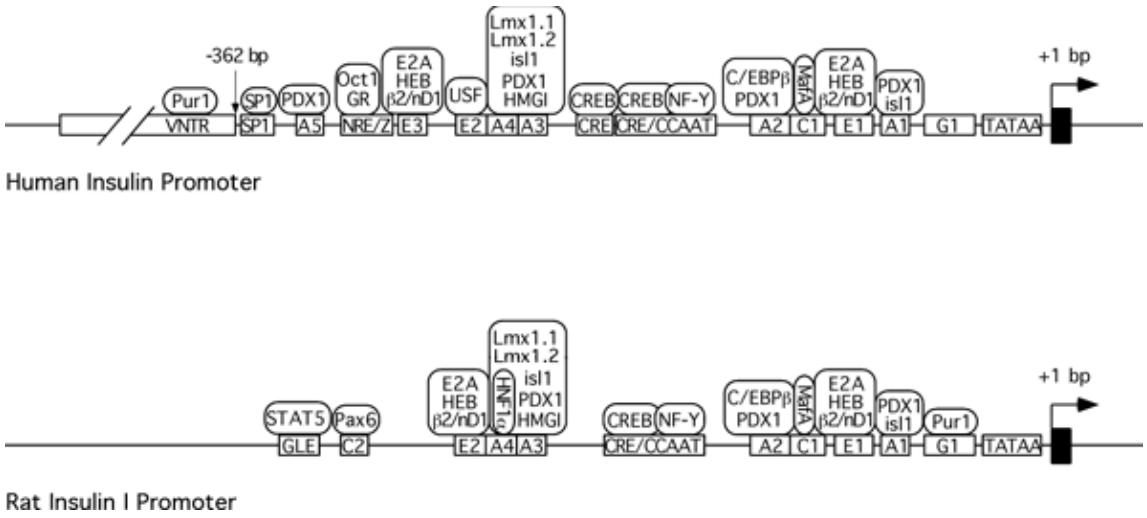

Figure 1.4 Insulin gene regulation. The insulin gene transcription is a highly regulated process in which many transcription factors bind the gene promoter. The level of expression and the combination of these transcription factors determine the rate of transcription. Figure from reference [16].

Glucose metabolism is necessary for the stimulation of the promoter activity [17] and the insulin gene contains multiple elements that respond to glucose [18]. In particular, the most studied factor is the Pancreatic and Duodenal Homeobox 1 (PDX-1): experiments in a human cell line, NES2Y, which lacks PDX-1, show that the insulin promoter is not sensitive to glucose stimulation. Reintroduction of PDX-1 recovers the glucose effect on insulin transcription [19]. Moreover, also the transactivation potency of PDX-1 is modulated by glucose [20].

The signalling pathways responsible for glucose induction of insulin gene transcription are not completely defined. Part of the stimulatory effect is determined by calcium, as indicated by the fact that insulin gene transcription is inhibited by calcium channel blockers [21]. Other pathways possibly involved are the cyclic AMP pathways, which have been shown to increase insulin mRNA level [21] or the activation of specific kinases or phosphatases that modify the phosphorylation status of sequence-specific transcription factors, such as protein kinase A (PKA), protein kinase C (PKC), members of the calcium calmodulin-dependent kinases (CaMK) and mitogen activated protein kinases (MAPK) [22].

1.1.2.1 Other factors regulating insulin secretion

In addition to carbohydrates, free fatty acids (FFAs) are also a critical metabolic constituent for normal β-cell function and insulin release. FFAs access the cytosol of the β-cell by freely diffusing through the plasma membrane, due to their lipophilic profile [23]. Once internalised, FFAs are metabolised to long-chain acyl-CoA (LC-CoA) by acyl-CoA synthase (ACS), then transported to the interior of the mitochondria by Carnitine Palmitoyl Transferase-1 (CPT-1), where they are oxidised via the β-oxidation pathway for energy production [24]. The ATP produced in this process sustains a basal release of insulin, in a K^+ ATP-dependent manner [25].

After a carbohydrate containing meal, fatty acid oxidation is inhibited, as citrate, generated from the glycolytic metabolism, is converted to malonyl-CoA by acetyl-CoA carboxylase (ACC). Malonyl-CoA sterically blocks CPT-1, inhibiting the transport of LC-CoA in the mitochondria (Figure 1.5) [26]. Accumulation of these intermediates in the cytosol leads to an increase in the intracellular calcium levels and to changes in the acylation state of proteins involved in the regulation of ion channel activity and exocytosis, amplifying insulin secretion [27]. In addition, LC-CoA can also enhance the fusion of insulin-secretory vesicles with the plasma membrane and insulin release, increasing membrane permeability [28]. Therefore, FFAs do not stimulate insulin secretion directly, but they are able to potentiate glucose stimulated insulin secretion (GSIS) in β-cells.

The amount of malonyl-CoA is mainly regulated by AMP-activated kinase (AMPK), which inhibits ACC by phosphorylation, leading to reduced conversion of citrate to malonyl-CoA (Figure 1.5) [24]. This process reduces the expression of active malonyl-CoA, facilitating FFAs esterification, increased entry in the mitochondria and enhanced β-oxidation. Indeed AMPK activity is inversely correlated with glucose concentration and is stimulated by palmitate in β-cell [29]. Downstream of AMPK, the transcription factor sterol-regulatory-element-binding-protein-1c (SREBP1c) regulates the transcription of genes involved in fatty acids synthesis, leading to enhanced lipogenesis [30].

Esterification of LC-CoA to triacylglycerol (TAG) also occurs in β-cells in the presence of glycerol 3-phosphate provided by glucose metabolism (Figure 1.5). The purpose of this process may be to provide insulinotropic lipid signalling molecules by lipolysis that can aid insulin vesicle assembly and exocytosis.

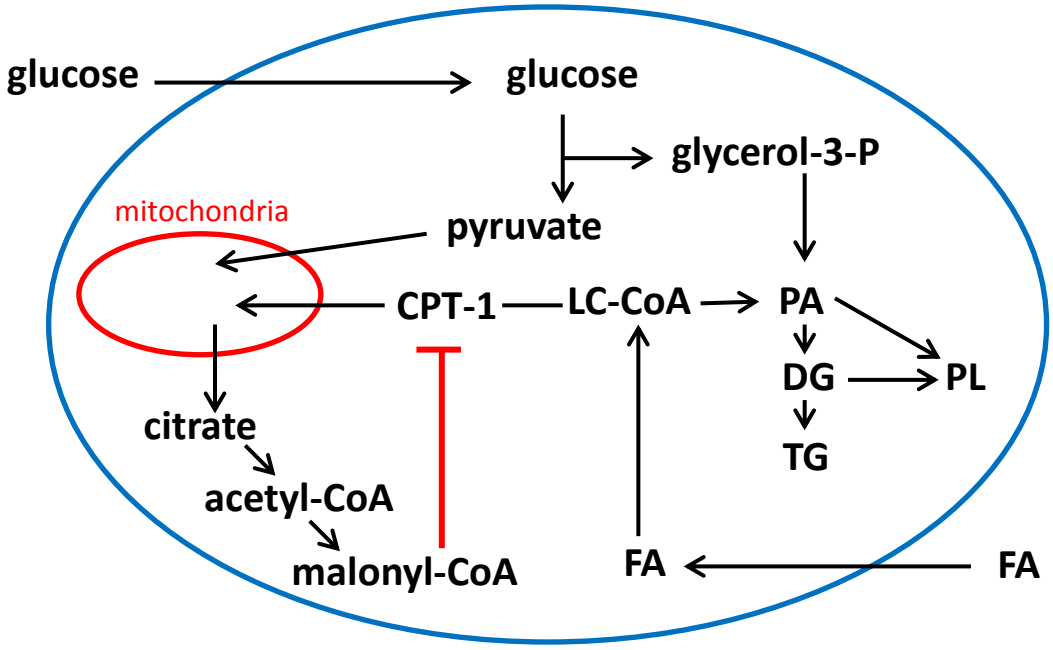

Figure 1.5 Effect of glucose on lipid partitioning in the β-cell. In the presence of glucose, the increase of malonyl-CoA derived from glucose metabolism inhibits the enzyme CPT-1 and consequently LC-CoA transport in the mitochondria is reduced. LC-CoAs accumulate in the cytosol where the esterification pathway is activated, generating phosphatidic acid (PA), diglycerides (DG), triglycerides (TG) and phospholipids (PL).

Another proposed mechanism by which lipids can stimulate insulin secretion is via interaction with the G-protein coupled receptors (GPRs) [31]. It is thought that GPRs amplify GSIS by enhancing calcium efflux from the ER [26].

Individual amino acids at physiological concentrations are poor insulin secretagogues. However, certain combinations of amino acids can augment GSIS [32], for example the combination of glutamine with leucine. Leucine can activate glutamate dehydrogenase, which converts glutamate to α-ketoglutarate. Glutamine, after conversion into glutamate by glutaminase in the cytosol, can enter the TCA cycle via α-ketoglutarate, which results in ATP production and enhancement of insulin secretion.

In addition, some amino acids can indirectly influence β-cell insulin secretion. During the fasting period, proteins in the skeletal muscles are catabolized and free amino acids, like alanine and glutamine, are released in the blood, acting as glucagon secretagogues. This results in elevation of blood glucose levels, which then triggers insulin secretion.

1.1.3 Insulin signalling and action

Insulin increases glucose uptake in muscle and fat and inhibits hepatic glucose production. It also stimulates cell growth and differentiation, and promotes the storage of substrates in fat, liver and muscle by stimulating lipogenesis, glycogen and protein synthesis, and inhibiting lipolysis, glycogenolysis and protein breakdown. Insulin increases glucose uptake in muscle and adipose cells by stimulating the translocation of the glucose transporter GLUT4 from intracellular sites to the cell surface [33].

Specifically, insulin binding to its receptor results in receptor autophosphorylation on tyrosine residues; this event results in the phosphorylation of the receptor substrates, among which insulin receptor substrates (IRS-1, IRS-2 and IRS-3) [34].

This event allows the association of IRSs with the regulatory subunit of phosphoinositide 3-kinase (PI3K) through its SRC homology 2 (SH2) domains (see Figure 1.6). This kinase, once activated, phosphorylates phosphoinositides at the 3' position of the inositol ring to produce phosphoinositides 3-phosphates, which bind to the pleckstrin homology (PH) domains of a variety of signalling molecules. It can also phosphorylate other proteins at serine residues. PI3K has a pivotal role in the metabolic and mitogenic actions of insulin and inhibitors of this enzyme or transfections with dominant negative constructs block most metabolic actions of insulin, including stimulation of glucose transport, glycogen and lipid synthesis [35]. In particular, PI3K activates the kinase 3-phosphoinositide dependent protein kinase 1 (PDK1), which in turn activates protein kinase B (PKB/Akt), a serine kinase [36]. PKB deactivates glycogen synthase kinase 3 (GSK-3), leading to activation of glycogen synthase and thus glycogen synthesis [37]. Activation of PKB also results in the translocation of GLUT-4 vesicles from their intracellular pools to the plasma membrane, where they allow the uptake of glucose into the cell. PKB also leads to activation of protein

synthesis mediated by the mammalian target of rapamycin (mTOR). mTOR is a member of the PI3K family of proteins that can control the mammalian translation machinery by direct phosphorylation and activation of p70 ribosomal S6 kinases as well as phosphorylation and inactivation of the initiation factor 4E for eukaryotic translation (eIF-4E) inhibitor [38].

In addition to PI3K activity, other signals seem to be required for insulin-stimulated glucose uptake, among which the pathway involving tyrosine phosphorylation of the Cbl protooncogene [39] (Figure 1.6). In most insulin-responsive cells, Cbl is associated with the adapter protein CAP, and upon phosphorylation, Cbl-CAP complex translocates to lipid rafts domains in the plasma membrane, recruiting the adapter protein CrkII. CrkII also forms a constitutive complex with the guanyl nucleotide-exchange protein C3G. Once translocated in the lipid rafts, C3G comes into proximity with the G protein TC10, and catalyses the exchange of GTP for GDP, activating the protein and providing a second signal to the GLUT4 proteins [40].

Other signal transduction proteins interact with IRS molecules, including GRB2 and SHP2, a tyrosine phosphatase (PTP) containing SH2 domains (Figure 1.6). GRB2, an adaptor protein, contains an SH3 domain, which is part of the cascade including RAS, RAF, MEK and extracellular signal-regulated kinase (ERK) that leads to activation of MAPK and mitogenic responses. Activated ERK can translocate into the nucleus, where it catalyses the phosphorylation of transcription factors such as p62, initiating a transcriptional programme that leads to cellular proliferation or differentiation [41].

SHC is another substrate of insulin receptor, which, when tyrosine phosphorylated, associates with GRB2 and can activate RAS/MAPK pathway independently of IRS-1.

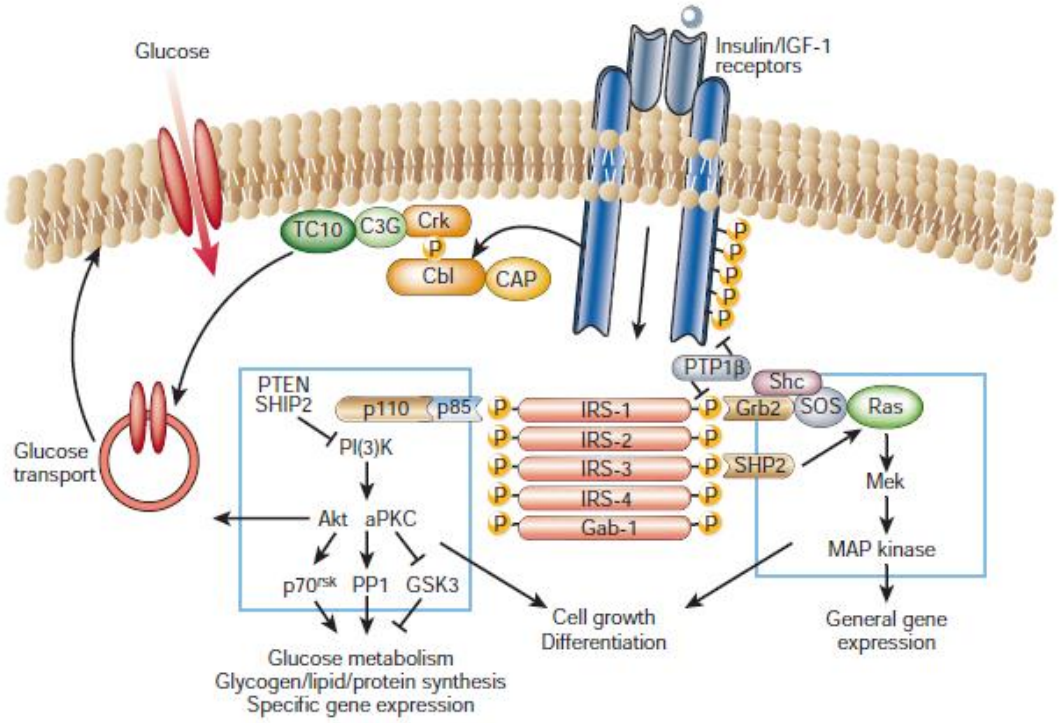

Figure 1.6 Insulin signalling mechanisms. The insulin receptor is a tyrosine kinase that undergoes autophosphorylation and catalyses the phosphorylation of cellular proteins such as members of the IRS family. Downstream they activate diverse signalling pathways, including PI3K, Ras and MAPK, which result in the regulation of glucose, lipid and protein metabolism. Figure from reference [33].

Insulin also inhibits the production and release of glucose by the liver by blocking gluconeogenesis and glycogenolysis. It directly controls the activities of a set of metabolic enzymes by phosphorylation and dephosphorylation and also regulates the expression of genes encoding hepatic enzymes of gluconeogenesis and glycogenolysis [42].

Insulin also promotes the synthesis of lipids and inhibits their degradation. Some studies suggest that many of these changes require an increase in SREBP-1c expression [43].

1.1.4 β-cell homeostasis

In adults, β-cells have an estimated life-span of ~60 days after which they undergo programmed cell death [44]. The senescent β-cells are replaced by processes of

replication (proliferation) and by neogenesis of new β-cells derived from progenitor cells that bud from the ducts of the exocrine pancreas. This balance is an important aspect for the maintenance of glucose homeostasis because the ability of the pancreas to produce sufficient insulin to meet the body's needs depends on the appropriate size of the β-cell mass [45]. Moreover, during adulthood, β-cell mass is highly adaptive to changes in metabolic homeostasis, as it is observed during the progression to diabetes.
Many factors are implicated in the regulation of β-cell mass, including nutrients (in particular glucose and fatty acids), insulin and other growth factors signalling, and incretin hormones such as glucagon-like peptide 1 (GLP-1).

It has been shown that glucose stimulates β-cell proliferation: mice subjected to glucose infusion demonstrated increased β-cell mass [46] and the same effect was also found in rat insulinoma cells (INS-1) [47]. One of the mechanisms responsible for this effect is the glucose dependent membrane depolarisation, calcium influx and the subsequent activation of the PI3K-Akt signalling pathways, which can induce cell survival and proliferation [48]. In addition, glucose can also induce mTOR signaling pathway, an important regulator of cell mass and proliferation [49]. Moreover glucose is able to increase β-cell function, stimulating insulin release. Finally, an increase in intracellular calcium could also play an important role in growth signals induced by glucose, through the activation of calcineurine, a calcium dependent phosphatase. It has been demonstrated that mice with a deletion in the regulatory subunit of calcineurine develop age-dependent diabetes, characterised by decreased β-cell proliferation and mass, reduced pancreatic insulin content and hypoinsulinemia [50].
FFAs are also able to influence β-cell homeostasis, as they are able to amplify GSIS and consequently to stimulate β-cell function. In addition, increased enteric nutrient supply, especially in the form of fats, may also result in β-cell mass expansion through increased GLP-1 production. GLP-1 is an incretin hormone, which has been shown to increase β-cell proliferation and decrease β-cell apoptosis [51]. Most of its effects in the β-cell are due to the activation of the PDX-1 gene [52], whose expression is essential for pancreogenesis and for the regulation of genes associated with pancreatic cell differentiation and maturation (insulin, GCK, GLUT2) [53].

Together with nutrients, insulin like growth factors (IGF-I and IGF-II) and insulin itself play an important role in the regulation of β-cell homeostasis. IGF-I bind to IGF-I receptor, stimulating its intrinsic tyrosine kinase activity, which in turn phosphorylates members of the IRS family and activates the molecular pathways described in paragraph 1.1.3. It has been shown that IGF-I and IGF-II are able to increase β-cell proliferation in rat islets and insulinoma cells *in vitro* [54]. In addition glucose enhances IGF-I mediated proliferation of insulinoma cells in culture through the activation of PI3K [47]. IGF-I is also able to activate the Ras/MAPK pathway and to induce mitogenesis in most mammalian cell types [55].

The effects of insulin receptor signaling in the β-cell have been assessed both *in vivo* and *in vitro*. Insulin infusion in mice induces β-cell proliferation and increases β-cell mass [56]. *In vitro*, insulin receptor knock-down in MIN-6 cells leads to decreased proliferation [57]. In particular, IRS2 plays an important role as it stimulates PI3K/Akt and ERK1/2 pathways and animal models deficient in IRS2 develop T2D because of failed compensation [58].

Other growth factors have been shown to regulate β-cell proliferation, including prolactin, placental lactogen (PL) and growth hormone (GH). *In vitro* experiments in islets showed that incubation with these hormones leads to increased β-cell proliferation [59]. This is due to activation of the Janus Kinase (JAK)/Signal Transduction and Activators of Transcription (STAT) pathway, which leads to activation of Cyclin 2, essential for β-cell proliferation [60].

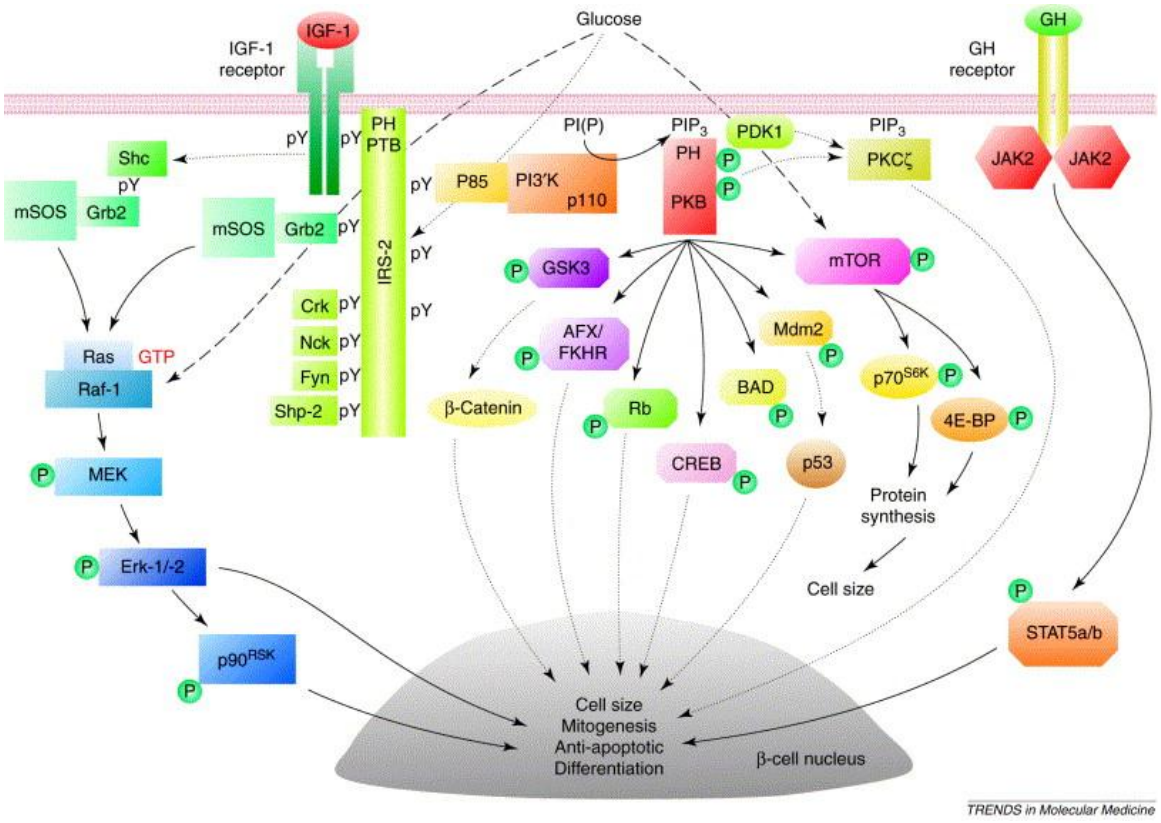

Figure 1.7 Intracellular pathways implicated in β-cell growth and survival. IGF-I, IRS-2, PI3K, mTOR and STAT are important players in the regulation of β-cell homeostasis. The disruption of these pathways leads to β-cell dysfunction and apoptosis. Figure from reference [61].

1.2 Diabetes Mellitus

Diabetes mellitus is a metabolic disease characterised by high levels of glucose in the blood, which is defined “hyperglycemia”. This condition is caused by defects in insulin secretion, defects in insulin action for a diminished tissue response, or both. Impairment of insulin secretion and defects in insulin action frequently coexist in the same person with diabetes, and it is often unclear which abnormality is the primary cause of the hyperglycemia [62].

The chronic hyperglycemia of diabetes is associated with long-term damage and dysfunction of various organs, especially eyes, kidneys, nerves, heart and blood vessels. In almost all high-income countries, diabetes is the leading cause of cardiovascular diseases, blindness, kidney failure and lower limb amputation.

There are two major types of diabetes. The causes and risk factors are different for each type:

- *Type 1 Diabetes* (T1D) can occur at any age, but it is most often diagnosed in children, teenagers, or young adults. This disease results from an autoimmune destruction of pancreatic β-cells. The subsequent lack of insulin leads to increased blood and urine glucose.

- *Type 2 Diabetes* (T2D) makes up 90% of diabetes cases. It most often occurs in adulthood. This form of diabetes develops often in people who are overweight and who do not exercise. T2D is considered a milder form of diabetes because of its slow onset (sometimes developing over the course of several years) and because it can be usually controlled with diet and oral medication. The consequences of uncontrolled and untreated T2D, however, are just as serious as those for T1D. Insulin injections are sometimes necessary if treatment with diet and oral medication is not working.

The World Health Organization states that 347 million people worldwide were suffering from diabetes in 2008, which equates to 9.5% of the adult population [63] and the

incidence is dramatically increasing. For this reason, the understanding of the molecular mechanisms of this disorder is becoming critical, in order to develop novel treatments that effectively target specific molecules and pathways.

The work in this thesis will focus its attention on the study of the molecular mechanisms of T2D.

T2D is characterised by defects in insulin secretion, defects in insulin action and an increased hepatic glucose output. Symptoms for this disease include frequent urination, lethargy, weight loss and an excessive thirst and hunger. The typical treatment for this disorder includes changes in diet, physical exercise, oral medications and daily injection of insulin.

It is generally agreed that T2D is a multifactorial disease, arising from the presence of T2D risk alleles in multiple genes and from environmental factors, which can also be responsible of modulation of the genetic risk [64].

Several lines of evidence support the principle of inherited genetic susceptibility as an important risk factor for T2D, but the mode of genetic transmission does not follow simple Mendelian patterns. Moreover, the risk of T2D is higher in certain ethnic groups, independent of metabolic risk factors profiles, such as Hispanics, African Americans, Pacific Islanders, and American Indians. Candidate gene association, linkage analysis and genome-wide association studies (GWAS) have identified some of the T2D susceptibility loci. Most of the T2D risk alleles identified correspond to gene that have impacts on glucose induced-insulin secretion: *TCF7L2*, *ADAMTS9*, *ADCY5*, *CDC123*/*CAMK1D*, *CDKAL1*, *CAPN10*, *CDKN2A/B*, *CENTD2*, *FOXO1*, *HHEX*, *IGF2BP2*, *KCNQ1*, *PROX1*, *PPARG*, *NOTCH2*, *WFS1*, *PCSK1*, *APOB* [65-67].

Sedentary lifestyles and high-fat diets are behavioural factors playing a role in the pathogenesis of the disease. It has been shown that lifestyle interventions (dietary modification, weight loss and exercise) in overweight adults with impaired glucose tolerance achieved 58% reduction in the incidence of diabetes [68].

T2D has a slow onset, progressing from an early asymptomatic stage with insulin resistance to mild postprandial hyperglycemia to T2D requiring pharmacological

intervention. Understanding the progression of diabetes is fundamental for effective treatments regimens, specific for the different stages of the disease.

1.2.1 Natural history of T2D

Insulin resistance is considered to be an early primary defect in T2D. It is characterised by an inadequate response to a given concentration of insulin and by the inability to increase glucose uptake and utilisation.

At first, the pancreatic β-cell is able to compensate this dysfunction, increasing the levels of insulin in a condition called hyperinsulinemia: higher levels of insulin correspond to higher insulin resistance. This compensation is able to keep glucose levels normalised for a period of time up to several years (Figure 1.8) [69] [70].

However, as insulin resistance worsens (due to genetic defects, obesity, decreased physical activity or aging), more global defects in insulin secretion occur, resulting also in increased hepatic glucose output. Together, these defects lead to a progressive elevation of fasting blood glucose, in an asymptomatic but still potentially pathologic stage characterised by mild hyperglycemia.

The progression from this stage to early T2D is marked by a decrease in the β-cell function and subsequently a decline in insulin secretion. It is a gradual and progressive failure because, as long as the pancreatic β-cell is able to compensate for insulin resistance by increasing insulin production and secretion, glucose level remains normal or near normal. It is only when the β-cell begins to fail, and insulin secretion decreases, that hyperglycemia occurs (Figure 1.8) [71].

Also obesity has an impact on the progression of the diabetic state: obese diabetic patients have a more profound degree of insulin resistance and compensatory hyperinsulinemia compared to lean patients [72].

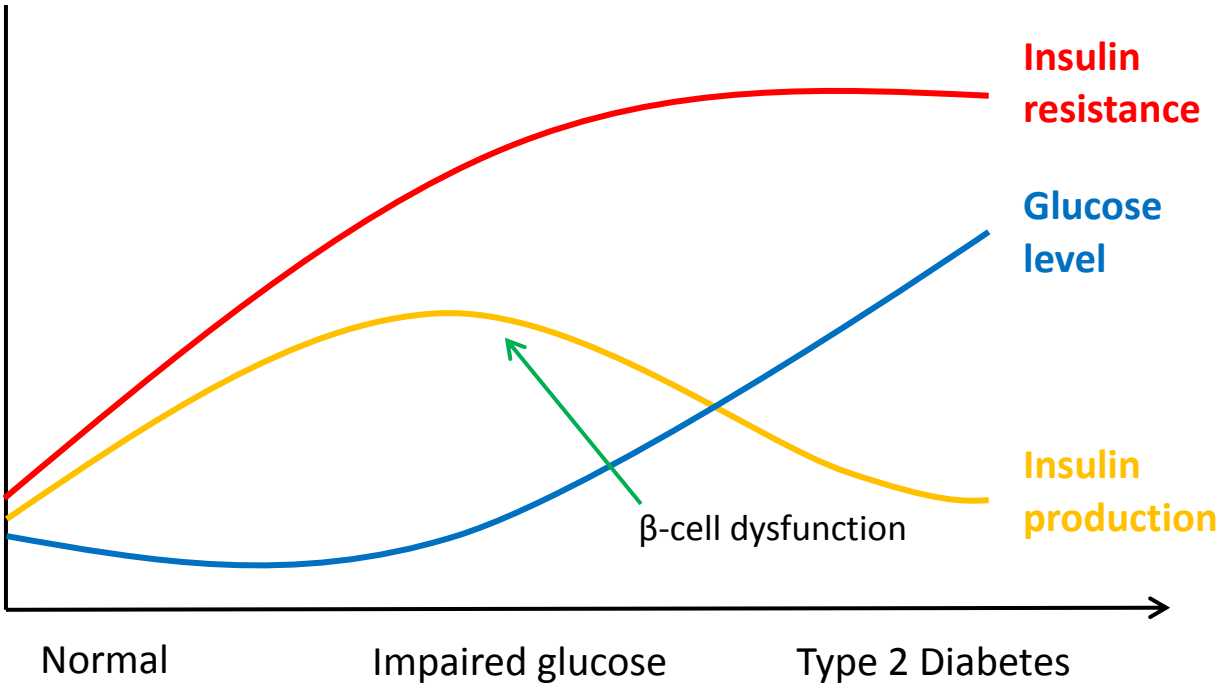

Figure 1.8 Natural history of T2D: T2D progresses from an initial phase of insulin resistance characterised by an increased insulin production that maintains normal glucose levels, to a gradual dysfunction of the β-cell, with increased insulin resistance and hyperglycemia.

Only a small fraction of obese individuals with insulin resistance progresses to T2D [73]. In addition, recent studies demonstrated that β-cell dysfunction is the critical determinant for T2D and it can occur also in absence of insulin resistance [74]. In particular, the United Kingdom Prospective Diabetes Study (UKPDS), which had the goal of understanding how to reduce long-term complications in patients with established diabetes, showed that treatments aimed to reduce insulin resistance were not able to stop the progression of β-cell dysfunction [75]. In general, the difficulty in maintaining normal glucose level has been attributed to the deterioration of β-cell function; such deterioration is the prerequisite to diabetes state, because many patients with intact β-cells are able to maintain normal glucose tolerance for their lifetimes.

1.2.2 β-cell compensation

The development of T2D is characterised by changes in the number, morphology and function of the β-cells, which progressively lose their differentiation feature and become unable to cope with the needs of the organism.

During the first phases of insulin resistance there is a compensation for the subnormal insulin function with an increase in β-cell mass and function, leading to increased insulin secretion (hyperinsulinemia). Increase in β-cell mass has been found in autopsy studies in obese humans [76] and rodent models of insulin resistance [77-78]. This is mostly due to increased cell number, but cell hypertrophy may also contribute.

The stimulating factors implicated in the compensatory islet responses include the same factors responsible of the maintenance of β-cell homeostasis, specifically, increased nutrient supply (in particular glucose and fatty acids), insulin and other growth factors signalling, and increased levels and sensitivity to incretin hormones such as GLP-1 [79].

Glucose, in particular, is considered the dominant factor in β-cell compensation process. Studies of islet β-cell compensation show an upregulation of glucose pathways [80-82], such as increased level of GCK, pyruvate carboxylase and glucose transporter GLUT2. It has also been shown that GCK is essential for the compensatory β-cell hyperplasia, as $GCK^{-/-}$ mice fed a high fat diet demonstrate decreased β-cell replication and hyperplasia [83].

However, with the progression of insulin resistance towards T2D, the β-cell is not able to cope anymore with the metabolic demand and hyperglycemia and hyperlipidemia negatively impact β-cell mass and function.

The toxic effect generated by chronic exposure to high glucose and fatty acids on the β-cell viability and function is generally called glucolipotoxicity and it is discussed in more details in the next paragraph (1.3).

1.3 Glucolipotoxicity

Glucolipototoxicity refers to the combined and deleterious effects of elevated glucose and fatty acids levels on pancreatic β-cell function and survival [84].

There is still debate about which molecular mechanisms are responsible for the β-cell failure during progression of diabetes, and in particular, recent attention is focussed on the identification of the mechanisms of glucose- and fatty acids-induced impairment of insulin production and secretion.

As discussed above, there is strong evidence of a gradual progression of the β-cell failure in glucolipotoxic conditions. In particular, after exposure to high concentrations of glucose and fatty acids, there is a compensatory phase during which there is increase of β-cell mass, leading to increased insulin gene expression and secretion. Upon prolonged exposure, the β-cell becomes unable to further compensate and this phase is characterised by reduced β-cell mass, reduction of insulin expression and secretion and ultimately β-cell failure.

1.3.1 Effect of glucolipotoxicity on β-cell viability

T2D is associated with a progressive decrease in β-cell mass and the inability to adapt to insulin resistance with an increase in β-cell replication and neogenesis. Rahier et al demonstrated that β-cell mass is 39% less in T2D subjects compared to matched controls [85]. It has also been shown that the pro-apoptotic genes Bad, Bid, and Bik are overexpressed in islets maintained in high glucose concentrations, while the anti-apoptotic gene Bcl-xl is reduced [86].

Many mechanisms could trigger β-cell apoptosis, including chronic hyperglycemia, chronic hyperlypidemia, increase in intracellular calcium, endoplasmic reticulum stress, oxidative stress and certain cytokines.

Glucotoxicity

As discussed above, transient increases in glucose levels within physiological range (i.e. after a meal) induce insulin secretion and β-cell proliferation. On the other hand, chronic hyperglycemia has detrimental effects on β-cell function and mass [87]. Currently, it is thought that chronic glucose exposure leads to oxidative stress in β-cells and to accumulation of reactive oxygen species (ROS), causing β-cell dysfunction and apoptosis [88-92]. When glucose enters the cell, it is converted by glycolysis to pyruvate, which then enters tricarboxylic acid cycle to undergo oxidative phosphorylation, with formation of ATP and ROS. However, when excess glucose is available to the cell, glucose is driven to alternative pathways and excess ROS can be formed [87]. The pathways involved in the generation of oxidative stress include the non-enzymatic glycosylation reaction with increased production of advance glycation end products (AGE), the disruption of the electron transport chain in the mitochondria, and the hexosamine pathway, with subsequent changes in gene expression (Figure 1.9). Also the polyol pathway is an established contributor to oxidative stress because the enzyme aldose reductase (responsible for detoxification of aldehydes to alcohols), in the presence of hyperglycemia, reduces glucose to sorbitol, which is then oxidised to fructose, consuming large quantities of NADPH. The depletion of NADPH leads to oxidative stress since this is a major cofactor for glutathione regeneration and a known antioxidant defence at the cellular level [93] (Figure 1.9).

The detrimental effects of oxidative stress in the β-cell might, in part, be caused by the activation of IκB kinase-β (IκKβ) and/or cyclooxygenase increasing the production of nitric oxide (NO) via NF-κB, activation of PKC, p38 mitogen-activated protein kinase and c-Jun N-terminal kinase (JNK) pathways [94-95]. Oxidative stress has also been shown to disrupt insulin signalling transduction (more details in paragraph 1.3.2).

Another pathway by which ROS can induce β-cell dysfunction and death is through the NLRP3 inflammosome, a complex of proteins responsible of the generation of inflammatory responses [96]. It has been shown that ROS can induce NLRP3 activation, facilitating the oxidative stress mediator thioredoxin-interacting protein (TXNIP) binding to inflammosome and its subsequent activation. NLRP3 then activates caspase

1, which induces cleavage of pro-IL-1β to IL-1β and the generation of an inflammatory cascade (see paragraph 1.4) [97].

Because of the relatively low expression of antioxidant enzymes such as catalase and glutathione peroxidase, β-cells are highly sensible to oxidative stress [98-99]. Consistent with this, it has been shown that overexpression of antioxidant enzymes in isolated islets prevented islets dysfunction in conditions that mimic prolonged hyperglycemia [100].

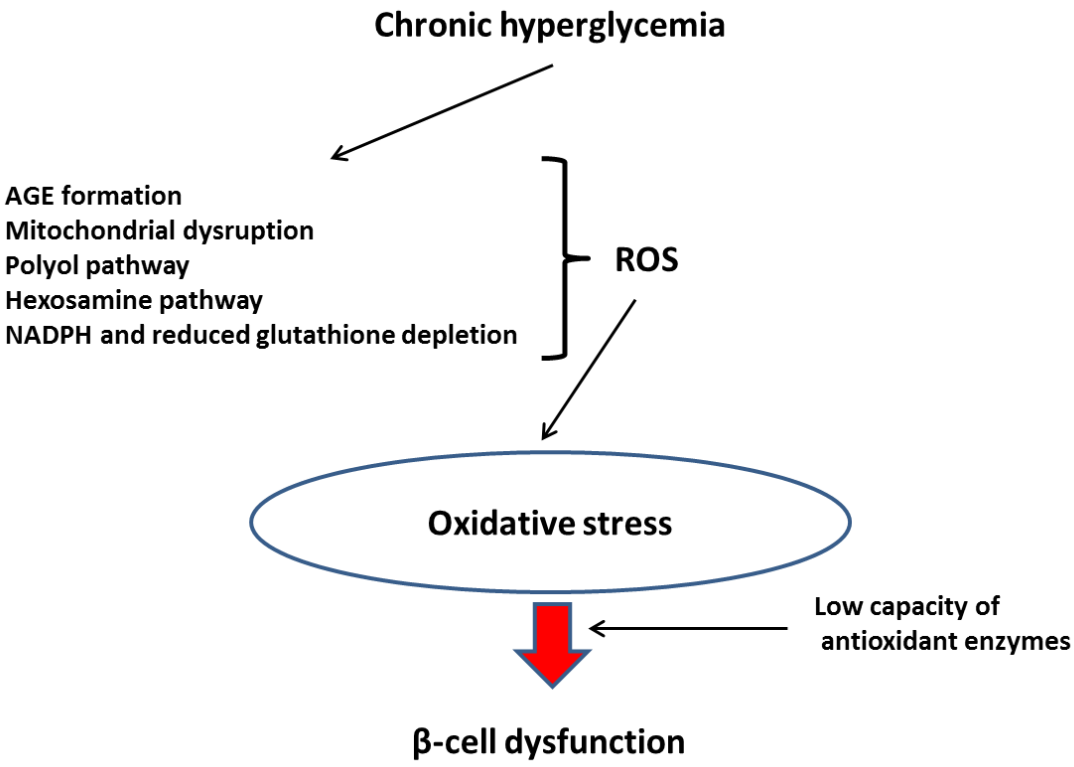

Figure 1.9 Chronic hyperglycemia leads to oxidative stress. Schematic representation of the factors implicated in the generation of oxidative stress under conditions of hyperglycemia.

In addition to oxidative stress, chronic hyperglycemia can induce ER stress (see below), increasing intracellular calcium and subsequent signalling. Chronic hyperglycemia leads to overstimulation and long term increase in cytosolic calcium that may be pro-apoptotic and induce β-cell dysfunction [101].

Moreover, high concentrations of glucose induce the production of interleukin-1 β (IL-1β), triggering an inflammatory response (more details in paragraph 1.4) [102] and of Fas receptor, activating the apoptotic pathway [103].

Finally, one of the downstream factors that can be influenced by hyperglycemia is IRS-2, which is especially involved in promoting β-cell survival. Increased IRS-2 expression can promote β-cell replication, neogenesis and survival, whereas decreased IRS-2 expression causes β-cell apoptosis. The promotion of β-cell replication is triggered by IRS-2 tyrosine phosphorylation, while serine/threonine phosphorylation leads to IRS degradation [104]. Chronic hyperglycemia can lead to the chronic activation of the mTOR, which can phosphorylate and downregulate IRS-2 [105].

Lipotoxicity

Long-term exposure of FFAs to β-cell has a more marked effect of inhibiting β-cell mitogenesis, as well as inducing β-cell apoptosis, especially in the presence of concomitant hyperglycemia. This can be explained by the fact that elevated glucose prevents fat oxidation via the AMPK/malonyl-CoA signalling network (see paragraph 1.1.2.1) and therefore the detoxification of fat [106]. This concept is supported by the findings that treatment with an inhibitor of fat oxidation promotes β-cell death, while treatment with an AMPK activator protects β-cell from glucolipotoxicity [107].

At the same time there is intracellular accumulation of LC-CoA, products of lipid peroxidation and/or ceramide derivatives, which are cytotoxic. Ceramide accumulation in β-cells is implicated in the apoptotic pathway because it increases the expression of inducible nitric oxide synthase (iNOS) through activation of NF-κB, and therefore it augments the production of the toxic NO [108].

Another potential mechanism by which FFAs may impair β-cell viability involves the expression of uncoupling protein-2 (UCP2), which is a mitochondrial carrier that regulates ATP production, catalysing the translocation of protons across the mitochondrial membrane. Chronic exposure of islets or insulinoma cells to elevated FFAs can induce an increase in UCP2 expression [109], increasing ROS production.

In addition, FFAs are able to activate Toll-like Receptor 4 (TLR4) [110], a molecule involved in the activation of the innate immune system. It has been shown that TLR4

activated macrophages contribute to IL-1β secretion from mouse and human islets [111].

ER stress

β-cell apoptosis can be further induced by endoplasmic reticulum stress. Because of the high secretory demand, the endoplasmic reticulum is very well developed and highly active in the β-cell. This also likely increases the susceptibility of these cells to ER stressors. ER stress might produce signals mediating glucose-induced impairment of function and death.

The molecular mechanisms by which glucolipotoxicity-induced ER stress causes β-cell apoptosis are not well understood, but can involve depletion of ER calcium stores [112]. It has been reported that the Akita mouse (a mouse model of diabetes) carrying a folding mutation in proinsulin that activates the ER stress response, develops diabetes and loss of β-cell mass, suggesting that an excessive demand on ER could cause β-cell damage [113].

Glucolipotoxicity also activates the Unfolded Protein Response (UPR), a mechanism that improves cellular ability to dispose unfolded proteins and increase the amount of chaperones in the ER. If unable to perform this task, the UPR triggers the apoptosis pathway [114].

ER stress can induce apoptosis by JNK, ATF-3 and inhibition of Bcl-2 [81]. In particular, activation of JNK could lead to suppression of the IRS/Akt signalling via serine phosphorylation of IRS-1, reducing survival and inducing apoptosis [115].

Mitochondrial dysfunction

Increased metabolism of glucose and FFAs through mitochondrial oxidation results in an increased mitochondrial membrane potential and superoxide production [116]. This can increase cell exposure to ROS and lead to the activation of UCP2 [117], which help to safely dissipate the elevated mitochondrial membrane potential and promote fuel detoxification. However, this occurs at the expense of ATP synthesis efficiency and consequently insulin secretion.

Islet inflammation and amyloid deposition

There is also strong evidence for the activation of inflammatory pathways in the presence of glucolipotoxicity. Chronic elevated glucose has been documented as inducing IL-1β production [102] and expression of Fas receptor [103]. A more detailed explanation of islet inflammation processes is presented in paragraph 1.4.

Also cytotoxicity from accumulation of IAPP may also be a factor contributing to T2D: this is the major component of islet amyloid and is co-secreted with insulin from β-cell [118]. In T2D this peptide aggregates to form intracellular microfibrils that can be toxic to the islet tissue, but the mechanisms responsible of amyloid formation remain unclear.

1.3.2 Effect of glucolipotoxicity on β-cell function

Prolonged exposure of the β-cell to high concentration of glucose and fatty acids leads to a β-cell dysfunction and impairment of insulin secretion and production. This phenomenon has been observed *in vivo* in rats [119] and humans [120]. Moreover, *in vitro* [107, 121-123] and *in vivo* [124] studies have provided evidence that lipotoxicity only occurs in the presence of concomitantly elevated glucose levels. This can be explained by the effects of glucose on lipid partitioning (explained in paragraph 1.1.2.1) and with the inhibition of β-oxidation and the concomitant accumulation of toxic intermediates in the cytosol.

In recent years, several potential mechanisms have been investigated that could be responsible for the impairment of insulin secretion in glucolipotoxicity. These include the upregulation of UCP2, the activation of novel isoforms of protein kinase C (PKCε), the activation of GPR40 and the effect on late exocytotic events.

Some evidence suggests that UCP2 might modulate insulin secretion and production and consequently play a role in glucolipotoxicity. This is based on the observations that increasing UCP2 expression in β-cells impairs insulin secretion [125] and that $UCP2^{-/-}$ mice have increased circulating insulin levels and are protected from diabetes [126]. However, more recent studies show that the increase in UCP2 expression levels after

high fat exposure likely represents a cellular defense mechanism against fuel overload and oxidative stress rather than a deleterious response [127].

Activation of PKCε (a novel isotype of PKC, a calcium independent serine/threonine kinase) has also been suggested as a potential mechanism for the decrease in insulin secretion in glucolipotoxicity. Biden and coworkers demonstrated that islets from PKCε$^{-/-}$ mice are protected from the deleterious effects of fatty acids on insulin secretion *in vitro* [128], probably due to the accumulation of lipolytic intermediates [129].

A role for GPR40 in mediating fatty acid inhibition of insulin secretion has been suggested by the observation that islets from GPR40$^{-/-}$ mice are insensitive to the inhibitory effects of prolonged fatty acid exposure, whereas overexpression of GPR40 in β-cells of mice leads to impaired β-cell function, hypoinsulinemia and diabetes [130].

Finally, evidence suggests that fatty acids may also alter one or more late steps of insulin exocytosis in the β-cell. It has been shown that expression of granuphilin, a molecule that plays a role in the docking of insulin secretory granules to the plasma membrane, is increased in islets exposed to palmitate, as a consequence of upregulation of SREBP1c, a transcription factor that targets granuphilin promoter and controls fatty acids synthesis. By contrast, ablation of granuphilin by knock-down or knock-out restored insulin secretion in these islets [131].

Also the induction of oxidative stress has detrimental effects on the β-cell function. As explained before, oxidative stress generates from accumulation of glucose metabolites produced after chronic exposure to high glucose concentrations. Takahashi et al demonstrated that exposing rat islets to increasing concentrations of D-glyceraldehyde is associated with oxidative stress, decreased insulin content and inhibition of GSIS [132].

In a recent study, Somesh and colleagues used rat islets and NIT-1 cells to clarify the molecular mechanisms involved in the reduction of insulin secretion in glucolipotoxicity. They demonstrated that islets show an impaired glucose uptake, with reduction of GLUT2 and GCK mRNA levels, and an increased fatty acid uptake. This general suppression in glucose metabolism correlates well with a decrease in mitochondrial number and activity and reduction in cellular ATP content. In addition, cytosolic calcium mobilization is lost and insulin granule docking is reduced, with decreased expression of Rab27a, a small GTPase involved in vesicles transport [133].

Prolonged exposure to fatty acids also impairs insulin gene expression in the presence of high glucose [121, 134], with distinct mechanisms from those involved in the impairment of insulin secretion. Generally, these mechanisms are not due to changes in mRNA stability, but to inhibition of glucose-induced insulin promoter activity [135]. This is associated with decreased binding activities and reduced expression of the transcription factors PDX-1 and MafA [136]. The accumulation of ceramide is considered as the leading mechanism in the impairment of insulin production and secretion. JNK is a known target of ceramide and can repress insulin gene transcription via inhibition of E1-mediated transcription and PDX-1 binding [137]. Moreover, ceramide formation from palmitate inhibits Akt activity [138], reducing the inhibition on the transcription factor Foxo-1, which translocates to the nucleus and activate gluconeogenesis. It has been shown that PDX-1 and Foxo-1 exhibit a mutually exclusive pattern of nuclear localization [139].

Also oxidative stress is able to decrease PDX-1 mRNA, PDX-1 protein, insulin mRNA and insulin content in HIT-T15 cells [140] and MafA binding [141].

ER stress is also associated with insulin transcription dysfunction, causing alterations in PDX-1 function [142] or insulin mRNA stability [143].

1.4 T2D and inflammation

Exposure of the β-cell to high concentrations of glucose and fatty acids can also induce the activation of inflammatory pathways. Initially, an inflammatory response is probably deployed to promote β-cell repair and regeneration. However, as it becomes chronic, auto-inflammatory processes can be activated that may become deleterious. Therefore T2D can also be considered an auto-inflammatory disease [144].

Supporting this hypothesis, inflammatory mediators such as cytokines and C-reactive protein have been shown to be elevated in patients with diabetes and they have been associated with the development and progression of cardiovascular complications [145-146]. Patients with diabetes have evidence of low-grade inflammation and abnormal peripheral blood mononuclear cells (PBMCs), that could relate to long term complications and susceptibility to infections [147].

IL-1β and TNF-α, alone or in combination, have been implicated in sustaining autoimmune reaction against β-cell in T1D [148]. TNF-α is also considered a major cytokine implicated in the inflammatory response, as it has been shown to be overexpressed in adipose tissue in obesity [149], and possibly contributing to insulin resistance and consequently to the development of T2D [150].

Of interest is the predominant role of IL-1β, which is upregulated in islets of patients with both T1D and T2D [151]. Moderately elevated glucose concentrations are sufficient to induce transcriptional activation of IL-1β expression in human islets. More recently it has been found that oleate, palmitate and stearate, can also stimulate IL-1β expression when added individually or in mixtures. The combination of FFAs with elevated glucose concentrations further increases IL-1β expression and the release of various cytokines and chemokines [152].

Elevated glucose and FFA initially induce the expression and release of low levels of IL-1β, required for the adaptive response of islet cells (Figure 1.10). Continuous or prolonged stimulation with nutrients (metabolic stress) leads to the activation of IL-1R leading to a further increase of IL-1β by an autostimulatory process and to the

production of IL-1β-dependent cytokines and chemokines. Autocrine and paracrine activation leads to a broad inflammatory response including elevated cytokines and chemokines production, attraction of macrophages, apoptosis and amyloidosis, fibrosis and impaired insulin secretion (Figure 1.10). Consistent with an important role of IL-1β in inflammation, it has been shown that IL-1 receptor antagonist (IL-1Ra) is able to protect cultured human islets from these deleterious effects [144, 153-154].

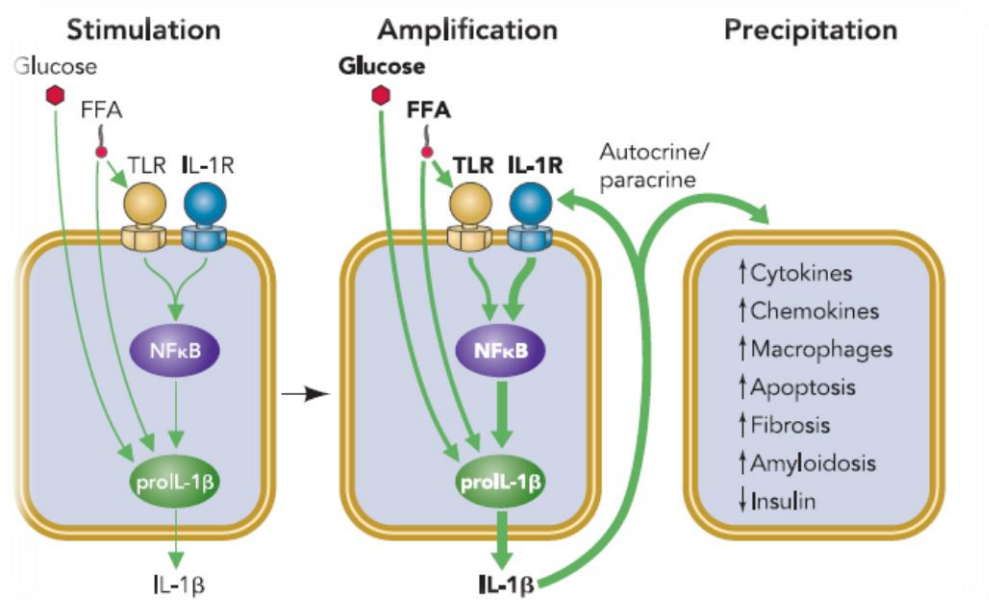

Figure 1.10 Regulation of IL-1β in islets by metabolic stress. Il-1β auto-stimulatory loop is one of the key factors implicated in the inflammatory response in T2D. Elevated glucose and FFA initially induce the expression and release of low levels of IL-1β, required for the adaptive response of islet cells. Continuous or prolonged stimulation with nutrients leads to the activation of IL-1R leading to a further increase of IL-1β by an autostimulatory process and to the production of IL-1β-dependent cytokines and chemokines. Autocrine and paracrine activation leads to a broad inflammatory response including elevated cytokines and chemokines production, attraction of macrophages, apoptosis and amyloidosis, fibrosis and impaired insulin secretion. Figure from reference [144].

IL-1β pathway is activated due to IL-1R accessory proteins docking to the intracellular side of the receptor, with the recruitment of IL-1R activated kinase (IRAK) via the adaptor protein MyD88. IRAK then interacts with and activates TNF receptor associated factor 6 (TRAF6) [155]. TRAF6 can lead to the activation of mitogen-activated protein (MAP) kinase (MAPK)/extracellular signal-regulated kinase (ERK) kinase kinase

(MEKK1). MEKK-1 then leads to the activation of the group of MAP/stress-activated protein kinases (MAP/SAPK) as well as NF-κB [156]. MAP/SAKs, which include ERK, p38, and JNK, are able to phosphorylate a broad spectrum of cellular proteins including transcription factors of the activator protein 1 family, NF-κB inhibitors and PKC, which are pathways linked to apoptosis in β-cells (Figure 1.11).

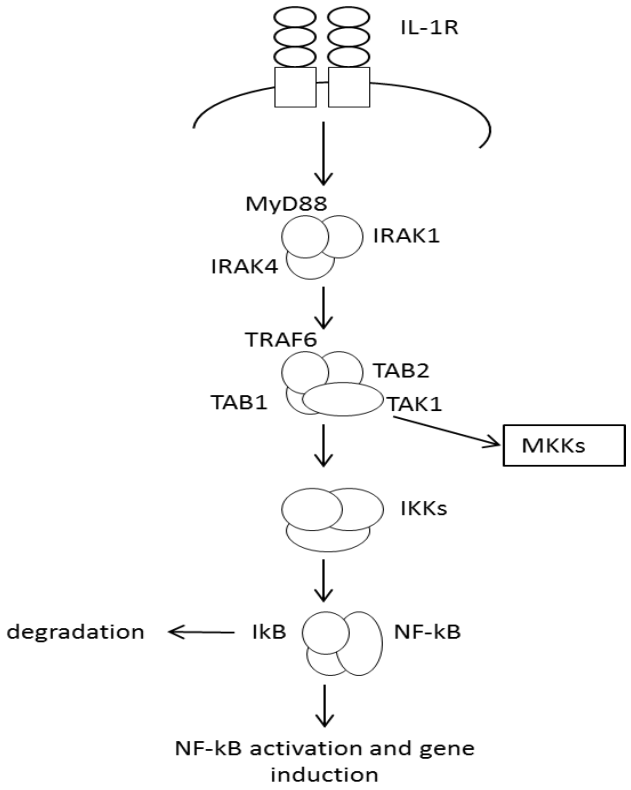

Figure 1.1 IL-1R signalling pathway. IL-1β pathway is activated with the recruitment of IL-1R activated kinase (IRAK) via the adaptor protein MyD88. IRAK then interacts with and activates TNF receptor associated factor 6 (TRAF6). TRAF6 can lead to the activation of MAP kinase kinase (MKKs) or IKKs, which phosphorylates IkB, leading to its degradation. This activates NF-κB and its inflammatory pathway.

As described before, IL-1β can be important for the consequent production of islets chemokines (IL-6, IL-8, MIP-1α, CXCL1) and their attraction of immune cells. These molecules are implicated in the stimulation of monocytes and neutrophils migration, and consequently in the increased number of islet-associated macrophages in T2D. This migration can be blocked by IL-8 neutralization [157]. All together, these factors lead to a chronic activation of the innate immune system.

IL-6 is another cytokine that is elevated in obesity and T2D and therefore it has been suggested as a predictive factor for the development of T2D. Both human and mouse islets respond to metabolic stress *in vitro* by increasing IL-6 release [144] and it has been shown that sustained treatment of human and rodent islets with IL-6 impairs GSIS [158].

IL-6 has also recently found to promote glucagon secretion from the pancreatic α-cell, induce α-cell proliferation and inhibit apoptosis [154]. Glucagon exerts opposite effects to insulin and it stimulates the release of glucose in the bloodstream. Thus, in contrast to the negative effects on the β-cell, IL-6 acts as a growth and survival factor and it promotes glucagon secretion in the α-cells. Pancreatic islet pathology in T2D is characterized not only by reduced β-cell function and mass, but also an increased proportion of α-cells relative to β-cells, together with relative hyperglucagonemia as a result of dysregulation of α-cell function.

Also IFN-γ has been shown to be involved in β-cell apoptosis and disruption of IFN-γ signalling pathway at the level of STAT1 prevents immune destruction of the β-cells [159].

These inflammatory effects are also amplified by the synergistic action of different cytokines at the same time; for example, TNF-α and IFN-γ works together to lead to caspase dependent apoptosis [160]. IFN-γ treatment confers susceptibility to TNF-α-induced apoptosis by STAT1 activation, followed by IFN regulatory factor (IRF)-1 induction. IRF-1 plays a central role in IFN-γ/TNF-α induced cytotoxicity because inhibition of IRF-1 induction by antisense oligonucleotides blocks IFN-γ/TNF-α induced cytotoxicity [161].

1.5 Tumor Necrosis Factor Receptors

Tumor necrosis factor (TNF) is a cytokine produced by many cell types, including macrophages, monocytes, lymphocytes, keratinocytes and fibroblasts, in response to inflammation, infection, injury and other environmental challenges. TNF-α is representative of a family of trimeric cytokines and cell surface proteins such as lymphotoxin-α (LT-α), Fas ligand (FasL), receptor-activator of NF-κB ligand (RANKL), CD40 ligand (CD40L), and TNF-related apoptosis-inducing ligand (TRAIL). These proteins display 25-30% sequence similarity mostly in the residues responsible for their trimerisation. By contrast, the external surface of the trimers, which accounts for receptor selectivity, shows little similarity [162]. These ligands bind to the respective receptors, triggering signalling cascades leading to cell proliferation, survival and differentiation. Most of the TNF/TNFR are expressed in the immune system, where their rapid and potent signalling capabilities are crucial in coordinating the proliferation and protective function of pathogen-reactive cells [163]. They have also roles in inflammation and apoptosis [164].

The different TNF receptors are listed in Table 1.1.

RECEPTOR	**SYSTEMATIC NOMENCLATURE**	**LIGANDS**	**ADAPTOR PROTEINS**
TNFR1	TNFRSF1A	TNF	TRADD
TNFR2	TNFRSF1B	TNF	TRAF1, TRAF2, TRAF5
Lymphotoxin β-receptor	TNFRSF3	Lymphotoxin $\beta_2\alpha_1$heterotrimer	TRAF3, TRAF4, TRAF5
OX40	TNFRSF4	OX-40 ligand	TRAF1, TRAF2, TRAF3, TRAF5
CD40	TNFRSF5	CD40 ligand	TRAF1, TRAF2, TRAF3, TRAF5, TRAF6
Fas	TNFRSF6	Fas ligand	FADD
Decoy receptor	TNFRSF6B	LIGHT, TL1A,	/

3		Fas ligand	
CD27	TNFRSF7	CD70	TRAF2, SIVA
CD30	TNFRSF8	CD30 ligand	TRAF1, TRAF2, TRAF3, TRAF5
4-1BB	TNFRSF9	4-1BB ligand	TRAF1, TRAF2, TRAF3
Death receptor 4	TNFRSF10A	TRAIL	FADD
Death receptor 5	TNFRSF10B	TRAIL	FADD
Decoy receptor 1	TNFRSF10C	TRAIL	/
Decoy receptor 2	TNFRSF10D	TRAIL	/
RANK	TNFRSF11A	RANK ligand	TRAF1, TRAF2, TRAF3, TRAF5, TRAF6
Osteoprotegerin	TNFRSF11B	RANK ligand, TRAIL	/
Death receptor 3	TNFRSF25	TL1A	TRADD
TWEAK receptor	TNFRSF12A	TWEAK	TRAF1, TRAF2, TRAF3
TACI	TNFRSF13B	BAFF, APRIL	TRAF2, TRAF5, TRAF6
BAFF receptor	TNFRSF13C	BAFF	TRAF3
HVEM	TNFRSF14	LIGHT, LTA, BTLA	TRAF2, TRAF3, TRAF5
Nerve growth factor receptor	TNFRSF16	NGF, NT-3, BDNF, NT-4	TRAF2, TRAF4, TRAF6
BCMA	TNFRSF17	BAFF, APRIL	TRAF1, TRAF2, TRAF3, TRAF5, TRAF6
GITR	TNFRSF18	TL6	TRAF1, TRAF2,

			TRAF3, SIVA
TAJ	TNFRSF19	LTA	TRAF1, TRAF2, TRAF3, TRAF5
RELT	TNFRSF19L	/	TRAF1
Death receptor 6	TNFRSF21	/	TRADD
/	TNFRSF22	/	/
/	TNFRSF23	/	/
Ectodysplasin A2 isoform receptor	TNFRSF27	ectodysplasin A2	TRAF1, TRAF3, TRAF6
Ectodysplasin 1, anhidrotic receptor	/	ectodysplasin A1	TRAF1, TRAF2, TRAF3

Table 1.1. List of TNF superfamily receptors.

1.5.1 TNFR structure

As their respective ligands, TNFRs undergo a trimerisation process following the binding of their ligands. Although different in their primary structure, the extracellular domains of all TNFR family members consist of cysteine-rich subdomains, which are thought to adopt a generally similar tertiary structure. The unique structural features of individual family members allow the TNFR family members to recognise their ligands with specificity and, in most cases, exclusivity [165].

TNFR-like receptors are type 1 transmembrane proteins that adopt elongated structures by a scaffold of disulfide bridges. The disulfide bonds arrange the typical cystein rich domains, responsive of ligand interaction. These 40 amino acids pseudorepeats are typically defined by 3 intra-chain disulfides generated by 6 well conserved cysteines [166]. The elongated receptor chains fit in the “grooves” within the ligand trimers (Figure 1.12) [163].

The cytoplasmic domains are rather small (46-221 residues) and generally lack sequence homology among themselves, suggesting major differences in signalling mechanisms. None of these domains possesses sequences implying catalytic activity [166].

The ligands are type 2 proteins that can exist as membrane-embedded or cleaved, soluble forms. Both forms are active as self-assembling noncovalent trimers, whose individual chains fold as compact "jellyroll" β-sandwiches and interact at hydrophobic interfaces (Figure 1.12) [167]. Certain ligands and receptors can bind more than one partner with specific high affinity, thereby enhancing regulatory flexibility and complexity [168]. After ligand binding, the receptor cytoplasmic tails form a 3:3 internal complex with signalling proteins such as TRAF2 or FADD.

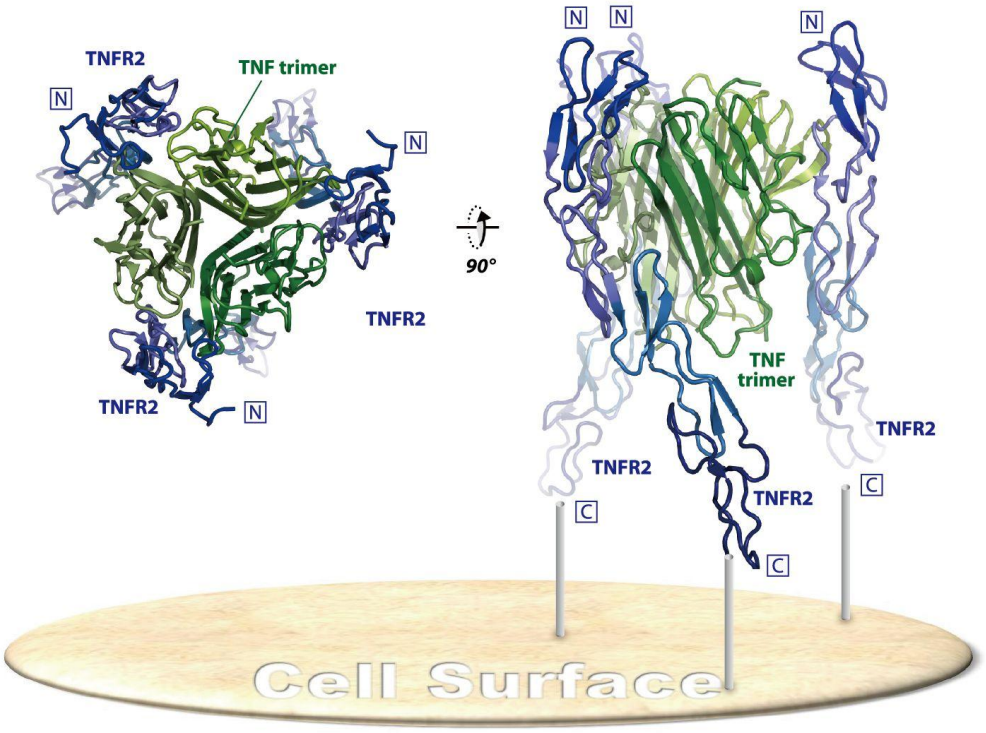

Figure 1.12 TNFR and ligand interactions. A trimerized TNF ligand interacts with a trimerized TNF receptor on the cell surface, triggering a signalling cascade inside the cell. Figure from reference [169].

1.5.2 TNFR signalling

Signalling of TNF receptors occurs through two principal classes of cytoplasmic adaptor proteins: TRAFs (TNF-receptor-associated factors) and death domain (DD) molecules. In mammals, at least 6 TRAF molecules and 37 non-receptor DD molecules have been identified and their genomic localisation is spread throughout the genome. The specific signalling adaptor is selected by whether the cytoplasmic tail of the receptor contains a DD or a TRAF binding domain. Signalling is extremely rapid and highly specific (Figure 1.13).

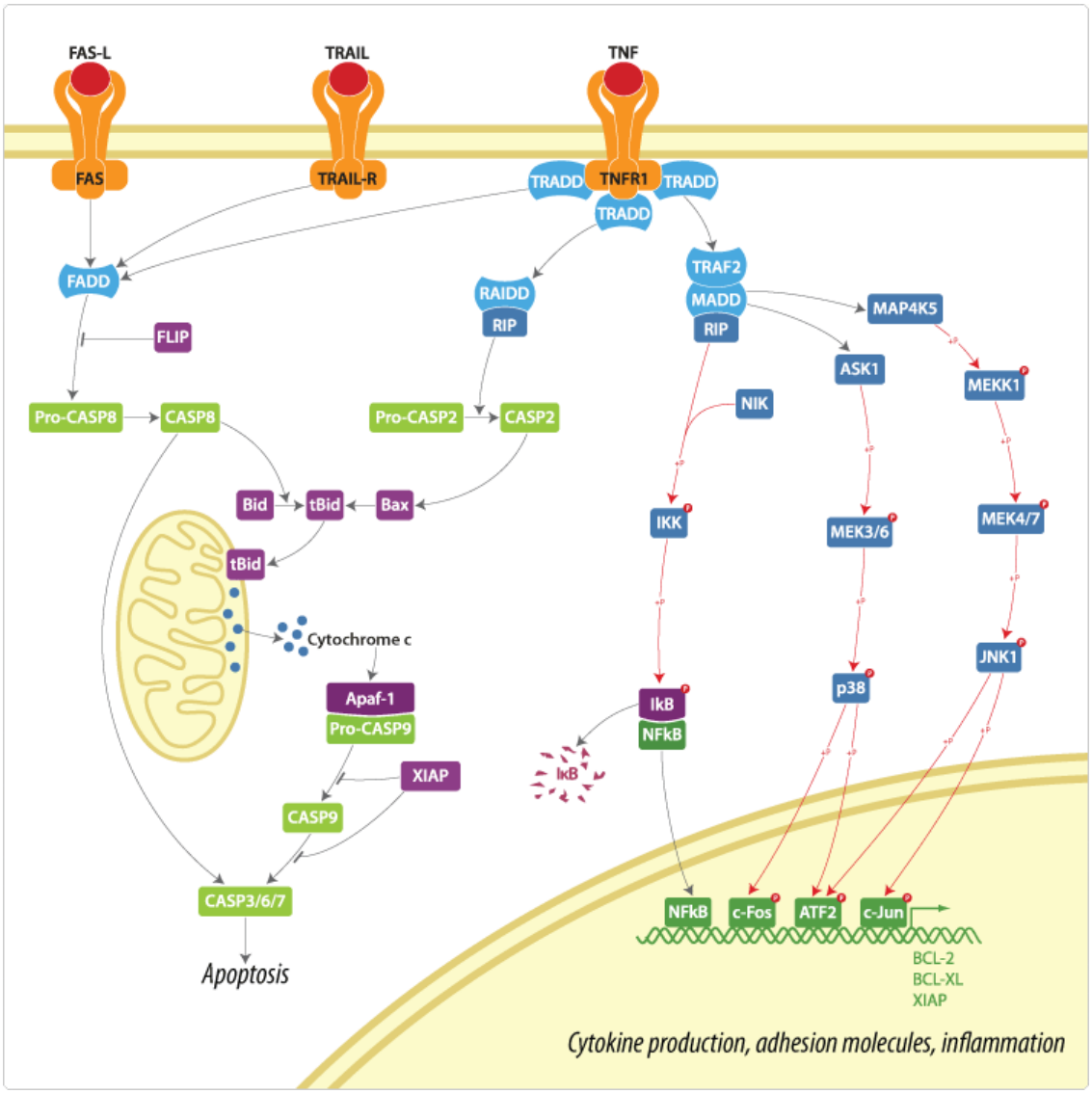

Figure 1.13 TNFR signalling pathways. Activation of TNFR leads to the recruitment of different cytoplasmic molecules: FADD molecules, which activate the apoptotic pathway, and TRAF2 that instead activate NF-κB and MAPK pathways. The specific combination of signalling molecules determines the different effects on the cell response. Figure adapted from Invitrogen website.

In the case of receptors containing DD domains, ligand engagement typically causes the association of adaptors such as Fas associated DD proteins (FADD) and TNFR-associated DD proteins (TRADD) that ultimately lead to caspase activation and cell death [163]. For example, binding of TNF-α to TNFR1 induces receptor trimerization and recruitment of TRADD, which serves as a platform to recruit at least three additional mediators: receptor-interacting protein 1 (RIP1), FADD and TRAF2 [170]. TRAF2 plays a central role in early events that lead to IKK and MAPK activation. On the other hand, activation of TNFR2 induces directly the binding of TRAF2 and the subsequent signal cascade [171]. In the specific, TNFR1 activation induces the formation of two different complexes, either at the cell surface (complex I) or following internalisation (complex II). The formation of complex I requires TRAF2 and RIP, leading to kinase cascade and pro-inflammatory gene expression. Alternatively, complex II is formed to induce apoptosis, triggered by proteolysis and internalisation of the receptor, with recruitment of FADD and pro-caspase 8 [172-173].

Another characteristic feature of the members of the TNFR family is the activation of NF-κB, mediated by TRAFs. How TRAFs mediate NF-κB activation is not completely clear but it has been shown that TRAF2 interact with the NF-κB inducing kinase (NIK) that in turn can activate NF-κB [174]. Genes that are regulated by NF-κB can suppress apoptosis. Thus cytokines like TNF activate both apoptosis and anti-apoptosis pathways, accordingly to the signalling molecules involved.

<u>TRAFs recruitment</u>

TRAFs are adaptor proteins that share a common structural domain at the C-terminus. This conserved region allows TRAFs to interact with cell surface receptors or other signalling molecules. They are able to serve as adaptor proteins for a wide variety of receptors involved in regulation of cell death, survival and cell response to stress [175].

To date, six different TRAF molecules have been identified in mammalian species.

TRAF1 has been shown to interact indirectly with TNFR2 [171] and directly with several other TNFR family members. TRAF1 has been shown to suppress [176] or stimulate NF-κB [177]; an explanation of these apparently divergent roles may be in part provided by the fact that TRAF1 is a substrate for caspases activated by TNF family death receptors [178]. The C-terminal domain is able to bind TRAF2, sequestering it from the TNFR1 complex, suppressing NF-κB induction [179]. The N-terminal fragment or the uncleaved TRAF1 instead have no effect on TNFR1 or TRAF2-mediated NF-κB activation. TRAF1 is upregulated by ligands of the TNF family and its promoter contains several functionally important NF-κB binding sites [177].

TRAF2 has been the most extensively studied TRAF, both in term of structure and function. Mutational analysis of TRAF2 has shown that distinct domains are involved in interaction with other proteins and signalling functions [180]. It is possible to identify two distinct subdomains (TRAF-N and TRAF-C) that appear to independently mediate self-association and interaction with TRAF1 to form heterodimers (Figure 1.14). Interaction with TNFR2 and TRADD requires both the TRAF-C and the TRAF-N domains, whereas interaction with RIP1 occurs via sequences at the N-terminus of the TRAF-C domain. The N-terminal RING finger and two adjacent zinc fingers are required for NF-κB activation (Figure 1.14). TRAF2 is able to mediate NF-κB activation through interaction with NIK, which contains a TRAF binding domain [181]. TRAF2 is also able to regulate AP-1, a transcriptional activator usually formed from a homo- or heterodimer of Jun, Fos and activating transcription factor (ATF) family member [182]. TRAF2 can bind the kinase MEKK1 [183], which, following a phosphorylation cascade, can activate the JNK and p38 kinases [184], responsible for AP-1 activation.

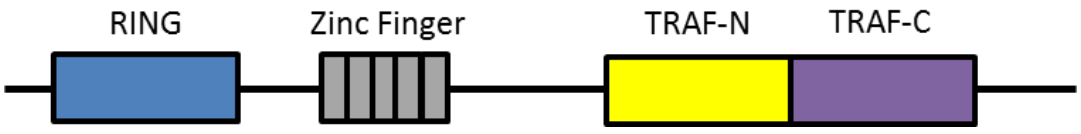

Figure 1.14 Schematic representation of TRAF2. TRAF2 is composed of four domains interacting with different proteins and signalling pathways. TRAF-N and TRAF-C are responsible for the association to the receptor and interaction with TRAF1. The N-terminal RING finger and the adjacent zinc fingers are required for NF-κB activation.

TRAF3 was first described as a molecule that binds CD40, in an interaction that is ligand dependent [185]. Its physical association with CD40 mediates its negative regulatory function, inhibiting CD40 signalling and NF-κB activation [186].

TRAF4 localises predominantly to the nucleus and has not been shown to regulate signalling through cell surface receptors [187].

TRAF5 is implicated in NF-κB activation through interaction with lymphotoxin β receptor (LTbR) and CD40 [188].

TRAF6 was initially identified as a signal transducer for IL-1 and it can activate JNK and p38 when overexpressed [181]; moreover, its oligomerisation with TRAF2 has been shown to be important for JNK activation [183]. TRAF6 can also interact with CD40, using a different site than TRAF1, 2 and 3, near the membrane proximal region [189].

MAPK activation

As mentioned before, TRAF2 and TRAF6 are able to activate MAPKs, in particular JNK and p38 [181]. It has been demonstrated that JNK and p38 activation by TNF is dependent on TRAF2, because their activation is blocked in $TRAF2^{-/-}$ cells [190]. Also MEKK1 is involved in TNF signalling [191] and it is also implicated in AP-1 and NF-κB activation [192]; the N-terminal domain of TRAF2 can also activate MEKK1 in an oligomerisation-dependent manner [183]. Another kinase implicated in TNF signalling is ASK1 [184], that interacts with the C-terminal oligomerization domain of TRAF2 [183]. The biological function of TNF-induced MAPK activation is under investigation, but it has been reported that JNK and p38 induce AP-1 activity, which contribute to the induction of TNF target genes [182].

NF-κB activation

As mentioned previously TRAF2 and TRAF5 are able to activate NF-κB pathways via the recruitment of the IKK complex. Such activation is dependent on the phosphorylation of two serines within the activation loop of IKKβ [193]. Several MAPK were proposed to provide a connection between TRAF2 and TRAF5 and the IKK complex, possibly through the phosphorylation of the IKKβ activation loop. One of these kinases is NIK, identified as a protein binding TRAF2 and capable of activating

NF-κB upon overexpression [174]. However, subsequent analysis of $NIK^{-/-}$ mice indicated that this kinase is not essential for induction of NF-κB DNA binding or transcriptional activity by TNF-α [194].
Another proposed mechanism of IKK activation is the recruitment of IKK to the TNFR1 complex through binding of the intermediate domain of RIP1 to IKKγ/NEMO [195].

Caspase activation

TNF-α is able to induce apoptosis through different pathways, among which the TRADD, FADD and caspase 8 pathway is the best characterised [196]. Upon activation by an apoptotic stimulus, the N-terminal prodomain of caspase 8 is cleaved, leading to an active heterodimeric enzyme, which in turn leads to activation of the downstream caspase 3, which in turn cleaves multiple cellular proteins, resulting in cell death [197].
The NF-κB pathway can be related to the apoptotic pathway through the activation of cellular inhibitors of apoptosis (cIAPs), which act as specific caspase inhibitors [198].

1.5.3 TNFR and Diabetes

Members of the TNFR superfamily have a unique and pivotal role in regulating cell fate and determine whether pro-apoptotic or anti-apoptotic signalling pathways will be activated, as well as having a role in cell proliferation and inflammation regulation.
Increasing evidence implicates dysregulation of TNF-α expression and signalling in the pathology of many diseases, including Crohn's disease, rheumatoid arthritis and neuropathologies such as stroke, multiple sclerosis and Alzheimer's disease [199].
The involvement of some members of the TNFR family in diabetes has been shown extensively in some studies on T1D. Walter et al reported increased expression of Fas and TNFR1 during the development of pancreatic inflammation (insulitis) in non obese diabetic (NOD) mice, a model for T1D [200]. In addition, NOD mice that are deficient for TNFR1 developed insulitis similarly to control NOD mice, but progression to diabetes was completely abrogated [201].
The TNFR pathway is also implicated in the pathogenesis of several processes involved in the development of insulin resistance. The principal role in obesity-related insulin

resistance is played by TNF-α, which is overexpressed in adipose tissue in many rodent models of obesity and it affects insulin sensitivity [149, 202]. Hossain and colleagues demonstrated an association of TNF-α with impaired insulin secretion and insulin resistance in a Bangladeshi population, and they suggested that it may have a causal relation with the insulin secretory defects in pre-diabetic patients [203]. It has also been demonstrated that TNF-α is able to induce insulin resistance in rat cells [150] and to reduce glucose-induced insulin secretion in INS-1 cells [204]. Solomon and coworkers showed also that treatment with anti-TNF-α agents improves fasting blood glucose values in the patients with T2D [205].

Also TNFR2 is implicated in insulin resistance and in the pathogenesis and susceptibility of T2D [206]. Mutational variants in TNF and TNFR2 genes identified in different studies are indicative of a genetic basis in the pathogenesis of the metabolic syndrome [207]. Moreover, soluble levels of TNFR2 have shown to be increased in patients with T2D [208].

The TNF signalling pathway is therefore a valuable target in the therapy of autoinflammatory and autoimmune diseases, and TNF blockers have the ability to interfere with inflammatory processes at multiple levels. However, this therapy has also some drawbacks, including risk of infection and malignancy and the onset of new auto-immune diseases. Some of these effects are caused by the fact that TNFR signalling can also have beneficial effects, related to the maintenance of the homeostasis of the immune system. For instance, the incidence of T1D is increased in anti-TNF treated patients with rheumatoid arthritis, due to dysregulation of T cell homeostasis [209-210], indicating that complete TNF inhibition is problematic. In such patients, TNFR1 signalling should be blocked, but TNF-TNFR2 immunomodulating signalling should be preserved [211].

A better understanding of the signalling mechanisms used by TNFRs could result in the development of small molecules that can successfully modulate the biological activity of these cytokines and provide new avenues for therapeutic intervention.

1.5.4 CD40

CD40 is a membrane glycoprotein and member of TNFR superfamily; as such it is sometimes referred to as TNFR5. It has the structure of a Type 1 transmembrane protein and it is a phosphorylated glycoprotein that migrates in SDS gel electrophoresis as a 48 kDa polypeptide.

The extracellular segment of CD40 is homologous to other members of TNFR family, in particular the 22 cysteine residues [165].

Its natural ligand, CD40L (or CD154) is a Type 2 transmembrane protein and a member of the TNF-α protein family.

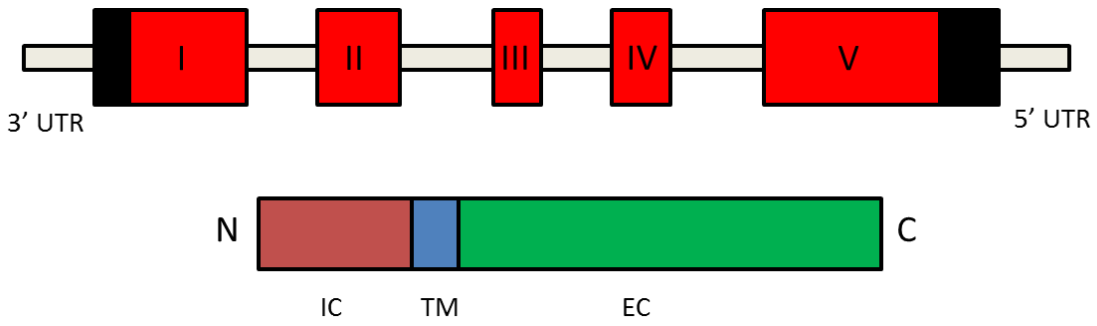

Figure 1.15 Schematic representation of CD40 gene and protein.

CD40 is expressed in many different immune and non-immune cell types. In B-lymphocytes, macrophages and APC cells, binding of CD40 by CD40L plays a central role in the immune system, inducing differentiation, cell survival, and proliferation [212]. CD40 expression is also reported in non-hematopoietic cells, and its activation is mostly associated with inflammatory responses. These events engage costimulatory molecules, inducing cytokines/chemokines synthesis and secretion, which results in recruitment and activation of immune cells [213].

As for the other members of TNFR superfamily, CD40 signalling is mediated mainly by TRAFs, linking CD40 to downstream signalling pathways. The cytoplasmic domain of CD40 contains two independent membrane TRAF-binding domains: a proximal region

that binds TRAF6 and a distinct distal domain that binds TRAF-1/2/3/5. Different TRAFs binding to CD40 triggers distinct signalling pathways leading to a variety of functional outcomes, depending on the cell types involved. For example, they can activate the canonical and non canonical NF-κB signalling pathways, the MAPK, PI3K and phospholipase Cc (PLCc) pathways [214]. Moreover, signalling may also occur independently from TRAF proteins, as Janus family kinase 3 (Jak3) has been found to bind directly to the cytoplasmic domain of CD40, inducing phosphorylation of STAT5 [215].

TRAF1 plays an important role in regulating the signalling of the other TRAF proteins, as it lacks the zinc finger domain and therefore it's unable to activate the downstream signalling pathways. Its binding site motif in the CD40 cytoplasmic tail overlaps with the binding site for TRAF2 and TRAF3, and it appears that TRAF1 can bind weakly in the absence of TRAF2 [189], demonstrating the importance of TRAF oligomerisation process. It has been shown that the recruitment of both TRAF1 and TRAF2 to CD40 is required for the activation of NF-κB pathways [216].

The engagement of TRAF2 leads to the activation of JNK, p38 and Akt pathways (number 2 in Figure 1.16). This was shown using TRAF2-deficient mouse embryonic fibroblasts and B cells, which exhibited attenuated activation of these pathways after CD40 engagement [190, 217]. The intermediate kinase responsible for TRAF2 pathways activation is MEKK1 (number 1 in Figure 1.16), which drives the phosphorylation of JNK and p38 and activates the respective pathways [218]. On the other hand, activation of NF-κB is mediated by NIK (number 3 in Figure 1.16): without CD40 stimulation, a complex is formed between family members of the cellular inhibitor of apoptosis (cIAP) 1 and 2, which interact with TRAF2, which in turn interacts with TRAF3 and NIK, inducing NIK degradation [219]. In contrast, after CD40/CD40L engagement, the complex is destabilised, leading to TRAF2 and TRAF3 binding to the cytoplasmic tail of CD40, with accumulation of NIK and activation of NF-κB (number 4 in Figure 1.16).

The function of TRAF3 signalling is controversial, as it seems to have opposite roles in different cell types. In B cells, a TRAF3-dominant negative protein can lead to the induction of NF-κB and JNK signalling upon CD40 engagement [220], suggesting a negative regulation; in contrast, in epithelial cells the overexpression of TRAF3 can

induce the activation of NF-κB pathways during CD40 stimulation [221]. These contrasting roles can be determined by different conformations assumed by the receptor and TRAF3, which lead to different downstream signalling [222] or by mechanisms involving receptor-mediated TRAF3 degradation [223].

TRAF5 forms heterodimers with TRAF3 and its siRNA mediated downregulation in B cells leads to an ablation of NF-κB pathways, with reduction of antibody production, proliferation and costimulatory molecules expression [224].

Finally, in mouse embryonic fibroblast of TRAF6$^{-/-}$ mice or epithelial cells where TRAF6 has been silenced by siRNA, there is a reduction in the activation of NF-κB, Jnk, p38 and Akt upon CD40 engagement, suggesting the importance of TRAF6 in the activation of these pathways. It can also interact with TRAF2, positively regulating CD40 signalling [225].

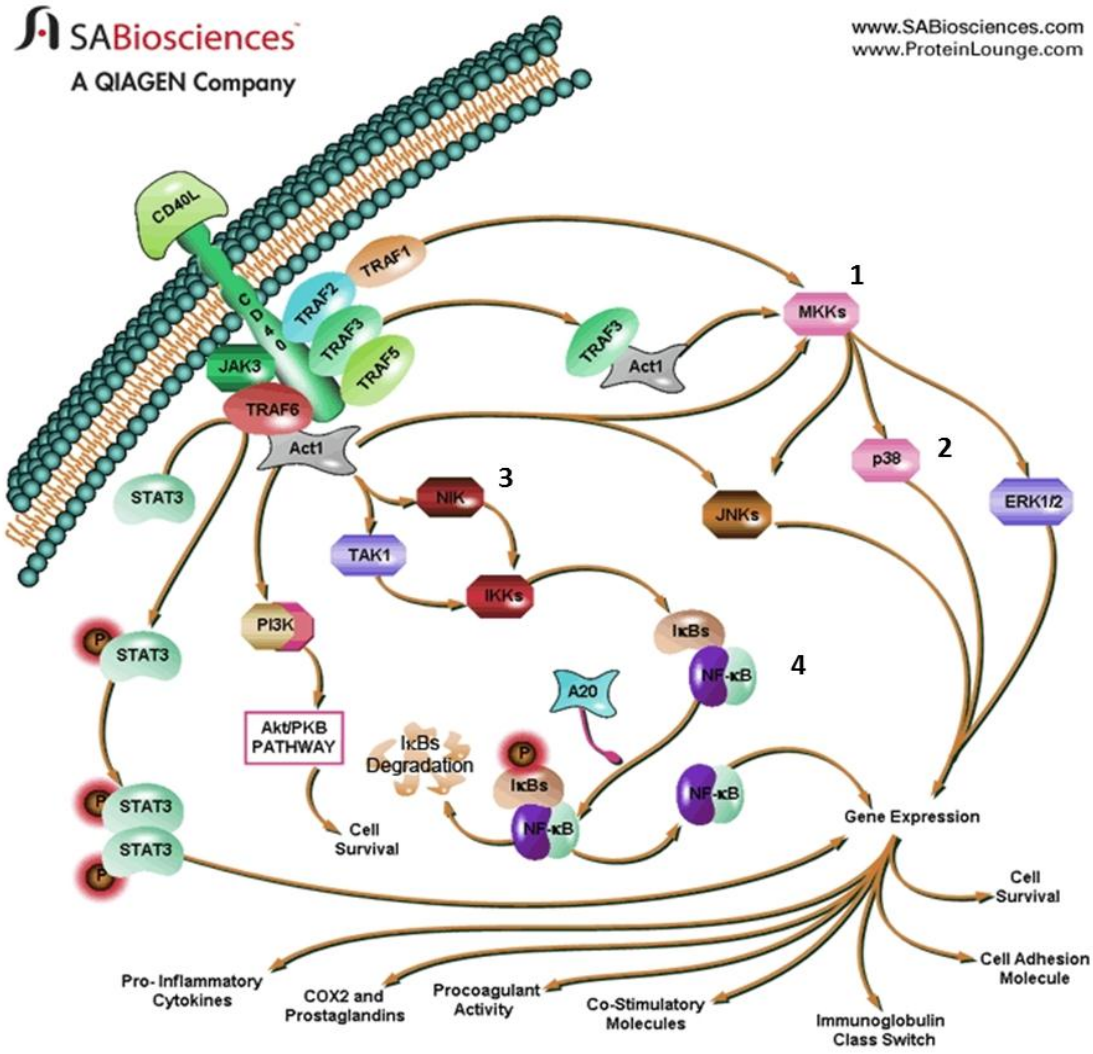

Figure 1.16 CD40 signalling pathway. CD40L binding to CD40 leads to TRAFs recruitment in the cytoplasmic tail of the receptor, with subsequent activation of NF-κB and MAPK pathways. The result is the induction of gene transcription in order to activate the inflammatory response. Figure adapted from SABioscience website.

To summarise, the two major effects of CD40 activation appear to be the activation of NF-κB pathways and of protein kinases. Since many CD40 inducible genes, including AZO, IL-6, ICAM, have NF-κB consensus sites in their 5' regulatory regions, it is likely that CD40-dependent NF-κB activation is responsible for the induction of these genes [226].

1.5.4.1 Biological effects of CD40 activation

CD40 activation drives the humoral immune response, in particular, the production of high titers of isotype-switched, high affinity antibodies and development of humoral immune memory. The engagement of CD40 expressed on the surface of antigen activated-B cells by CD40L expressed on activated CD4+ T cells triggers adhesion, sustains proliferation, expansion, differentiation and antibody isotype switching in vitro [226-227]. In vivo, CD40 engagement is required for germinal centre formation and progression, antibody isotype class switching and affinity maturation, in order to generate memory B cells and long-lived plasma cells [228].

The most compelling evidence for a critical role of CD40 activation in B-cell function is the observation that a fatal immunodeficiency in children (hyper-IgM syndrome), which is characterised by lack of circulating IgG and IgA and by the absence of germinal centres, can be attributed to a genetic defect in CD40L [229]. Consistent with this, mice deficient in either CD40 or CD40L display a phenotype similar to hyper-IgM syndrome patients [230]. In view of the critical role of CD40-CD40L interactions in humoral immune response, strategies have been developed to either decrease or increase these responses. Blocking anti-CD40L antibodies have been used in animal models to inhibit unwanted antibody production, for example in systemic lupus erythematosus (SLE) nephritis, and experimental autoimmune encephalomyelitis (EAE) [231-232]. On the other hand, administration of agonistic anti-CD40 antibodies can result in stronger isotype switched antibody responses [233].

It has also been shown that CD40 has a role in T cell priming [234], and have been suggested to inhibit tolerance induction. Therefore, interference with CD40 activation has been extensively investigated to prolong the survival of experimentally transplanted organs, including heart, skin, aorta and pancreatic islets [235].

In addition, CD40 and CD40L have a role in inflammation. CD40 engagement on macrophages induces the production of pro-inflammatory cytokines, including TNF-α, IL-6 and IL-1β [236]. Treatment with anti-CD40L antibodies has been shown to reduce the development of atherosclerosis [237] and to prevent pulmonary inflammation and fibrosis caused by oxygen-induced respiratory distress syndrome [238]. Moreover,

CD40 can promote IL-10 production from macrophages during Leishmania infections [239]. Platelets might also contribute to immunity and inflammation and CD40L-positive T cells have been shown to enhance platelet activation [240]. Interestingly, CD40 is also present on fibroblasts and during fibrotic conditions (such as inflammation-induced lung fibrosis), fibroblasts are bound to T lymphocytes through surface CD40L [241].

1.5.4.2 CD40 in β-cells

A functional CD40 is also expressed on the surface of mouse β-cells (mouse islets and NIT-1 insulinoma cells) and its expression is upregulated by a cocktail of pro-inflammatory cytokines (IL-1β, IFN-γ, TNF-α). The receptor is active, as it is able to activate NF-κB [242]. CD40 is expressed also in pancreatic duct cells, but not in α-cells [243].

It has been demonstrated that CD40L binding triggers the secretion of pro-inflammatory cytokines/chemokines (IL-6, IL-8, MCP-1, MIP-1β) through Raf/MEK/ERK and NF-κB pathways [244]. Moreover, it has been reported that CD40 signalling activates pathways of MAPK involved in inflammatory responses.

Additionally, activated CD40 enhances expression of intercellular adhesion molecule (ICAM)-1 (CD54) on the surface of β-cells: this molecule is known for its critical role in the patho-physiology of inflammation [244].

1.5.4.3 CD40 and diabetes

Previous studies have suggested an emerging role for CD40-CD40L interactions in T1D, as established diabetogenic T cell clones are CD40 positive, whereas nondiabetogenic clones are CD40 negative. High levels of CD40 T cells were found in thymus, spleen and pancreas of NOD mice [245].

In addition, interference with the CD40 pathway using blocking antibodies against CD40L inhibits the spontaneous development of T1D in NOD mice [246-247] and,

together with NF-κB blocking, prolongs allogeneic islet graft survival in rats [248] and in non human primates [249].

Increased cellular CD40 and CD40L have been observed in patients with both T1D and T2D [250-251] and CD40L soluble levels may be related to the severity of the disease [251].

No direct correlation to insulin metabolism has been elucidated so far, but Poggi et al demonstrated that obese $CD40L^{-/-}$ mice have preserved insulin sensitivity and low plasma insulin levels compared to obese $CD40L^{+/+}$ mice [247]. In addition, specific blockage of CD40-TRAF6 interactions improved insulin sensitivity, reduced adipose tissue inflammation and decreased hepatosteatosis in diet-induced obesity [252].

It has also been shown that diabetes-mediated hyperglycemia can result in monocyte recruitment associated with upregulation of CD40L in the vascular wall [253]. These processes might be integral with the development of atherosclerosis in patients with diabetes.

Specific inhibition of CD40L-CD40 signalling may become a promising strategy to improve inflammation in diabetes mellitus, thereby reducing the occurrence of vascular complications.

1.6 Transcriptome profiling

The transcriptome is the entire repertoire of transcripts of a cell and represents the key link between the information encoded in the DNA and the phenotype. To achieve mRNA regulation, a concerted action of multiple cis-acting proteins that bind to gene flanking regions is necessary [254]. In particular, core elements, located at exons' boundaries, are strictly required to initiate the pre-mRNA processing events, whereas auxiliary elements, variable in number and location, are crucial for their ability to enhance or inhibit the basal splicing activity of a gene. Until 10 years ago, the transcriptome was considered to mainly consist of ribosomal RNA (rRNA, 80-90%), transfer RNA (tRNA, 5-15%), mRNA (2-4%) and a small fraction of intragenic and intergenic noncoding RNA (ncRNA, 1%) with undefined regulatory functions [255]. More recently, it has been shown that the amount of noncoding DNA increases with organism complexity, ranging from 0.25% in procaryotic genome to 98.8% in human genome [256]. Additional complexity is added by the fact that most of the transcripts identified so far have been found only in specific cell types, in particular growth conditions and in particular tissues. Based on this, discovering and interpreting the complexity of the transcriptome represent a crucial aim to understand the functional elements of a genome. The analysis of the complexity of the genetic code of living organisms will drive towards a more complete knowledge of many biological issues such as the onset of disease and progression.

The main goal of transcriptome analyses is to identify, characterise and catalogue all the transcripts expressed within a specific cell/tissue, at a particular stage. This can also potentially determine the correct splicing patterns and the structures of the genes, and quantify the differential expression of transcripts in both physiological and pathological conditions [257].

With the completion of the human genome project, monitoring changes in the whole cellular transcriptome is an increasingly attractive method to dissect the molecular basis of a disease.

Tools for profiling RNA have been available for years, such as Northern Blots, reverse transcription PCR (RT-PCR), expressed sequence tags (ESTs), and serial analysis of gene expression (SAGE). However, the rapid and high-throughput quantification of the transcriptome became a possibility only with the development of gene expression microarrays (see paragraph 1.6.1). The development of these high-throughput techniques has allowed transcriptome profiling of model of diseases both *in vitro* and *in vivo* in an unbiased and highly sensitive manner, without previous knowledge of the genes involved in a particular disease. With the more recent advent of techniques for direct sequencing of the transcriptional output of the genome, it is now possible to perform a complete transcriptional characterisation of all organisms.

1.6.1 Microarrays

Expression microarrays are high throughtput techniques that allow the measurement of the expression of multiple genes simultaneously. The starting point for a microarray is a set of short oligonucleotide probes representing the genomic DNA. A typical modern microarray consists of patches of such probes complementary to the transcripts whose presence is to be investigated, and immobilised on a solid substrate. Probe design is based on genome sequence or on known or predicted open reading frames and usually multiple probes are designed per gene model. Transcripts are extracted from cells or tissues, labelled with fluorescent dyes, hybridised to the arrays, washed and scanned with a laser. Probes that correspond to transcribed RNA hybridise to their complementary target. Because transcripts are labelled with fluorescent dyes, light intensity can be used as a measure to quantify gene expression (Figure 1.17) [258].

Initially, microarrays designed by different companies appeared to produce different results with the same samples [259]. Moreover the fluorescent readout of hybridisation intensities varied between different laser scanners and there was lack of reproducibility between different laboratories. The recognition of these limitations and bias by individual laboratories and organisations, such as the Microarray Quality Control (MAQC) consortium, has led to the development of quality control standards that operate to ensure the running of a well performed microarray experiment [260].

Specialised microarrays have also been designed, for examples arrays with probes spanning exon junctions can be used to detect and quantify distinct spliced isoforms [261]. In addition, genomic tiling microarrays (a microarray that uses a set of overlapping oligonucleotide probes for a subset of the whole genome), that represent the genome at high density and resolution, allow the mapping of transcribed regions to a very high resolution [262].

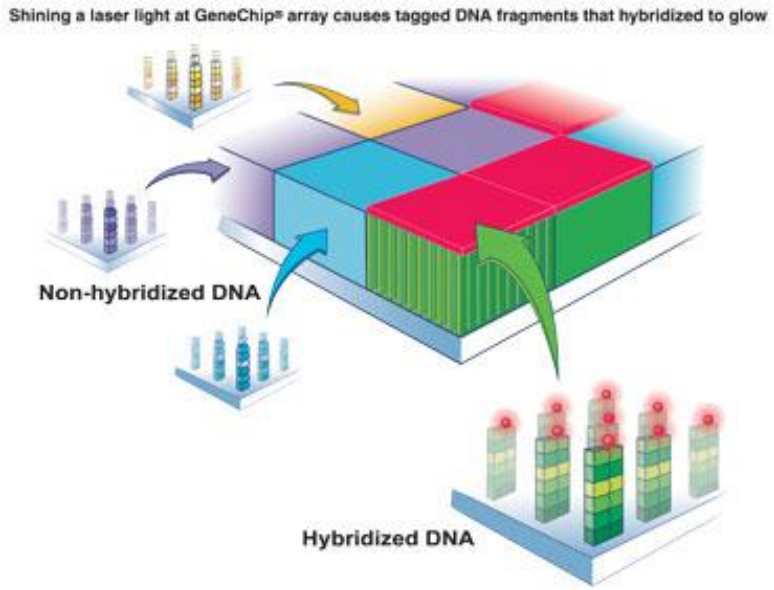

Figure 1.17 Microarrays technique. Short oligonucleotides probes are immobilised on a solid surface. Transcripts are extracted from cells or tissues, labelled with fluorescent dyes, hybridised to the microarrays, washed, and scanned with a laser. Figure adapted from Affymetrix website.

Microarrays technique has been very successful and extensively used for the identification of differentially expressed genes in different conditions. For example, Wada et al used this technique to monitor gene expression in whole kidneys of streptozotocin (STZ)-induced diabetic mice and identified differential expression of 81 genes (16 upregulated and 65 downregulated), 44 of which were novel genes [263]. Some studies investigated the effect of β-cell exposure to high concentration of glucose [264-265], identifying clusters of genes differentially expressed at specific glucose concentrations.

However, hybridisation-based approaches have several limitations because they need to rely on existing knowledge of genome sequence, they have high background levels due to cross-hybridisation, and a limited dynamic range of detection due to both background and saturation of signals.

1.6.2 RNA sequencing

Nucleic acid analysis has been recently revolutionised by the development of tools for massive parallel sequencing of DNA molecules. These techniques have then been extended to the analysis of the transcriptome, with a procedure called RNA-seq. This method has clear advantages over existing approaches and it is expected to revolutionise the way in which eukaryiotic transcriptomes are analysed. Rather than using molecular hybridisation to capture transcript molecules of interest, RNA-seq analyses transcripts present in the starting material by direct sequencing. Sequences are then mapped back to a reference genome. Reads that map back to the reference are then counted to assess the level of gene expression, as the number of mapped reads being the measure of expression level for that gene or genomic region.

A schematic overflow of RNA-seq technique is presented in figure 1.18. A population of RNA (total or fractionated) is converted to a library of cDNA fragments with adaptors attached to one or both ends. For small RNAs such as miRNAs there is first a process of preferential isolation via a small RNA-enrichment method or size selection on an electrophoresis gel.

Each molecule, with or without amplification, is then sequenced in a high-throughput manner to obtain short sequences from one end (single-end sequencing) or both ends (pair-end sequencing). The reads are typically 30-400 bp, depending on the sequencing technology used. Illumina's Genome Analyser and HiSeq instruments as well as Applied Biosystems' SOLID instruments and Roche 454 Life Science are the most common platforms used for high-throughput sequencing.

After sequencing, the resulting reads are either aligned to a reference genome or assembled de novo without the genomic sequence to produce a genome-scale transcription map that consists of both the transcriptional structure and/or level of

expression for each gene [266]. Expression levels are obtained from the total amount of reads that map to the exons of a gene, normalised by the length of the exons. The presence and amount of each RNA can be calculated and subsequently compared with the amount in any other sequenced sample.

Results obtained with this approach have shown close correlation with those of quantitative PCR and RNA-spiking experiments, which are normally used to calibrate measurements in DNA microarrays.

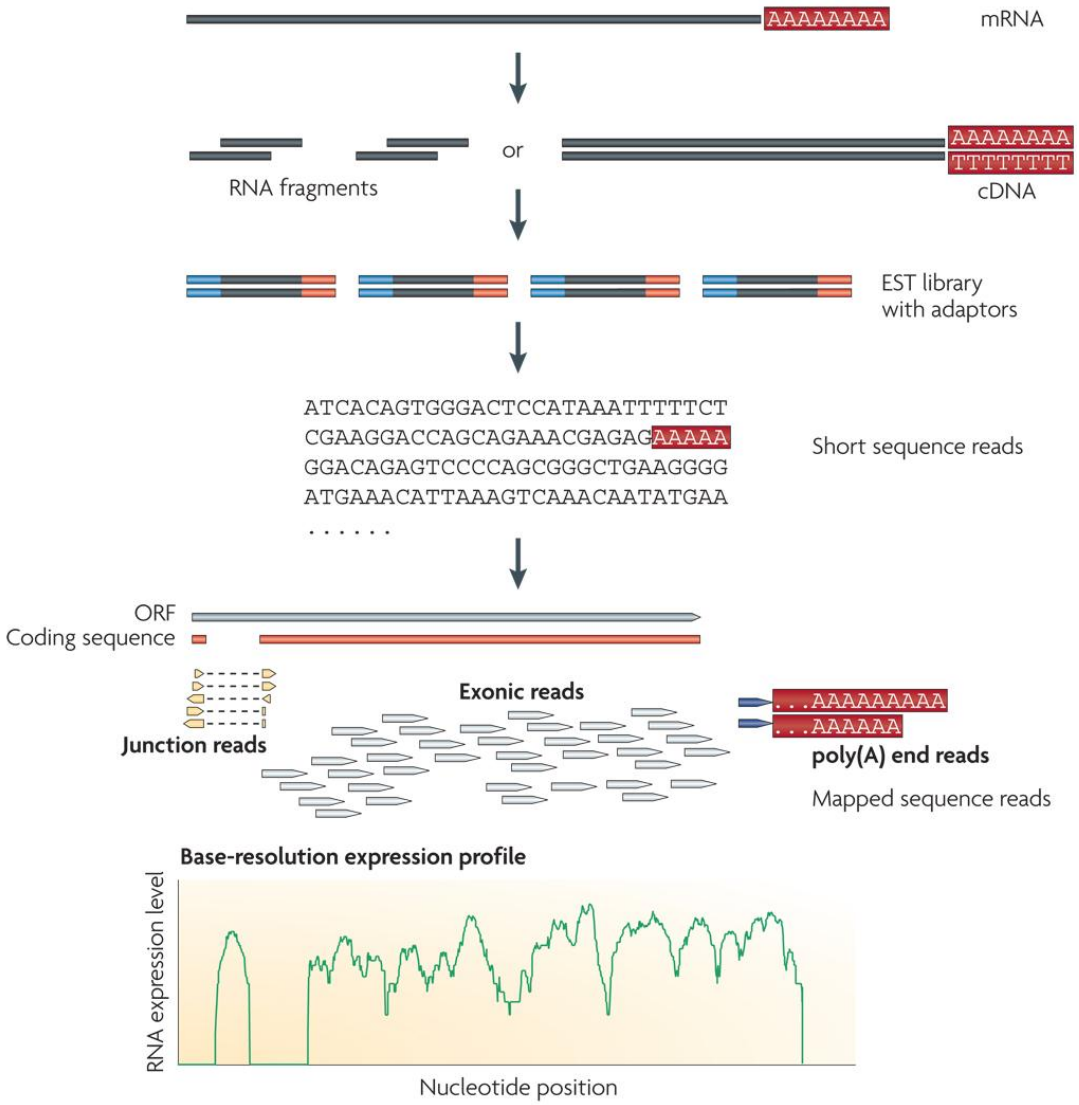

Figure 1.18 A typical RNAseq experiment. Long RNAs are first converted to a library of cDNA fragments and sequencing adaptors are added to each extremity. The fragments are then sequenced and the obtained reads are then mapped to a reference genome. Figure from reference [266].

There are some advantages in the use of RNA-seq compared to microarrays. Because RNA-seq provides direct access to the sequence with single base resolution, junctions between exons can be assayed without prior knowledge of the gene structure. 3' boundaries can be mapped precisely by searching for poly(A) tags, and introns can be mapped by searching for tags that span GT-AG splicing sites [267].

RNA editing events can also be detected, and knowledge of polymorphisms can provide direct measurement of allele-specific expression. Because RNA-seq provides direct access to the sequence, this technique can be used on species for which a full genome sequence is not available.

In addition to this, expressed regions of the genome that correspond to genes not currently identified (novel genes) might be easier to detect with sequencing than with microarrays, because detection depends only on where reads map in the genome and not on whether that region is annotated [268]. Gene annotation is the process of identifying the locations of genes and all the coding regions in a genome and determining what those genes do.

Another strength of RNA-seq is the quantification of individual transcript isoforms and splicing diversity, as sequencing can provide direct access to reads that span exon/exon boundaries and in principle it makes possible to study the expression of different isoforms for a gene and to make comparisons of isoforms diversity and abundance. In humans 31618 known splicing events were confirmed by RNA-seq and 379 novel splicing events were discovered [268-269].

Moreover, RNA-seq has very low, if any, background signal because DNA sequences can been uniquely mapped to single regions of the genome.

RNA-seq does not have an upper limit for quantification, indicating that it has a high dynamic range. By contrast, DNA microarrays lack sensitivity for genes expressed at very low or very high levels and they have a smaller dynamic range [266].

RNA-seq data also show high levels of reproducibility for both technical (repeated measurements of the same sample) and biological (parallel measurements of biologically distinct samples) replicates.

On the other hand, currently, the main advantage of arrays is their relative low cost compared to sequencing. Another advantage is knowledge of biases in array data with the possibility of developing analysis strategies and experimental design to deal with them. By comparison, sources of bias in sequencing data are still being actively researched and at the same time RNA-seq continues to evolve.

One of the most important concerns about sequencing RNA is the depth of sequencing to effectively analyse the transcriptome. This equates to how many times to sequence a sample. For highly expressed genes, small amounts of sequencing are sufficient, but for the middle and low end of expression levels, it is clear that many reads are needed. Failure to obtain sufficient coverage and check the representation of this coverage (that is the library complexity) will provide erroneous values of gene expression and lead to false inferences even for genes that are detected.

Another source of bias in sequencing is the heterogeneity of reads across an expressed region, which is the uneven sequencing depth along the length of a transcript. This heterogeneity in coverage will influence expression estimates for transcripts and needs to be corrected. Coverage and heterogeneity are not an issue in microarrays because of the fixed nature of probes that capture the transcripts by hybridisation.

A final consideration about arrays and sequencing is the quantity and size of the data. In expression arrays the raw data are composed of image files, typically TIFF files that may be around 30 MB per array. These TIFF files are then transformed into txt files that contain fluorescence intensities for each gene. The Illumina instrument instead generates sequence files that are an order of magnitude larger than those from arrays and because of the large file size, Python, Perl, Unix command line and other scriptings are necessary to sort and experiment with these files. Using spreadsheet softwares will not be an option and therefore bioinformatics support is necessary.

RNA sequencing has been used to characterise the β-cell transcriptome, with the identification of β-cell specific genes, splicing events and intergenic RNA that could play important role in the regulation of the cell function [270]. In addition, long noncoding RNAs were also identified by RNA sequencing in human pancreatic islets and some of these transcripts were found to be dysregulated in diabetes [271].

In a recent study, Cnopp et al investigated the effects of fatty acids exposure on the β-cell. They observed that palmitate changed the expression of 1325 genes in human islets, in particular related to ER stress, ubiquitin and proteasome function, autophagy and apoptosis. Palmitate also inhibited transcription factors involved in the regulation of the β-cell phenotype (PAX4 and GATA6) and also shifted alternative splicing of 3525 transcripts [272].

1.6.3 microRNAs

As described before, the mammalian transcriptome is very complex and it contains a wide percentage of noncoding regulatory transcripts. Non-coding RNA genes include highly abundant and functionally important RNAs such as tRNAs and rRNAs, as well as small nucleolar RNAs (snoRNAs), microRNAs, siRNAs, small nuclear RNAs (snRNAs), extracellular RNAs (exRNAs) and Piwi interacting RNAs (piRNAs).
In particular, miRNAs are endogenous ~22 nucleotides long RNAs that play important regulatory roles in animals and plants by targeting mRNAs for cleavage or translational repression. They normally bind to the 3'-UTR of their target mRNA through imperfect base pairing. miRNAs were firstly described in a nematode, Caenorhabditis elegans, in which it was discovered that two miRNAs, lin-4 and let-7 control the timing of the organism development [273-274].
Over 500 miRNAs have been found in the human genome [275] and it has been extimated that they could regulate 74-92% of all protein coding mRNAs. They can control both physiological and pathological processes such as development, metabolism, cancer and, relevant to this thesis, insulin resistance and diabetes [276].

1.6.3.1 miRNAs biogenesis

Although miRNAs were initially described in Caenorhabditis elegans more than a decade ago, their presence in the vertebrates was confirmed only in 2001 [277]. In mammals, primary miRNAs are transcribed by RNA polymerase II [278], generating transcripts that are usually several kilobases long and contain local stem-loop structures

(Figure 1.19). miRNAs are then edited by ADARs (adenosine deaminase acting on RNAs), an enzyme that modifies adenosine into inosine. Because base-pairing properties of inosine are similar to those of guanine, the editing process of miRNA precursors may change their sequence and target recognition abilities.

miRNAs are subsequently processed in order to cleave the transcript at the stem of the hairpin structure, which release a small hairpin, termed pre-miRNA (Figure 1.19). This reaction takes place in the nucleus by the nuclear RNase III-type protein Drosha [279]. Together with a co-factor, DGCR8 (DiGeorge syndrome critical region gene 8), Drosha forms a large complex called Microprocessor complex. The two RNase domains of Drosha cleave the 5' and 3' arms of the pri-miRNA hairpin, whereas DGCR8 stably interacts with the pri-miRNA and functions as a molecular ruler to determine the precise cleavage site [280].

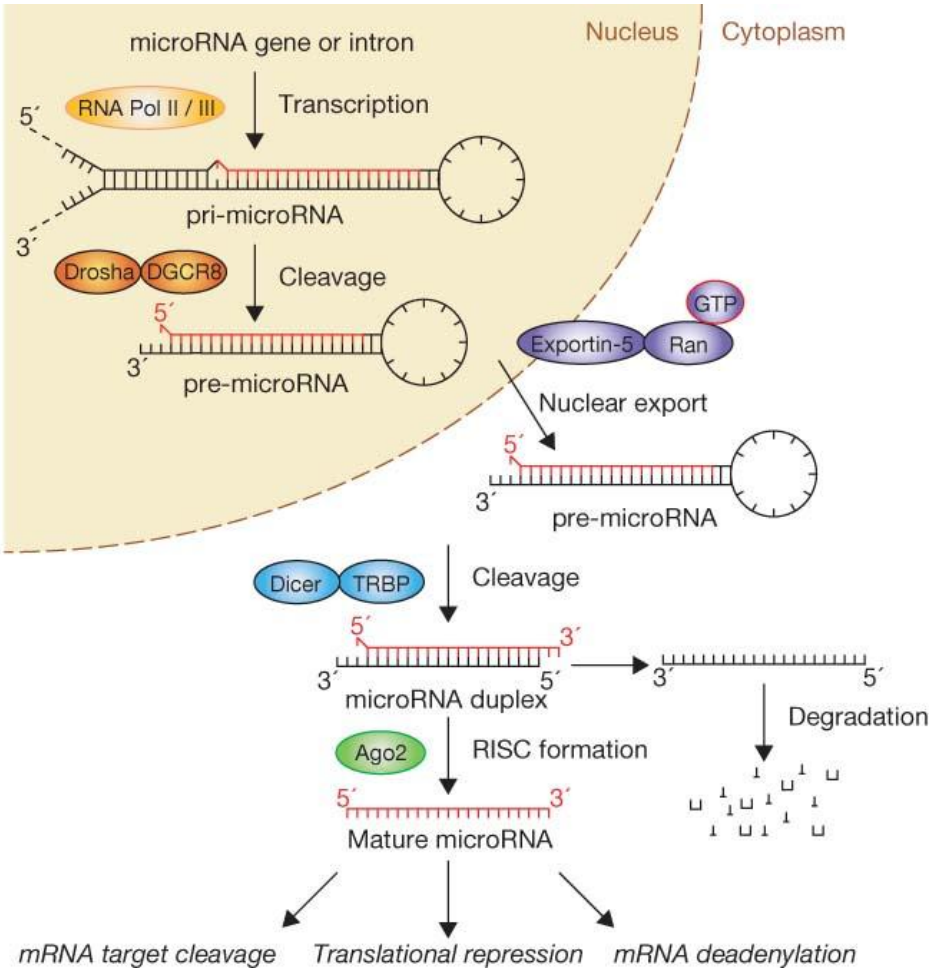

Figure 1.19 Biogenesis of miRNAs. miRNAs are 22 nt long transcripts generated by the cleavage of longer hairpin-structured RNAs performed in the nucleus by the enzyme Drosha. The pre-microRNA is then transported in the cytoplasm where it is processed by the protein Dicer to form the mature microRNA, which is recruited in the RNA-induced silencing complex (RISC) to perform translational repression or mRNA cleavage. Figure from reference [281].

However, Drosha mediated processing of pri-miRNAs is not the obligatory pathway. miRNAs derived from gene introns (mirtrons) are released from their host transcripts after splicing. If the intron resulting from the action of the splicing machinery has the appropriate size to form a hairpin resembling a pre-miRNA, it bypasses Drosha cleavage and is further processed in the cytoplasm by Dicer (Figure 1.20).

Figure 1.20 Formation of mirtrons. Splicing can replace Drosha processing if the miRNA derives from gene introns and it has the appropriate size. Figure from reference [281].

After nuclear processing, pre-miRNAs are exported to the cytoplasm. This process is mediated by exportin 5 (EXP5), a member of the nuclear transport receptor family [282]. EXP5 binds cooperatively to its target and to the GTP-bound form of the cofactor Ran in the nucleus, and subsequently releases the cargo in the cytoplasm with hydrolysis of GTP.

After export from the nucleus, pre-miRNAs are cleaved near the terminal loop by Dicer, releasing ~22 nt duplexes with two nucleotides protruding as overhangs at each 3' end [283]. Dicer is a highly conserved enzyme found in almost all eukaryotic organisms and it associates with some proteins: TRBP (TAR RNA-binding protein) and PACT (protein activator of PKR) that contribute to the formation of the RNA-induced silencing complex (RISC). TRBP and PACT are not essential for Dicer-mediated cleavage of the pre-miRNA but they facilitate it, and TRBP stabilises Dicer [284]. After Dicer cleavage, the resulting 22 nt is loaded into an Ago protein to complete the effector complex, RISC. One strand of the 22 nt RNA duplex remains in Ago as a mature miRNA (the guide strand or miRNA), whereas the other strand (the passenger strand or miRNA*) is degraded. Some evidence suggests that the miRNA duplex is released from Dicer after cleavage and the stable end of the duplex is bound to TRBP in the RISC, whereas the other end interacts with the Ago protein [285]. In principle, the miRNA duplex could give rise to two different mature miRNAs. However, only one strand is usually incorporated into RISC, while the other is degraded. This asymmetry depends on the termodinamic stability of the base pair at the end of the duplex: the miRNA strand with the less stable base pair at its 5' end is loaded into RISC. Ago proteins exert multiple

functions in the miRNA pathway, as they are the RISC effector proteins mediating mRNA degradation, destabilisation or translational inhibition [286-287].

1.6.3.2 miRNAs function

miRNAs can direct the RISC complex to downregulate gene expression by two post-transcriptional mechanisms: mRNA cleavage or translational repression. According to the prevailing model, the choice of the post-transcriptional mechanism is determined by the identity of the target: once incorporated in the cytoplasmic RISC complex, the miRNA will specifically cleave the mRNA if there is sufficient complementarity or it will repress translation if the mRNA does not have sufficient complementarity [288].

When a miRNA guides cleavage, the cut occurs between the nucleotides pairing to residues 10 and 11 of the miRNA [289]. Therefore, the cut site appears to be determined by the miRNA residues, not miRNA:target base pairs. After cleavage of the corresponding mRNA, the miRNA remains intact and can guide the recognition and destruction of additional targets.

When instead a miRNA induces transcriptional repression, the active single stranded miRNA enters the RISC complex, which interacts with the 3'UTR of target mRNAs. The miRNA-mRNA sequence mismatch impairs translation initiation, with mechanisms that frequently affect the initiation step, although regulation of later stages such as elongation, termination or release of the stable polypeptide has been reported. It was shown that mRNAs that are translationally repressed by miRNAs collect P bodies, within or adjacent to processing, and these are large cytoplasmic aggregates that serve as sites for mRNA degradation [290]. The detailed mechanisms by which miRNAs trigger sequestration of their mRNA targets in the P-bodies are not understood.

Humphreys et al demonstrated that miRNAs can block the initiation phase of the translation via inhibition of the initiation factor 4E/cap and poly(A) tail function [291]. Another study conducted by Pillai et al [292] reported similar findings, namely that miRNAs can block the initiation phase of translation, possibly by interfering with the cap recognition step.

In contrast to miRNAs, short interfering RNAs (siRNAs) are not encoded by the genome but derive from exogenous or endogenous long, double stranded RNAs. They achieve gene silencing by promoting cleavage of the perfectly matched mRNAs. This different mode of action explains why siRNAs repress single genes, while miRNAs are promiscuous and can target up to 200 transcripts.

Analysis of the miRNA target site indicates that genes with longer 3'UTRs usually have higher density of miRNA-binding sites and are mainly involved in development, whereas genes with shorter 3'UTRs usually have lower density of miRNA-binding sites and are involved in basic cellular processes [293]. This fact emphasizes the importance of the 3'UTR in the interaction with the miRNAs.

1.6.3.3 miRNAs and diabetes

In order to study the potential involvement of miRNAs in diabetes, a wide range of *in vitro* and *in vivo* strategies can be performed. A common and straight-forward approach is to expose cell lines or isolated primary cells to pathophysiological conditions, for example elevated concentration of glucose and/or FFAs, or cytokines. This method allows detailed analysis of the signalling pathways leading to changes in miRNAs expression, the study of the functional impact of individual miRNAs and the elucidation of the molecular mechanisms of their action. Another approach is to correlate the alterations in miRNA expression with the development of diabetes in animal models [294].

Some miRNAs have been shown to be involved in the pancreatic β-cell failure in T2D. A role for miRNAs in T2D was first estabilished by Poy et al, who showed that Mir-375 is directly involved in the regulation of insulin secretion (see below) [295]. This study was one of the first to demonstrate that a miRNA could be tightly linked to a disease phenotype. Recently, many additional miRNAs have been identified as components of pathways involved in the aetiology of T2D. The discovery of novel miRNAs and their relative regulatory pathways will lead to a greater understanding of the disease and possibly provide novel diagnostic, prognostic and treatment alternatives.

Mir-375 is essential for β-cell development and function. Poy et al demonstrated that Mir-375 knock out in mice influences pancreatic α and β-cell mass, as Mir-375 regulates a cluster of genes involved in cellular growth and proliferation [296]. Specifically, in Mir-375$^{-/-}$ mice, it has been observed a decrease of β-cell mass, accompanied by a 1.7 fold increase in the number of α-cell, which suggests that Mir-375 could play different functions in α and β cells [296]. The levels of Mir-375 and Mir-7 increase during the development of human pancreatic islets, which correspond to an increase in insulin transcription level [297].

Functional studies conducted in insulin secreting MIN-6 cells and primary β-cells revealed that Mir-375 is essential for insulin secretion. The overexpression of this miRNA impairs exocytosis of insulin-containing intracellular vesicles due to aberrant regulation of the Mir-375 target myotropin (also called V-1) [295], an antiapoptotic factor involved in maintaining β-cell viability and in exocytosis [298]. Another potential target of Mir-375 is PDK1 [299], a kinase involved in the PI3K pathway of regulation of cell survival and proliferation. Overexpression of Mir-375 attenuates proliferation and insulin gene transcription, reducing glucose-induced insulin secretion. This overexpression does not affect ATP production, nor the increase in intracellular calcium triggered by glucose, but it does affect a late step in the insulin secretory pathway through its effect on myotropin. In addition, Mir-375 is repressed by glucose via the cAMP-PKA pathway, which represents another way to enhance long-term insulin release. The transcription factor CREM is a potential mediator in this pathway, as it is activated by PKA through phosphorylation and is transcriptionally upregulated by glucose [300]. These studies revealed for the first time that nutrients can regulate the expression of miRNAs, particularly those related to β-cell. Moreover, the levels of Mir-375 in pancreatic islets have found to be reduced in obese BTBR-ob/ob mice as well as in spontaneously diabetic GK rats [299, 301]. These data could seem controversial, as Mir-375 inhibits insulin secretion therefore it would be expected to be upregulated in diabetic conditions, but its reduction can be correlated to the loss of β-cell mass. Overall, it is becoming clear that Mir-375 targets genes that negatively regulate cellular growth and proliferation and that aberrant loss of this miRNA leads to reduction of β-cell mass, leading to low levels of insulin, hyperglycemia and diabetes [296].

Many other additional miRNAs play a role in insulin exocytosis in β-cell (Figure 1.21). Among those, Mir-9 regulates insulin secretion by repressing the transcription factor Onecut-2, and in turn, increasing the level of granuphilin/Slp4, a Rab GTPase effector associated with β-cell secretory granules, which exerts a negative control on insulin release. Plaisance et al demonstrated that overexpression of Mir-9 in insulin secreting cells causes a reduction in glucose or potassium stimulated exocytosis [302].

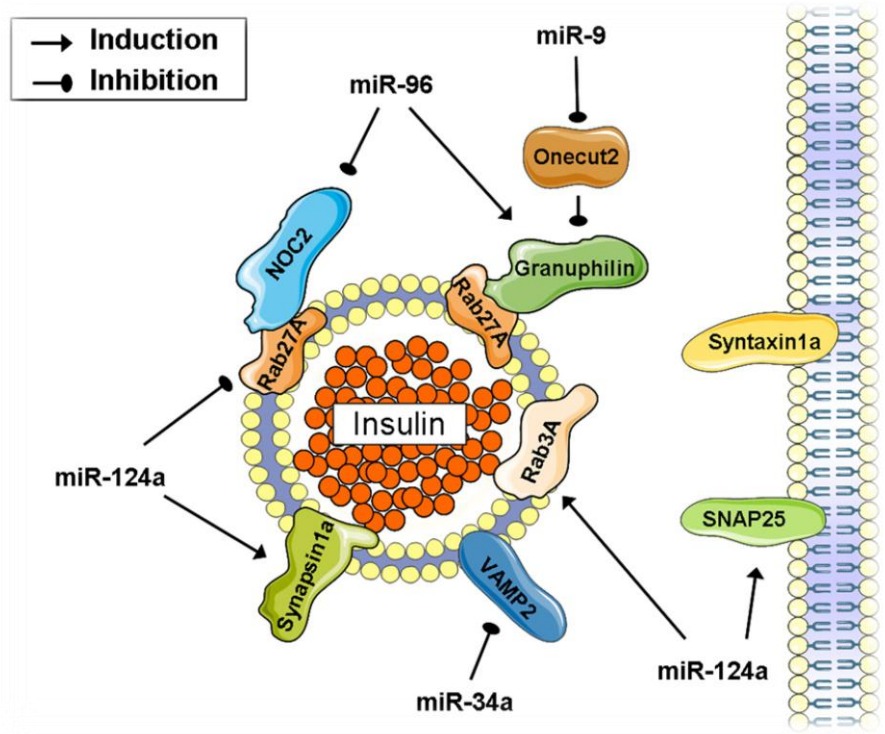

Figure 1.21 miRNAs involved in T2D and insulin release. The figure represents the miRNAs that directly or indirectly control the expression of key components required for insulin exocytosis machinery. Figure from reference [294].

Mir-96 negatively regulates insulin exocytosis by targeting granuphilin and reducing the level of Noc2 (a protein involved in insulin exocytosis) in MIN6 cells, resulting in lower ability of cells to respond to secretagogues [303].

Mir-124a is upregulated in the β-cell in the presence of glucose [304], and this leads to reduced glucose induced-insulin secretion, through targeting the transcription factor Foxa2. This protein downregulates PDX-1, which directly regulates insulin gene transcription. Moreover, Mir-124a also decreases levels of Rab27 and Noc2 and

upregulates Snap25, Rab3a, and Synapsin1a, which regulate the late steps of insulin exocytosis [303-304].

Mir-187 has been connected to diabetes, as its expression is increased in human islets from individuals with T2D and it is associated with decreased GSIS [305]. This correlation was also observed, in the same study, in primary rat islets and INS-1 cells, where overexpression of Mir-187 decreased GSIS [305]. A possible target for this miRNA is homeodomain–interacting protein kinase-3 (HIPK3), a known regulator of insulin secretion, whose expression resulted reduced in islets from individuals with T2D.

Another candidate miRNA in the pathogenic pathway to β-cell dysfunction and T2D is Mir-34a. Fatty acids are able to induce Mir-34a expression and, consequently, its levels are elevated in islets of obese mice [301]. It has been shown that Mir-34a is involved in the fatty acids-induced apoptotic process, probably by inhibition of the anti-apoptotic gene Bcl-2 [306]. It has also been demonstrated that Mir-34a can directly inhibit the translation of VAMP2 (vesicle-associated membrane protein 2), a SNARE protein involved in exocytosis. This inhibition can be responsible for the reduced insulin secretion in the presence of fatty acids [303]. Therefore, it is possible that Mir-34a overexpression in islets of obese mice can induce a reduction of insulin secretion and participate in the lipotoxic effects observed in obesity and metabolic syndrome, leading to defective β-cell function and cell death.

As described before, T2D is characterized also by an inflammatory status with upregulation of different cytokines and chemokines, with a detrimental effect on the pancreatic β-cell. Global miRNAs profiling perfomed on the insulin secreting cell line MIN6 treated with pro-inflammatory cytokines revealed a strong induction of Mir-21, Mir-34-a, Mir-146 [307]. In particular, Mir-21 is upregulated *in vivo* and *in vitro* in inflammatory conditions and targets Pclo, a protein involved in vesicle trafficking [308]. Moreover, a blockade of these miRNAs using antisense molecules prevents the reduction in glucose-induced insulin secretion induced by cytokine exposure. Blockade of Mir-34-a prevents the reduction in Bcl2 expression, whereas the blockade of Mir-146-a allows the attenuation of c-Jun induction triggered by cytokines [307].

Tang and colleagues studied the differential expression of a large set of miRNAs after exposure of the pancreatic cell line MIN6 to high levels of glucose. In particular, Mir-124-a, Mir-107 and Mir-30-d result to be upregulated in hyperglycemic conditions, whereas Mir-296, Mir-484 and Mir-690 are downregulated. Overexpression of Mir-30-d causes a reduction in insulin gene expression [304].

Specific miRNAs have been recently demonstrated to abundantly and stably exist in serum and to be potentially disease-specific. Evidence suggests that miRNAs are not present in the blood in the native form but are released in microvesicular structures, such as exosomes or apoptotic bodies, and circulate inside these vesicles that protect them from degradation. Zampetaki et al showed that a plasma signature of 5 miRNAs (Mir-15a, Mir-29b, Mir-126, Mir-223, Mir-28-3p) can accurately differentiate patients with a high likelihood of developing diabetes from healthy controls [309]. Similarly to this, Pescador et al found that the combined down-regulation of Mir-138 and Mir-503 in plasma can effectively distinguish between patients with T2D and obese patients and healthy controls [310].

Considering that T2D is often associated with obesity, miRNAs in adipose tissue are strongly dysregulated in response to obesity-induced molecular changes and environmental signals. For example the Mir-29 family of miRNAs is induced by hyperglycemia and hyperinsulinemia in adipose tissue [311], Mir-320 increases insulin sensitivity in insulin resistant adipocytes [312] and Mir-27b impairs human adipocyte differentiation [313]. Therefore, dysfunction of these miRNAs in insulin targeting tissues can reflect the degree of disturbance and deregulation in diabetes.

1.6.3.4 miRNAs as potential targets for diabetes

As outlined before, serum circulating miRNAs can be used as biomarkers for T2D. It has been suggested that these miRNAs could be not only useful indicators of early disease onset, but they can also be responsible for the disease progression [314]. This

idea makes them a good target for an early intervention, and restoration of miRNA functions to normal levels is an attractive therapeutic strategy.

Different chemically modified oligonucleotides have been used to modulate miRNAs expression. MiRNA mimic oligonucleotides increase the expression of the miRNA of interest, whereas anti-miRs, antagomirs and morpholinos are efficient inhibitors of miRNA functions and are also effective *in vivo* [315-316]. The use of oligonucleotides for gene therapy has to face different obstacles because these molecules are relatively unstable and their effects are transient. Therefore, they need to be injected at high doses and with repeated deliveries. They also need a cell-specific targeting.

One method to obtain a temporally controlled elevation of miRNA expression *in vivo* is the generation of vectors in which miRNA mimics are placed under the control of an inducible promoter, which can be activated only in a specific-cell type. Kota et al used this vector to overexpress Mir-26a in liver cancer cell, showing an important protection from hepatic cancer progression without toxic effects [317]. Also, adenoassociated virus (AAV) vectors have shown promising results for gene therapy and the use of an insulin promoter can specifically deliver the vector to pancreatic β-cells [318]. This method opens an interesting prospective on the use of AAV-miRNA strategy for miRNAs highly expressed in normal tissues and underexpressed in T2D.

On the other hand, the most promising approach to reduce miRNA activity involves the use of “miRNA sponges”. These are artificial structures that bind and hold native miRNAs, competing with their natural targets, thus creating a loss of function of the miRNA of interest [319]. This approach has been used *in vivo* to decrease the activity of Mir-31 and to investigate its role in cancer development [320].

The discovery of novel miRNAs involved in T2D and the identification of their functions in the insulin secreting system could open the way to new therapeutic strategies that can be able to treat the disease at an early stage.

1.7 Aim of the thesis

The incidence of T2D continues to grow at an alarming rate, and individual pharmacological intervention therapies often become less effective in patients over time. For this reason, there is an urgent need to better understand the causes of diabetes and to develop novel treatments that effectively targets specific molecules and pathways associated with diabetogenesis. With the advent of new techniques for transcriptome profiling, there has been a huge progress in the understanding of the molecular mechanisms involved in the pathogenesis of diabetes. In particular, some studies have been perfomed using transcriptome profiling to identify molecules differentially expressed in β-cells or islets exposed to glucose or fatty acids. However, these projects relied only on microarrays results (while RNA sequencing would give a more complete view of the effects of glucolipotoxicity) or they only considered the effects of exposure to high glucose or fatty acids alone.

The aim of this thesis is to define the molecular mechanisms involved in glucolipotoxicity, with the purpose to discover novel molecules implicated in the impairment of the β-cell function that could be potential targets for therapeutic strategies.

To address this aim, a combined approach of microarray, RNAseq, RT-qPCR and Western Blots has been used to elucidate the pathways affected after chronic exposure to high concentrations of both glucose and fatty acids.

Particular attention has been focussed on the TNFR pathway, which is involved in the inflammatory process in T2D. This thesis focusses especially on CD40 and its signalling pathway, in order to understand its involvement in glucolipotoxicity and insulin secretion.

RNAseq has been used to confirm and expand the microarray analysis, as this next generation technique is the instrument of choice to determine differential expression between experimental conditions and discover novel genes at the same time. This will open the possibility of discovering unknown proteins involved in T2D.

Chapter 2

Materials and Methods

2.1 Reagents and solutions

2.1.1 Reagents

Unless otherwise stated, all the reagents were purchased from Sigma Aldrich, UK. All the plasticware was purchased from VWR, UK.

2.1.2 Solutions and buffers

SOLUTION	COMPOSITION
Krebs-Ringer solution	125 mM NaCl, 1.2 mM KH_2PO_4, 5 mM KCl, 2 mM Mg SO_4, 1.67 mM glucose, 0.1% BSA, 25 mM HEPES
NP40 buffer	500 mM Tris HCl, 1 M NaCl, 1% Triton X-100, pH 7.2
Sample buffer	40% glycerol, 240 mM Tris HCl, 8% SDS, 0.04% Blue Bromophenol, 5% β-mercaptoethanol, pH 6.8
Lower buffer	1.5 M Tris HCl, 0.4% SDS, pH 8.8
Upper buffer	1.5 M Tris HCl, 0.4% SDS, pH 6.8
Running Buffer	0.25 M Tris HCl, 2.5 M glycine, 1% SDS, pH 8.3
Transfer buffer	1 M Tris Base, 1 M glycine, 2% SDS, 20% methanol
Ponceau solution	5 ml acetic acid, 90 ml water, 5 g Ponceau
PBS 10X	137 mM NaCl, 2.7 mM KCl, 10 mM Na_2HPO_4, 2 mM KH_2PO_4
Stripping buffer	6.25 ml Tris HCl 0.5M pH 6.8, 5 ml SDS 20%, 347 µl β-mercaptoethanol

Table 2.1 List of solutions and buffers.

2.2 Cell culture

2.2.1 Cell line

The cell line used in the experiments performed in this thesis was the following:

CELL LINE	ORGANISM	CHARACTERISTICS
INS-1	Rat	Rat insulinoma cell line immortalized by radiation. INS-1 cells respond to glucose in the physiological range and they contain a relatively high amount of insulin. They require β-mercaptoethanol in culture medium for their growth [321].

Table 2.2 Description of the cell line used.

2.2.2 Cell culture and propagation

INS-1 rat pancreatic β-cells were cultured in RPMI-1640 media supplemented with 11 mM glucose, 26 mM sodium bicarbonate, 10 mM HEPES, 50 μM β-mercaptoethanol, pH 7.4. Medium was supplemented with 10% v/v foetal bovine serum (FBS) (Life Technologies, UK), 1% v/v sodium pyruvate (Life Technologies, UK), 1% v/v Penicillin/Streptomycin/Glutamine (Life Technologies, UK).
Cells were plated in T75 flasks and incubated at 37°C in a 95% air/5% CO_2 atmosphere.

2.2.3 Cell amplification and passage

Cell lines were passaged when 80-85% confluent. Growth medium was aspirated and cells were washed in 5 ml of sterile phosphate buffered saline solution (PBS) and then incubated in 5 ml Trypsin-EDTA (Life Technologies, UK) for 3 minutes at 37°C to detach cells. Cells were then harvested in 5 ml of complete growth media and gently pipetted up and down before being collected by centrifugation at 200 RCF for 5 minutes at room temperature. Cell pellets were resuspended in the appropriate amount of growth media and re-plated as required in new tissue culture flasks or plates.

2.2.4 Cryo-conservation and recovery of cells

INS-1 cells were collected when 80-85% confluent. Growth medium was aspirated and cells were washed in sterile PBS and then incubated in 5 ml Trypsin-EDTA (Life

Technologies, UK) for 3 minutes at 37°C to detach cells. Cells were then harvested in 5 ml of complete growth media and pipetted up and down before being collected by centrifugation at 200 RCF for 5 minutes at room temperature. Cells pellets were resuspended in 1 ml of 90% FBS: 10% DMSO (Sigma Aldrich, UK) and the total volume transferred in cryovials. Cells were stored in -80°C for at least 24h before being transferred in liquid nitrogen for long-term storage.

2.2.5 Mycoplasma check

All cells used in this thesis were regularly tested for Mycoplasma infection, using VenorGeM Mycoplasma detection kit (Cambio Ltd, UK). This system utilizes a PCR reaction to detect Mycoplasma infections in cell cultures. The primer set is specific to the 16s rRNA coding region in the mycoplasma genome and the generated amplicon shows a size of approximately 267 bp.

Templates for PCR analysis were prepared by incubating the supernatant of cell cultures for 5 minutes at 95°C and subsequently centrifuged for 5 seconds to pellet cellular debris.
The reaction was set up as follow:

REAGENT	x 1 REACTION	x 3 REACTIONS
PCR grade water	14.3 µl	42.9 µl
10X reaction buffer (for Platinum Taq Polymerase, Invitrogen)	2.5 µl	7.5 µl
Primers/Nucleotide Mix	2.5 µl	7.5 µl
Internal control	2.5 µl	7.5 µl
Platinum Taq Polymerase, Invitrogen	0.2 µl	0.6 µl
$MgCl_2$	1 µl	3 µl

Table 2.3 PCR reaction for Mycoplasma detection.

2 µl of samples and controls (one positive and one negative control) were added respectively and the tubes centrifuged briefly, taking care of avoiding cross-contaminations.

The PCR program used was the following:

1 cycle	94°C for 2 min
39 cycles	94°C for 30 sec 55°C for 30 sec 72°C for 30 sec
Cool down to 4°C	

Table 2.4 PCR reaction program for Mycoplasma detection.

Samples were then run on a 1.5% agarose gel in TBE buffer 1X (Life Technologies, UK) for 20 minutes at 100 V. We expected a 191 bp band for the internal control and a 265-278 bp band for Mycoplasma.

Figure 2.1 shows an example of not contaminated cells.

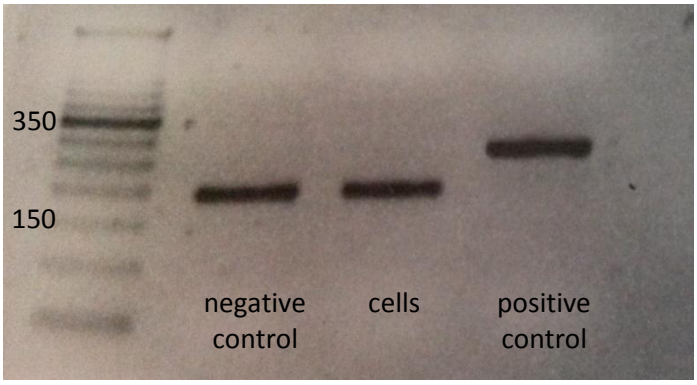

Figure 2.1 Detection of Mycoplasma infections by PCR. PCR reaction was performed on the supernatant of cultured cells. In this picture cells show a band at 191 bp, corresponding to the internal control. In case of contamination, cells show a band at 270 bp, in correspondence to the positive control.

2.2.6 Decontaminating cells from Mycoplasma

In order to clean cells from Mycoplasma infections, we used MycoZap, Mycoplasma elimination reagent (Lonza Ltd, UK). This solution eliminates Mycoplasma using a combination of antibiotic and antimetabolic agents. 500 µl of the specific Reagent 1 was added to the cell culture medium, containing not more than 5% v/v FBS and cells were grown for 2-3 days. Cells were than passaged in normal culture medium, adding 500 µl of Reagent 2 for the following 3 passages. After the end of the treatment with Reagent 2, cells were free from Mycoplasma infections.

2.3 Mice

2.3.1 Mice strains

The mice used in these experiments were C57Bl/6 mice (Charles River, UK). They were fed a high-fat diet (60% fat-58Y1; Test Diets, USA) or a standard rodent diet (CON) for 10 weeks. After 10 weeks, mice were killed in the fed state (between 08.00 h and 10.00 h) by overdose of anaesthetic for isolation of pancreatic islets. Mice were maintained on a 12 h light/12 h dark cycle. All animal experiments were conducted in accordance with the UK Home Office Animals (Scientific Procedures), 1986, with local ethical committee approval. cDNA from islets of mice fed high fat diet was prepared by Paul Caton (Blizard Institute).

2.3.2 Islet extraction and digestion

Islets were isolated by collagenase digestion using a modified technique first described by Lacy and Kostianovskey (1967). Ice-cold 1 mg/ml collagenase P (Roche Applied Science; Basel, Swtzerland) and 0.15 mg/ml DNAse 1 (Roche Applied Science; Basel, Swtzerland) in RPMI-1640 was injected into the pancreas using a 1 ml syringe and G25 needle. After the pancreas was inflated, it was excised and placed in a 5 cm Petri dish containing ice-cold RPMI on ice and cut into very small pieces with surgical scissors.

The resultant solution containing pancreas pieces and collagenase was transferred into a 25 ml conical flask and sealed with parafilm. The sealed flask was incubated at 37°C for 7 minutes under static conditions, with vigorous shaking by hand every 2 minutes and at the end of the incubation period, until the pancreas tissue was digested adequately. The digested pancreas solution was then transferred to a 15 ml falcon tube on ice and topped up with RPMI and allowed to settle. Then the supernatant was removed and the solution containing islets was transferred into a black bottomed Petri dish and free islets were handpicked under a microscope using a p200 pipette. The free islets were collected into a Petri dish containing RPMI and incubated at 37°C.

2.4 Human islets

2.4.1 Human islets extraction and digestion

Islets were similarly extracted post-mortem from human donors with local Ethics Board approval, in Piero Marchetti laboratory (University of Pisa, Italy). Islets were hand-picked into RPMI 1640 media (containing 11 mM glucose, supplemented with 10% (v/v) heat-inactivated FBS; 100 U/ml penicillin and 100 μg/ml streptomycin; all Sigma Aldrich, UK). Isolated islets were then picked into RPMI and immediately lysed for either RNA extraction or protein separation.

2.5 Preparation of experimental conditions

2.5.1 Preparation of BSA conjugated fatty acids and media conditions

To replicate diabetic extracellular glucolipotoxicity conditions *in vitro*, INS-1 cells were incubated for 72h in RPMI medium containing 27 mM glucose, 200 μM oleic acid, 200 μM palmitic acid, either alone or in combination. The experimental conditions were chosen accordingly to [123]. The high glucose concentration used (27 mM) was determined by the fact that INS-1 cells were cultured in 11 mM glucose in normal

conditions. This justifies the use of experimental glucose concentrations much higher than the physiological concentrations in human blood. The fatty acids concentrations used were not so elevated in comparison to other studies [107], but we wanted to recreate experimental conditions that did not affect cell viability. In physiological conditions, fatty acids concentrations range from around 300-600 μM in the overnight fasting state to 1300 mM after a 72h fast [322]. These concentrations decrease during the fed state, due to the secretion of the hormone insulin, which exerts an antilipolytic action.

Stock solution of oleic acid and palmitic acid conjugated to fatty acids free BSA (Roche Applied Science; Basel, Swtzerland) were prepared as follows. One hundred millimolar solutions of oleic acid dissolved in 50% ethanol and of palmitic acid dissolved in 100% ethanol were used to supplement the RPMI-1640 media prior to experimental incubation. This media was supplemented with 2% BSA and filtered with 0.2 μM filters; after the addition of fatty acids, the solution was incubated at 37°C for 1 h, to allow fatty acids binding to BSA. Individual experimental glucose and fatty acid concentrations are indicated in the text and figures. Control and high glucose conditions were supplemented with the corresponding amounts of ethanol and BSA.

2.6 Cell function analysis

2.6.1 Cell counting

Cells were seeded in 6 or 12 well plates and incubated in the desired conditions for 72h. In all the experiments described, cells were washed with PBS and detached using Trypsin EDTA (Life Technologies, UK). Trypsin was neutralised using 1 volume of complete growth media and the cell suspension was transferred in an Eppendorf tube. Cells were centrifuged at 2000 RCF for 5 minutes. The supernatant was then removed and the pellet was resuspended in 1 ml of culture media. Cells were counted manually using a Neubauer chamber, using 10 μl of cells suspension. Three of the big squares indicated as 1 in Figure 2.2 were counted and cell number was calculated with the formula:

$$\text{Concentration} = \frac{\text{Number of cells x 10000}}{\text{Number of squares x dilution}}$$

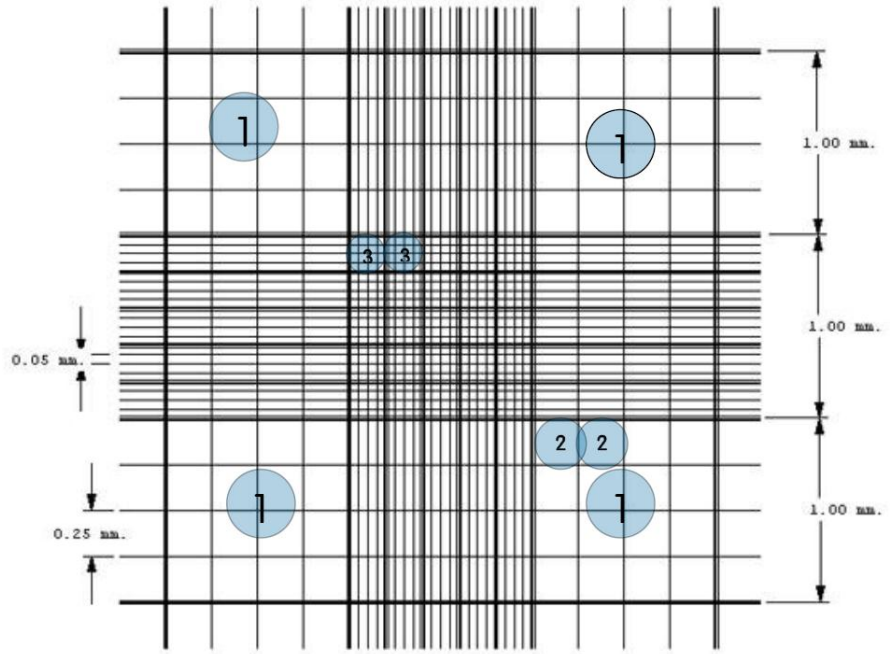

Figure 2.2 Schematic representation of a Neubauer chamber. Neubauer chamber was used for cell counting. Three of the big squares indicated as 1 were counted and multiplied by 10000 to obtain the cell concentration. Figure adapted from Celeromics website.

2.6.2 MTT (3-(4,5-Dimethylthiazol-2-yl)-2,5-diphenyltetrazolium bromide) assay

MTT assay was used to assess cell viability, in particular mitochondrial metabolic activity. The principle of the MTT assay is that for most viable cells mitochondrial activity is constant and thereby an increase or decrease in the number of viable cells is linearly related to mitochondrial activity. The mitochondrial activity of the cells is reflected by the conversion of the tetrazolium salt MTT into formazan crystal, which can be solubilised for homogenous measurements. Thus, an increase or decrease in the number of viable cells can be detected by measuring formazan concentration, reflected in optical density measurements.

Cells were seeded in 12-well plates and allowed to grow in the desired conditions. At the indicated time, 100 µl of MTT solution 5 mg/ml (Sigma Aldrich, UK) was added to the cells, followed by 2 hours incubation at 37°C in a 95% air/5% CO_2 atmosphere. After the incubation period, DMSO was added to the cells for 15 minutes on a shaking rotor. The absorbance was read at 570-650 nm using a spectrophotometer.

2.6.3 Caspase 3 activity assay

The activation of caspase 3 (CPP32/apopain), which has substrate specificity for the amino acid sequence Asp-Glu-Val-Asp (DEVD), has been shown to be important for the initiation of apoptosis. For the detection of its activity we used EnzCheck Caspase-3 Assay Kit #2 (Life Technologies, UK). The basis for the assay is rhodamine 110 bis-(N-CBZ-L-aspartyl-L-glutamyl-L-valyl-L-aspartic acid amide) (Z-DEVD-110), which contains DEVD peptides covalently linked to each of R110's amino groups, suppressing the dye's visible absorption and its fluorescence. Upon enzymatic cleavage, the nonfluorescent bisamide substrate is converted in the fluorescent product, with peak excitation and emission wavelengths of 496 nm and 520 nm.

The assay was performed following manufacturer's instructions. Briefly, cells were harvested after the desired length of time and washed in PBS. Each cell sample was then resuspended in 50 µl of 1X lysis buffer and incubated on ice for ~30 minutes. Lysed cells were centrifuged to pellet cellular debris at 8000 rpm for 5 minutes and 50 µl of the supernatant of each sample was transferred to a 96 wells plate. 50µl of the 2X substrate working solution (containing Z-DEVD-100 substrate) was added to each sample and control. The samples were then incubated at room temperature for approximately 30 minutes. Fluorescence (excitation/emission ~496/520 nm) was measured using a spectrophotometer. Because the assay is continuous, measurements could be made at multiple time points.

2.6.4 Fluorescence-activated cell sorting (FACS)

Cell cycle analysis

Cell-cycle analysis experiments were performed using flow cytometry to distinguish cells in different phases of the cell cycle. Before analysis, cells were permealised and treated with a fluorescent dye (propidium iodide) that stained DNA quantitatively. The fluorescence intensity of the stained cells at certain wavelength therefore correlated with the amount of DNA they contain.

In the specific, cells were seeded in T25 flasks and incubated with the desired conditions for 24, 48 or 72 hours. Cells were then washed with PBS, harvested and fixed in ice cold 70% ethanol, added with a Pasteur pipette on a vortex. Cells were then incubated at 4°C from 30 minutes to a week. At the time of analysis cells were pelletted and washed twice in PBS. 400 µl of a solution of 100 µg/ml RNAse (Sigma Aldrich, UK) and 50 µg/ml Propidium Iodide (PI) (Sigma Aldrich, UK) was added to each sample. Samples were then incubated at RT for 15 minutes and subsequently analysed by flow cytometry collecting 25000 events per sample.

2.6.5 Insulin secretion assay

Cells were seeded in poly-D-lysine coated 6-well plates and allowed to grow near confluency ($2x10^6$ cells/well) in each of the test media conditions for 72h. Cells were then washed with Krebs-Ringer solution (see table 2.1) and subsequently incubated for 2h in Krebs-Ringer solution with or without insulin secretagogue cocktail (10 mM glucose, 1 µM phorbol 12-myristate 13-acetate, 1 mM isobutyl-methylxanthine, 1 mM tolbutamide, 10 mM leucine, 10 mM glutamine, all Sigma Aldrich, UK). Supernatant was collected and spun down to remove cell debris and insulin concentration determined following standard ELISA kit protocols (Mercodia, Uppsala, Sweden). Cellular protein content was assayed with BCA kit protocol (Thermo Fisher Scientific, Waltham, MA) and used to normalise secretion data (see paragraph 2.8.1).

2.6.6 Insulin content assay

Cells were grown in 6-well plates in the desired test media conditions for 72h. The total protein content was measured using BCA kit (Thermo Fisher Scientific, Waltham, MA) and used to normalize insulin values obtained. Media was removed from the remaining wells of each plate and 500 µl of extracting solution containing 1.5% hydrochloric acid (37%), 18.5% distilled water, 80% ethanol (95%) were added to each well. After 24 hours at 4°C, 500 µl of 0.1 M sodium hydroxide was added to neutralise the samples, which were then assayed for insulin content using standard ELISA protocols (Mercodia, Uppsala, Sweden).

2.7 RNA analysis

2.7.1 RNA extraction

Total RNA was extracted from cells and whole islets using the Pure Link RNeasy mini kit (Life Technologies, UK). Briefly, cells were harvested and lysed in the appropriate volume of lysis buffer, before centrifuging the samples at maximum speed for 3 minutes. An equal volume of 70% ethanol was added to the supernatant, thoroughly mixed and vortexed and transferred to the RNeasy spin columns. Once the RNA in the sample had bound to the column, a series of washes followed, each time discarding the flow-through. Finally, the bound RNA was eluted with 30-50 µl of nuclease free water and stored at -80°C.

2.7.2 RNA quantification and quality assessment

Total RNA was analysed using a NanoDrop 1000 spectrophotometer (Thermo Fisher Scientific, Waltham, MA) to determine concentration and quality. The NanoDrop calculates RNA concentration by measuring the absorbance at 260 nm; absorbance correlates with concentration in a linear manner (Beer-Lambert law). RNA absorbs at 260 nm while proteins and other contaminants (such as phenol and ethanol) absorb at

280 nm. Therefore the ratio of absorbance at 260 nm over 280 nm shows RNA purity: a ratio of 2 or above is indicative of a pure RNA sample.

2.7.3 Reverse transcription

2 µg of total RNA for each sample were used to be reverse-transcribed to cDNA using cDNA synthesis kit (Thermo Fisher Scientific, Waltham, MA). The reaction was set up as follow:

REAGENT	X 1 REACTION	X 10 REACTIONS
Oligo dT primers	1 µl	10 µl
Reaction buffer 5X	4 µl	40 µl
RNAse inhibitor	1 µl	10 µl
dNTPs	2 µl	20 µl
M-MULV RT	2 µl	20 µl

Table 2.5 PCR reaction for reverse transcription.

RNAse free water was added to reach a total volume of 20 µl for each sample.
The PCR reaction was performed at 37°C for 60 minutes, followed by 5 minutes at 70°C. Once reverse transcribed, cDNA was diluted 1:5 in RNAse free water.

2.7.4 Quantitative PCR

Real time qPCR is a technique that permits to measure the amount of PCR product after each round of amplification, using a fluorescence label. During amplification a fluorescence dye binds, either directly or indirectly via a labeled hybridazing probe, to the accumulating DNA molecules, and fluorescence values are recorded during each cycle of the amplification process. The fluorescence signal is directly proportional to the DNA concentration over a broad range, and the point at which fluorescence is first detected as statistically significant above the background is called the threshold cycle or Ct value. The higher the initial amount of sample DNA, the sooner the accumulated product is detected in the fluorescence plot and the lower the Ct value.

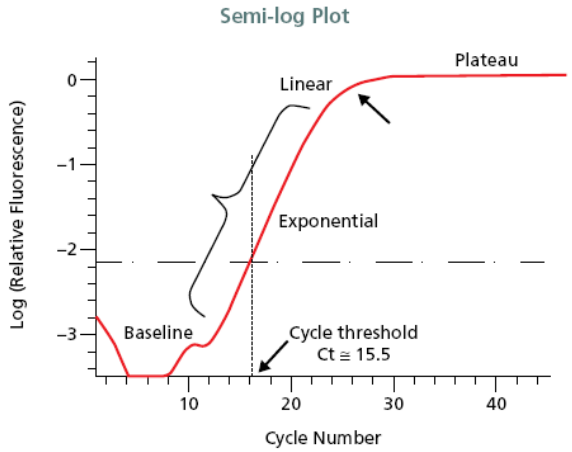

Figure 2.3 Plot representing qPCR amplification. The fluorescence signal is directly proportional to the DNA concentration over a broad range, and the point at which fluorescence is first detected as statistically significant above the background is called the threshold cycle or Ct value. Figure adapted from Sigma Aldrich website.

qPCR primers design

Primers were designed using the program Primer 3 (http://primer3.ut.ee/). Specific intron spanning or intron flanking qPCR primers were designed of 18-25 bp long, with a GC content of 30-80% and a melting temperature (Tm) of 55-62°C. Designing intron spanning or intron flanking primers prevented the amplification of genomic DNA. Specificity of the primers was determined by nucleotide blast-search. The corresponding amplicons were between 100 and 150 bp, to obtain a high level of fluorescence without compromising PCR efficiency.

To assess primer quality and specificity, a consecutive melt curve was acquired at the end of the qPCR reaction. A single peak for every sample is indicative of good primers specificity (Fig 2.4 A), instead the presence of different peaks is indicative of formation of primers dimers or aspecificity (Fig 2.4 B).

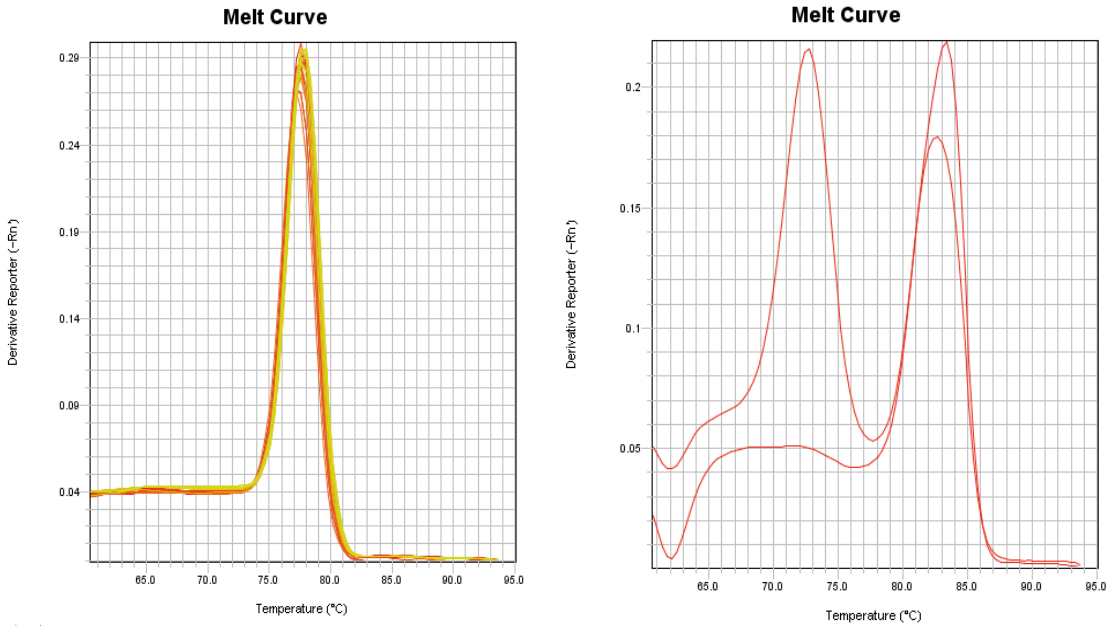

Figure 2.4 Melt curve to assess primer specificity. A) A single peak for every sample is indicative of good primers specificity; B) the presence of different peaks is indicative of formation of primers dimers or aspecificity.

The primers used in this thesis are listed in Appendix A.

Reaction set-up

Real-time qPCR reactions were performed using Maxima SYBR Green/ROX qPCR Master Mix (Thermo Fisher Scientific, Waltham, MA) and the primers specific for each gene. 1-5 µl of cDNA were added to the reaction composed of:

REAGENT	X 1 REACTION	X 10 REACTIONS
Primer Forward	1 µl	10 µl
Primer Reverse	1 µl	10 µl
Maxima Master Mix	10 µl	100 µl

Table 2.6 qPCR reaction set-up.

RNAse free water was added to reach a total volume of 20 µl for each sample and the reactions were performed in Optical 96 well plates (Applied Biosystems, Life Technologies, UK).

The 7500 Software v2.0.6 (Applied Biosystems, Life Technologies, UK) was used for the Real Time reaction and analysis. The following thermal profile was used:

1 cycle	50°C for 2 min
1 cycle	95°C for 10 min
40 cycles	95°C for 15 sec 60°C for 1 min
Melting curve	95°C for 15 sec 60°C for 1 min 95°C for 15 sec 60°C for 15 sec

Table 2.7 qPCR reaction program.

Data analysis

Data were analysed using the comparative delta delta Ct ($\Delta\Delta_{CT}$) method. This relative quantisation requires calculation of the ratio between the amount of target template and a reference template in a sample. The advantage of this technique is that using an internal standard can minimize potential variation in sample preparation and handling. In this thesis every gene expression is normalised to 18s expression.

Having obtained a Ct value for each well, the Δ_{CT} equation can be used to calculate fold change relative to the control sample, known as calibrator. In these experiments the control conditions or the transfection with a scrambled siRNA were used as calibrators.

The fold change relative to the calibrator sample was calculated as follows:

1. Δ_{CT} = Ct target gene – Ct endogenous control (normalisation to housekeeping gene to minimize sample to sample variations)
2. $\Delta\Delta_{CT}$ = Δ_{CT} sample - Δ_{CT} calibrator
3. $2^{\Delta\Delta CT}$ = fold change relative to the calibrator sample.

2.8 Protein analysis

2.8.1 Protein samples preparation from cell lysates

Cells were plated in 6 well plates and treated with the required media solution. After the incubation time (usually 72h) cells were washed twice in PBS and lysed in 300 μl of cold NP-40 lysis buffer (see Table 2.1), containing 1X protease and phosphatase inhibitors tablets (Roche Applied Science, Basel, Swtzerland). Scrapers were used to detach the cells from the plates and destroy cellular integrity. Lysates were collected in 1.5 ml tubes and centrifuged at 8000 rpm for 5 minutes, in order to clear from cell debris. The supernatants were transferred in a clean 1.5 ml tube and used for subsequent analysis.

BCA protein assay

Protein concentration was determined using Pierce™ BCA (bicinchoninic acid) Protein Assay Kit (Thermo Fisher Scientific, Waltham, MA). The principle of this system is that the peptide bonds in the proteins are able to reduce the Cu^{2+} ions from the cupric sulfate to Cu^{+} and the amount of Cu^{2+} reduced is proportional to the amount of protein present in the solution. Subsequently two molecules of bicinchoninic acid are able to chelate with Cu^{+} ions forming a purple-colored product that absorbs light at 562 nm. This absorbance is nearly linear with increasing protein concentrations over a broad working range (20-2000 μg/ml).

Bovine Serum Albumin (BSA) included in the kit was used to establish a standard calibration curve for protein quantification as seen in Table 2.8.

VIAL	VOLUME OF DILUENT (µl)	VOLUME AND SOURCE OF BSA (µl)	FINAL BSA CONCENTRATION (µg/ml)
A	0	300 of stock	2000
B	125	375 of stock	1500
C	375	325 of stock	1000
D	175	175 of vial B dilution	750
E	325	325 of vial C dilution	500
F	325	325 of vial E dilution	250
G	325	325 of vial F dilution	125
H	400	100 of vial G dilution	25
I	400	0	0=blank

Table 2.8 List of calibrators. Preparation of BSA calibrators for the generation of a standard curve.

An adequate volume of Working solution was prepared following manufacturer instructions, mixing 50 parts of BCA Reagent A with 1 part of BCA Reagent B. 200 µl of Working solution were added to each well of a 96-well plates and subsequently 10 µl of samples and calibrator were pipetted thoroughly in the solution. The plate was covered and incubated at 37°C for 30 minutes and absorbance was read at 562 nm.
The linear equation for the standard curve was set using Microsoft Excel, plotting BSA concentration (X axis) and absorbance values (Y axis). The concentration values of the samples were extrapolated from this graph.
Protein samples were normalised and diluted in 5X denaturating sample buffer and heated at 95°C for 5 minutes. The denaturated protein samples were used for Polyacrylamide gel Electrophoresis and Western Blot analysis.

2.8.2 Western Blot

SDS gels preparation

Small gels were hand poured using the BioRad system. Briefly, a running gel mix was prepared as listed in table 2.8, poured between the assembled glasses and allowed to set. Subsequently the stacking gel mix was poured onto the running gel with a ten or fifteen teeth comb in place.

Alternatively, pre-casted gels (Life Technology, UK) were used, together with the Invitrogen apparatus, following manufacturer procedures.

INGREDIENTS FOR 12.5% GEL (8 ML)	RUNNING GEL	STACKING GEL
Water	2.5 ml	2.6 ml
40% Acrylamide Bis-Acrylamide 29:1	3.3 ml	1 ml
Lower buffer	2.08 ml	1.3 ml
Temed	8 µl	50 µl
APS 10%	80 µl	5 µl

Table 2.9 Preparation of a 12.5% polyacrylamide gel.

Loading and separation of protein samples

The gels were placed in an electrophoretic tank containing running buffer and the comb removed. 20-30 µg of denatured protein samples were loaded per lane alongside a protein molecular weight marker and run with a constant voltage of 110V for 90 minutes. Subsequently the proteins were transferred to a nitrocellulose membrane using a semi dry Hoefer TE transfer unit soaked in transfer buffer.

Immunoblotting

Membranes were blocked with 5% (w/v) milk in PBS to prevent non specific binding for 45 minutes and incubated with the specific primary antibody (see Table 2.9) diluted in PBS + 0,1% Tween-20 (v/v) overnight at 4°C. The following day the membranes were washed 3 times in PBS + 0,1% Tween (v/v) and incubated with the appropriate infra-red (IR) secondary antibody (anti mouse, goat or rabbit IgG) for 1 hour at room temperature. The membranes were then washed 3 times in PBS + 0,1% Tween (v/v) and 1 time in PBS and the signals revealed using LI-COR Odyssey system.
Alternatively, after washing, membranes were incubated with the appropriated peroxidise-conjugated (HRP) secondary antibody, diluted in PBS 0.1% Tween-20 (v/v).

Membranes were then washed 3 times in PBS 0.1% Tween-20 (v/v) and once in PBS before being incubated with ECL Plus Mix solution (Amersharm, GE Healthcare, UK) for 1 minute, sealed in a plastic sheet and exposed to a chemioluminescence sensitive film (Kodak, Rochester, NY).

ANTIGEN	MANUFACTURER	CAT NUMBER
CD40	Santa Cruz Biotechnology, USA	sc-975
Actin	Santa Cruz Biotechnology, USA	sc-1616
NF-κB p65	Santa Cruz Biotechnology, USA	sc-372
TRAF sampler kit (TRAF1, TRAF2, TRAF3, TRAF6)	Cell signalling Technologies, Danvers, MA	8347
Anti Rabbit IgG-IR	Li-COR Biosciences, UK	926-32211
Anti Goat IgG-IR	Li-COR Biosciences, UK	926-68024
Anti Rabbit IgG-HRP	Cell signalling Technologies, Danvers, MA	7074

Table 2.10 List of antibodies.

Stripping membranes

Membrane were incubated in stripping solution (see Table 2.1) for 20 minutes at 37°C and then washed repetitively in PBS and subsequently re-incubated with the desired primary antibody.

2.8.3 Immunofluorescence

Cells were seeded in 12-well plates onto coverslips for 72h in different media conditions. After the incubation period cells were fixed in 4% paraformaldehyde in PBS for 30 minutes and subsequently washed 3 times in PBS and store at 4°C overnight. The following day, cells were permeabilized by exposure to 0.1% Triton X-100 in PBS for 5 minutes to create pores in the membrane and allow the entrance of the antibody and

washed once in 0.1% Triton in PBS. The specific primary antibody was then added, diluted 1:500 in PBS + 30 mg/ml BSA + 0.1% Triton X-100 and cells incubated for 2h at room temperature on a shaker.

Coverslips were then washed 3 times in PBS + Triton X-100 and then incubated with the specific secondary antibody conjugated with a fluorescence dye (AF488) diluted 1:500 in PBS + 30 mg/ml BSA + 0.1% Triton X-100, for 1h at room temperature.

After the incubation period, cells were washed 3 times in PBS + 0.1% Triton for 5 minutes.

Nuclei were stained by incubating cells in 1 µg/ml DAPI (Life Technologies, UK) in PBS for 1 minute and then washed in PBS + 0.1% Triton. After that, cells were washed again 3 times in PBS, to remove any trace of Triton and the coverslips washed in water, dried and put on glass slides.

Images have been taken with the microscope Leica DM5000 epi-fluo.

2.9 siRNA transfection

2.9.1 Transfection with Lipofectamine RNAi max

Transient knock-down of target genes was achieved using siRNA duplex technology. Efficient transfections of CD40 siRNAs were performed using Lipofectamine RNAiMAX (Life technologies, UK) and siRNA purchased from Dharmacon, GE Healthcare, UK. During the optimisation process, Lipofectamine 2000 (Life Technologies, UK) and siRNA purchased from Qiagen (Venlo, Netherlands) were also used. See table 2.10 for the list of sequences used.

In this procedure, INS-1 cells were plated in 6 well plates in order to have 40-50% confluence at the time of transfection. The following day siRNA-Lipofectamine complexes were prepared for each transfection sample (one well of a 6 well plate) as follows: in a sterile 1.5 ml tube, 7 µl of siRNA (20 µM) were diluted in 243 µl of Optimem (Invitrogen) without serum and mixed gently. In a separate sterile 1.5 ml tube, 7 µl of Lipofectamine RNAimax were added to 243 µl of Optimem without serum and mixed gently. These solutions were incubated for 8 minutes at room temperature. After

the incubation period, the diluted siRNA was combined with the diluted Lipofectamine RNAimax and mixed gently with the pipette. The solution was incubated for 25 minutes at room temperature. Media was removed from cells and 1.5 ml of RPMI with serum but without antibiotics was added. 500 µl of transfection solution was then added to each well.

After 24h, media was removed and replaced with complete RPMI. Knock-down was detected 48-72h after transfection.

SiRNA	TARGET SEQUENCE	MANUFACTURER
Rn_Tnfrsf5_1	AGCCGGGAAACCGACTAGTTA	Qiagen, Venlo, Netherlands
Rn_Tnfrsf5_2	CACCGACACTGCGAACTCAAT	Qiagen, Venlo, Netherlands
Rn_Tnfrsf5_3	CCGCGGTTTCAGACACTGTTT	Qiagen, Venlo, Netherlands
CD40 5	GATTTGTGCCAGCCGGGAA	Dharmacon, GE Healthcare, UK
CD40 6	GAGATGTCTTGCTGCGGTT	Dharmacon, GE Healthcare, UK
CD40 7	GCTGATGGTCCTACGGGAA	Dharmacon, GE Healthcare, UK
CD40 8	GGTAAAGAGAGTCGCATCT	Dharmacon, GE Healthcare, UK
Non-targeting siRNA	TGGTTTACATGTCGACTAA	Dharmacon, GE Healthcare, UK

Table 2.11 List of siRNA sequences.

2.9.2 Transfection with Amaxa nucleofector

During the optimisation process, transfections were performed also using electroporation with Amaxa Nucleofector II. Briefly, cells were resuspended in 100 µl of nucleofector solution (Nucleofector kit V; Lonza, Basel, Switzerland) and the specific siRNA was added to a final concentration of 1 µM. The samples were transferred into an Amaxa certified cuvette and inserted in the machine where the specific program was

run (T-020). Cells were then resuspended in pre-warmed medium and plated in 6-wells plates.

2.10 RNA sequencing

RNA sequencing is a high-throughput sequencing method for both mapping and quantifying transcriptomes, namely the complete set of transcripts in a cell. It involves direct sequencing of complementary DNAs (cDNAs) using high-throughput DNA sequencing technologies followed by the mapping of the sequencing reads to the genome. It is a very informative technique, because it allows the identification of exons and introns, the mapping of their boundaries, the identification of the 5' and 3' ends of genes and of the transcription start sites. It is also a genome-wide technique, allowing the study of the effects of a certain treatment on global transcriptome regulation. It is therefore possible to compare the genome-wide effects of a treatment to control conditions.

2.10.1 RNA extraction

Cells were incubated in the appropriate conditions for 72h, then harvested and RNA extracted using mirVana miRNA isolation kit (Life Technologies, UK). This specific kit was used because the same samples were used subsequently for miRNAs extraction.
Briefly, 1 ml of Binding Buffer was added to cell pellets and the solution vortexed to disperse any aggregates. 100 µl of miRNA homogenate additive were added and mixed well inverting the tube several times; the solution was then incubated on ice for 10 minutes. Subsequently, a process of phenol-chloroform extraction was performed, adding 1 ml of acid-phenol:chloroform solution to each sample and mixing well by vortexing. After centrifugation at 10000 g for 5 minutes at RT aqueous and organic phases were separated. The aqueous phase was kept for the subsequent RNA extraction. 1250 ml of 100% ethanol were added to the solution and the mixture was transferred into a filtered column. Once the RNA in the sample had bound to the column, a series of washes followed, each time discarding the flow-through. Finally, the bound RNA was

eluted with 100 µl of nuclease free water and stored at -80°C. 1 µl of RNAse OUT (Life Technologies, UK) was added to the RNA solution, to avoid RNA degradation.

2.10.2 DNAse treatment

In order to remove contaminant genomic DNA from the RNA solution, samples were DNAse treated using DNA-free, DNA removal kit (Life Technologies, UK).
Briefly, 0.1 volume of 10X DNAse buffer was added to the RNA solution, mixed gently and incubated at 37°C for 10 minutes. 0.1 volumes of DNAse inactivation agent was added and incubated at RT for 2 minutes, mixing occasionally. Samples were then centrifuged at 10000 g for 1.5 minutes and RNA transferred to a fresh tube.

2.10.3 Assess RNA quality using Agilent Bioanalyser

Before performing a genome-wide analysis using RNA sequencing, it is compulsory to check the high quality of the extracted RNA. Quality of RNA can be detected using NanoDrop 1000 spectrophotometer (Thermo Scientific), reading the 260/280 ratio: a ratio of 2 or above is indicative of a pure RNA sample. However, this system is not able to assess other parameters of RNA quality, like RNA degradation. For this purpose, in this thesis, RNA integrity was determined with improved accuracy using a technology developed by Agilent (Santa Clara, CA), in which the abundance of two rRNA species are used to assess the integrity of RNA. In this system a microfabricated chip is used to perform elecrophoretic separation of RNA samples. Because of a constant mass-to-charge ratio and the presence of a sieving polymer matrix, the molecules are separated by size. Dye molecules intercalate into RNA strands and these complexes are detected by laser-induced fluorescence. Data is translated into gel-like images (bands) and electropherograms (peaks). Total RNA shows two distinct ribosomal peaks corresponding to 18s and 28s and a relatively flat baseline between 5s and 18s ribosomal peaks. 28s and 18s exist in equal concentrations in the cell, but 28s is double fluorescent. As RNA degradation occurs, there is a gradual decrease in the 18s to 28s ribosomal band ratio and an increase in the baseline signal between the two ribosomal

peaks and the lower marker. Consequently, a 28s/18s ratio of two is considered to be good quality RNA.

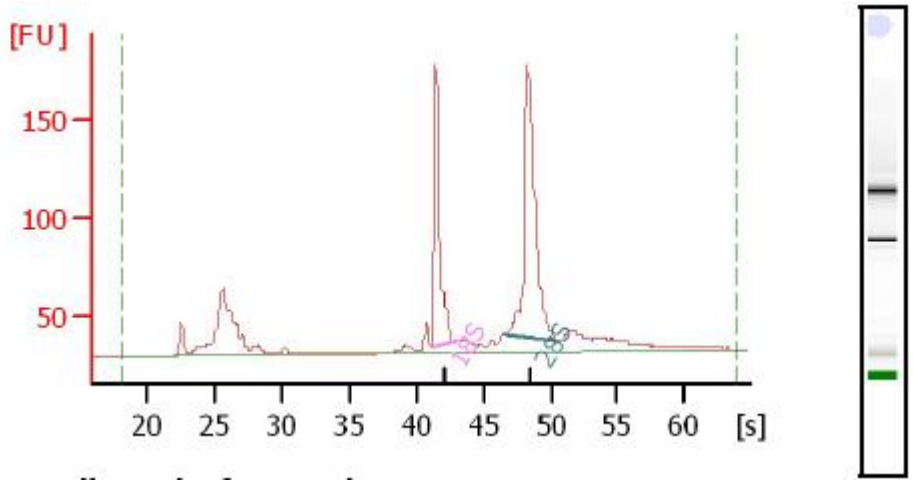

Figure 2.5 Electropherogram and gel images showing RNA integrity. Total RNA shows two distinct ribosomal peaks corresponding to 18s and 28s. As RNA degradation occurs, there is a gradual decrease in the 18s to 28s ribosomal band ratio and an increase in the baseline signal between the two ribosomal peaks and the lower marker. Consequently, a 28s/18s ratio of two is considered to be good quality RNA.

RIN number

In order to standardize the process of RNA integrity interpretation, Agilent Technologies has introduced a new tool for RNA quality assessment: the RNA Integrity Number (RIN). The RIN software algorithm allows for the classification of total RNA based on a numbering system from 1 to 10, with 1 being the most degraded profile and 10 being the most intact.

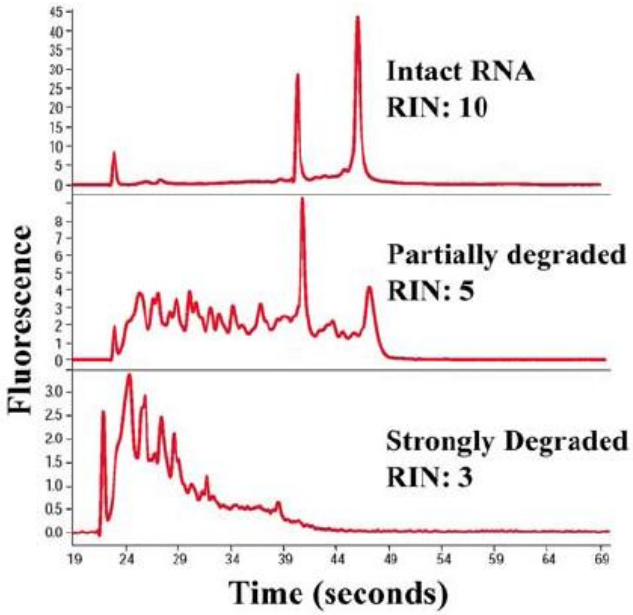

Figure 2.6 RNA integrity number. RIN number is a tool to assess RNA quality and integrity. It is based on a numbering system from 1 to 10, with 1 being the most degraded profile and 10 being the most intact. Figure adapted from Agilent Technologies website.

Agilent method

RNA samples were analysed using a RNA 6000 Nanochip (Agilent, Santa Clara, CA), in accordance to the manufacturer's instructions. Briefly, wells were preloaded with the appropriate gel and a fluorescent dye. Subsequently, 1 µl of each sample and of a molecular weight ladder were added to the chip. Once the wells and channels are filled, the chip becomes an integrated electrical circuit. The chip was then vortexed and analysed using the Agilent Bioanalyzer software.
All samples used in this study were assigned a RIN number of 8 or above.

2.10.4 Library preparation

High quality RNA was then sent to Sarah Lamble laboratory in Oxford for the subsequent stages of library preparation and sequencing, using an Illumina mRNA seq Sample preparation kit (Illumina, San Diego, CA).

Briefly, RNA was initially ribo-depleted, to remove the vast majority of rRNA and to allow a better analysis of smaller changes in trascriptomes and less abundant sequences.
Library was then generated with the fragmentation of the mRNA in small pieces using divalent cations under elevated temperature and the fragments were converted to first strand cDNA using reverse transcriptase and random primers. Subsequently the RNA template was removed and a replacement cDNA strand was synthesized, generating a double strand-cDNA. The fragments were then end-repaired, in a process that converts the overhangs into blunt ends, using T4 DNA polymerase and Klenow DNA polymerase. The 3' to 5' exonuclease activity of these enzymes removes 3' overhangs and the polymerase activity fills in the 5' overhangs. 3' ends were then adenylated, adding an A base to the 3' end of the blunt phosphorylated DNA fragments, using the polymerase activity of Klenow fragment. This step prepares the DNA fragments for the ligation to adapters, which have a single T base overhang at their 3' end.
Adapters were then ligated to the end of the DNA fragments, preparing them to be hybridised to a single read flow cell. Subsequently, cDNA samples were purified on a gel to select a size range of templates (around 200 bp) for downstream enrichment. The purified cDNA templates were enriched using PCR to amplify the cDNA in the library, using primers that anneal to the ends of the adapters.
The library was then validated performing a quality control analysis to quantify DNA concentration, using Agilent Bioanalyzer.

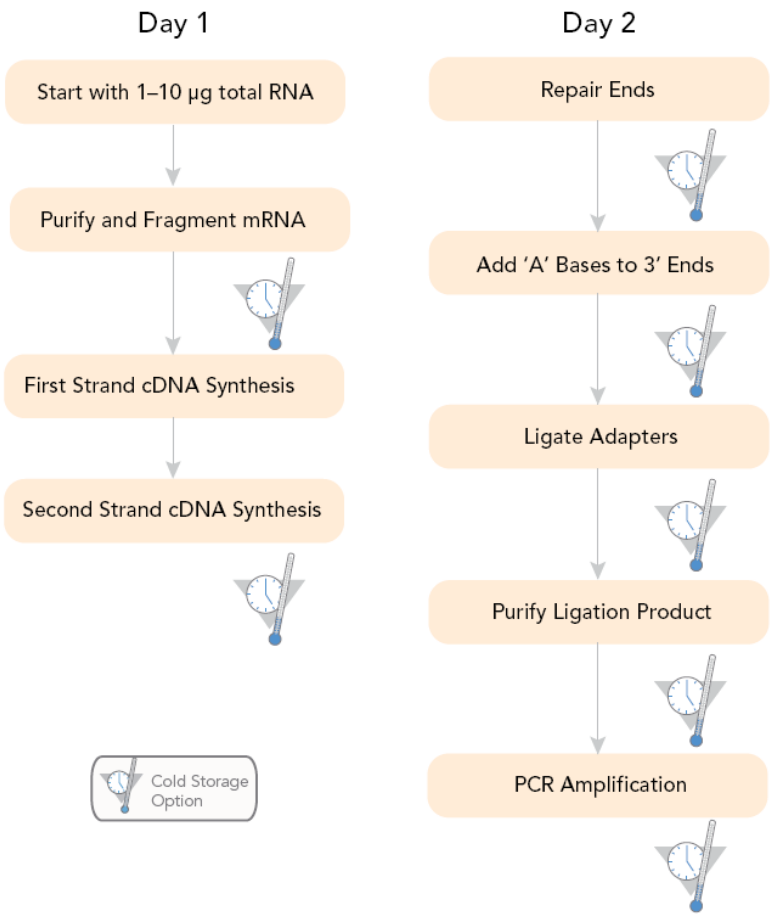

Figure 2.7 RNAseq library preparation workflow. RNA was ribodepleted, fragmented in small pieces and converted to cDNA using reverse transcriptase and random primers. The fragments were then end-repaired, polyadenylated and adapters were added, preparing them to be hybridised to a single read flow cell. Figure adapted from Ilumina website.

2.10.5 Sequencing

Library was used to perform paired end sequencing over one lane of a flow cell on an Illumina-HiSeq 2000 instrument in Oxford. This sequencing technology relies on the attachment of randomly fragmented genomic DNA to a planar, optically transparent surface. Attached DNA fragments were extended and bridge amplified to create an ultra-high density sequencing flow cell with hundreds of millions of clusters, each containing ~1000 copies of the same template. The templates were sequenced using a robust four-colour DNA SBS (sequencing by synthesis) technology that employs reversible terminators with removable fluorescent dyes.

Figure 2.8 Illumina Hi-Seq 2000 platform. After library preparation, the fragments were amplified to create clusters, each containing ~1000 copies of the same template. The samples were then sequenced using SBS (sequencing by synthesis) technology. Figure adapted from Illumina website.

2.10.6 Data analysis

Raw RNAseq data were analysed by Dr. Rob Lowe (Blizard Institute). In the sequencing process, the Illumina instrument produced quality-scored base calls during the run. The sequencing output files (compressed FASTQ files) were then used for the secondary analysis.

Reads were aligned to an annotated reference genome using Top Hat v 2.0.9: http://tophat.cbcb.umd.edu. Reads aligned to exons, genes and splice junctions were counted using the reference genome "rn4", extracted from UCSC (http://genome.ucsc.edu/goldenPath/credits.html#rat_credits).

Data visualisation and interpretation, calculating gene as well as transcript expression, then reporting differential expression, was done using the HTseq-count program: (http://www-huber.embl.de/users/anders/HTSeq/doc/count.html).

Normalisation process, which correct for in-sample distributional differences within the read counts, such as differences in total counts (sequencing depths), and within sample gene-specific effects, such as gene length or GC-content effects, was performed using the program DEseq:
(http://www.bioconductor.org/packages/devel/bioc/html/DESeq.html)

The statistical significance of fold changes was calculated by comparing the experimental read values to the control samples and the p values were subsequently adjusted at genome wide level using Bonferroni formula.

2.10.7 Pathways analysis

In order to identify enriched pathways and functions between our differentially expressed genes, data were loaded in pathways analysis programs: PANTHER (http://www.pantherdb.org/), Metacore (http://thomsonreuters.com/metacore/), Gene Venn (http://genevenn.sourceforge.net/).

PANTHER and Metacore allow the identification of enriched pathways, molecular functions, biological processes, cellular components, protein classes and associated diseases among a given list of genes. The programs calculate the number of genes that are enriched with a specific pathway and give also the statistical significance of any enrichment. Enrichment is considered statistical significant when there are more genes in the list associated with a particular pathway than it would be expected by chance based on the total number of genes associated with that pathway.

GeneVenn was used to draw Venn diagrams and to identify logical relations between our sets of data.

2.11. Small RNA analysis

2.11.1 miRNAs extraction

Total RNA was previously extracted using mirVana miRNA isolation kit (Life Technologies, UK) (see paragraph 2.10.1). Small RNAs were then separated from total RNA following manufacturer's instructions. Briefly, total RNA was mixed with 5 volume of binding buffer. 1/10 volume of miRNA homogenate additive was added and the samples mixed well by vortexing. Samples were then incubated on ice for 10 minutes. 1/3 volume of 100% ethanol was added and the mixture was pipetted onto a filter column. After centrifugation at 5000 rpm for 1 minute, the filter contained the

RNA fraction depleted of small RNAs. Small RNAs passed through the filter and, in order to purify them, 2/3 volume of 100% ethanol was added and the mixture transferred to a second filter column. Once the small RNA in the sample had bound to the column, a series of washes followed, each time discarding the flow-through. Finally, the bound RNA was eluted twice with 50 µl of nuclease free water and stored at -80°C. 1 µl of RNAse OUT (Life technologies, UK) was added to the small RNA solution, to avoid RNA degradation.

2.11.2 miRNA reverse-transcription

Small RNAs were retro-transcribed to cDNA using TaqMan® MicroRNA Reverse Transcription Kit (Applied Biosystems, Life Technologies, UK) with the specific assay for each miRNA.
A RT master mix was prepared using the following reagents:

REAGENT	X 1 REACTION	X 10 REACTIONS
100 mMdNTPs	0.15 µl	1.5 µl
MultiScribe™Reverse Transcriptase, 50 U/µL	1 µl	10 µl
10x reverse transcription Buffer	1.5 µl	15 µl
RNase inhibitor, 20 U/µl	0.19 µl	1.9 µl
Nuclease-free water	4.16 µl	41.6 µl

Table 2.12 PCR reaction for miRNAs reverse transcription.

For each reaction, 5 µl of RNA (1-10 ng) were then added, followed by addition of 3 µl of the specific RT primer. Tubes were incubated on ice for 5 minutes, before performing the following reaction:

30 min	16°C
30 min	42°C
5 min	85°C
Cool down to 4°C	

Table 2.13 PCR reaction program for miRNAs reverse transcription.

2.11.3 Taqman miRNA assay

Taqman miRNA assay kit (Applied Biosystems, Life Technologies, UK) was used to perform a qPCR on the cDNA retro-transcribed from the small RNA. Each reaction was performed as follows:

REAGENT	X 1 REACTION
Taqman microRNA assay 20x	1 µl
Product from RT reaction (minimum 1:15 dilution)	1.33 µl
Taqman 2X universal PCR master Mix	10 µl
Nuclease-free water	7.67 µl

Table 2.14 qPCR reaction for miRNAs.

The reaction was set up as follows:

Hold stage	95°C for 10 minutes
40 cycles	95°C for 15 seconds 60°C for 60 seconds

Table 2.15 qPCR reaction program for miRNAs.

Data were then analysed using the comparative delta delta Ct ($\Delta\Delta_{CT}$) method (see 2.7.4).

2.12 Statistical analysis

All the values were expressed as mean + standard deviation. Statistical analyses were carried out using two-tailed, unpaired *t*-test using Microsoft Excel and a p-value of <0.05 was considered significant.

Chapter 3

Glucolipotoxicity of the pancreatic β-cell

3.1 Introduction

T2D is a metabolic disorder characterised by insulin resistance and pancreatic β-cell dysfunction and β-cell death due to molecular mechanisms mainly generated by chronic exposure to high concentrations of glucose and fatty acids.

Different factors can be responsible for β-cell dysfunction (in particular for the impairment of insulin secretion and production) including glucotoxicity, lipotoxicity, ER stress, mitochondrial dysfunction and inflammation.

It has been shown that after exposure to glucose and fatty acids, the β-cell initially responds with a compensation process, in which it increases β-cell mass and insulin production and secretion [76, 78, 80]. However, recent studies demonstrated that β-cell dysfunction is the critical determinant for T2D and it can occur also in absence of insulin resistance [74]. In general, prolonged exposure of the β-cell to high concentrations of glucose and fatty acids leads to β-cell dysfunction, impairment of insulin secretion and production and ultimately β-cell death [119]. Moreover, different studies have provided evidence that lipotoxicity only occurs in the presence of concomitantly elevated glucose levels [121, 123]. This can be explained by the effects of glucose on lipid partitioning and with the concomitant accumulation of toxic intermediates. After a carbohydrate containing meal, fatty acid oxidation is indeed inhibited, as citrate, generated from the glycolitic metabolism, is converted to malonyl-CoA by ACC. Malonyl-CoA sterically blocks CPT-1, inhibiting the transport of LC-CoA in the mitochondria and inducing its accumulation in the cytosol.

Also inflammation is involved in the glucolipotoxicity process in T2D, and elevation of inflammatory markers as cytokines and C-reactive protein have been shown to be a feature of diabetes pathogenesis [145]. As a consequence, also some inflammatory mediators can be implicated in the process of impairment of insulin secretion or production, for example TNF-α [323] and IL-6 [324].

Although some molecular mechanisms have been proposed to be involved in this β-cell dysfunction [125, 128, 130-132], additional studies are required to completely understand this process, in order to discover new molecules involved in the process of

impairment of insulin production and secretion and to identify novel targets for specific therapeutic strategies.

The aim of this study was to characterise the effects of chronic exposure to high concentrations of glucose and fatty acids on β-cell dysfunction. Since we were specifically interested in defining the mechanisms of glucolipotoxicity-induced β-cell dysfunction, we focussed on experimental conditions that were able to impair insulin secretion, but that did not affect massively cell viability. We then focussed on gene expression changes in these conditions in order to identify novel molecules involved in the process of glucolipotoxicity, which can lead to identify novel potential targets for future therapeutic strategies at an early stage of the disease.

3.2 Effect of glucolipotoxicity on cell viability

In order to study the effects of glucolipotoxicity on the pancreatic β-cell, we used rat insulinoma cells (INS-1), which are pancreatic β-cell immortalised by radiation. They are a simple and reliable model of study and they show a good insulin response to glucose.

To replicate the chronic glucolipotoxic conditions, INS-1 cells were incubated for 72 hours in the presence of the following experimental conditions:

1- Control (RPMI-1640 containing 11 mM glucose);
2- High glucose (RPMI-1640 containing 27 mM glucose);
3- High fat (RPMI-1640 containing 11 mM glucose, 200 µM oleic acid, 200 µM palmitic acid);
4- High glucose, high fat (RPMI-1640 containing 27 mM glucose, 200 µM oleic acid, 200 µM palmitic acid).

In particular, we decided to test the effects of glucose and fatty acids alone or in combination. Firstly we investigated the effects of these experimental conditions on cell viability, assessing cell morphology, apoptosis, cell cycle progression and mitochondrial activity.

3.2.1 Effect of glucolipotoxicity on cell morphology

INS-1 cells were cultured for 72h in the 4 experimental conditions of glucolipotoxicity. Images were taken after 72h to assess any visible change in cell morphology in the different conditions. We did not observe major changes in cell morphology when cells were incubated in the presence of high glucose, whereas a slight increase in cell size was detected in cells in the presence of fatty acids (Figure 3.1). When INS-1 cells viability is compromised, cells start to change their morphology, assuming a rounded shape and reducing adherence to the plate [325-326]. This effect was not observed in our experimental conditions.

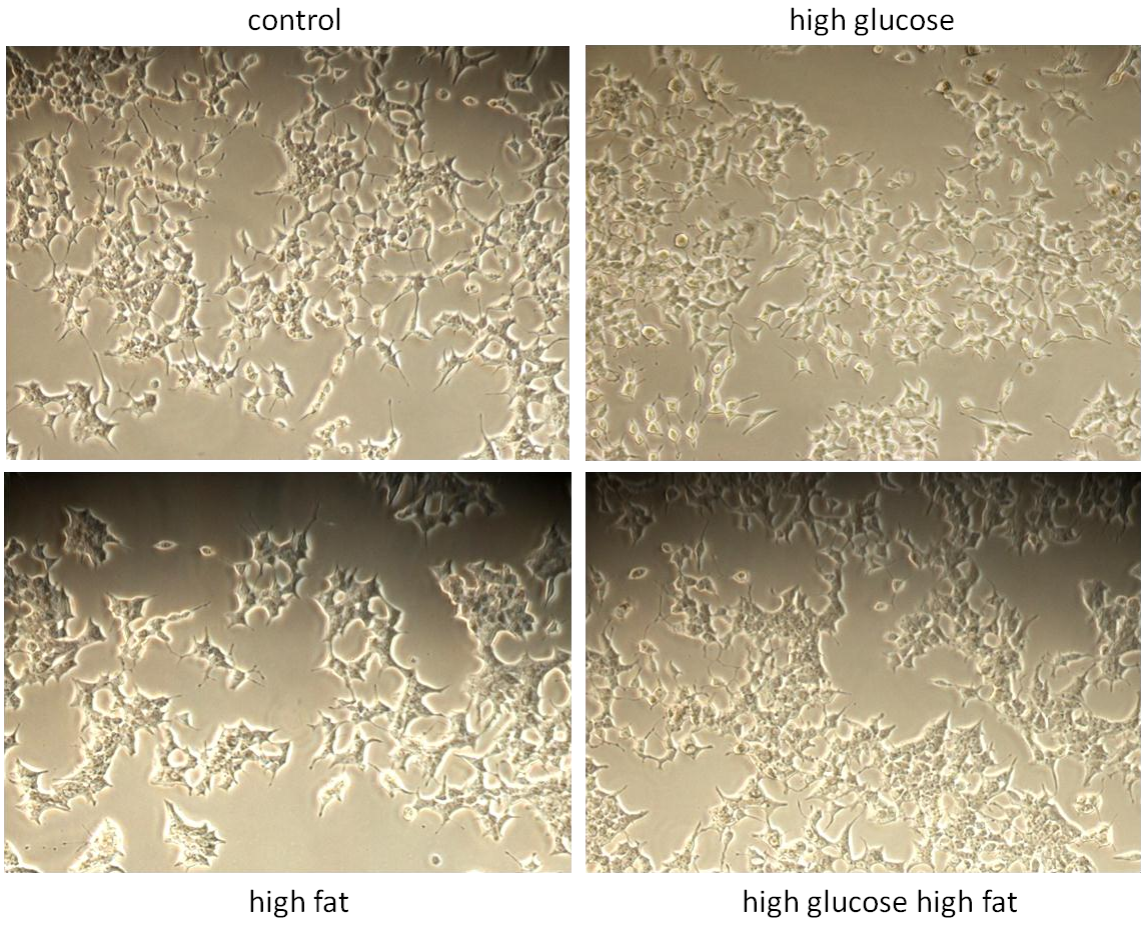

Figure 3.1 Effect of glucolipotoxicity on cell morphology. INS-1 cells were incubated for 72 hours in the presence of high glucose (27 mM glucose), high fat (200 µM oleic acid, 200 µM palmitic acid) or the combination of the two. Images were taken using a microscope with camera, with a 10x objective. These are representative images of 3 independent experiments.

3.2.2 Effect of glucolipotoxicity on caspase 3 activation

Since it has been previously reported that glucolipotoxic conditions can induce apoptosis in β-cells, we next determined whether incubation for 72h in the 4 different conditions was able to activate this process. Apoptosis was determined measuring caspase 3 activity with the appropriate kit (EnzCheck Caspase-3 Assay Kit #2, Life Technologies, UK). Caspase 3 is a member of the cysteine-aspartic acid protease (caspase) family, which plays a central role in the execution phase of cell apoptosis. Caspase 3 is activated by initiation caspases (caspases 8, 9 and 10) and in turn executes apoptosis by cleaving targeted cellular proteins. An increased caspase 3 activity reflects an increase in the apoptotic process.

Figure 3.2A shows the effect of incubation of INS-1 cells for 24h with 5 μM of staurosporine, as a positive control. Staurosporine is a protein kinases inhibitor, known to induce apoptosis. As a confirmation of the validity of the assay, staurosporine induced 14 fold change in activation of caspase 3 in this experimental system. No increase in the caspase 3 activity was detected in any of the 3 experimental conditions in comparison to control (Figure 3.2B). Consequently no activation of apoptosis was observed in these conditions. Although it appeared that there was a reduction in caspase 3 activity in presence of fatty acids, these fluctuations were due to the fact that basal caspase 3 activity in control conditions was very low, almost undetectable.

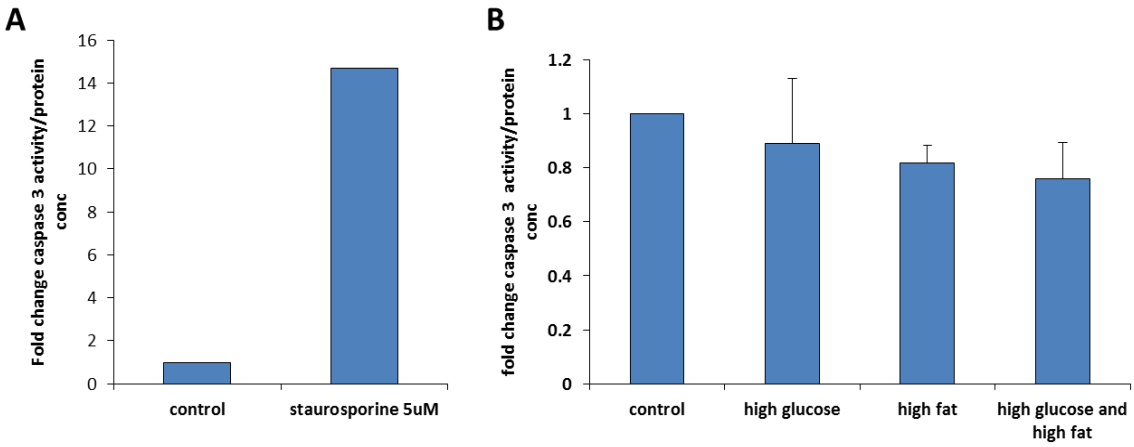

Figure 3.2 Effect of glucolipotoxicity on caspase 3 activation. A) Cells were incubated for 24h in normal RPMI and in RPMI containing 5 μM staurosporine and apoptosis was determined by caspase 3 activity. Data represent fluorescence values at ~496/520 nm normalised to total protein concentration and are expressed as fold change compared to cells grown in control conditions. Values are from 1 experiment. B) Cells were incubated for 72h in the 4 experimental conditions and apoptosis determined by caspase 3 activity. Data represent fluorescence values at excitation/emission ~496/520 nm normalised to total protein concentration and are expressed as fold change compared to cells grown in RPMI containing 11 mM glucose (control). Values are means + SD from 3 independent experiments performed in duplicate.

3.2.3 Effect of glucolipotoxicity on cell cycle progression

Consistent with data obtained in the caspase assay, we did not detect any difference in the percentage of cells in subG1 phase by FACS analysis. Specifically, cells were incubated for 72h in the 4 experimental conditions, fixed and incubated in a solution of propidium iodide. Cells were then sorted using a FACS machine, which separate them based on their DNA content.

CONTROL	HIGH GLUCOSE	HIGH FAT	HIGH GLUCOSE HIGH FAT
1.6 %	1.5 %	1.7 %	1.3 %

Table 3.1 Percentage of cells in subG1. Values are from one experiment representative of 2 independent experiments.

Table 3.1 shows the percentage of cells in subG1 phase after FACS sorting. There was no significant change in the amount of fragmented DNA, therefore neither apoptosis nor necrosis could be detected.

No significant change in the percentage of cells at each phase of the cell cycle could be detected in any of the conditions (Figure 3.3).

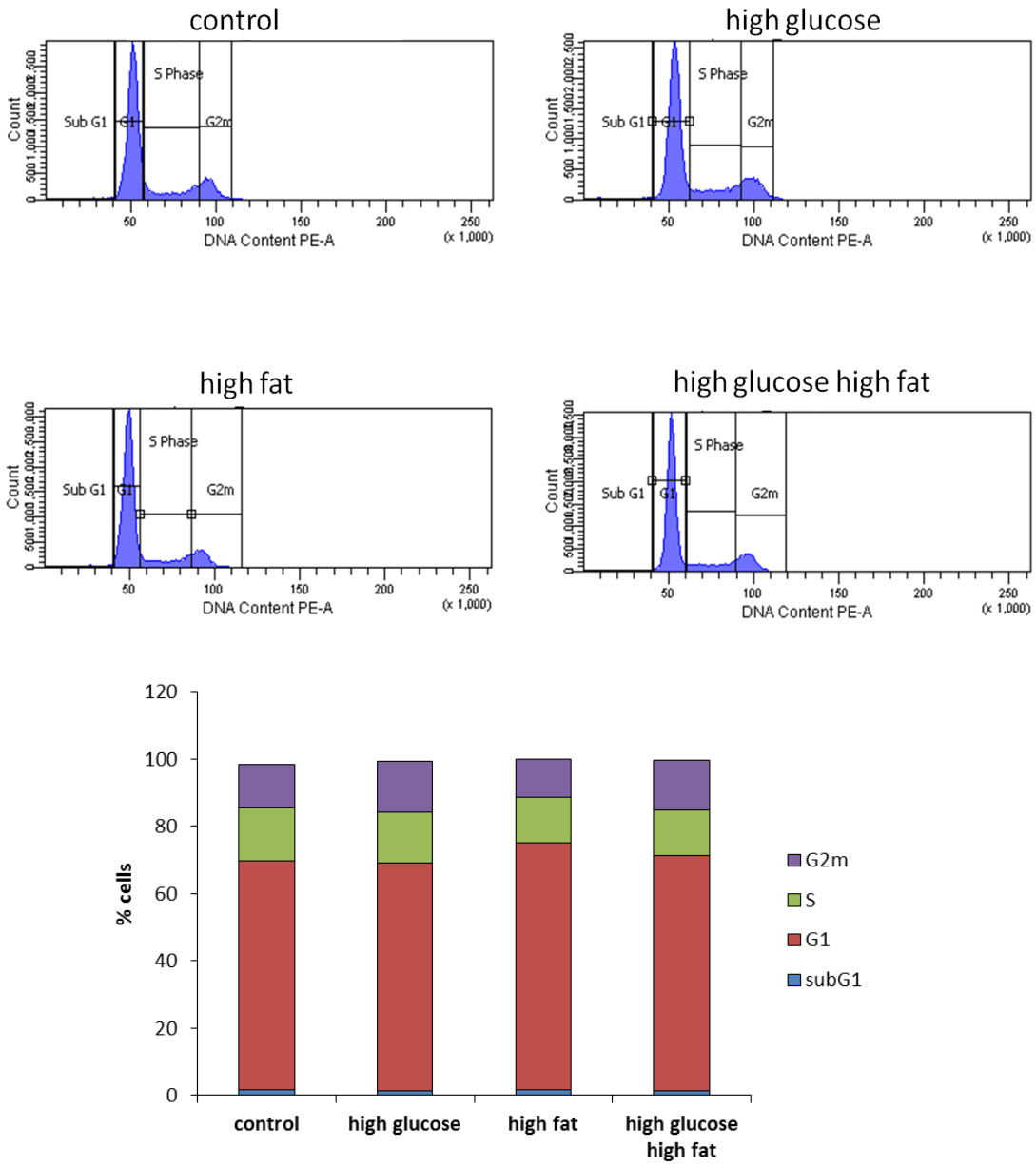

Figure 3.3 Effect of glucolipotoxicity on cell cycle progression. Cells were incubated for 72 h in the 4 experimental conditions and cell cycle analysed by FACS, using propidium iodide as DNA marker. Data are from one experiment representative of 2.

3.2.4 Effect of glucolipotoxicity on mitochondrial activity

Cell viability was measured also using an MTT assay, which assesses cell metabolic activity and therefore reflects the number of viable cells. Cells were incubated for 72h in the 4 different conditions and subsequently incubated with the appropriate MTT solution for 2 hours. Cell viability was measured by the absorbance read at 570 nm minus the absorbance at 650 nm, to subtract the background. There was a slight increase (10%) of the absorbance with high concentrations of glucose, and a slight reduction of cell viability in presence of high concentrations of fatty acids (20% with high fat, $p<0.05$, 23% with high glucose high fat, $p<0.05$) (Figure 3.4). These results shows that, in presence of fatty acids, cells started to have impairment in their metabolic activity, but this reduction was not reflected in an increased apoptosis.

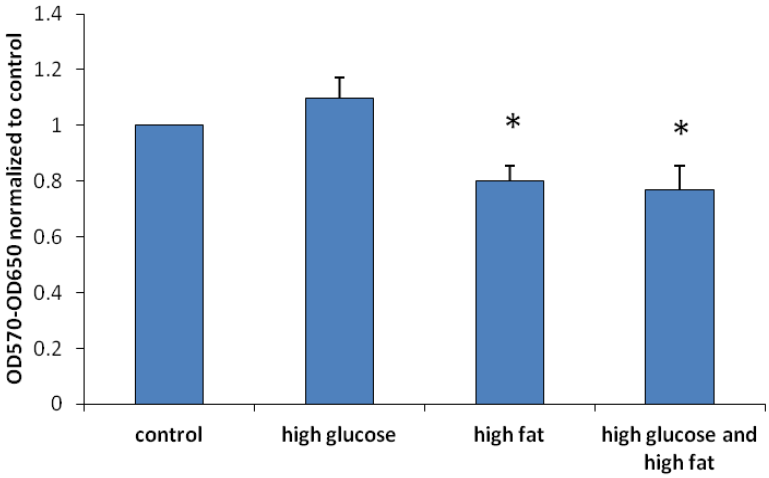

Figure 3.4 Effect of glucolipotoxicity on mitochondrial activity. INS-1 cells were incubated for 72 h in the four experimental conditions and cell viability was determined using a MTT assay. Data show absorbance values at 570-650 nm and are expressed as a fold change compared to cells grown in RPMI (control). Data are means + SD from 3 independent experiments performed in duplicate (*$p<0.05$).

3.3 Effect of glucolipotoxicity on pancreatic β-cell function

In order to study if conditions of glucolipotoxicity impair the normal β-cell function, we determined the effects of high concentrations of glucose and fatty acids on insulin secretion, insulin content and insulin biosynthesis. The production and secretion of insulin is a specific feature of the β-cell and the impairment of these functions in glucolipotoxicity leads to the loss of mechanisms important for the β-cell homeostasis.

3.3.1 Effect of glucolipotoxicity on insulin secretion

INS-1 cells were incubated for 72 hours in the 4 experimental conditions of glucolipotoxicity and basal and stimulated insulin secretion was measured using standard ELISA protocols (Mercodia, Uppsala, Sweden). Basal insulin secretion was measured after incubation of cells with Krebs buffer, which induces the release of the docked insulin vesicles. Insulin secretion was then stimulated by incubation in a secretagogue cocktail (10 mM glucose, 1 μM phorbol 12-myristate 13-acetate, 1 mM isobutyl-methylxanthine, 1 mM tolbutamide, 10 mM leucine, 10 mM glutamine). Incubation was for 2h in order to induce the release of the pool of vesicles not associated with the plasma membrane.

There was a decrease in stimulated insulin secretion when INS-1 cells were cultured with high concentrations of glucose (55% decrease) (Figure 3.5). Fatty acids exerted a slight effect, with a small reduction of stimulated insulin secretion compared to control (17% decrease) (Figure 3.5). The combination of high glucose and fatty acids caused a further decrease in insulin secretion (68% decrease), confirming the observations that fatty acids exert a negative effect on β-cell function only in presence of concomitant high glucose concentrations (Figure 3.5). Based on this data, high glucose appeared to be the main driver of insulin secretion impairment.

In addition, Figure 3.5 shows also a reduction (20% decrease) in basal insulin secretion in all conditions compared to control, but no differences could be detected between the conditions.

These results indicate that our experimental conditions did not affect cell viability, as demonstrated previously, but were able to impair β-cell function.

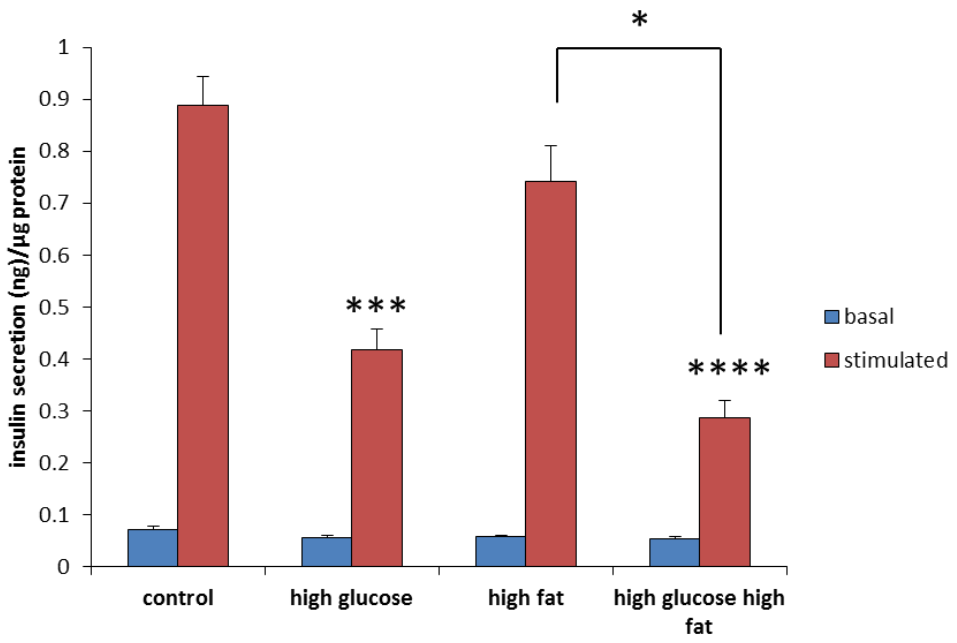

Figure 3.5 Effect of glucolipotoxicity on insulin secretion. Cells were incubated for 72h in the 4 experimental conditions and basal and stimulated insulin secretion was measured using Mercodia ELISA kit. Data indicate ng of insulin secreted per µg of total protein. Data are means + SD from 3 independent experiments performed in duplicate (*p<0.05, ***p<0.005, ****p<0.001).

3.3.2 Effect of glucolipotoxicity on insulin content

We next investigated whether the decreased secretion was due to decreased synthesis of insulin or to a defect in the secretory machinery, measuring the total amount of insulin in the cell. Specifically, INS-1 cells were cultured for 72 hours in condition of glucolipotoxicity and subsequently lysed by acid-ethanol extraction. Total insulin content was measured using standard ELISA protocols (Mercodia, Uppsala, Sweden), normalizing the values obtained to the total protein content.

Figure 3.6 shows that high concentrations of glucose induced a 47% decrease in insulin content ($p<0.05$), whereas fatty acids induced a 31% decrease, but not statistically

significant. A further decrease in insulin content was observed when glucose and fatty acids were combined (57% decrease, $p<0.005$).

These data indicate that glucolipotoxicity reduces β-cell insulin content, which eventually leads to reduced insulin secretion.

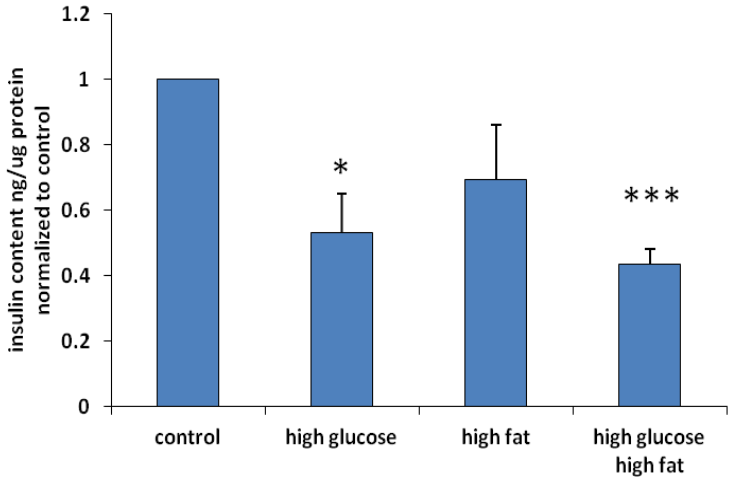

Figure 3.6 Effect of glucolipotoxicity on insulin content. Cells were incubated for 72h in the 4 experimental conditions and subsequently lysed by acid-ethanol extraction. Insulin content was measured using Mercodia ELISA kit. Data indicate ng of insulin secreted per μg of total protein. Data are means + SD from 3 independent experiments (*$p<0.05$, ***$p<0.005$).

3.3.3 Effect of glucolipotoxicity on insulin mRNA

We next investigated whether the decreased insulin content was due to the degradation of insulin protein or to a decreased level of insulin mRNA transcription. INS-1 cells were cultured for 72h in RPMI containing high glucose and fatty acids in different combinations. Cells were lysed, total RNA was extracted and insulin mRNA levels measured by a RT-qPCR using insulin specific primers. Our data showed a decrease in insulin mRNA in the presence of high glucose (59% decrease, $p<0.005$), a slight decrease in the presence of fatty acids (31%) and a slightly higher reduction when glucose and fatty acids were combined (61%, $p<0.0005$) (Figure 3.7).

These data indicate that glucolipotoxicity is able to impair insulin biosynthesis and production, and therefore to affect insulin secretion.

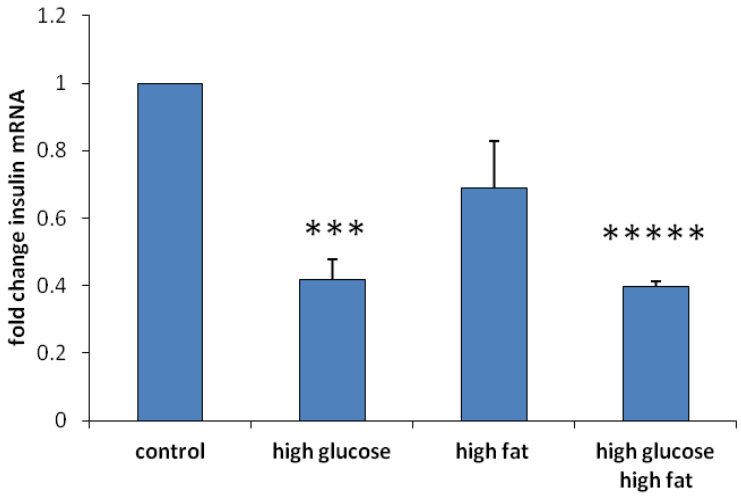

Figure 3.7 Effect of glucolipotoxicity on insulin mRNA levels. Cells were incubated for 72h in the 4 experimental conditions and subsequently lysed and total RNA extracted. RT-qPCR was performed using primers specific for the insulin gene. Data represent ΔΔCt values expressed as fold change compared to cells grown in RPMI (control). Data are expressed as means + SD of 3 independent experiments (***$p<0.005$, *****$p<0.0005$).

3.3.4 Insulin mRNA gradually decreases with the progression of glucolipotoxicity

During the progression to diabetes, the β-cell is subjected to different changes in function, culminating in a gradual impairment of insulin secretion and production. In order to determine if the reduction of insulin mRNA was due to a gradual impairment of the β-cell function during the 72 hours of incubation, we performed a timecourse experiment. INS-1 cells were incubated for 24, 48 and 72h in presence of 27 mM glucose and 200 μM oleic acid, 200 μM palmitic acid (high glucose, high fat). Cells were lysed, total RNA extracted and RT-qPCR performed using primers specific for the insulin gene. Figure 3.8 shows a gradual decrease of insulin mRNA, with a 15% decrease after 24h, which progressively decreased to 29% after 48h, to reach a 55% decrease after 72h.

This result shows that the β-cell function is gradually impaired upon exposure to chronic glucolipotoxic conditions, similarly to what is observed in patients with diabetes.

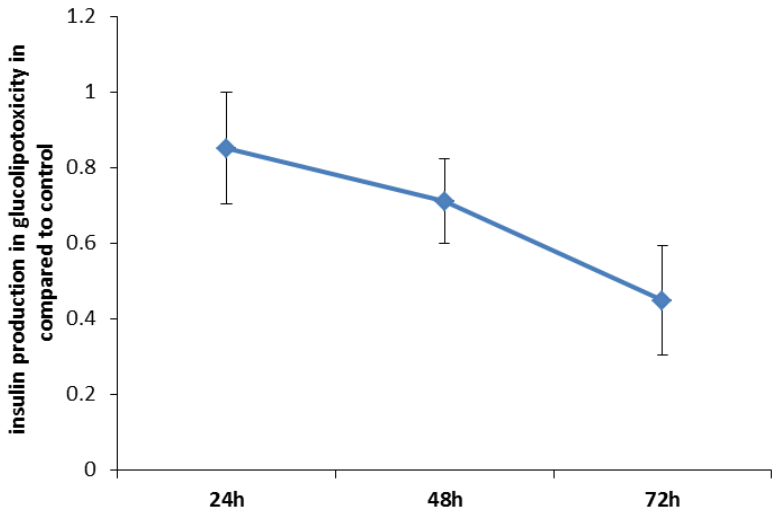

Figure 3.8 Timecourse of insulin production in glucolipotoxicity. INS-1 cells were incubated for 24h, 48h and 72h in conditions of 27 mM glucose, 200 μM oleic acid, 200 μM palmitic acid, lysed and total RNA extracted. RT-qPCR was performed using primers specific for the insulin gene. Data represent ΔΔCt values expressed as fold change compared to cells grown in RPMI (control) at each time point. Data are expressed as means ± SD of 3 independent experiments.

3.4 Effect of glucolipotoxicity on gene expression

Data so far indicate that exposure of INS-1 cells to high concentrations of glucose and/or fatty acids does not affect cell viability but impairs β-cell function. In particular, we observed a decrease in insulin biosynthesis, content and secretion, driven mainly by high glucose.

In order to gain further insight into the complex nature of the β-cell dysfunction in diabetogenesis and to discover novel mechanisms that can affect insulin secretion, a transcriptome profiling of the β-cell in conditions of glucolipotoxicity compared to control conditions was performed. In particular, previously in my group, Dr. C. Marshall and Dr. W. Ogunkolade performed an Affymetrix microarray screening in order to identify pathways involved in glucolipotoxicity.

3.4.1 Affymetrix array and pathway analysis

In order to investigate how chronic exposure to high glucose and fatty acids might trigger impairment of the β-cell function, in this previous experiment, INS-1 cells were incubated for 72h in RPMI-1640 media supplemented with 27 mM glucose, 200 μM oleic acid, 200 μM palmitic acid. RNA was isolated, converted to cDNA, fragmented and hybridised overnight at 45°C to Affymetrix high density GeneChip RatGenome 230 2.0 arrays. Chips were then washed and stained with streptavidin-phycoerythrin (SAPE). The fluorescent pixel intensities for each probe were determined using a confocal laser scanner, processed, quantified, background adjusted and scaled using Affymetrix Microarray Suite 5.0 software. Data analysis was compared using three independent experiments.

When statistically significant data ($p<0.05$) were analysed for expression change, it was found that approximately 10% of INS-1 transcripts underwent 2-fold or greater change in expression. Of relevance to preservation of β-cell mass and function, it was found that expression of a number of genes linked to apoptosis and related signalling pathways, biological oxidation, and fidelity of nucleic acid processing and repair was affected by glucolipotoxic conditions (Figure 3.9).

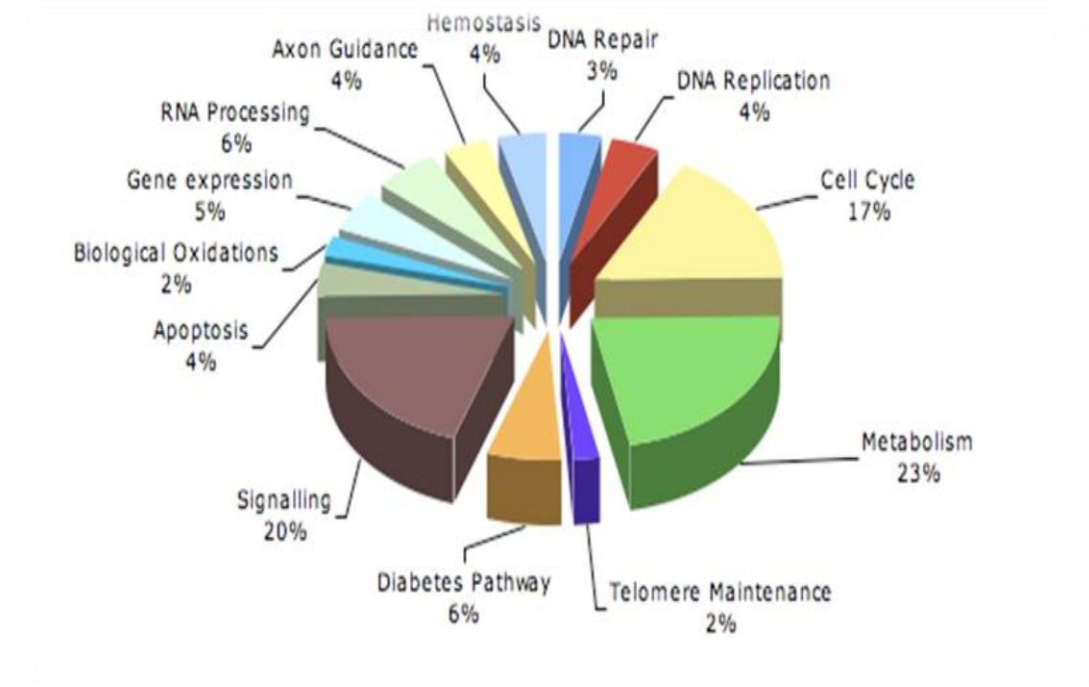

Figure 3.9 Altered gene expression in glucolipotoxicity. Pathway analysis of altered gene expression in INS-1 cells incubated for 72h in RPMI-1640 media supplemented with 27 mM glucose, plus 200 µM oleic acid, and 200 µM palmitic acid compared to cells grown in normal conditions. Cells were lysed, RNA extracted, and hybridised to Affymetrix® high density microarrays each containing 31,000 probe set. Significant differentially expressed genes were determined using Partek® software, based on a p value < 0.05 and with a fold change > 2 from three independent experiments. These were then grouped based on their biological function.

Validation of some of the results obtained in the array revealed that the expression of TNFR members and their associated factors was affected by glucolipotoxic conditions. Of these, *TNFRSF5*, the gene encoding TNFR5 (also known as CD40), was found to be the most highly upregulated, with a 2.23 fold increase in its expression (Table 3.2).

TNFRSF1	*TNFRSF5/CD40*	*TNFRSF6*
N.S.	2.23 ($p<0.0001$)	1.59 ($p<0.05$)

Table 3.2 TNFR family members. Analysis of individual expression data for the TNFR superfamily members *TNFRSF1*, *TNFRSF5*, and *TNFRSF6* based on Affymetrix array data.

3.4.2 CD40 mRNA levels are increased in glucolipotoxicity

As TNFR5/CD40 resulted to be the most upregulated member of TNFR family from the Affymetrix array, we decided to focus our investigations on this receptor. In addition, the potential role of CD40 in diabetes and glucolipotoxicity has not been described before, which makes it an interesting subject for further investigations.

In order to validate the Affymetrix data, INS-1 cells were incubated in 27 mM glucose, 200 μM oleic acid, 200 μM palmitic acid in different combinations, lysed and total RNA extracted. RT-qPCR was performed using primers specific for CD40. Figure 3.10A shows the increased expression of CD40 in conditions of glucolipotoxicity. We detected a 4.5 fold increase ($p<0.0.5$) in CD40 expression when INS-1 cells were incubated in high concentrations of glucose. Fatty acids alone did not exert any effect, whereas the combination of glucose with fatty acids triggered increased CD40 expression more than glucose alone, reaching a 6-fold increase ($p<0.05$) (Figure 3.10A).

Figure 3.10B shows the effects of fatty acids taken singularly in combination with glucose. Palmitic acid, a saturated fatty acid, exerted a slight stronger effect than oleic acid in increasing CD40 expression, but, in all the conditions studied, high glucose was the main driver of expression changes.

A

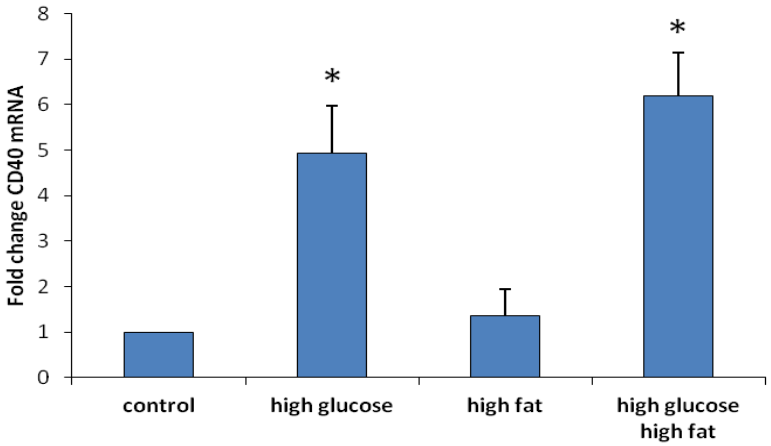

B

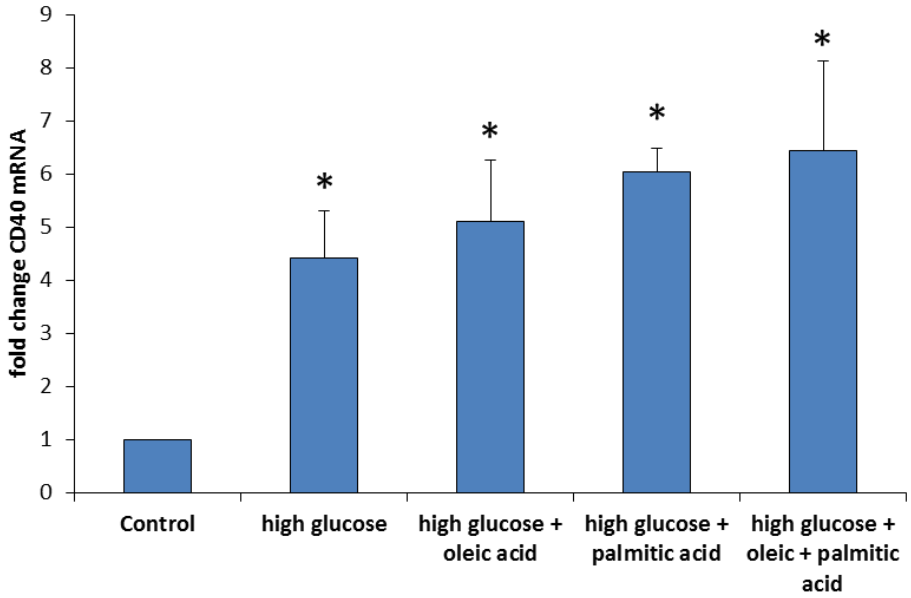

Figure 3.10 CD40 mRNA levels are increased in glucolipotoxicity. INS-1 cells were incubated for 72h in glucolipotoxic conditions, subsequently lysed and total RNA extracted. RT-qPCR was performed using primers specific for CD40 gene. Data represent ΔΔCt values expressed as a fold change compared to cells grown in RPMI (control). Data are expressed as means + SD of 3 independent experiments (*$p<0.05$). A) Incubation of INS-1 cells in control (11 mM glucose), high glucose (27 mM glucose), high fat (200 µM oleic acid, 200 µM palmitic acid) and high glucose high fat (27 mM glucose, 200 µM oleic acid, 200 µM palmitic acid); B) Incubation of INS-1 cells in control (11 mM glucose), high glucose (27 mM glucose), high glucose plus oleic acid (27 mM glucose plus 200 µM oleic acid), high glucose plus palmitic acid (27 mM glucose plus 200 µM palmitic acid) and high glucose plus oleic and palmitic acid (27 mM glucose, 200 µM oleic acid, 200 µM palmitic acid).

3.4.3 CD40 protein is overexpressed in glucolipotoxicity

To determine whether the increase in mRNA results in increased protein levels we incubated INS-1 cells for 72h in the glucolipotoxic conditions listed above. Cells were then lysed and protein separated on a 12.5% SDS PAGE, transferred to nitrocellulose membranes and immunoblotted with anti CD40 polyclonal antibody.

The combination of glucose and fatty acids induced the strongest (2-3 fold, $p<0.05$) upregulation in the CD40 protein (Figure 3.11). In particular, palmitate was the most powerful fatty acid, and it was able to induce a 1.7 fold increase, but the variability of the response did not lead to a statistical significance.

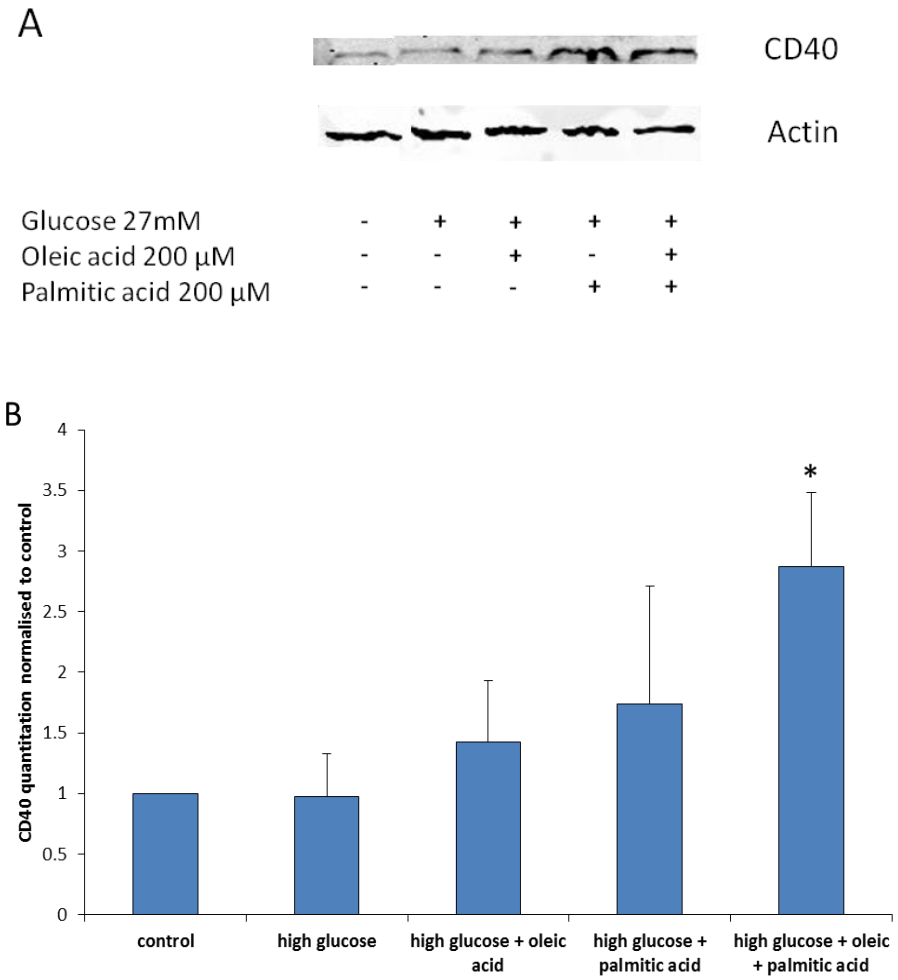

Figure 3.11 CD40 protein is overexpressed in glucolipotoxicity. Cells were incubated for 72h in 27 mM glucose, 200 µM oleic acid, 200 µM palmitic acids in different combinations. Cells were subsequently lysed and lysates separated on 12.5% polyacrylamide gels. Membranes were then incubated with CD40 specific antibody. A) Representative image of a Western Blot, representative of 3 indipendent experiments; B) Quantification of anti-CD40 western blot bands, normalised to internal actin control. Data are expressed as means + SD of 3 independent experiments (*$p<0.05$).

This biochemical data was also supported by immunofluorescence experiments (Figure 3.12), in which a strong increase in CD40 intensity (green) in INS-1 cells incubated for 72h in the presence of high glucose and both fatty acids could be detected.

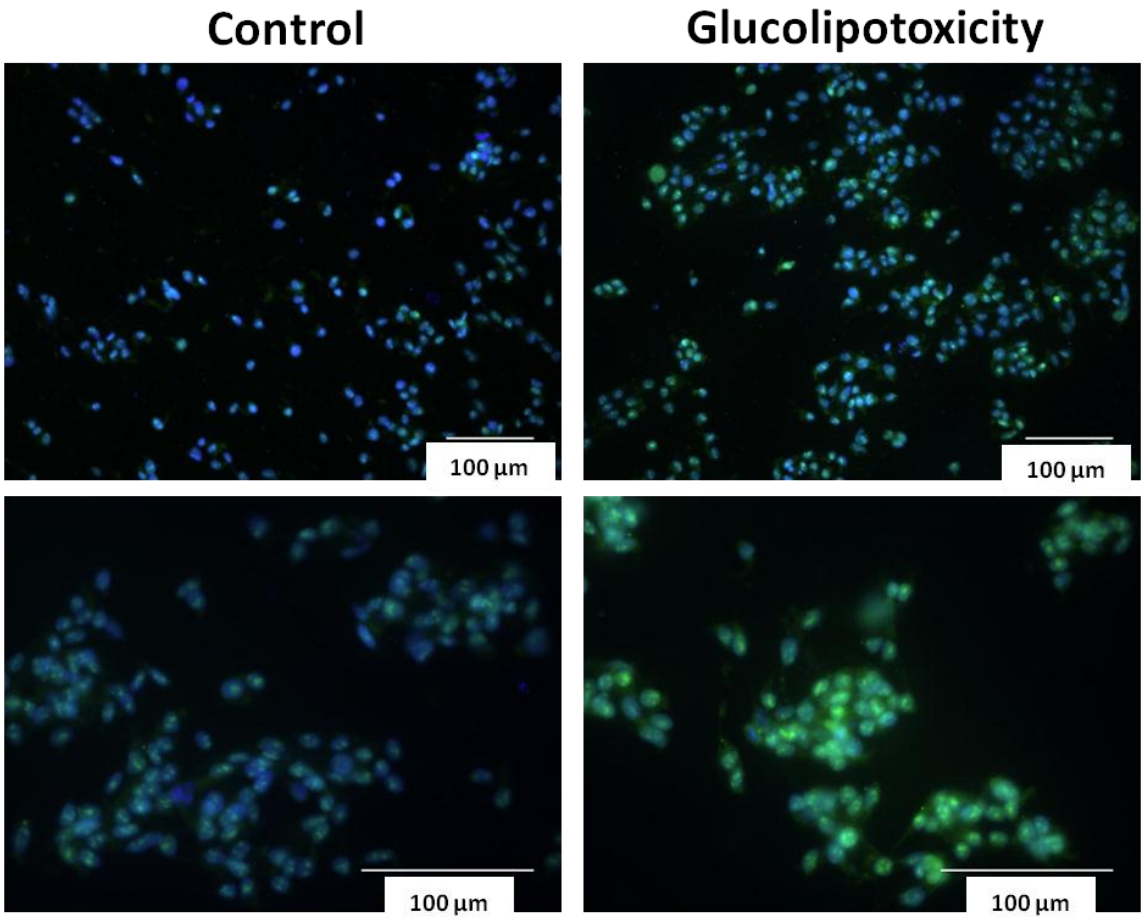

Figure 3.12 CD40 is overexpressed in glucolipotoxicity. Cells were incubated for 72h in RPMI with or without 27 mM glucose, 200 µM oleic acid, 200 µM palmitic acids. Cells were subsequently fixed and stained with CD40 antibody followed by incubation with AF488 secondary antibody (green) and DAPI (blue) to identify the nucleus. Images were taken with a Leica Epi-fluo microscope using a 20x objective (first row) and 40x objective (second row). Representative image of 3 independent experiments.

Taken together these data indicate that chronic exposure of INS-1 cells to elevated levels of glucose and fatty acids leads to the upregulation of CD40 at both mRNA and protein level.

3.4.4 CD40 expression gradually increases in glucolipotoxicity

Upregulation of CD40 expression in all the experiments so far was evaluated after 72h of incubation in glucolipotoxic conditions. In order to define the timecourse of CD40

overexpression, INS-1 cells were incubated for 24, 48 and 72h in RPMI-1640 supplemented with 27 mM glucose, 200 μM oleic acid, 200 μM palmitic acid. Cells were then lysed, total RNA extracted and RT-qPCR performed using CD40 specific primers. Interestingly we observed that CD40 mRNA levels increased in cells grown in normal medium for 72h (2.3 fold, $p<0.05$) (Figure 3.13A). In addition, CD40 mRNA further increased in glucolipotoxic conditions at each time point investigated (Figure 3.13B). Specifically we detected a 3-fold increase ($p<0.01$) after 24h that gradually reached a 7-fold increase ($p<0.01$) after 72h. Consequently, the basal levels of CD40 mRNA increased during the incubation period and it was further increased under glucolipotoxic conditions.

These results were also confirmed at the protein level, as INS-1 cells were cultured in glucolipotoxic conditions, lysed and protein separated on a 12.5% SDS PAGE gel. A slight increase in CD40 protein expression was detected after 48h and a further increase in chronic conditions, after 72h (Figure 3.13C).

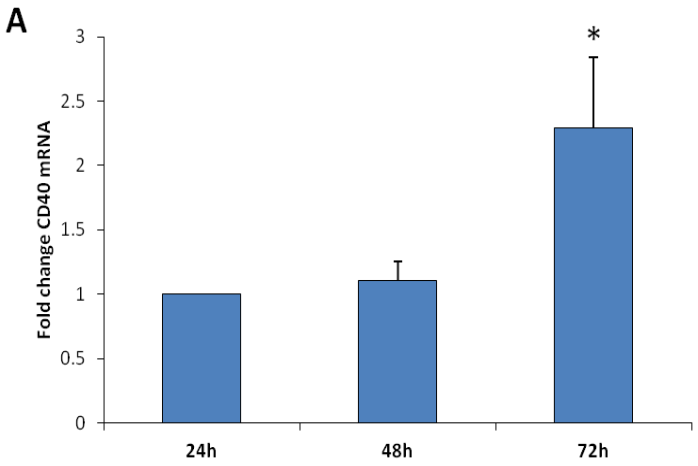

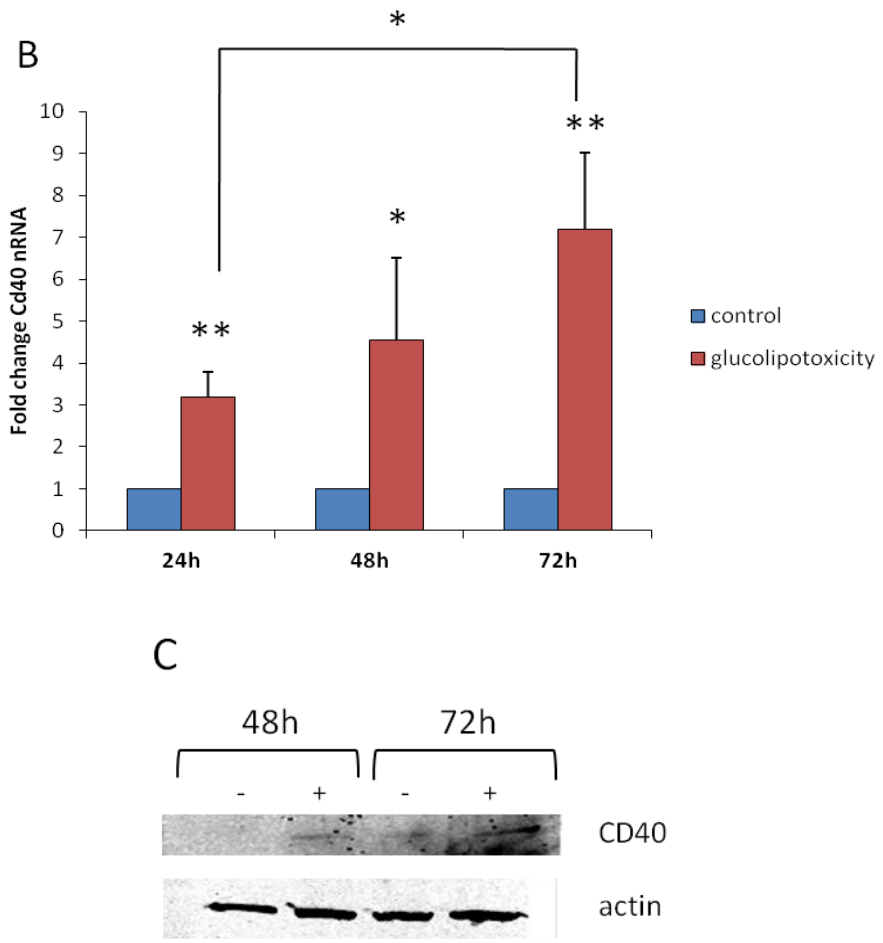

Figure 3.13 Timecourse of CD40 expression. A) INS-1 cells were incubated for 24, 48 and 72 h in control RPMI-1640. After the respective incubation times, cells were lysed, total RNA extracted and RT-qPCR performed using CD40 specific primers. Data represent ΔΔCt values expressed as a fold change compared to cells cultured for 24h. Data are expressed as means + SD of 4 independent experiments (*p<0.05). B) INS-1 cells were incubated for 24, 48 and 72 h in control RPMI-1640 and RPMI supplemented with 27 mM glucose, 200 µM oleic acid, 200 µM palmitic acid. After the respective incubation times, cells were lysed, total RNA extracted and RT-qPCR performed using CD40 specific primers. Data represent ΔΔCt values expressed as a fold change compared to cells cultured in RPMI (control) at each timepoint. Data are expressed as means + SD of 4 independent experiments (*p<0.05, **p<0.01). C) INS-1 cells were cultured in control (-) and glucolipotoxic conditions (+) for 48 and 72h, lysed and protein separated on a 12.5% SDS PAGE gel. The image is a representative western blot of 3 indipendent experiments. Actin was used as loading control.

3.4.5 Increased level of CD40 mRNA *in vivo*

INS-1 cells offer a consistent response to experimental manipulation, which makes them an ideal choice for microarray analysis where large numbers of repeat experiments are

costly. However, transformed β-cell lines are not fully representative of primary β-cell biology, so it became important to determine whether these results were representative of whole animal physiology.

To this end, we determined the levels of CD40 mRNA in cDNAs extracted from the pancreatic islets of C57BL/6 mice fed a high fat diet for 10 weeks (kindly donated from Dr. Paul Caton, Blizard Institute). RT-qPCR was performed using specific primers for CD40. Consistent with our results obtained in INS-1 cells, RT-qPCR analysis of extracted RNA indicated a 3-fold increase ($p<0.05$) in CD40 mRNA levels in the high fat fed mice relative to lean controls (Figure 3.14).

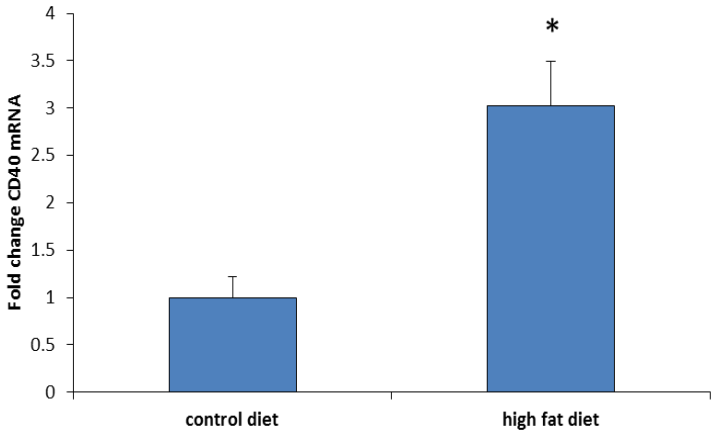

Figure 3.14 Increased level of CD40 mRNA *in vivo*. C57BL/6 mice were fed a high fat diet for 10 weeks prior to sacrifice, pancreas removed and total RNA extracted from isolated islets. RT-qPCR was performed using specific primers for CD40. Data represent ΔΔCt values expressed as a fold change compared to the expression in mice fed a control diet. Data are expressed as means + SD of 3 independent experiments (*$p<0.05$).

3.4.6 Increased level of CD40 mRNA in human islets

In collaboration with Prof. Piero Marchetti (University of Pisa, Italy), CD40 mRNA levels were then measured in islets isolated post-mortem from human donors. These islets were incubated for 24h in RPMI-1640 supplemented with 0.5 mM palmitate, total RNA extracted and RT-qPCR performed using primers specific for CD40. All these experiment were perfomed at University of Pisa. Consistent with previous data, we

observed a statistically significant upregulation of CD40 (1.4 fold, $p<0.05$) (Figure 3.15). This indicates a similar pattern of upregulation of CD40 in rodent and human islets exposed to a glucolipotoxic environment.

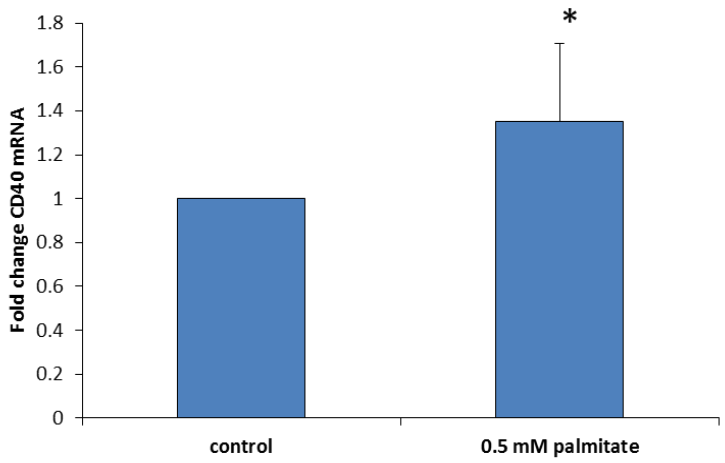

Figure 3.15 Increased levels of CD40 mRNA in human islets. Islets were isolated post-mortem from human donors and left untreated (control) or incubated for 24h in RPMI-1640 supplemented with 0.5 mM palmitate. Total RNA was extracted and RT-qPCR was performed using primers specific for CD40. Data represent ΔΔCt values expressed as a fold change compared to islets incubated in normal RPMI (control). Data are expressed as means + SD of 6 independent experiments (*$p<0.05$).

3.5 Discussion

The concept of glucolipotoxicity refers to the combined and deleterious effects of elevated glucose and fatty acids levels on pancreatic β-cell function and survival [84]. Prolonged exposure of the β-cell to high concentrations of glucose and fatty acids leads to a progressive impairment of β-cell function and gene expression and, ultimately, to β-cell death. In particular, glucolipotoxicity affects the β-cell function, namely insulin secretion and production [119-120]. In humans, oleate (C18:1), palmitate (C16:0), and stearate (C18:0) comprise around 80% of the circulating FFA at a ratio of 1.6:1:0.5. Oleate is the most prominent FFA in the human pancreas [327].

Therefore, to recreate conditions of glucolipotoxicity, we incubated rat pancreatic β-cells, INS-1 cells, in the presence of 27 mM glucose, 200 μM oleic acid, 200 μM palmitic acid, in different combinations for 72h.

We demonstrated that these conditions were not able to affect negatively cell morphology (Figure 3.1) and cell cycle (Figure 3.3), and we detected no activation of caspase 3 (Figure 3.2) and induction of apoptosis after 72h (Table 3.1). Fatty acids alone were able to slightly affect mitochondrial activity, as we observed a 20% decrease of cell viability measured by MTT assay (Figure 3.4), which was not reflected in an increased in apoptosis via caspase 3.

Previous studies had reported an increase in apoptosis in INS-1 cells after incubation with high concentrations of glucose and fatty acids. In particular Zhou et al, demonstrated that INS-1 cells incubated with 30 mM glucose and 200 μM palmitic acid for 72h showed an increased apoptosis with progressive activation of caspase 3 [328]. One possible explanation of our contrasting results is the fact that these authors did not use oleic acid in their experimental conditions, and it has been shown previously that oleate can partly protect from the deleterious effects of palmitate [329]. Considering that oleate is the most abundant fatty acids in human diet, our experimental conditions are more representative of a real physiological condition. Similarly, El-Assaad et al, showed that incubation of INS-832/13 with different combinations of glucose and fatty acids induced apoptosis [107]. However, in this study, they used different concentrations of fatty acids, and they showed apoptosis with 300-400 μM palmitic acid, which are double the concentration that we used in our study.

Our data showed that incubation of INS-1 cells for 72h in RPMI-1640 supplemented with 27 mM glucose, 200 μM oleic acid and 200 μM palmitic acid induced a decrease in insulin secretion (Figure 3.5), content (Figure 3.6) and mRNA levels (Figure 3.7). In particular, our data indicates that high glucose appeared to be the main driver in the reduction of insulin levels and secretion, whereas fatty acids alone exerted little or no effects. On the other hand, the combination of glucose and fatty acids together potentiated the effect of glucose in impairing insulin secretion and production. These results are in line with previous investigations showing that fatty acids exert a negative effect on insulin only in the presence of concomitant elevated glucose concentrations

[121-124]. Moreover, the detrimental effect of glucolipotoxicity on insulin biosynthesis could be detected already after 24h of incubation (Figure 3.8).

In conclusion, our experimental conditions of glucolipotoxicity do not affect cell viability, but impair β-cell function, namely insulin secretion and production. As a consequence, the β-cell is at an early stage of its dysfunction, in which cells are not dying but mitochondrial activity is slightly reduced in presence of fatty acids and β-cell function is impaired.

As these experimental conditions affect insulin secretion and production at an early stage of β-cell dysfunction, the study of the differential gene expression can lead to the discovery of novel molecules involved in the early stages of β-cell failure. Affymetrix microarray analysis performed previously in the group had identified several genes differentially expressed in conditions of 27 mM glucose, 200 μM oleic acid, 200 μM palmitic acid compared to control. Among them we focussed our attention on CD40, a member of the TNFR superfamily, implicated in immune response and inflammation. A functional CD40 protein is also expressed in mouse and human pancreatic β-cells and is able to induce inflammatory responses [242-244]. The Affimetrix array showed that CD40 was upregulated more than 3 times in glucolipotoxic conditions (Table 3.2).

In this study we demonstrated that CD40 was upregulated 6 times at the mRNA level (Figure 3.10) especially with the combination of high glucose and fatty acids. Its overexpression was detectable also at the protein level, as shown by western blot and immunofluorescence (Figure 3.11, Figure 3.12). Moreover its upregulation was highly sensitive to chronic exposure to a glucolipotoxic environment, as CD40 expression was higher after 72h of incubation (Figure 3.13).

As a confirmation of the results in the cell line, CD40 mRNA levels resulted upregulated also in islets of mice fed a high fat diet compared to lean controls (Figure 3.14), as well as in human islets cultured for 24h in 500 μM palmitate (Figure 3.15). All these results confirm the upregulation of CD40 in glucolipotoxicity in different systems, suggesting, for the first time, an important role for CD40 in glucolipotoxicity conditions and possibly in glucolipotoxicity-induced inflammation, as observed in diabetes.

Exposure of β-cells to high levels of glucose and fatty acids results in an increase in CD40 expression, which has been reported to induce the activation of inflammatory

pathways and NF-κB, leading to cell death [243-244]. Previous work has shown that subjects from India with diabetes have approximately 3 times higher soluble CD40L levels in their plasma than individuals with normal glucose tolerance [330]. Similar findings were also reported in a subsequent study in Europeans with T2D [331]. As a consequence, the combination of high soluble CD40L levels in diabetes along with upregulated expression of functional receptor in β-cells suggests that CD40 signalling can have an important role in the development of inflammation in glucolipotoxicity induced diabetes.

These preliminary studies open the way to the investigations performed in the next chapter, in order to characterise CD40 and its function in the β-cell in relation to glucolipotoxicity.

Chapter 4

New role for CD40 in pancreatic

β-cell

4.1 Introduction

CD40 is a membrane glycoprotein and member of the TNFR superfamily, as such as it is sometimes referred to as TNFR5.

CD40 is expressed in many different immune and non-immune cell types. In B-lymphocytes, macrophages and APC cells, binding of CD40 by CD40L plays a principal role in the immune system, inducing differentiation, cell survival, and proliferation. CD40 expression is also reported in non-hematopoietic cells, and its activation is mostly associated with non-specific inflammatory responses. A functional CD40 is also expressed in mouse and human pancreatic β-cells and is able to induce inflammatory responses [242-244]. These events activate inflammatory pathways, inducing cytokine/chemokine synthesis and secretion, which results in recruitment and activation of immune cells and downstream activation of NF-κB [213].

Like other members of TNFR superfamily, CD40 signalling is mediated principally by TRAFs, that link CD40 to downstream signalling pathways [213]. The cytoplasmic domain of CD40 contains two independent membrane TRAF-binding domains: a proximal region binding TRAF6 and a distinct distal domain that binds TRAF-1/2/3/5. Different TRAFs binding to CD40 triggers distinct signalling pathways leading to a variety of functional outcomes, depending on the cell types involved. For example, they can activate the canonical and non canonical NF-κB signalling pathways, the mitogen MAPK, PI3K and phospholipase Cc (PLCc) pathways [214].

In the previous chapter we demonstrated that CD40 expression is upregulated in INS-1 cells after chronic exposure to high concentrations of glucose and fatty acids. These results were confirmed *in vivo*, in islets of mice fed a high fat diet and in human islets cultured in palmitate.

These data suggest a role for CD40 in the development of glucolipotoxicity-induced inflammation during the progression to T2D and it opens the possibility that CD40 has a potential new role in regulation of β-cell function.

In this chapter, we aimed to characterise the role of CD40 in the β-cell. In particular, we investigated whether CD40 had a role in cell viability and β-cell function. We analysed

if CD40 was able to influence insulin secretion and production and if it regulated the expression of downstream genes in its pathway, in particular TRAF proteins.

4.2 CD40 is able to activate NF-κB

Previous studies demonstrated that activation of CD40 with pro-inflammatory cytokines is able to activate NF-κB [244]. NF-κB is a transcription factor composed of different subunits. When it is activated by an inflammatory stimulus, NF-κB subunit p65 translocates to the nucleus where it is able to activate the transcription of downstream genes. As a consequence, NF-κB p65 expression in the nucleus is a good readout of its activation. Downstream NF-κB activation is important in regulating cellular responses and it controls many genes involved in inflammatory processes. Its prolonged activation is partly responsible for the inflammatory status and β-cell failure observed during the progression to T2D [144].

Here, we investigated if CD40 was able to activate NF-κB in our experimental system, in order to determine if CD40 upregulation and activation in glucolipotoxicity could induce NF-κB responses. We used immunofluorescence to analyse NF-κB p65 subunit translocation in the nucleus and we activated CD40 using CD40L.

4.2.1 Activation of CD40 induces NF-κB p65 translocation in the nucleus

In order to determine if the activated CD40 is able to activate NF-κB, INS-1 cells were cultured onto coverslips and incubated with CD40L (1 μg/ml) for 6h. This timepoint was chosen according to experiments performed previously in my group, showing activation of CD40 after 6h incubation with CD40L. Cells were then fixed and stained with NF-κB p65 polyclonal antibody (green) and DAPI (blue).

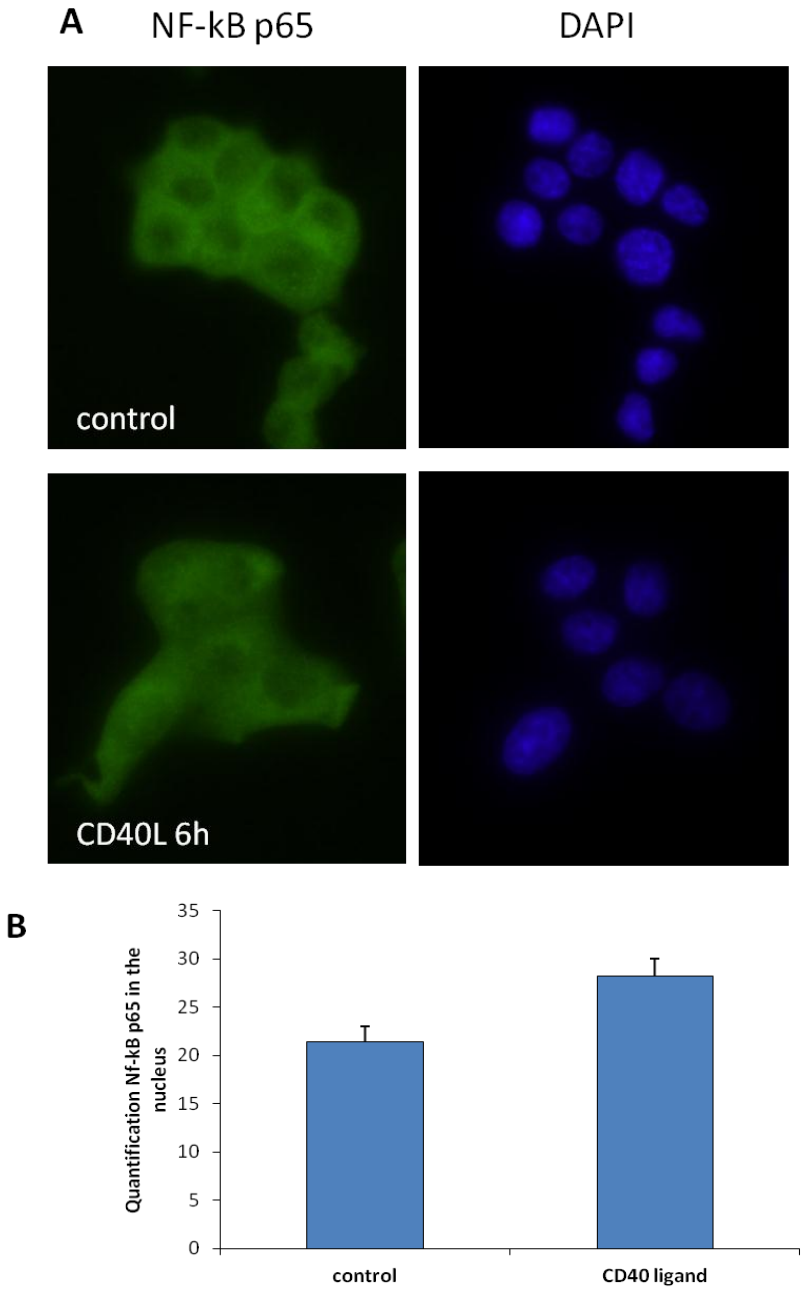

Figure 4.1 Activation of CD40 can induce NF-κB p65 translocation to the nucleus. INS-1 cells were cultured onto coverslips and incubated with CD40L (1 μg/ml) for 6h. Cells were then fixed and stained with NF-κB p65 polycolonal antibody (green) and DAPI (blue). A) Images were taken with a Leica EpiFluo microscope with a 63x objective (representative image of 3 independent experiments). B) Quantification of p65 translocation in the nucleus using the program Image J. Data are expressed as mean + SD of 10 cells from one experiment.

Figure 4.1A shows that, in control conditions, no p65 staining (green) was detected in the nucleus, indicating that p65 was located mainly in the cytoplasm. Instead, in presence of CD40L, we observed a quantitative increase of the green signal in the nucleus. P65 translocation was also quantified using the program ImageJ, which is an image processing program that allows the quantification of the fluorescence signals. Figure 4.1B shows a 20% increase in p65 signal in the nucleus when INS-1 cells were incubated with CD40L. This result indicates that CD40 activation by CD40L is able to induce p65 translocation in the nucleus and, consequently, NF-κB activation, which will likely induce the transcription of the target genes.

These data were also confirmed by other experiments performed by Dr. Nedjai in my group, who measured NF-κB p65 translocation in the nucleus using Transam NF-κB ELISA kit (Active Motif, Carlsbad, CA). Briefly, oligonucleotides containing NF-κB consensus binding site were immobilized onto 96-well plates and p65 subunit activity detected in INS-1 cells treated with either high glucose, TNF-α, or CD40L. These data showed that 72h incubation of INS-1 cells in 28 mM glucose resulted in an increased level of NF-κB activity similar to that observed following 2h exposure of cells to 100 ng/ml of TNF. INS-1 cells incubated under standard glucose concentrations elicited a half-maximal induction of NF-κB activity when exposed for 6h to 1 μg/ml CD40L (Figure 4.2). As a consequence CD40 upregulation and activation could be responsible of most of the NF-κB activation in glucolipotoxicity.

These results were consistent with previous data reported in the literature [243-244].

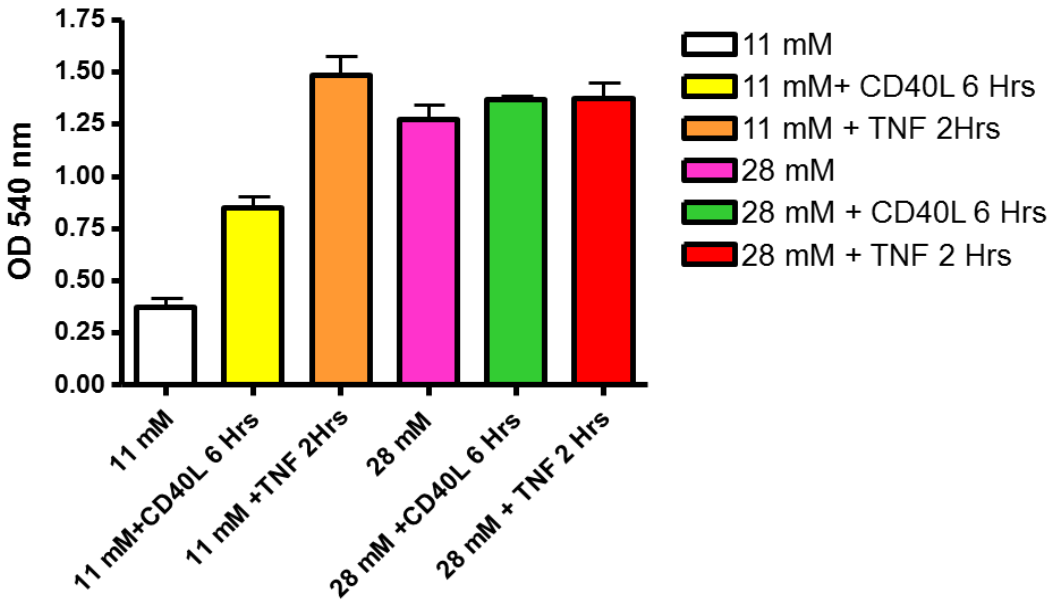

Figure 4.2 Activation of CD40 is responsible of most of NF-κB activation in glucolipotoxicity. INS-1 cells were cultured in RPMI containing 11 or 28 mM glucose and subsequently incubated with CD40 ligand (1 μg/ml) or TNF-α (100 ng/ml) for 6h. Lysates were then used to measure NF-κB p65 translocation in the nucleus, using Transam NF-κB ELISA kit (Active Motif, Carlsbad, CA). Data are expressed as mean + SD of 3 independent experiments performed in duplicate.

4.3 Effect of CD40 downregulation on cell viability

While the role of CD40 in NF-κB activation has already been reported, nothing is currently known on the effect of CD40 on cell viability and function in the context of the β-cell and in relation to glucolipotoxicity. The most straightforward way to investigate this would be to overexpress CD40, therefore simulating the situation observed in glucolipotoxicity, and to determine the effects of this overexpression in the β-cell. However, INS-1 cells are quite difficult to transfect, therefore it would have been difficult to obtain a good level of gene overexpression. For this reason we decided to perform the opposite approach, i.e. downregulating CD40 using siRNA technology to investigate the effects on the β-cell.

Specifically, in these experiments, we aimed to determine if CD40 has a role in the regulation of cell number, apoptosis, mitochondrial activity and cell cycle progression.

4.3.1 CD40 knock-down optimisation

To investigate the effect of CD40 silencing on the β-cell viability and function, it is necessary to obtain at least a 75% knock-down of the gene of interest at RNA level, in order to see the biological effects at the protein level in the cells. Therefore, an optimisation process was required to identify the optimal experimental conditions for CD40 downregulation.

First we used specific siRNAs purchased from Qiagen (Venlo, Netherlands), using electroporation as a transfection method. INS-1 cells were transfected with 1 μM (5 μl from stock 20 μM) of a "scrambled", not targeting siRNA and 3 different siRNAs specific for CD40. Cells were lysed after 72h and total RNA extracted. RT-qPCR was performed using primers specific for CD40. Figure 4.3 shows a slight decrease in CD40 expression using siRNA1, but it reached only a 25% of knock-down, which was not enough to see an effect at the protein level.

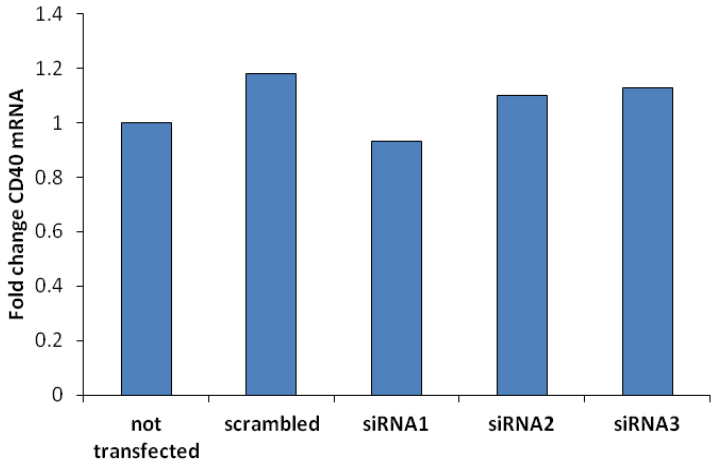

Figure 4.3 CD40 downregulation using electroporation and Qiagen siRNAs. INS-1 cells were transfected with 5 μl of a scrambled and 3 different siRNAs and after 72h lysed and total RNA extracted. RT-qPCR was performed using primers specific for CD40. Data represent ΔΔCt values expressed as a fold change compared to not transfected cells (control). Data are from one experiment.

We then tested whether CD40 downregulation could be achieved by chemical transfection, using Lipofectamine 2000 or RNAiMax (Life Technologies, UK) as transfection reagents. INS-1 cells were transfected with 80 or 320 nM of siRNA1 and

Lipofectamine 2000 or RNAimax, lysed after 72h and total RNA extracted. RT-qPCR was performed using primers specific for CD40. No effect on CD40 mRNA levels was detected using these experimental conditions (Figure 4.4).

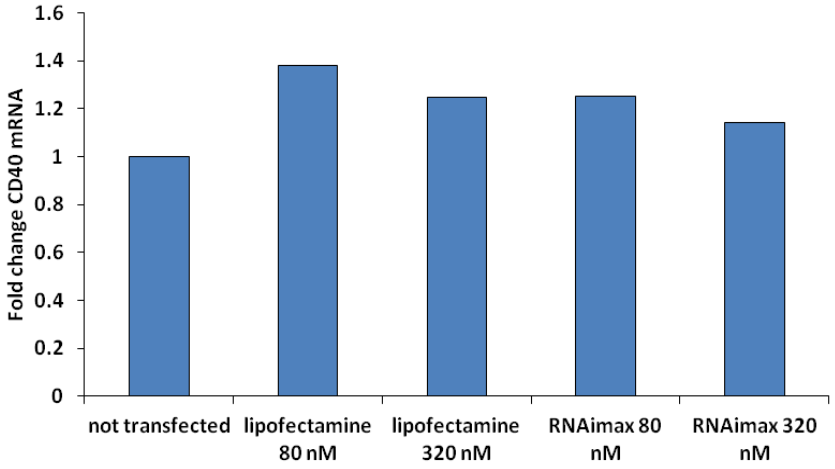

Figure 4.4 CD40 downregulation using lipofectamine and Qiagen siRNAs. INS-1 cells were transfected with 80 or 320 nM of siRNA1 using Lipofectamine or RNAimax as transfection reagents (10 µl). After 72h cells were lysed and total RNA extracted. RT-qPCR was performed using primers specific for CD40. Data represent ΔΔCt values expressed as a fold change compared to not transfected cells (control). Data are from one experiment.

As the Qiagen sequences were not very effective in our experimental system, we decided to try different sequences, purchased from Dharmacon (GE Healthcare, UK), and to transfect them using either electroporation or Lipofectamine RNAimax. In Figure 4.5A, INS-1 cells were transfected with 200 nM of a "scrambled" and 4 different siRNAs specific for CD40, using 30 µl RNAimax. Cells were lysed after 72h and total RNA extracted. RT-qPCR was performed using primers specific for CD40. Using this protocol, siRNAs 6 and 8 were able to downregulate CD40 mRNA levels compared to the scrambled sequence (55% knock-down). On the other hand, siRNA 7 led to a 45% downregulation and siRNA 5 had no effect at all. In Figure 4.5B INS-1 cells were transfected by electroporation with 1 µM of the 4 different siRNAs specific for CD40. Cells were lysed after 72h and total RNA extracted. RT-qPCR was performed using primers specific for CD40. In these experimental conditions only siRNA 6 led to a 20% downregulation, whereas the other siRNAs had no effect.

Considering that chemical transfection gave better results than electroporation in this experimental system, we decided to use RNAimax as a transfection reagent for all the future experiments. We needed, however, to further optimise the conditions, varying the concentrations of siRNA and RNAiMax, in order to obtain a more efficient downregulation.

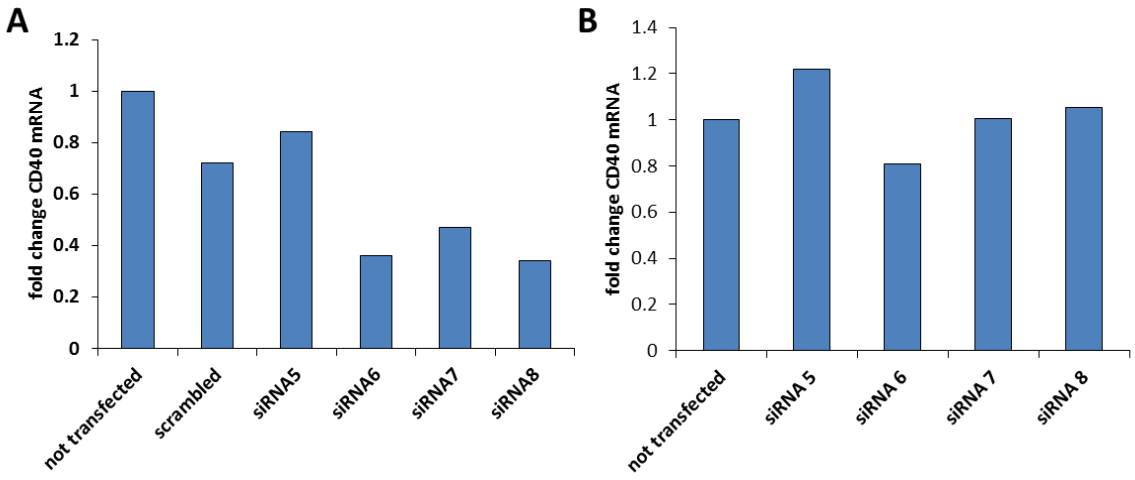

Figure 4.5 CD40 downregulation using Dharmacon siRNAs. A) INS-1 cells were transfected with 200 nM of a "scrambled" and 4 different siRNAs specific for CD40, using 30 µl RNAimax. After 72h cells were lysed and total RNA extracted. RT-qPCR was performed using primers specific for CD40. B) INS-1 cells were transfected with 1 µM of 4 different siRNAs specific for CD40, by electroporation. Cells were lysed after 72h and total RNA extracted. RT-qPCR was performed using primers specific for CD40. Data represent ΔΔCt values expressed as a fold change compared to not transfected cells (control). Data are from one experiment.

Based on the data in Figure 4.5A, we decided to further optimise siRNA 6 and 8 which proved to be the most effective in inducing CD40 downregulation. We used also siRNA 5 as a negative control. We changed the amounts of lipofectamine and siRNA used, in order to optimise the protocol, transfecting INS-1 cells with 70 nM of a "scrambled" and 3 different siRNAs specific for CD40, using 7 µl of RNAimax. RT-qPCR was performed as before. Figure 4.6 shows that this protocol induced a strong downregulation in cells transfected with siRNA 6 (85% knock-down) which would be sufficient to see a biological effect in the β-cell. Therefore, these conditions were used in all the subsequent experiments presented in this chapter.

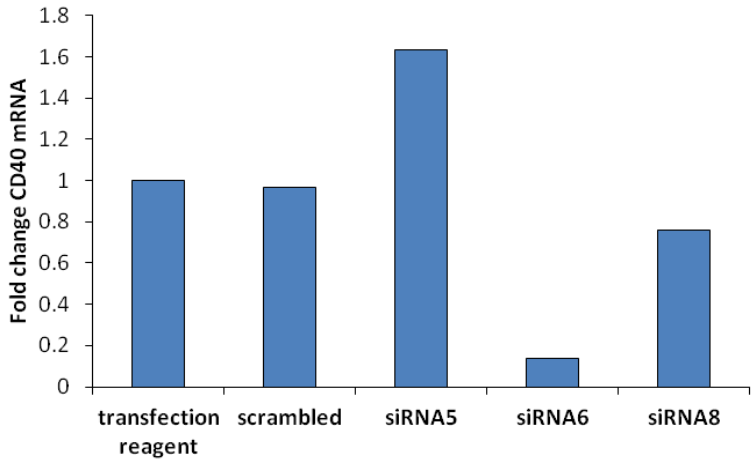

Figure 4.6 CD40 downregulation optimisation using RNAimax. INS-1 cells were transfected with 7 µl of a "scrambled" and 3 different siRNAs specific for CD40, using 7 µl of RNAimax. Cells were lysed after 72h, total RNA extracted and RT-qPCR was performed using primers specific for CD40. Data represent ΔΔCt values expressed as a fold change compared to not transfected cells (control). Data are from one experiment.

4.3.2 Validation of CD40 downregulation at the protein level

Given that RNA expression does not always equate to protein expression, it became necessary to check if also CD40 protein expression decreases after 72h of transfection with siRNA 6. INS-1 cells were transfected with a "scrambled" and a siRNA specific for CD40. After 72h cells were lysed in Triton-X100 buffer and protein separated on a 12.5% SDS PAGE gel. The gel was then transferred to nitrocellulose and immunoblotted with anti CD40 polyclonal antibody. Figure 4.7 shows that siRNA6 was able to induce a 50% reduction of CD40 protein expression compared to scrambled siRNA, indicating that CD40 was successfully downregulated at protein level.

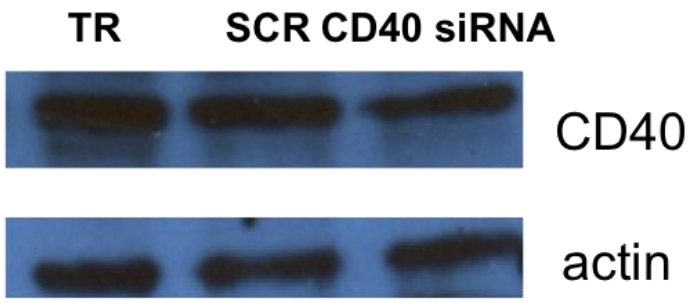

Figure 4.7 CD40 downregulation at the protein level. INS-1 cells were transfected with RNAiMax alone (TR), "scrambled" (SCR) and a siRNA specific for CD40. Cells were lysed in Triton-X100 buffer after 72h and protein separated on a 12.5% SDS PAGE gel. The gel was then transferred to nitrocellulose and immunoblotted with anti CD40 polyclonal antibody. Actin was used as a loading control. Image is representative of 3 independent experiments.

4.3.3 Effect of CD40 downregulation on cell number

In order to assess if CD40 has a role on cell viability in control conditions, INS-1 cells were transfected with a "scrambled" and a siRNA specific for CD40. After 72h cells were collected and counted using a Neubauer chamber. Figure 4.8 shows no change in cell number upon CD40 downregulation, indicating that CD40 is not involved in cell viability.

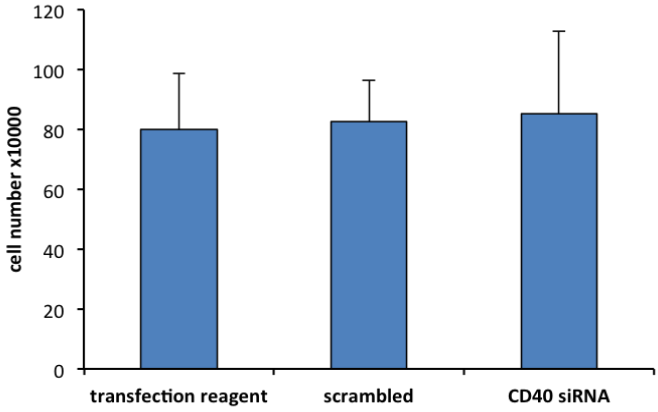

Figure 4.8 Effect of CD40 downregulation on cell number. INS-1 cells were transfected with a scrambled and a siRNA targeting CD40 gene. After 72h cells were collected and counted using a Neubauer chamber. Data represent number of cells expressed as absolute value. Data are means + SD of 3 independent experiments performed in duplicate.

4.3.4 Effect of CD40 downregulation on caspase 3 activation

We demonstrated above that CD40 downregulation does not affect cell number, and, as a consequence, it does not stimulate or reduce cell proliferation. In addition to this, we further investigated if CD40 downregulation could have an effect on apoptotic events, such as the activation of caspase 3.

In order to test this, INS-1 cells were transfected with a scrambled and a siRNA targeting CD40 gene. After 72h, cells were lysed and caspase 3 activity was measured using EnzCheck Caspase-3 Assay Kit #2 (Life Technologies, UK). No significant changes in caspase 3 activity were detected upon downregulation of CD40 (Figure 4.9).

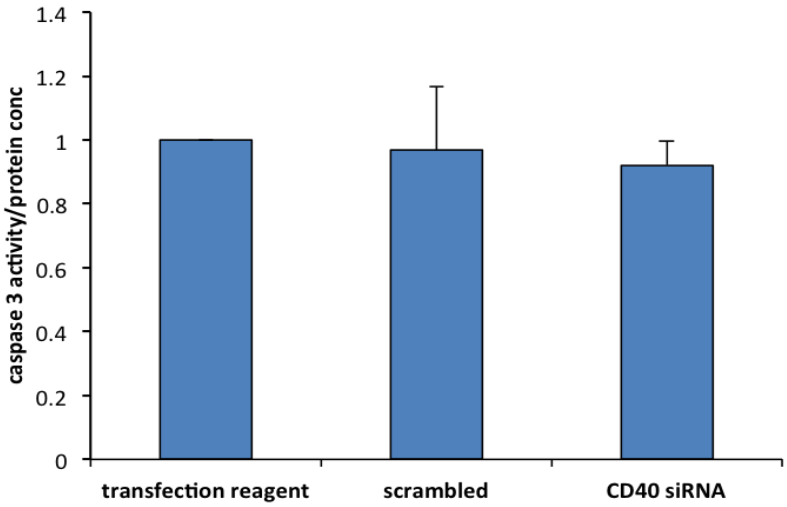

Figure 4.9 Effect of CD40 downregulation on caspase 3 activation. INS-1 cells were transfected with a scrambled and a siRNA targeting CD40 gene. After 72h cells were lysed and apoptosis determined via caspase 3 activity. Data represent fluorescence values at excitation/emission ~496/520 nm normalised to total protein concentration and are expressed as fold change compared to cells transfected with only the transfection reagent. Values are means + SD from 3 independent experiments performed in duplicate.

4.3.5 Effect of CD40 downregulation on cell cycle

Consistent with data obtained with caspase 3 assay, no change in the number of cells in subG1 phase was observed by FACS. Cells were transfected for 72h with a "scrambled" and a siRNA specific for CD40, fixed and incubated in a solution of propidium iodide.

Cells were then sorted using a FACS machine, separating them according to their DNA content to determine the percentage of cells in the distinct phases of the cell cycle.

TRANSFECTION REAGENT	SCRAMBLED	CD40 siRNA
2.2 + 0.9 %	2 + 0.7 %	2.3 + 1.0 %

Table 4.1 Percentage of cells in subG1. Numbers represents the percentage of cells in subG1 phase. Values are mean + SD from 3 independent experiments.

Table 4.1 shows the percentage of cells in subG1 phase and indicates that there was no significant difference in the number of cells in subG1 upon CD40 downregulation, indicating no activation of apoptosis.

Figure 4.10 shows the results of cell cycle analysis upon CD40 downregulation. Data indicate a slight increase of cells in G1 phase and decrease in G2 phase in cells lacking CD40, compared to scrambled cells. During G1 phase cells increase their size and synthesize mRNA and proteins. Given these results, we can hypothesise that the downregulation of CD40 induced a slight increased cell activity that could influence also β-cell function.

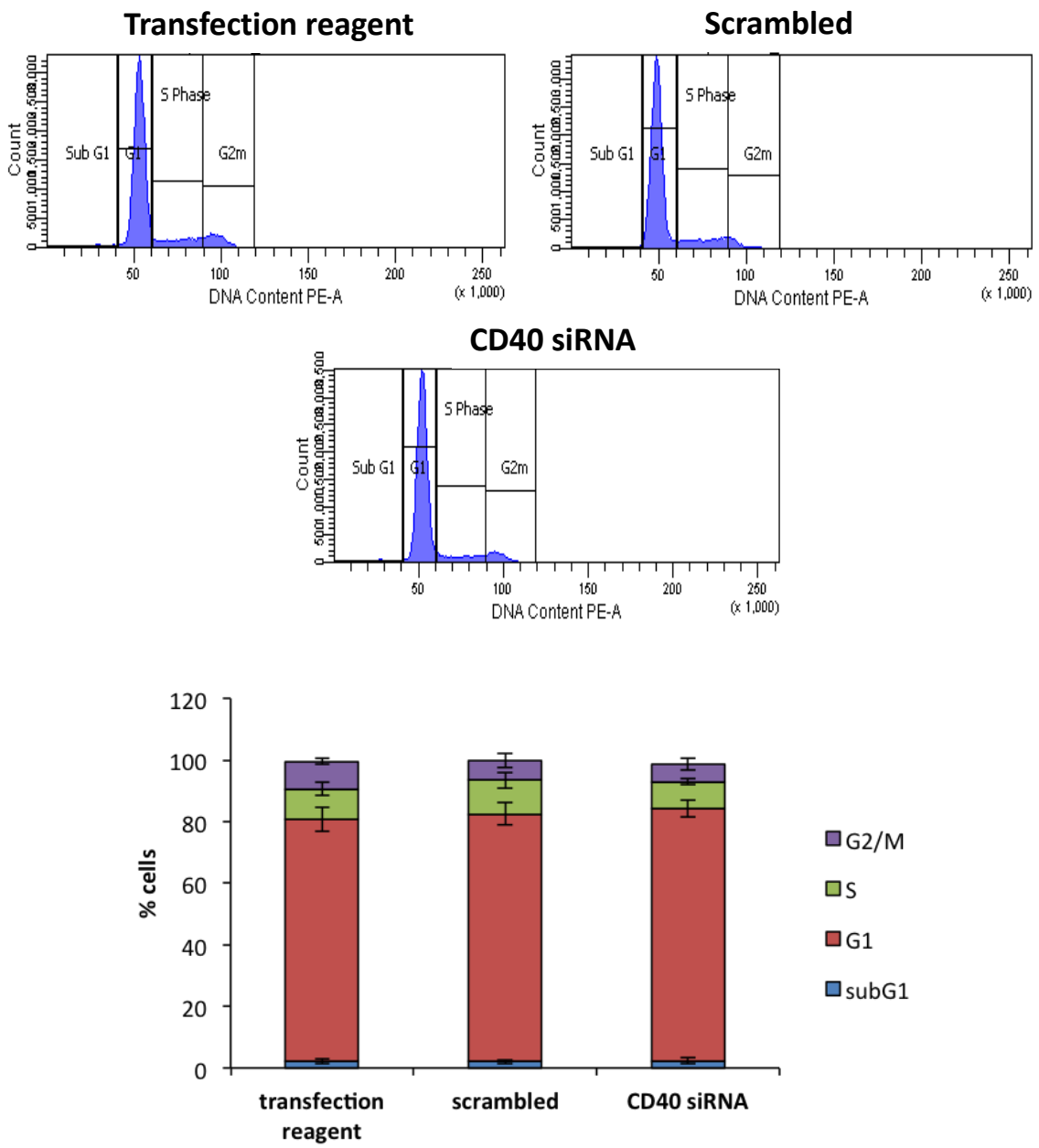

Figure 4.10 Effect of CD40 downregulation on cell cycle progression. Cells were transfected for 72h with a scrambled and a siRNA specific for CD40, fixed and sorted by FACS to analyse the cell cycle. Values are means ± SD from 3 independent experiments.

4.4 CD40 and insulin secretion and production

In the previous chapter we demonstrated that glucolipotoxicity reduces insulin production and secretion, impairing β-cell function. At the same time, glucolipotoxicity

increases the expression of CD40, revealing a role for this receptor in the β-cell. Here we wanted to determine if the increase in CD40 expression could be partly responsible for the reduction of insulin in glucolipotoxicity, and therefore if CD40 is able to influence insulin secretion and production.

In order to address this aim, we investigated the effect of CD40 downregulation on insulin mRNA levels, insulin content and secretion.

4.4.1 Effect of CD40 downregulation on insulin mRNA levels

In order to determine if CD40 downregulation can influence insulin mRNA expression, INS-1 cells were transfected with a "scrambled" and a siRNA specific for CD40. After 72h, cells were lysed, RNA extracted and RT-qPCR performed using primers specific for the insulin gene.

Figure 4.11A shows that the siRNA used as control (scrambled siRNA) did not affect insulin mRNA levels in our experimental system.

Importantly, downregulation of CD40 induced a 1.7 fold increase ($p<0.05$) in insulin mRNA (Figure 4.11B). This result suggests a potential new role for CD40 in the regulation of β-cell function.

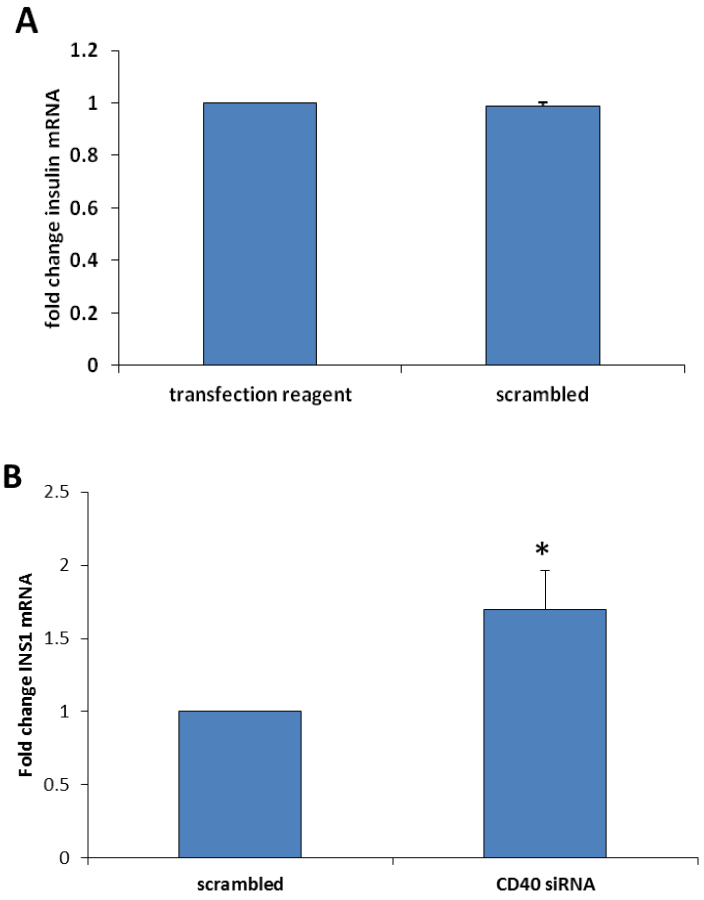

Figure 4.11 Effect of CD40 downregulation on insulin mRNA levels. INS-1 cells were transfected with transfection reagent alone, a scrambled and a siRNA specific for CD40. Cells were lysed after 72h, RNA extracted and RT-qPCR performed using primers specific for insulin gene. A) Data represent ΔΔCt values expressed as a fold change compared to cells transfected with transfection reagent only. Data are expressed as means + SD of 2 independent experiments. B) Data represent ΔΔCt values expressed as a fold change compared to cells transfected with a scrambled siRNA. Data are expressed as means + SD of 4 independent experiments (*$p<0.05$).

4.4.2 Effect of CD40 downregulation on insulin content

Insulin biosynthesis at RNA level may not be indicative of the amount of insulin protein inside the cell. In order to assess if CD40 downregulation is able to influence the total insulin content, INS-1 cells were transfected with a "scrambled" and a siRNA specific for CD40. After 72h cells were lysed using acid-ethanol extraction and total insulin content measured using Mercodia ELISA kit (Uppsala, Sweden). As shown in Figure 4.12 CD40 downregulation induced a 1.3 fold increase in the total insulin content.

Taken together, these results indicate that the downregulation of CD40 increases both insulin mRNA and insulin content.

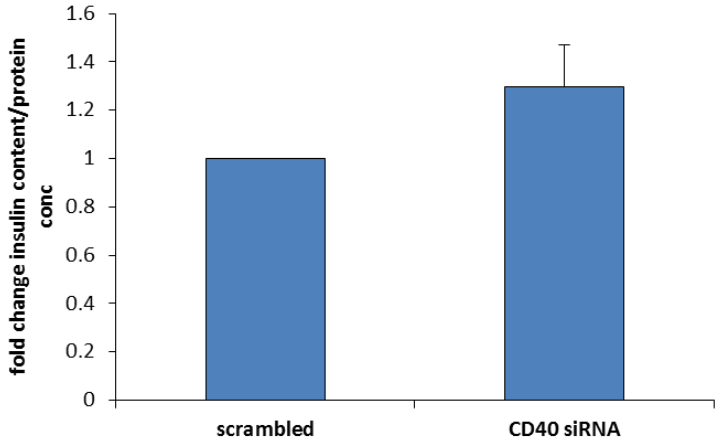

Figure 4.12 CD40 downregulation and insulin content. INS-1 cells were transfected with a scrambled and a siRNA specific for CD40. Cells were lysed after 72h using acid-ethanol extraction and total insulin content measured using Mercodia ELISA kit. Data represent ng of insulin secreted per µg of total protein. Data are means + SD from 3 independent experiments.

4.4.3 Effect of CD40 downregulation on insulin secretion

We then decided to investigate the effect of CD40 downregulation on insulin secretion. To this end, INS-1 cells were transfected with a "scrambled" and a siRNA specific for CD40. After 72h, cells were treated with a secretagogue cocktail to stimulate insulin secretion and the amount of secreted insulin measured using Mercodia ELISA kit (Uppsala, Sweden).

Figure 4.13 shows the effect of CD40 downregulation on insulin secretion. A 1.5 fold increase ($p<0.05$) in insulin secretion was detected in cells lacking CD40, indicating that CD40 also regulates insulin secretion.

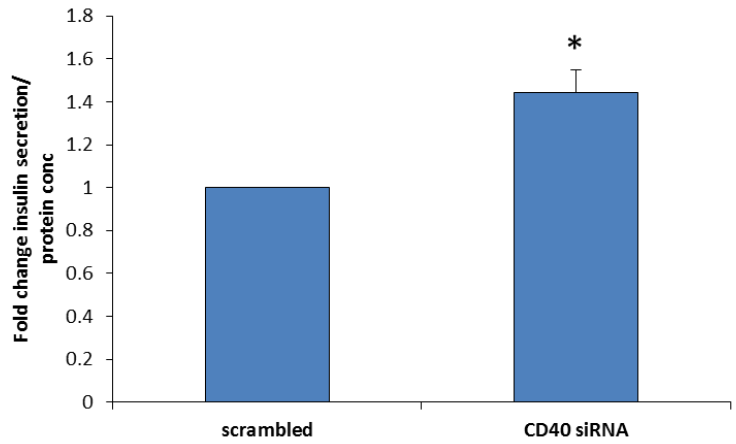

Figure 4.13 Effect of CD40 downregulation on insulin secretion. INS-1 cells were transfected with a scrambled and a siRNA specific for CD40. After 72h, cells were treated with a cocktail to stimulate insulin secretion and the amount of insulin secreted measured with Mercodia ELISA kit. Data represent ng of insulin secreted per μg of protein. Data are means + SD from 3 independent experiments (*$p<0.05$).

4.4.4 CD40 downregulation in glucolipotoxicity

Previously we showed that insulin mRNA levels decrease and CD40 expression increases when INS-1 cells are exposed to glucolipotoxic conditions. In addition, when CD40 is downregulated, in normal RPMI (11 mM glucose) conditions, insulin mRNA levels increase.

We then decided to investigate if the downregulation of CD40 in glucolipotoxicity is able to restore the impaired insulin expression. In order to assess this, INS-1 cells were transfected with a "scrambled" and a siRNA specific for CD40 gene. The following day cells were incubated in RPMI-1640 media supplemented with 27 mM glucose, 200 μM oleic acid, 200 μM palmitic acid for 72h. After the incubation time, cells were lysed, RNA extracted and RT-qPCR performed using primers specific for CD40 and insulin gene.

Figure 4.14 shows the effect of CD40 knock-down on CD40 and insulin mRNA levels in control and in glucolipotoxic conditions. Figure 4.14A shows the expression of CD40: glucolipotoxicity induced an increase in CD40 expression also in presence of CD40 siRNA. These RNA levels almost equated the level in scrambled cells in control

conditions. Figure 4.14B shows the expression of insulin: a 1.5 fold increase in insulin mRNA could be detected with CD40 knock-down also in glucolipotoxic conditions, indicating that the downregulation of CD40 was able to partly restore the impaired insulin expression in glucolipotoxicity. However, in these experimental conditions, CD40 mRNA levels were higher in glucolipotoxicity than in control conditions, also when cells were transfected with CD40 siRNA. Therefore, CD40 mRNA levels were not reduced enough to see a complete recovery of insulin expression in glucolipotoxicity.

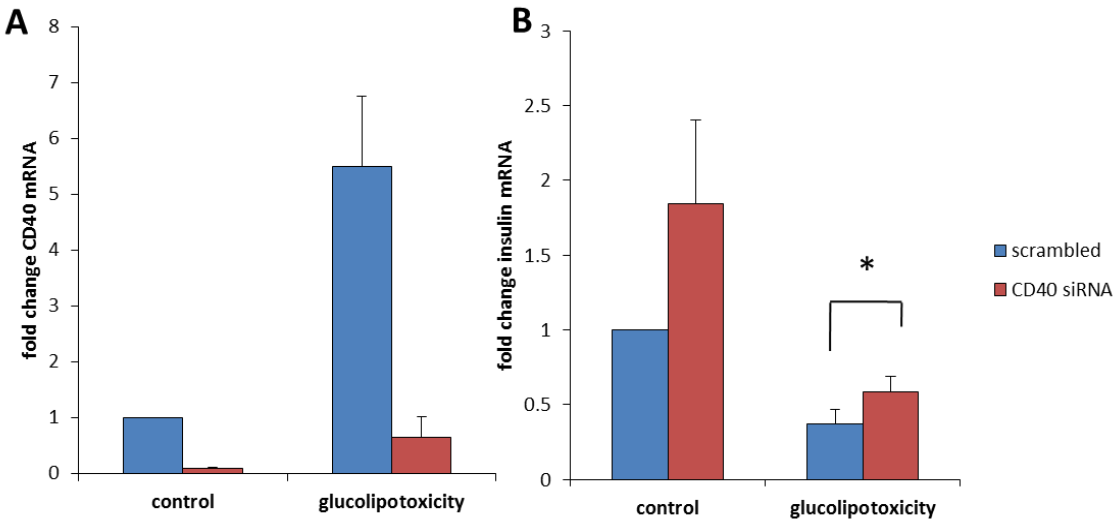

Figure 4.14 Effect of CD40 downregulation on insulin in glucolipotoxicity. INS-1 cells were transfected with a scrambled and a siRNA specific for CD40. The following day, the transfected cells were treated with RPMI-1640 supplemented with 27 mM glucose, 200 μM oleic acid, 200 μM palmitic acid. After 72h, cells were lysed, RNA extracted and RT-qPCR performed using primers specific for CD40 (A) and for insulin gene (B). Data represent ΔΔCt values expressed as a fold change compared to cells transfected with a scrambled siRNA in control conditions (normal RPMI). Data are expressed as means + SD of 3 independent experiments (*$p<0.05$).

4.4.5 Effect of CD40 downregulation on insulin transcription factors

We showed above that downregulation of CD40 is able to increase insulin biosynthesis, both in control than in glucolipotoxic conditions.

It is known that insulin promoter is regulated by different transcription factors, and high concentrations of glucose and fatty acids can affect not only their binding activity but

also their expression. In particular, PDX-1 and MafA, the main insulin transcription factors, show a reduced mRNA expression in glucolipotoxicity [136].

To assess whether CD40 can influence insulin transcription by affecting the expression of one or more of its transcription factors, INS-1 cells were transfected with a "scrambled" and a siRNA specific for CD40. RT-qPCR was performed using primers specific for PDX-1, TFAM, HNF1, MafA as before. Figure 4.15 shows the results of the qPCR performed on the insulin transcription factors. Data indicate that downregulation of CD40 did not affect the expression of any of the transcription factors analysed.

These results suggest that CD40 influences insulin transcription through a mechanism that is independent from the expression of its transcription factors.

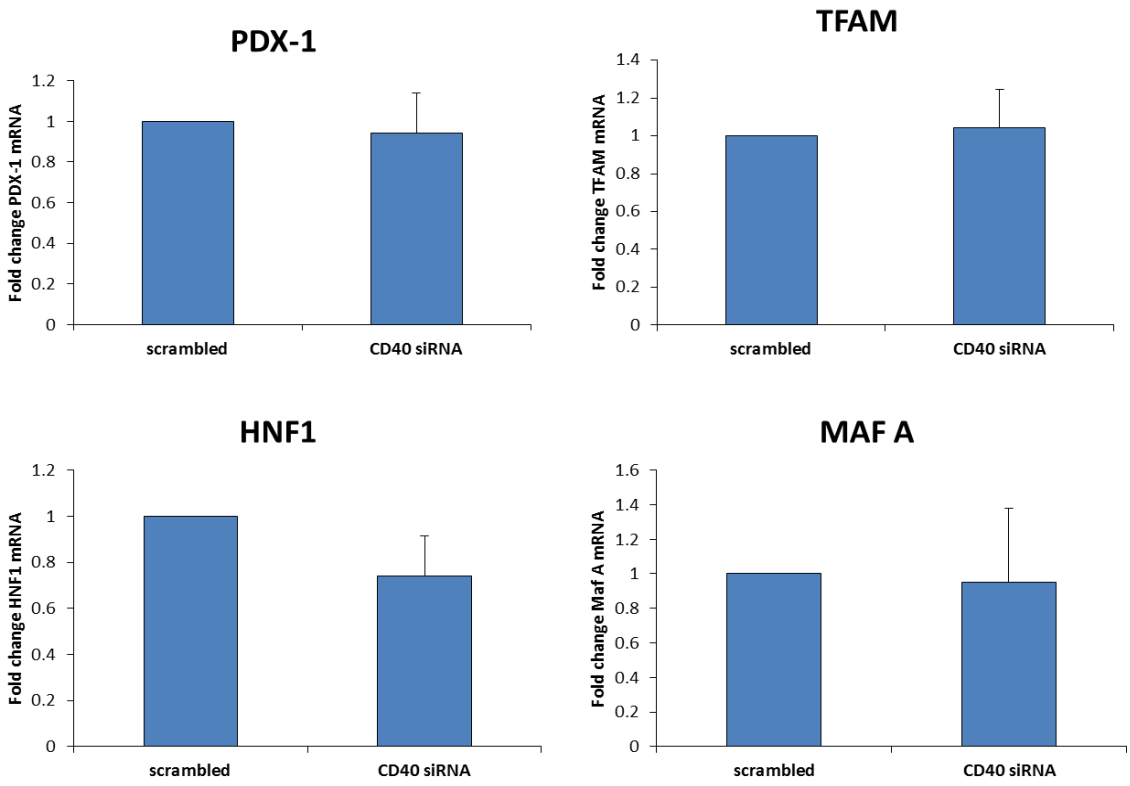

Figure 4.15 Effect of CD40 downregulation on the mRNA levels of insulin transcription factors. INS-1 cells were transfected with a scrambled and a siRNA specific for CD40. After 72h cells were lysed, RNA extracted and qPCR performed using primers specific for PDX-1, TFAM, HNF1, Maf A. Data represent ΔΔCt values expressed as a fold change compared to cells transfected with a scrambled siRNA. Data are expressed as means + SD of 3 independent experiments.

4.4.6 Presence of NF-κB binding sites on insulin promoter

In the previous paragraph we showed that CD40 downregulation does not affect the expression of the insulin transcription factors, indicating that the increase of insulin secretion and production observed upon CD40 downregulation is not due to a mechanism involving the expression of conventional insulin transcription factors.
We therefore hypothesized that CD40 could either:

- influence the binding of insulin transcription factors or
- activate NF-κB, which, in turn, could influence insulin transcription.

Our previous data indicated that CD40 is able to activate NF-κB, therefore, to determine if NF-κB can regulate insulin, we checked if there are some NF-κB consensus binding sites ahead of the insulin gene. NF-κB consensus sequence is known to be 5'GGGACTTTCC-3', but we did not find this nucleotide sequence in the insulin promoter area. However, NF-κB is able to bind also to the generic sequence 5'GGGRNNYYCC-3', where R is a purine and Y a pyrimidine. We subsequently used the online program TF search (http://www.cbrc.jp/research/db/TFSEARCH.html), which allows the identification of the potential transcription factors binding sites in a given sequence. This program identified a possible p65 binding site, laying 1600 bp ahead of the insulin gene.
This finding opens the possibility that CD40 could regulate insulin transcription through NF-κB. Further investigations are necessary to establish if NF-κB is able to effectively bind insulin promoter and if CD40 downregulation could modify NF-κB binding.

4.5 Effect of CD40 downregulation on downstream signalling

In the previous paragraphs we demonstrated that downregulation of CD40 does not influence cell viability but is able to affect insulin biosynthesis and secretion. In order to determine if CD40 downregulation affects other β-cell functions, as the expression of other genes of the TNFR pathway, we checked the expression of these genes in scrambled and in knock-down cells. In particular, because of the potential link with the NF-κB pathway, we focused on TRAF proteins, adaptor molecules downstream of

CD40 signalling, analysing their expression with CD40 downregulation and their role in glucolipotoxicity.

4.5.1 Role of CD40 on TRAFs expression levels

To determine if CD40 signalling is able to influence the expression of other members of the TNFR pathway, we determined the effect of its downregulation. RT-qPCR was performed as before using primers specific for TRAF1, TRAF2, TRAF3 and TRAF6. Figure 4.16 shows the expression of TRAFs proteins upon CD40 downregulation. These data indicate a trend for a decrease in TRAF1 (25%), TRAF2 (25%) and TRAF6 (30%) expressions upon CD40 knock-down; TRAF3 expression, on the other hand, was not affected.

These results suggest the possibility of a link between CD40 and the downstream TRAF proteins, in particular TRAF1, TRAF2 and TRAF6. Interestingly, it has ben shown that TRAF1, TRAF2 and TRAF6 are able to activate NF-κB [176, 180]. The fact that CD40 downregulation could be able to modulate TRAFs expression suggests that CD40 blockade may possibly inhibit NF-κB activation and the consequent inflammatory process. These data open the possibility of development of novel therapeutic strategies, blocking CD40 and its downstream signalling.

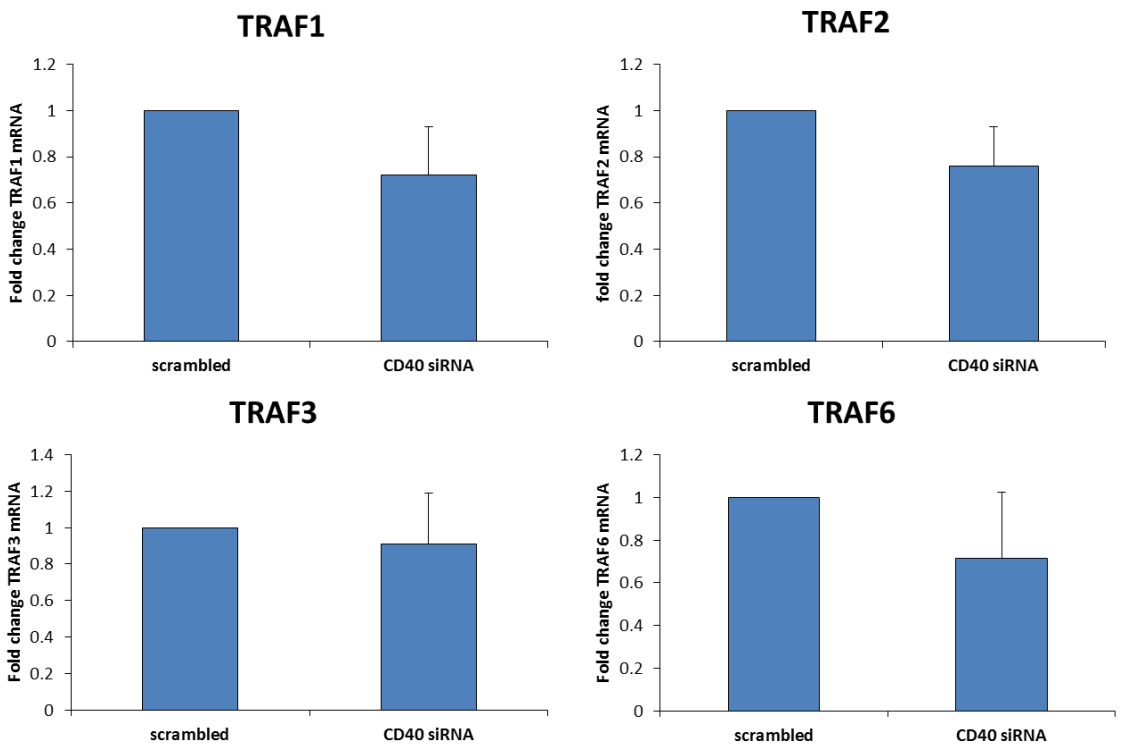

Figure 4.16 Effect of CD40 downregulation on TRAF proteins. INS-1 cells were transfected with a scrambled and a siRNA specific for CD40. Cells were lysed after 72h, RNA extracted and qPCR performed with primers specific for TRAF1, TRAF2, TRAF3 and TRAF6. Data represent ΔΔCt values expressed as a fold change compared to cells transfected with a scrambled siRNA. Data are expressed as means + SD of 3 independent experiments.

4.5.2 TRAFs mRNA levels in glucolipotoxicity

As TRAF1, TRAF2 and TRAF6 mRNA levels decrease when CD40 expression decreases, we decided to assess their levels in glucolipotoxicity, when CD40 is overexpressed. To investigate this, INS-1 cells were cultured for 72h in RPMI-1640 supplemented with 27 mM glucose, 200 μM oleic acid, 200 μM palmitic acid in different combinations. After the incubation time, cells were lysed, RNA extracted and qPCR performed using primers specific for TRAF1, TRAF2, TRAF3 and TRAF6.

Figure 4.17 shows that all TRAFs mRNA levels were similar in control conditions.

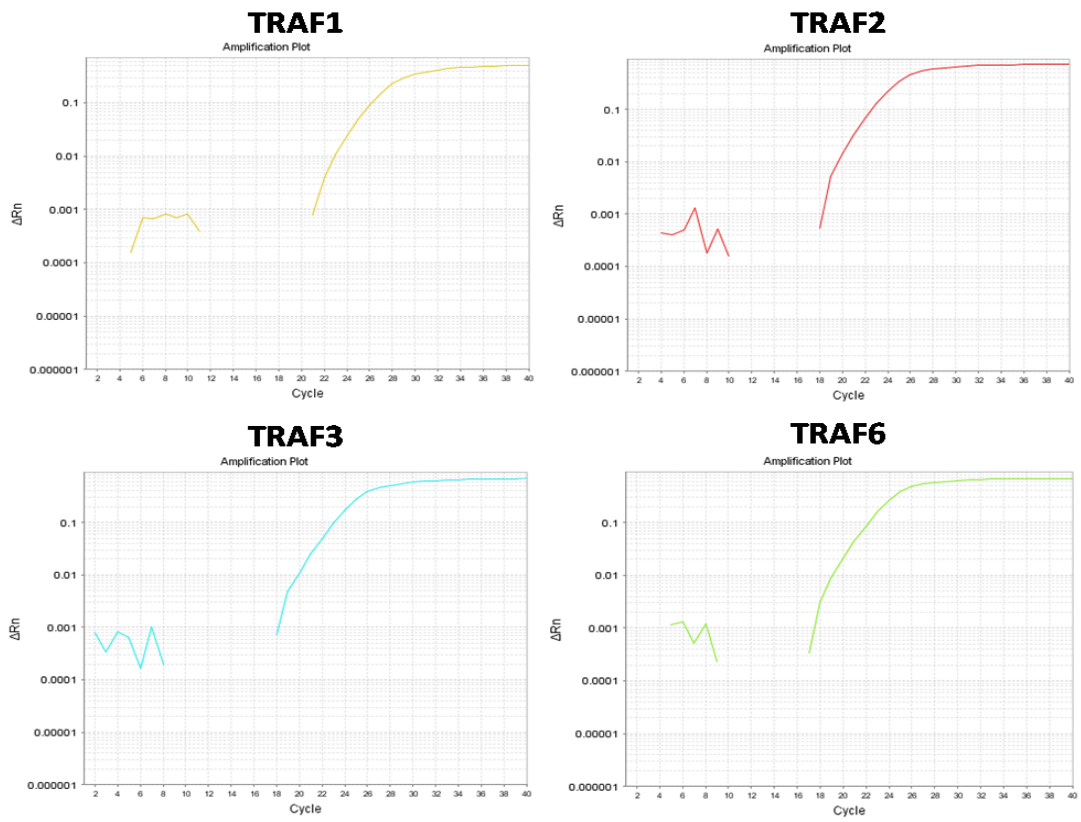

Figure 4.17 TRAFs expression level. INS-1 cells were cultured for 72h in RPMI-1640, cells were lysed, RNA extracted and qPCR performed using primers specific for TRAF1, TRAF2, TRAF3 and TRAF6. Data represent amplification plots of the respective TRAFs in control conditions.

Figure 4.18 shows TRAFs mRNA levels in glucolipotoxicity. There was a significant increase in TRAF2 expression, especially with incubation of both glucose and fatty acids (1.7 fold, $p<0.05$). There was a trend towards the increase of TRAF1 and TRAF6 mRNA levels (2.5 and a 2.2 fold respectively), with combination of glucose and fatty acids, whereas TRAF3 showed a trend towards decreased levels in glucolipotoxicity.

These results suggest that TRAF1, TRAF2 and TRAF6 mRNA levels could be linked to CD40 expression, as they show the same pattern of overexpression in glucolipotoxicity.

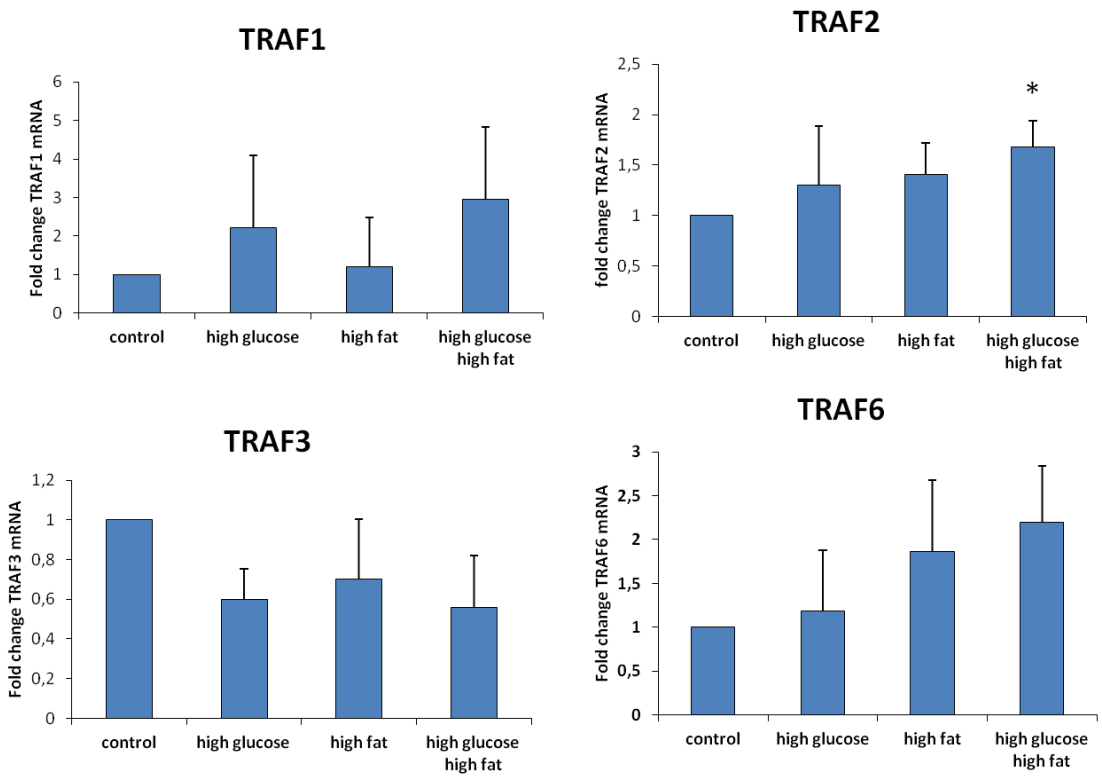

Figure 4.18 Effect of glucolipotoxicity on TRAFs expression. INS-1 cells were cultured for 72h in RPMI-1640 supplemented with 27 mM glucose, 200 μM oleic acid and 200 μM palmitic acid in different combinations. After the incubation time, cells were lysed, RNA extracted and qPCR performed using primers specific for TRAF1, TRAF2, TRAF3 and TRAF6. Data represent ΔΔCt values expressed as a fold change compared to cells grown in normal RPMI (control). Data are expressed as means + SD of 3 independent experiments (*$p<0.05$).

4.5.3 TRAFs protein expression in glucolipotoxicity

To determine whether the changes in mRNA levels correspond to differences at the protein level, INS-1 cells were cultured as before. After the incubation time, cells were lysed with TritonX-100 buffer and protein separated on a 12.5% SDS PAGE gel. The gel was then transferred on a membrane and then immunoblotted with anti-TRAF1, TRAF2, TRAF3 and TRAF6 polyclonal antibodies. Figure 4.19 shows that the expression of TRAF1, TRAF2 and TRAF6 increased in glucolipotoxicity, while TRAF3 expression was unaffected. In particular, TRAF1 increased with incubations of high glucose or high fat alone, and its overexpression was more evident in the presence of both high glucose and high fat. TRAF2 expression increased especially with high

glucose and high fat. TRAF6 appeared to increase in all the conditions compared to control, but it is barely detectable in these experimental conditions. Further optimisation of the blotting technique is necessary to obtain clearer results.

These results confirm the data observed at the RNA level and suggest a potential role of TRAF2 and TRAF6 in glucolipotoxicity. However, these experiments need to be repeated in order to reach statistical significance.

A

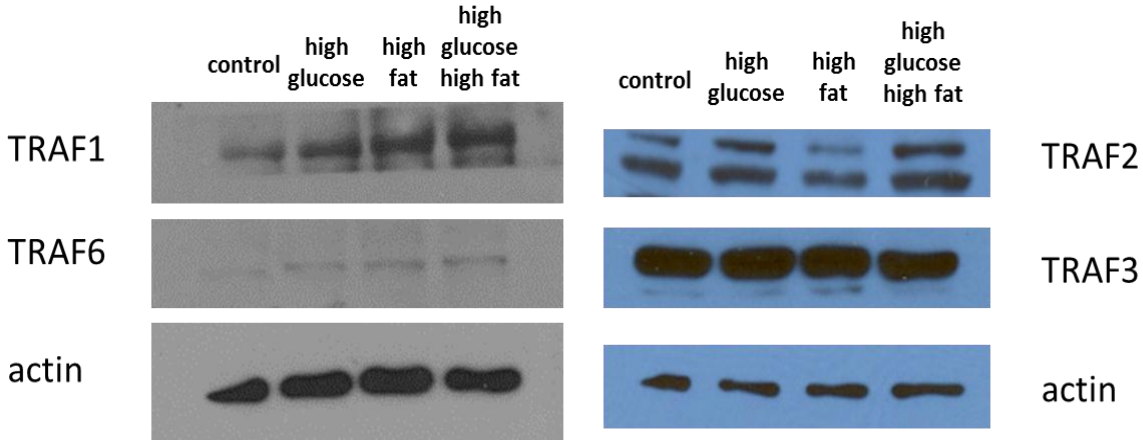

B

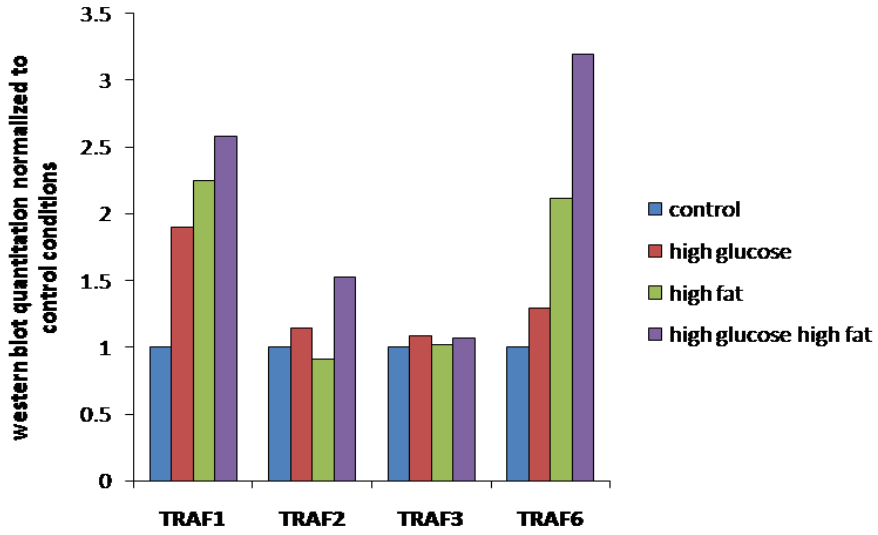

Figure 4.19 TRAFs protein expression in glucolipotoxicity. INS-1 cells were cultured for 72h in RPMI-1640 supplemented in 27 mM glucose, 200 µM oleic acid, 200 µM palmitic acid in different combinations. After the incubation time, cells were lysed with TritonX-100 buffer and protein separated on a 12.5% SDS PAGE gel. The gel was then transferred on a membrane and

then immunoblotted with anti TRAF1, TRAF2, TRAF3 and TRAF6 polyclonal antibodies. A) Western blots are representative of 3 independent experiments; B) Quantitation of the previous western blots using the program Image J. Bands are normalised using actin as a loading control and subsequently normalised to control conditions.

4.5.4 TRAFs expression *in vivo*

To determine whether upregulation of TRAF2 and TRAF6 also occurred *in vivo*, we performed RT-qPCR analysis using islets from C57BL/6 mice fed a high fat diet for 10 weeks or control mice. Data indicate a significant increase in TRAF2 mRNA levels (2 fold, $p<0.05$) in the high fat diet mice compared to lean control. TRAF6 did not show any significant change. The increase seemed to be specific for TRAF2 as TRAF6 mRNA did not seem to be affected (Figure 4.20).

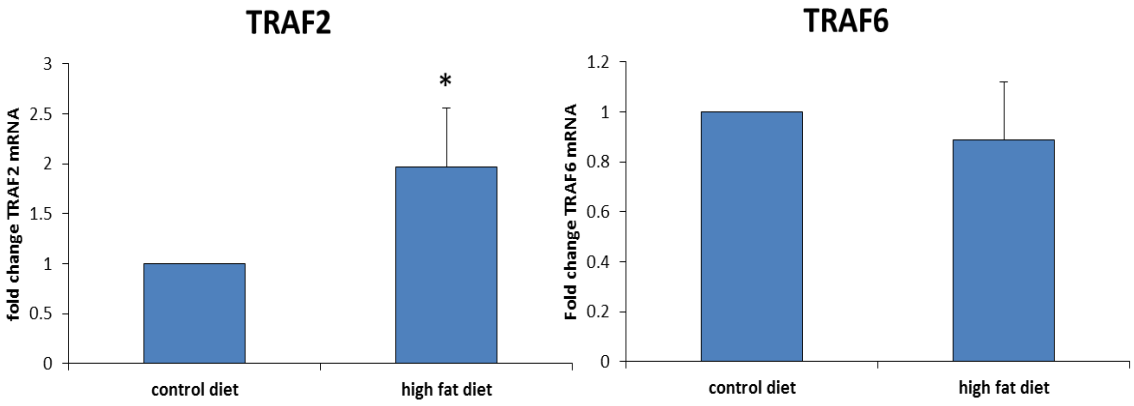

Figure 4.20 TRAFs expression *in vivo*. C57BL/6 mice were fed a high fat diet for 10 weeks prior to sacrifice, pancreas removed and total RNA extracted from isolated islets. RT-qPCR was performed using specific primers for TRAF2 and TRAF6. Data represent ΔΔCt values expressed as a fold change compared to the expression in islets of mice fed a control diet. Data are expressed as means + SD of 3 independent experiments (* $p<0.05$).

4.6 Discussion

CD40 is a member of the TNFR superfamily that plays a key role in the immune system and it is also associated with inflammatory responses in non-immune cells. A functional

CD40 is also expressed in mouse and human pancreatic β-cells and is able to induce inflammatory responses, upon activation of NF-κB [213, 242-244].

We demonstrated in the previous chapter that CD40 is overexpressed in INS-1 cells incubated under chronic conditions of high glucose and fatty acids, suggesting that it may be involved in the inflammatory process of glucolipotoxicity induced inflammation during the progression to T2D.

In this chapter, we characterised the role of CD40 in the β-cell, with particular focus on its potential role on β-cell function. We first demonstrated that CD40 activation by CD40L is able to induce NF-κB p65 translocation to the nucleus, and consequently NF-κB activation (Figure 4.1 and 4.2). The combination of high level of CD40L in diabetes along with upregulated expression of functional receptor in β-cells suggests that CD40 signalling may be responsible for much of the NF-κB-dependent islet inflammation. Since NF-κB activity is known to induce islet cell death [144], this lead to the hypothesis that a prolonged CD40 signalling through this pathway is likely to be a major contributor to islet cell death in the presence of chronically elevated levels of glucose and fatty acids.

To establish the specific role of CD40 in the pancreatic β-cell, we then performed a targeted knock-down of the gene in INS-1 and we determined cell viability in control conditions. We demonstrated that CD40 downregulation did not affect cell number (Figure 4.8) and did not activate caspase 3 (Figure 4.9), indicating that CD40 silencing is not involved in regulation of survival/apoptosis, at least in normal conditions.

In addition, we observed an increased number of cells in G1 phase upon CD40 downregulation, indicating that the absence of CD40 could induce a slight increase metabolism in the β-cell. These data were also confirmed by the effect of CD40 downregulation on insulin. We showed an increase in insulin gene transcription (Figure 4.11), insulin content (Figure 4.12) and secretion (Figure 4.13) in INS-1 cells transfected with a siRNA specific for CD40. These results suggest a new role for CD40 in the pancreatic β-cell. CD40 is able to regulate the function of the β-cell, and its downregulation was able to partially improve the impaired insulin production in glucolipotoxicity (Figure 4.14). In literature, no direct correlation between CD40 and insulin metabolism has been reported so far, although Poggi et al demonstrated that

obese CD40L$^{-/-}$ mice have preserved insulin sensitivity and low plasma insulin levels compared to obese CD40L$^{+/+}$ mice [247]. Our study is the first to suggest a direct correlation between CD40 and β-cell function.

The increase in insulin production observed in CD40 knock-down cells is independent to changes in the expression of insulin transcription factors (Figure 4.15), suggesting that downregulation of CD40 could either affect the binding activity of these transcription factors or act through NF-κB. We showed before that CD40 can activate NF-κB and we found a predicted NF-κB binding site 1600 bp ahead of the insulin promoter. The absence of CD40 would reduce the negative effect of NF-κB on insulin promoter, inducing insulin transcription.

Like the other members of TNFR superfamily, CD40 signalling is mediated principally through TRAFs, linking CD40 to downstream signalling pathways, among which activation of NF-κB. In this chapter, we showed that there was a trend towards a reduction in the expressions of TRAF1, TRAF2 and TRAF6 upon CD40 downregulation (Figure 4.16), suggesting a potential direct connection between CD40 and its downstream effectors. In addition, TRAF1, 2 and 6 expressions resulted upregulated in glucolipotoxicity (Figure 4.18, 4.19, 4.20), when also CD40 expression increases, showing that TRAFs expression perfectly reflects CD40 expression. Interestingly, CD40 results to be able to influence the expression of the downstream effectors, and this discovery can open the way to new therapeutic approaches, blocking the pathways activated by CD40. TRAF5 was not considered in the present analysis because it is the least studied TRAF in CD40 signalling. Future studies could include investigations on its role in glucolipotoxicity and in relation to CD40.

Taken together these results suggest a potential link between CD40 and insulin, as represented in Figure 4.21. In glucolipotoxic conditions, CD40 expression increases, leading to an increase of TRAFs expression, which can then activate NF-κB. NF-κB in turn binds to the insulin promoter and blocks the transcription of the gene. Given these results, an interesting therapeutic approach would be the blockage of the CD40 pathway. Upon CD40 downregulation, also TRAFs expression decreases, with subsequent reduction in the activation of NF-κB and subsequent increase in the transcription of the insulin gene.

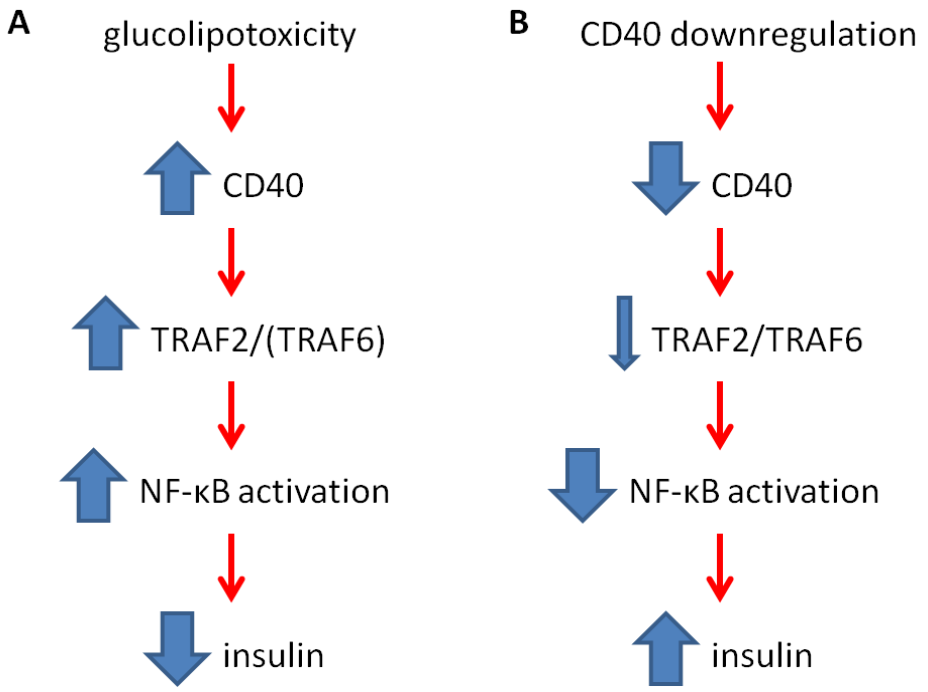

Figure 4.21 Hypothetic mechanism linking CD40 to insulin. A) In glucolipotoxic conditions; B) with CD40 downregulation.

The results of this chapter suggest the possibility that it would be possible to enhance islet function in glucolipotoxicity through targeted disruption of CD40 signalling pathways. A similar approach has been employed as a general immunosuppressant strategy following transplantation, and also to treat people suffering from lupus and different types of cancer. Intervention has not always been successful however, as there are a number of reports where anti-CD40L monoclonal antibodies have been shown to trigger thromboembolic events [332-333]. Importantly, these dangerous side effects have not been observed when the receptor, rather than the ligand, is targeted. Indeed there are now numerous promising clinical trials taking place involving a number of different anti-CD40 monoclonal antibodies [334-335], which may be worth consideration for use as an adjunct therapy for people with a history of poorly controlled T2D. Lucatumumab in particular would appear a strong initial candidate for this role. It is a human monoclonal antibody against CD40 and not only it is reported to be well tolerated [336], at least in moderate and intermediate strength doses [337], but it has also

previously been shown to prevent induction of NF-κB activity in multiple myeloma cells [338].

Chapter 5

Transcriptome profiling of the β-cell in glucolipotoxicity

5.1 Introduction

The transcriptome is the entire repertoire of transcripts in a species and represents a key link between the information encoded in the DNA and the phenotype. Discovering and interpreting the complexity of the transcriptome represents a crucial method of understanding the functional elements of the genome. This analysis can lead to a more complete understanding of many biological issues such as the onset of disease and progression.

The main goal of the whole transcriptome analysis is to identify, characterise and catalogue all the transcripts differentially expressed within a specific cell/tissue, at a particular stage. It has the potential to determine the correct splicing patterns and the structures of the genes, and to quantify the differential expression of transcripts in both physiological and pathological conditions [257]. Evolution of high-throughput techniques has allowed transcriptome profiling of model of diseases both *in vitro* and *in vivo* in an unbiased and highly sensitive manner, without previous knowledge of the genes involved in a particular disease. Next generation sequencing technology also tolerates de novo assembly of the reads, with access to transcriptional variations across the whole genome and not restricted only to sequences on certain particular probes. Moreover, with adaptations of next generation techniques, it is now possible to identify differentially expressed small RNAs, in particular miRNAs. MiRNAs are endogenous ~22 nucleotides long RNAs that play important regulatory roles in animals and plants by targeting mRNAs for cleavage or translational repression [281]. They can regulate both physiological and pathological processes such as development, metabolism, cancer and, relevant to this thesis, insulin resistance and diabetes.

The aim of this part of the thesis was to explore the molecular mechanisms activated in the β-cell under chronic exposure to high concentrations of glucose and fatty acids, using RNA sequencing. As reported in chapter 3, previous experiments in our lab identified several genes that are differentially expressed in glucolipotoxic conditions using Affymetrix microarrays. However, microarray analyses have several limitations because they need to rely on existing knowledge about the genome sequence, they have

high backgrounds levels due to cross-hybridisation, and a limited dynamic range of detection due to both background and saturation of signals [266]. RNAseq experiments allowed to expand the information gained through the microarray analysis, allowing the identification of expression changes at all the genome level, and the potential to discover novel transcripts, corresponding to molecules which structure and functions had not been elucidated so far.

Specifically we were interested in the investigation of novel molecules differentially expressed in conditions of glucolipotoxicity, which could be potential new targets for therapeutic strategies. These targets could be further studied to determine if they could have a role in regulating β-cell function.

5.2 Experiment set-up

We chose to perform RNA sequencing experiments to identify novel molecules involved in β-cell function impairment in glucolipotoxicity. The information gained from this study represented a broader view of the expression changes during glucolipotoxicity compared to the previous Affymetrix microarray data (Chapter 3). We chose to use INS-1 cells as they are a reliable model to study changes in gene expression and insulin secretion.

5.2.1 Experimental conditions

In order to discover novel mechanisms involved in the process of glucolipotoxicity, INS-1 cells were incubated in four experimental conditions, as those used for all the previous experiments of this thesis:

1- Control (RPMI-1640 containing 11 mM glucose) (C)
2- High glucose (RPMI-1640 containing 27 mM glucose) (HG)
3- High fat (RPMI-1640 containing 200 μM oleic acid, 200 μM palmitic acid) (HF)
4- High glucose high fat (RPMI-1640 containing 27 mM glucose, 200 μM oleic acid, 200 μM palmitic acid) (HGHF).

We used the same conditions adopted for the Affymetrix study, in order to compare some of the results obtained. In addition, differently from the Affymetrix experiment where only the combination of high glucose and high fat was used, in this RNAseq experiment we also evaluated the effects of glucose and fatty acids alone.
INS-1 cells were cultured for 72h in the 4 experimental conditions, subsequently lysed and RNA extracted (see Chapter 2, section 2.10.1). The experiment was performed in triplicate, in order to minimise experimental errors, for a total of 12 samples.

5.2.2 Extraction and quality control of RNA

The quality of the 12 RNA samples was confirmed using the Agilent Bioanalyser, using the protocol described in the Material and Methods section (Chapter 2, section 2.10.3). A RIN number (a tool that estimates the integrity of the RNA sample) between 8 and 10 was assigned to all samples, indicating that they consisted of high quality RNA. A representative electropherogram is shown in picture 5.1.

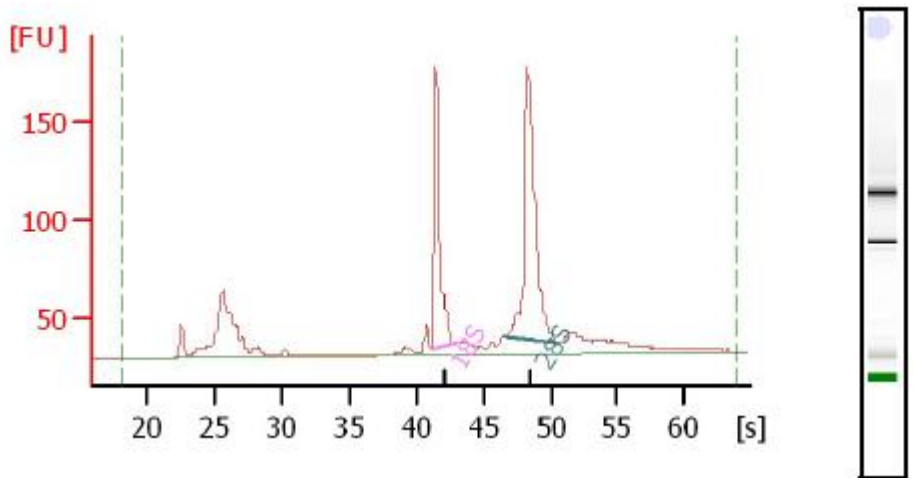

Figure 5.1 Agilent Bioanalyser analysis of RNA samples. The 12 samples of RNA extracted from INS-1 cells were run on an Agilent Bioanalyser system, in order to assess quality of the RNA. All the samples were assigned a RIN number between 8 and 10, indicative of high quality RNA.

The electropherograms for all the samples and the correspondent RIN numbers are presented in Appendix B.

5.2.3 Obtaining expression data

High quality RNA was then sent to Dr. Sarah Lamble laboratory in Oxford for the subsequent stages of library preparation and sequencing, performed over one lane of a flow cell on an Illumina-HiSeq 2000 instrument. The statistics of the RNAseq experiment are presented in Appendix C.

Raw RNAseq data were then analysed by Dr. Rob Lowe (Blizard Institute). In the sequencing process, the Illumina instrument produced quality-scored base calls during the run. The sequencing output files (compressed FASTQ files) were then used for the secondary analysis.

Reads were aligned to an annotated reference genome using Top Hat v 2.0.9: http://tophat.cbcb.umd.edu. Reads aligned to exons, genes and splice junctions were counted using the reference genome "rn4", extracted from UCSC (http://genome.ucsc.edu/goldenPath/credits.html#rat_credits).

Data visualisation and interpretation, calculating gene as well as transcript expression, then reporting differential expression, was done using the HTseq-count program: (http://www-huber.embl.de/users/anders/HTSeq/doc/count.html).

Normalisation process, which correct for in-sample distributional differences within the read counts, such as differences in total counts (sequencing depths), and within sample gene-specific effects, such as gene length or GC-content effects, was performed using the program DEseq:

(http://www.bioconductor.org/packages/devel/bioc/html/DESeq.html)

The statistical significance of fold changes was calculated by comparing the experimental read values to the control samples and the p values were subsequently adjusted at genome wide level using Bonferroni formula.

5.3 Multivariance analysis to identify sample clusters

After data were analysed, we performed the following comparisons:

- HG vs C

- HF vs C
- HGHF vs C
- HG vs HF
- HG vs HGHF
- HF vs HGHF.

For the subsequent analysis we focussed on the genes differentially expressed in the 3 experimental conditions compared to control conditions (HG vs C, HF vs C, HGHF vs C).

Genes were considered to be differentially expressed if reads changed more than 2 fold up/down compared to control with the adjusted p value of $p<0.05$.

The following numbers of genes resulted differentially expressed with an adjusted p-value of $p<0.05$:

- HG: 2701 differentially expressed genes, 588 upregulated and 2113 downregulated;
- HF: 2561 differentially expressed genes, 5 upregulated and 2556 downregulated;
- HGHF: 7994 differentially expressed genes, 1724 upregulated and 6270 downregulated.

Venn diagrams using the program Gene Venn (http://genevenn.sourceforge.net/) were used to identify differentially expressed genes common to more than one condition, hence to identify logical relations between our sets of data. Venn diagrams are representations useful to identify relationships between groups of objects.

Figure 5.2 represents the Venn diagrams of the number of genes differentially expressed in the 3 different conditions compared to control, with a p value of $p<0.05$. This analysis shows that most of the genes that were differentially expressed in high glucose compared to control (red diagram) were also differentially expressed in condition of high glucose/high fat (green diagram) (2568 genes). Similar results were obtained for genes differentially expressed in high fat compared to control (yellow diagram) (2463 genes). 4377 genes were differentially expressed only in high glucose/high fat, whereas 1415 genes were differentially expressed in all the three conditions. These results indicate that, in most of the cases, high glucose alone or high fat alone did not affect

gene expression significantly but the combination of high glucose and high fat cooperated in altering gene expression. In very few cases (8) high glucose alone and high fat alone had opposite effects on gene expression, leading to a null effect when glucose and high fat were used together.

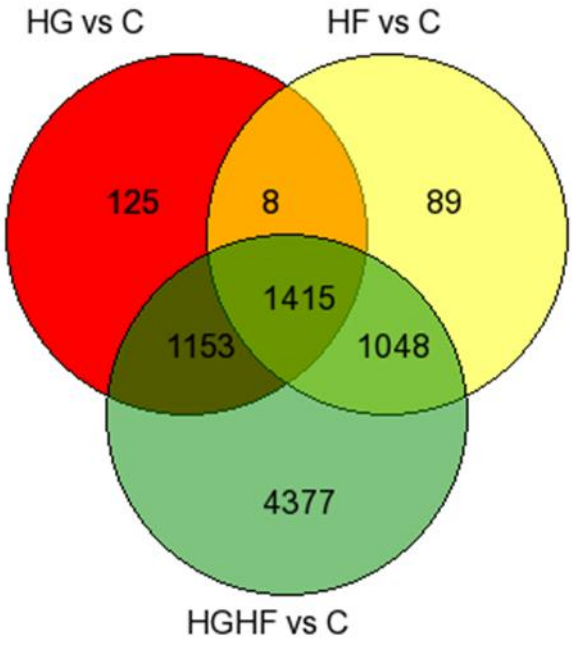

Figure 5.2 Venn diagrams showing the correlation between differentially expressed genes in the 3 conditions compared to control with p<0.05. The red diagram represents the genes differentially expressed in HG vs C, the yellow diagram the genes in HF vs C and the green diagram the genes in HGHF vs C. The numbers corresponds to the differentially expressed genes with a p value p<0.05.

The distribution of genes expressions in in the different conditions compared to control conditions was then investigated using scatter plots. Figure 5.3 shows the scatter plot of statistical significant genes (p<0.05) in each of the three experimental conditions compared to control. Each graph represents the comparison between the expressions of a gene in an experimental condition to its expression in control conditions. The red line corresponds to control conditions and each blue dot represents a gene: dots above the red line are genes overexpressed; dots below the red line are downregulated.

High glucose (Figure 5.3 A) triggered both upregulation and downregulation of genes, but expression values were not very different from control conditions. High fat treatment (Figure 5.3 B) induced in general downregulation of gene expressions but values were very similar to control conditions. Finally, in conditions of high glucose/high fat (Figure 5.3 C), genes were both upregulated and downregulated and expression values were more different and spread from control conditions.

These results are in line with our previous experiments showing that the combination of high glucose and high fat is able to affect more β-cell function than each condition alone. Examples of this cooperation can be seen in the impairment of insulin secretion and expression and in the increase of CD40 and TRAFs expression in glucolipotoxicity.

A

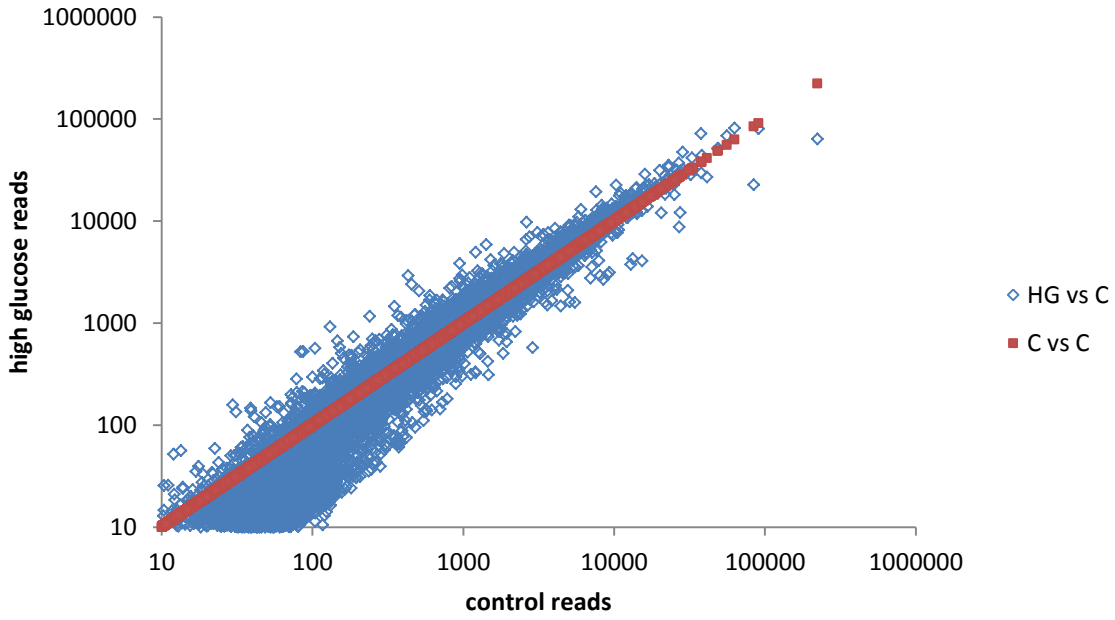

B

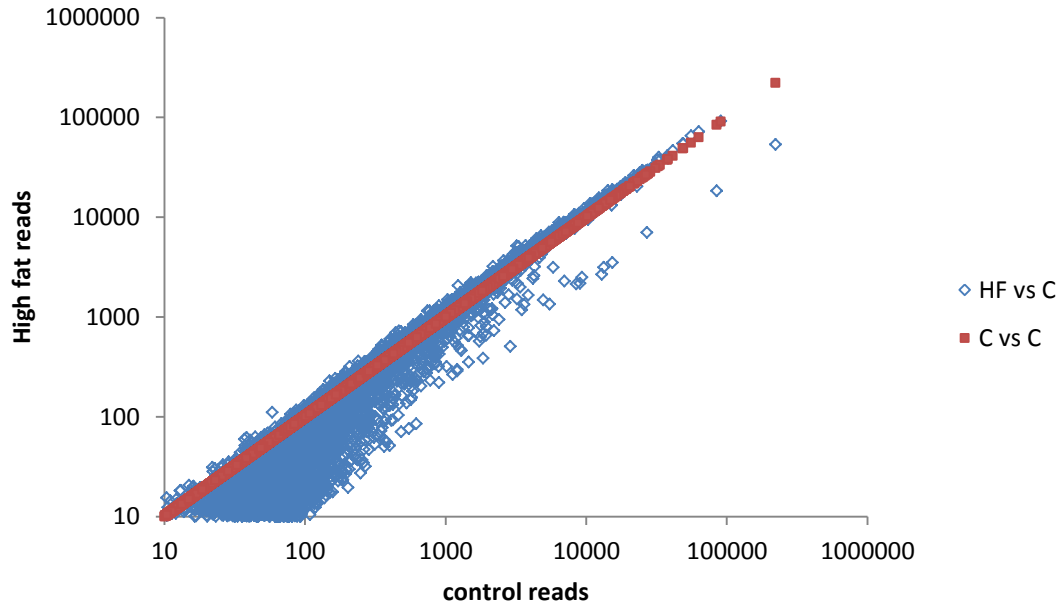

C

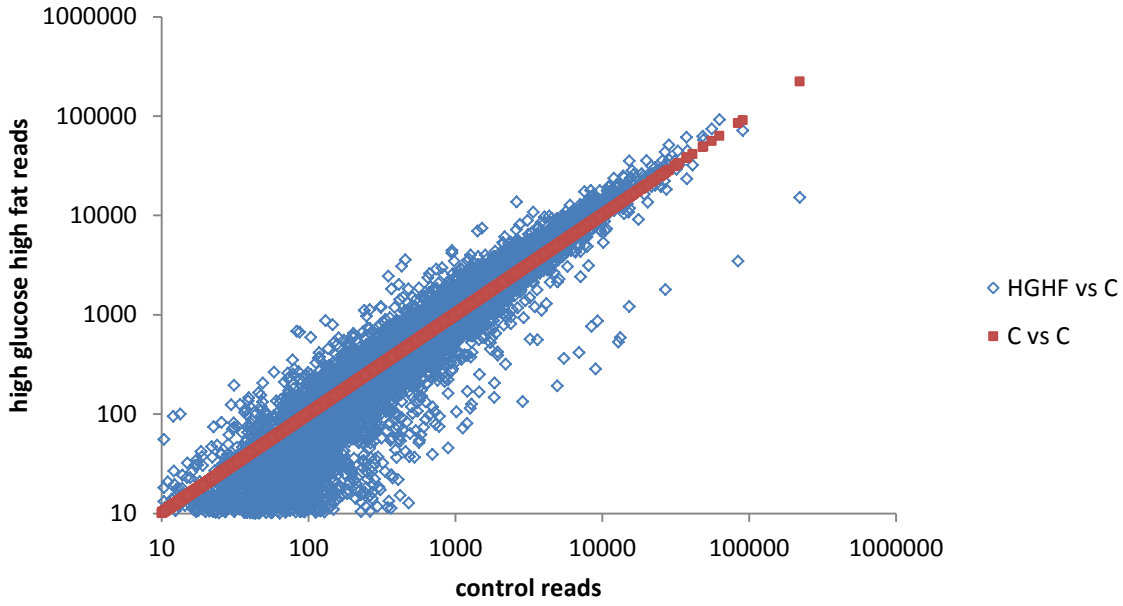

Figure 5.3 Scatter plots of differentially expressed genes in comparison to control. A) High glucose vs control; B) High fat vs control; C) High glucose/high fat vs control. Each graph represents the comparison between the expression of a gene in each condition and the expression in control conditions. The red line corresponds to control conditions. Each dot represents a gene: dots above the red line are genes overexpressed, dots below the red line are downregulated. Values below 10 are considered as baseline and not represented. Only genes with a significant p value of $p<0.05$ are represented.

5.3.1 Hierarchical clustering

In order to determine how these different conditions relate to each other, according to gene expression, hierarchical clustering was performed. Hierarchical clustering is a method to visualise correlation between different samples and conditions. The program regroups genes with a similar pattern of expression, which will be represented close to each other. The bigger is the distance between two genes or conditions, the bigger is the difference among them.

Figure 5.4 represents the cluster plots of the differentially expressed genes with an adjusted p value $p<0.001$ in high glucose vs control conditions (A), high fat vs control (B) and high glucose high fat vs control (C). The cluster analysis was performed by Dr. Rob Lowe (Blizard Institute). In Figure 5.4 the rectangles represent each gene and the colour indicates the level of its expression, ranging from blue (low expression) to red (high expression). The expression of each significant gene is considered in each of the 12 experimental samples independently.

In Figure 5.4A (HG vs C), the first rows represent genes overexpressed in high glucose and the lower part of the graph represents genes downregulated in high glucose. Control and high fat conditions clustered together, while high glucose and high glucose/high fat clustered together, indicating that most of the genes differentially expressed in high glucose were also differentially expressed in high glucose high fat. Not all these genes were differentially expressed also in high fat conditions.

Among the genes differentially expressed in high fat vs control (Figure 5.4B) with $p<0.001$, nearly all the genes were downregulated. In this case, high glucose, high fat and high glucose/high fat clustered together, indicating that, when genes were differentially expressed in high fat, with high probability they were also differentially expressed in the other conditions compared to control.

Figure 5.4C represents the cluster plot of the genes differentially expressed in high glucose/high fat. The first rows represent genes that were upregulated with a p value $p<0.001$. This analysis shows that high fat conditions presented a pattern of colour similar to controls. High glucose conditions started to differentiate from control, while high glucose/high fat conditions contained the most varied expression levels compared

to controls. The rows in the second part of the diagram represent genes that were downregulated in glucolipotoxicity. Downregulation was similar for conditions of high glucose and high fat, while high glucose/high fat conditions together showed the most effective downregulation.

A

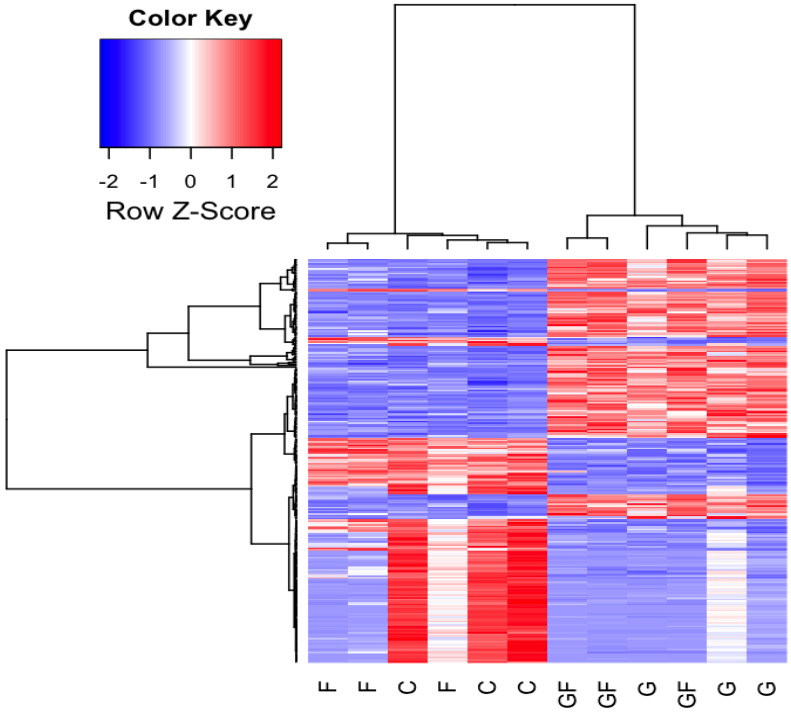

B

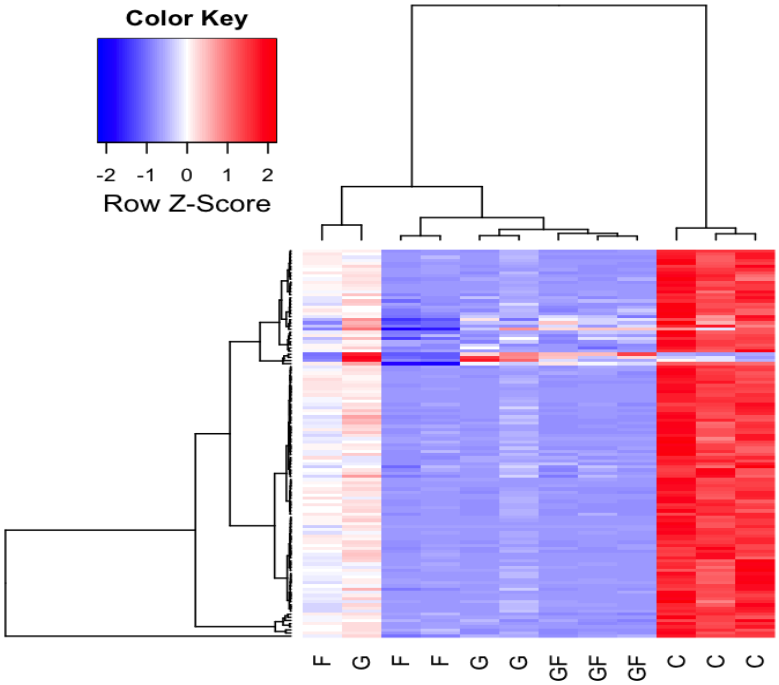
Color Key
-2 -1 0 1 2
Row Z-Score
F G F F G G GF GF GF C C C

C

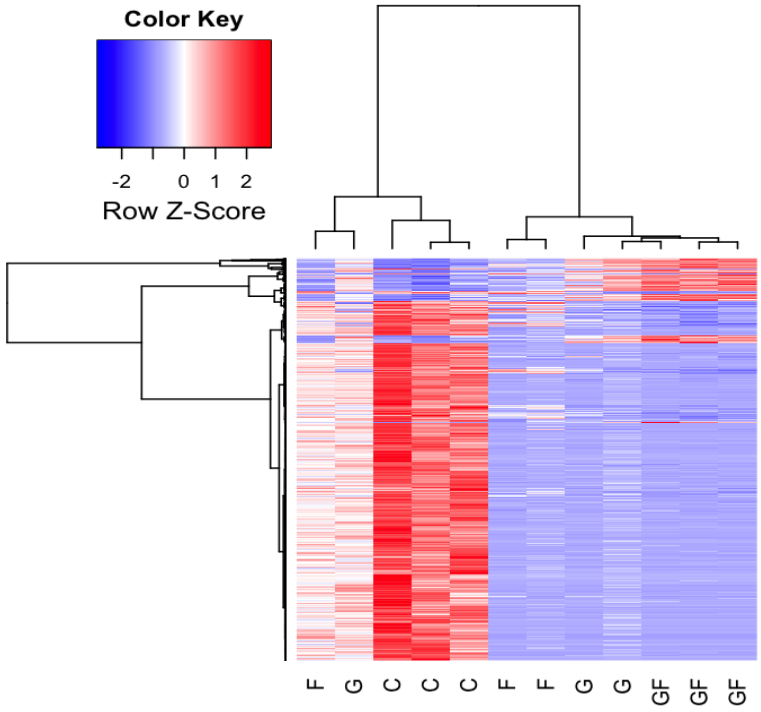
Color Key
-2 0 1 2
Row Z-Score
F G C C C F F G G GF GF GF

Figure 5.4 Hierarchical clustering of differentially expressed genes with p value p<0.001. The rectangles represent each gene (rows) and the colour indicates the level of its expression, ranging from blue (low expression) to red (high expression). The expression of each significant gene is considered in each of the 12 experimental samples. A) High glucose vs control B) High fat vs control C) High glucose high fat vs control. (C=control, G=high glucose, F=high fat, GF=high glucose high fat).

In conclusion, the hierarchical clustering shows that high glucose and high fat alone are able to change genes expression, but the combination of these conditions has additional effect.

These results are in line with the cluster plots shown previously, confirming that most of the genes are downregulated by the treatments and that the combination of high glucose/high fat leads to a stronger effect than each condition alone.

It is also worth noticing that this downregulation is not caused by a toxic effect or by β-cell death, as MTT assays and caspase 3 activity assays (Chapter 3, Figure 3.2 and 3.4) revealed no activation of apoptosis in these experimental conditions. Only the function of the β-cell resulted affected at the time point considered.

Clustering showed us that expression profiles of high fat samples are similar to control, while the combination of high glucose/high fat gives the highest difference in expression changes.

Considering that most of genes differentially expressed in high glucose alone and high fat alone are also differentially expressed in the combination of the two conditions, in all further analyses we focussed on the comparison between high glucose/high fat and control conditions.

5.4 Pathway analysis

Once the list of genes differentially expressed in our experimental conditions was obtained, we decided to determine which pathways are mainly affected by glucolipotoxic conditions. To assess this, we used the programs Panther (http://www.pantherdb.org/) and Metacore (http://thomsonreuters.com/metacore/) to identify enriched pathways, enriched functions and associated diseases.

5.4.1 Identification of enriched pathways

The program Panther allows the identification of enriched pathways, molecular functions, biological processes, cellular components and protein classes among a given list of genes. In this case, the list of genes differentially expressed in conditions of high glucose/high fat in comparison to control with a statistical significance of $p<0.05$ was uploaded to the program. The program calculates the number of genes that are enriched with a specific pathway and gives also the statistical significance of any enrichment. Enrichment is considered statistical significant when there are more genes in the list associated with a particular pathway than it would be expected by chance based on the total number of genes associated with that pathway. Table 5.1 lists the significantly enriched pathway (p value $p<0.05$). In the table, the number of genes for each pathway that would be expected by chance are also indicated ("expected"), compared to the number of genes of that pathway that are differentially expressed in our experiment. The list includes pathways involved in glucose metabolism (glycolysis), inflammation mediated by chemokine and cytokine signalling pathways, and vesicle trafficking.

PATHWAYS	**EXPECTED**	**HGHF P<0.05**	**P VALUE**
Glycolysis	44.23	12	3.78 E-10
Blood coagulation	15.91	35	9.17 E-09
Heterotrimeric G protein signaling pathway-Gi alpha and Gs alpha mediated pathway	42.95	68	2.34 E-05
Huntington disease	73.81	46	2.42 E-04
Cadherin signalling pathway	48.68	74	3.27 E-04
Heterotrimeric G protein signalling pathway-Gq alpha and Go alpha mediated pathway	35.63	57	4.18 E-04
Nicotinic acetylcholine receptor signalling pathway	23.86	40	5.72 E-04

Inflammation mediated by chemokine and cytokine signalling pathway	76.68	100	1.54 E-03
Synaptic vesicle trafficking	8.91	17	5.81 E-03
Endothelin signalling pathway	26.09	39	1.01 E-02
Ionotropic glutamate receptor pathway	14.95	25	1.07 E-02
Thyrotropin-releasing hormone receptor signalling pathway	13.68	23	1.07 E-02
Phenylethylamine degradation	1.91	6	1.31 E-02
Dopamine receptor mediated signalling pathway	18.77	29	1.35 E-02
Plasminogen activating cascade	5.41	11	1.69 E-02
Alzheimer-disease-presenilin pathway	38.18	51	2.27 E-02
Wnt signalling pathway	92.90	112	2.68 E-02
Integrin signalling pathway	58.22	73	2.88 E-02
Muscarinic acetylcholine receptor 1 and 3 signalling pathway	14.32	22	3.36 E-02
5HT2 type receptor mediated signalling pathway	15.27	23	3.52 E-02
Nicotine pharmacodynamics pathway	11.45	18	3.85 E-02

Table 5.1 List of enriched pathways in HGHF vs C $p<0.05$.

As expected, most of the identified pathways were associated to diabetes or its molecular complications:

- *Glycolysis* is the metabolic pathway that converts glucose to pyruvate, so this process is strictly connected to the amount of glucose in the blood. In addition, insulin either directly or indirectly increases the rate of glycolysis [339], and in β-cells it has been observed that chemical glycolytic oscillations are consistent with insulin oscillations at both high and low initial concentrations of glucose [340].

- *Cadherin signalling pathway, inflammation mediated by cytokines and chemokines and endothelin signalling pathway* are all involved in the inflammatory process induced by chronic exposure of the β-cell to high concentrations of glucose and fatty acids. A detailed explanation of the role of inflammation in T2D is described in chapter 1.4.
- *Nicotinic acetylcholine receptors* are known to interact with anti-inflammatory pathways and have been implicated in the control of appetite and body weight, as well as lipid and energy metabolism [341]. It has been shown that acetylcholine can bind its receptor in the β-cells, triggering intracellular pathways which culminate in the rise of intracellular calcium and insulin secretion [342].
- *Vesicle trafficking* is also involved in the development of T2D, especially in relation to insulin exocytosis. Disruption of the microtubule network responsible of vesicle trafficking impairs granule movement and the exocytotic response [9].
- Altered *glutamatergic transmission* may contribute to the impaired insulin secretory response in the β-cell, as it has been shown that glutamate pathways are involved in insulin secretion [343].
- *Dopamine receptor signalling* is implicated in glucolipotoxicity. The number of dopaminergic receptors as well as central dopaminergic transmission are increased in diabetes [344]. It has been shown that dopamine D2-like receptors are expressed in the pancreatic β-cell and mediate inhibition of insulin secretion [345].
- *Alzheimer's disease* pathway can be connected to T2D and glucolipotoxicity could influence the expression of molecules involved in this pathway in the β-cell. This can be explained by the fact that the pancreas is a highly innervated organ that shares a number of molecular similarities with brain at the level of transcriptome and proteome. Diabetes could increase the likehood of Alzheimer's disease, due to the impact of insulin abnormalities, insulin resistance and advanced glycation end products on the development of amyloid plaques and neurofibrillary tangles. T2D and Alzheimer's disease are both characterised by localised amyloid deposits that progress during the course of the disease [346].

- *Wnt signalling pathway* plays an important role in intestinal tumorigenesis but it has also been associated to T2D. Wnt can increase cellular sensitivity to insulin, regulating the transcription of IRS-1 [347], therefore the disruption of this pathway could be involved in the development of diabetes. In addition GLP-1 stimulates Wnt signalling in pancreatic β-cell, enhancing cell proliferation; thus positive feedback between GLP-1 and Wnt signalling may result in increased proliferation, and inhibition of apoptosis in pancreatic β-cells [348]. Wnt signalling is also a strong activator of mitochondrial biogenesis, which leads to increased production of ROS known to cause DNA and cellular damage [347].
- *5HT2 type receptor signalling pathway* has been reported to have lipolytic action on adipocytes, increasing plasma level of free fatty acids. It has also been shown that 5HT2 receptors are expressed in pancreatic β-cells and they have a role in the inhibition of insulin secretion [349].
- *Signalling pathways associated to protein G, receptors and metabolism* result to be implicated in glucolipotoxicity. This is explained by the fact that β-cell function and insulin production and release are related to many signalling and metabolic pathways (glucose metabolism, IGF pathways, PI3K pathway), which involve signalling through protein G and receptors. As a consequence, disruption of these pathways leads to a condition of impairment of insulin production and secretion.
- *Thyrotropin-releasing hormone receptor signalling pathway* will be further investigated in chapter 6 of this thesis, as a future topic of study.

In summary, this pathway analysis revealed that glucolipotoxicity is able to change the expression of molecules involved in pathways related to inflammation and signalling in T2D. This confirms the fact that our experimental conditions resemble the detrimental conditions of T2D and its molecular complications.

5.4.2 Identification of enriched molecular functions

Figure 5.5 shows the enriched molecular functions between our list of differentially expressed genes in high glucose/high fat compared to controls and with a p value $p<0.05$. This analysis indicates that among our significantly differentially expressed genes there were more genes associated with the molecular functions represented in the pie chart than it would have been expected by chance.

The functions affected in glucolipotoxicity were mainly involved in catalytic activity, receptor activity and protein binding transcription factor activity. This is in line with the fact that many molecules implicated in the impairment of insulin secretion and production are involved in signalling pathways, and consequently receptor activity and catalytic activity are obviously impaired. Moreover, a differential expression of transcription factors and proteins that regulate their binding are required to induce gene expression changes.

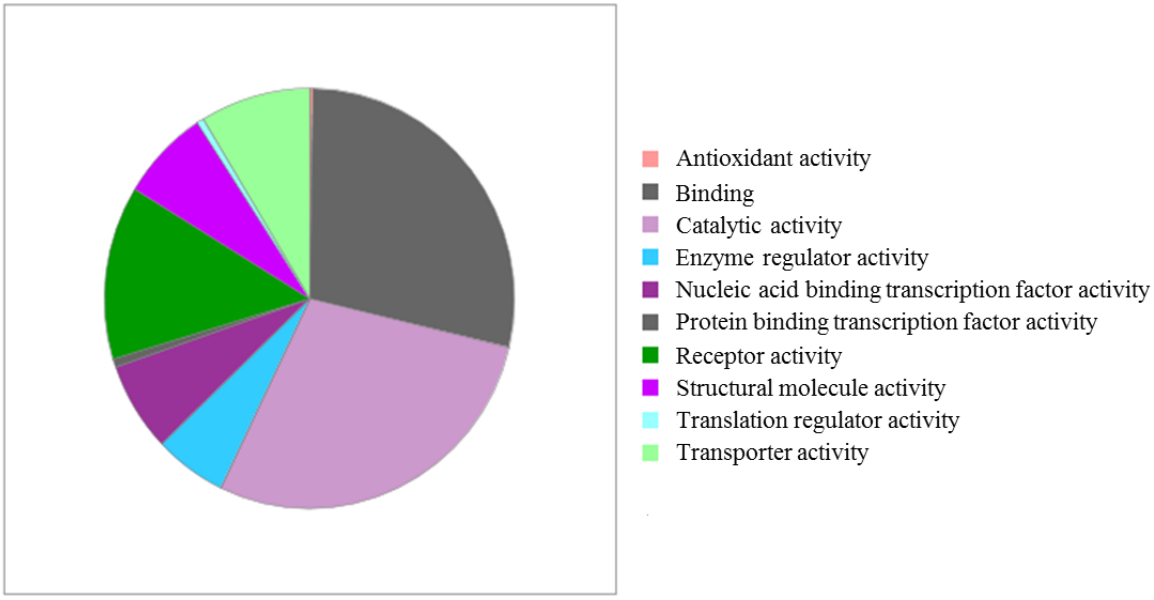

Figure 5.5 Enriched molecular functions in HGHF vs C with $p<0.05$. The pie chart represents the enriched molecular functions among the differentially expressed genes in high glucose/high fat compared to control with a p value $p<0.05$.

5.4.3 Identification of enriched biological processes

Figure 5.6 shows the enriched biological processes involved in conditions of glucolipotoxicity. This analysis indicates that among our significant differentially expressed genes there were more genes associated with the biological processes represented in the pie chart than it would have been expected by chance.

The pie chart reveals that the biological processes mostly affected were apoptotic processes, cellular processes, metabolic processes, showing that there was an enrichment of processes involved in metabolism and cellular activity. This can be explained by the impairment of the β-cell function, activity and insulin metabolism in glucolipotoxicity. In addition, the detrimental effects of glucolipotoxicity start leading to the activation of apoptotic pathways, culminating with β-cell death. Our results showed no activation of apoptosis in the experimental conditions tested, although we cannot rule out the activation of early stages of the apoptotic pathway, which has yet to have an impact on cell viability during the time period considered.

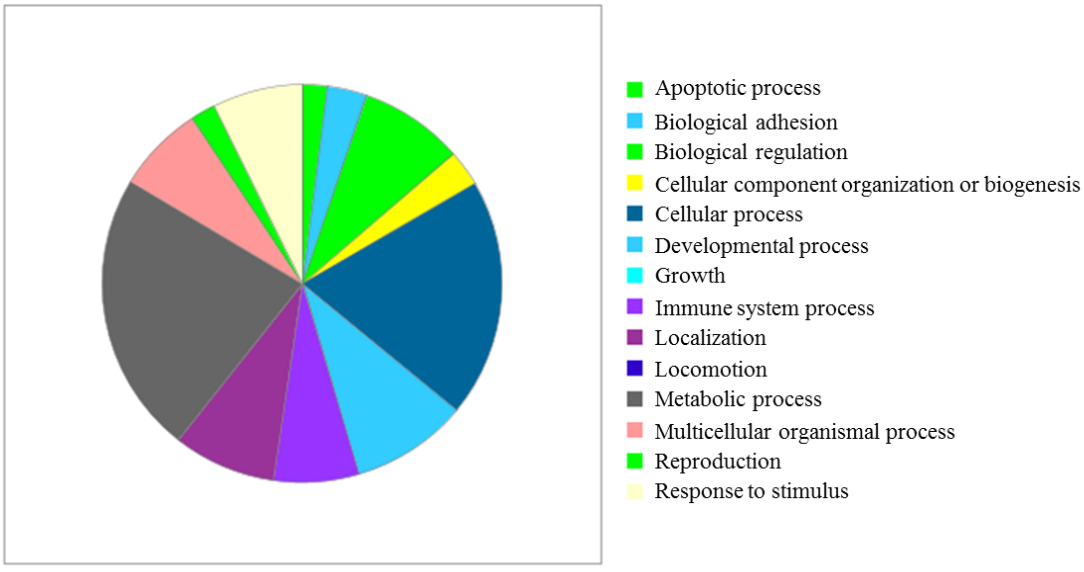

Figure 5.6 Enriched biological processes in HGHF vs C with p<0.05. The pie chart represents the enriched biological processes among the differentially expressed genes in high glucose high fat in comparison to control with a p value p<0.05.

5.4.4 Identification of enriched cellular components

Figure 5.7 shows the enriched cellular components among the genes differentially expressed in our conditions. This analysis indicates that among our significant differentially expressed genes there were more genes located in the cellular components represented in the pie chart than it would have been expected by chance.

Most of the molecules differentially expressed were located in organelles or on the membrane. This is in line with the finding that many of the molecules involved in glucolipotoxicity are signalling molecules or receptors, so they can be located in the membrane. Moreover, considering that glucolipotoxicity has also effect on ROS production and energy, it can affect the expression of mitochondrial molecules. Transcription factors and molecules involved in regulating their binding are located in the nucleus.

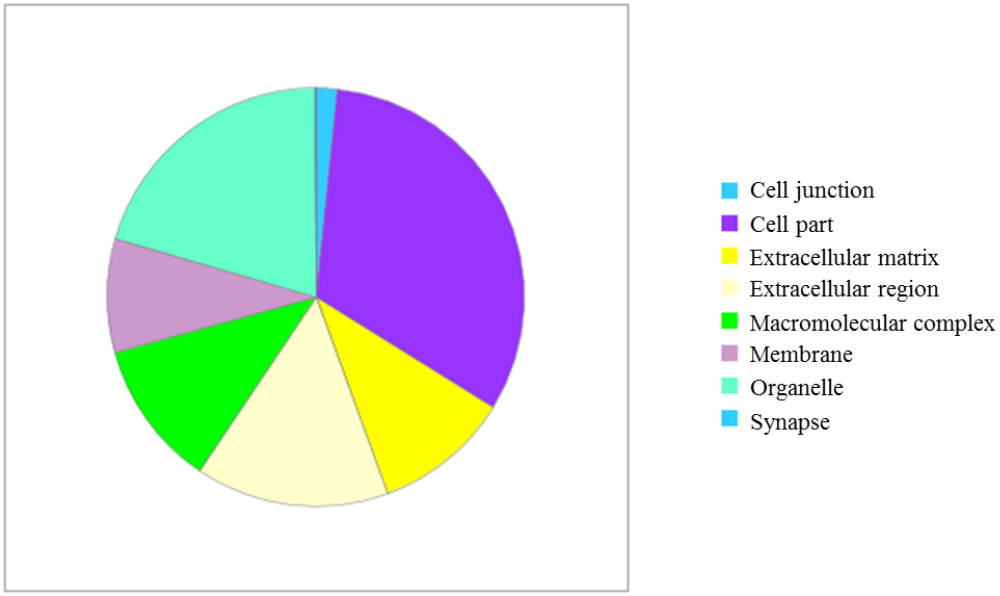

Figure 5.7 Enriched cellular components in HGHF vs C with p<0.05. The pie chart represents the enriched cellular components among the differentially expressed genes in high glucose/high fat in comparison to control with a p value p<0.05.

5.4.5 Identification of enriched protein classes

Table 5.2 shows the classes of the molecules involved in glucolipotoxicity. This analysis indicates that among our significant differentially expressed genes there were more genes associated with the protein classes listed in the table than it would have been expected by chance. Proteins differentially expressed in high glucose/high fat compared to control were mainly receptors, nucleic acid binding molecules, signalling molecules and transporters. This is consistent with the fact that the molecules involved in glucolipotoxicity are implicated in signalling pathways, in regulating transcription factors binding and in molecular transport.

PROTEIN CLASS	P VALUE
Receptor	1.88 E-38
G-protein coupled receptor	1.67 E-24
RNA binding protein	3.54 E-20
Ribosomal protein	1.54 E-18
Signalling molecule	1.28 E-17
Nucleic acid binding	2.91 E-17
Transporter	8.91 E-16
Immunoglobulin	1.13 E-13
Ion channel	2.72 E-13
Cell adhesion molecule	4.58 E-11

Table 5.2 Enriched protein classes in HGHF vs C with $p<0.05$

5.4.6 Identification of associated diseases

Interestingly, the molecules resulted differentially expressed in our experiment were also found to be important in other diseases, therefore they are indicative of the presence of a pathologic condition. The predicted associated diseases to our experimental conditions of glucolipotoxicity were identified using the program Metacore. Table 5.3 lists the first 50 diseases associated with the list of differentially expressed molecules in

HGHF vs C with a p value $p<0.05$. The table indicates also the enrichment, expressed as the ratio of the number of genes that would be associated to each disease by chance compared to the number of the differentially expressed genes in our list associated with the disease.

The table indicates the presence of diseases associated with inflammation, obesity, T2D and insulin resistance, which confirms that our experimental conditions influenced the expression of molecules implicated in diabetes and insulin resistance. In addition, the list includes other diseases associated with diabetes, which may have a common aetiology, for example, cardiovascular diseases and hypertension. These are generated mainly by the inflammatory process and oxidative stress characteristic of T2D.

In addition, Table 5.3 lists many forms of neoplasm associated with our conditions of glucolipotoxicity. Chronic exposure of the β-cell to high concentrations of glucose and fatty acids can alter the expression of molecules involved in the aetiology of cancer and epidemiologic evidence suggests that people with diabetes are at significantly higher risk for many forms of cancer [350]. Several studies indicate an association between diabetes and the risk of liver, pancreas, endometrium, colon/rectum, breast and bladder cancer. Mortality is also moderately increased in subject with diabetes. Common risk factors such as age, obesity, physical inactivity and smoking may contribute to increased cancer risk in diabetic patients. In addition, hyperinsulinemia most likely favours cancer in diabetic patients as insulin is a growth factor with metabolic and mitogenic effects, and its action in malignant cells is favoured by mechanisms acting at both the receptor and post-receptor level [351].

As explained before, also Alzheimer's disease is connected with diabetes, for the similarity of the β-cells to neurons, which could justify the common aetiology of the two diseases.

Moreover, some autoimmune and inflammatory diseases are listed, including Rheumatoid Arthritis, Systemic Lupus Erythematosus and Multiple Sclerosis, confirming that conditions of glucolipotoxicity generate the activation of an inflammatory status.

In conclusion, our experimental system supports many of the known molecular changes evolving or associated with T2D.

ASSOCIATED DISEASES	RATIO	P VALUE
Lung Neoplasms	5326/16891	1.23 E-71
Neoplasms	1520/20277	3.38 E-36
Arthritis, Rheumatoid	629/1592	2.81 E-35
Wounds and Injuries	400/980	6.81 E-34
Stomach Neoplasms	1459/3803	9.20 E-34
Breast Neoplasms	2995/8967	6.52 E-32
Inflammation	392/898	8.36 E-31
Prostatic Neoplasms	3287/9711	1.90 E-30
Rectal Neoplasms	2329/6608	3.68 E-30
Colorectal Neoplasms	1526/9302	9.89 E-30
Multiple Sclerosis	830/2278	1.01 E-28
Hypertension	304/606	1.76 E-25
Lupus Erythematosus, Systemic	411/928	2.11 E-23
Skin Neoplasms	1612/4478	2.62 E-22
Carcinoma, Non-Small-Cell Lung	1139/3021	4.34 E-22
Asthma	647/1608	8.66 E-22
Arthritis	239/1798	1.52 E-21
Sjogren's Syndrome	286/584	5.43 E-21
Depressive Disorder, Major	428/966	1.14 E-20
Endometrial Neoplasms	3350/10214	1.35 E-20
Fibrosis	226/498	6.61 E-20
Pulmonary Disease, Chronic Obstructive	468/1103	2.58 E-19

Laryngeal Neoplasms	876/2278	3.23 E-19
Melanoma	1278/3867	5.09 E-19
Cardiovascular Diseases	191/3605	3.87 E-18
Coronary Artery Disease	248/508	5.19 E-18
Myocardial Infarction	247/508	1.15 E-17
Infection	416/1186	2.66 E-17
Melanoma, Cutaneous Malignant	405/938	2.96 E-17
Kidney Neoplasms	2892/9603	3.14 E-17
Obesity	438/1069	4.00 E-17
Colonic Neoplasms	645/1659	3.12 E-16
Neoplasm Metastasis	312/704	5.46 E-16
Bipolar Disorder	316/706	5.46 E-16
Idiopathic Pulmonary Fibrosis	136/243	7.97 E-16
Migraine Disorders	75/111	1.14 E-15
Arteriosclerosis	195/709	1.49 E-15
Ovarian Neoplasms	1214/3403	2.21 E-15
Diabetes Mellitus, Type 2	601/1529	2.50 E-15
Carcinoma	660/5784	4.50 E-15
Glioblastoma	994/2714	6.01 E-15
Carcinoma, Ductal, Breast	578/1470	1.70 E-14
Coronary Disease	181/658	5.03 E-14
Stroke	176/406	6.32 E-14
Mouth Neoplasms	1303/4289	6.32 E-14
Infarction	139/261	7.17 E-14

Alzheimer Disease	415/1257	1.37 E-13
Glioma	256/5175	2.03 E-13
Insulin Resistance	217/775	1.59 E-12
Bronchitis, Chronic	48/63	1.60 E-12

Table 5.3 Associated diseases in HGHF vs C p<0.05.

5.5 Comparison with QTL and GWAS data

QTLs (Quantitative Trait Loci) are stretches of DNA containing or linked to genes that are believed to make a significant contribution to the expression of a particular phenotype. QTLs are usually associated with more than one gene and with the environment, and include several medically significant traits (e.g. blood pressure, obesity).

In human, association of complex common diseases to a particular chromosomal region uses the differential frequency of single nucleotide polymorphisms (SNPs) between patients compared to controls. The study of such SNP variations genome wide, known as GWAS (Genome Wide Association Study), has allowed researchers to identify genes as well as chromosomal regions associated with complex diseases like diabetes.

In order to investigate if the differentially expressed genes in glucolipotoxicity are associated with known diabetic genes or regions, we studied their connection to known data of QTL regions or GWAS studies.

In order to understand if the differentially expressed genes are located in the rat diabetic QTLs regions, which are regions of the genome that have been associated to diabetes, we used the database RGD (Rat Genome Database: http://rgd.mcw.edu/) to localise diabetic QTLs on the rat chromosomes. Figure 5.8A represents the localisation of 110 QTLs associated with diabetes (blue bars). Figure 5.8B represents the localisation of the first 500 statistical significant differentially expressed genes of our list (red bars). First, it must be noticed that these significant genes were spread all over the 21 rat

chromosomes, therefore there was not a particular chromosome enrichment. In addition, they mainly overlapped with the rat diabetic QTLs, therefore they were located in regions of the genome known to be associated with diabetes.

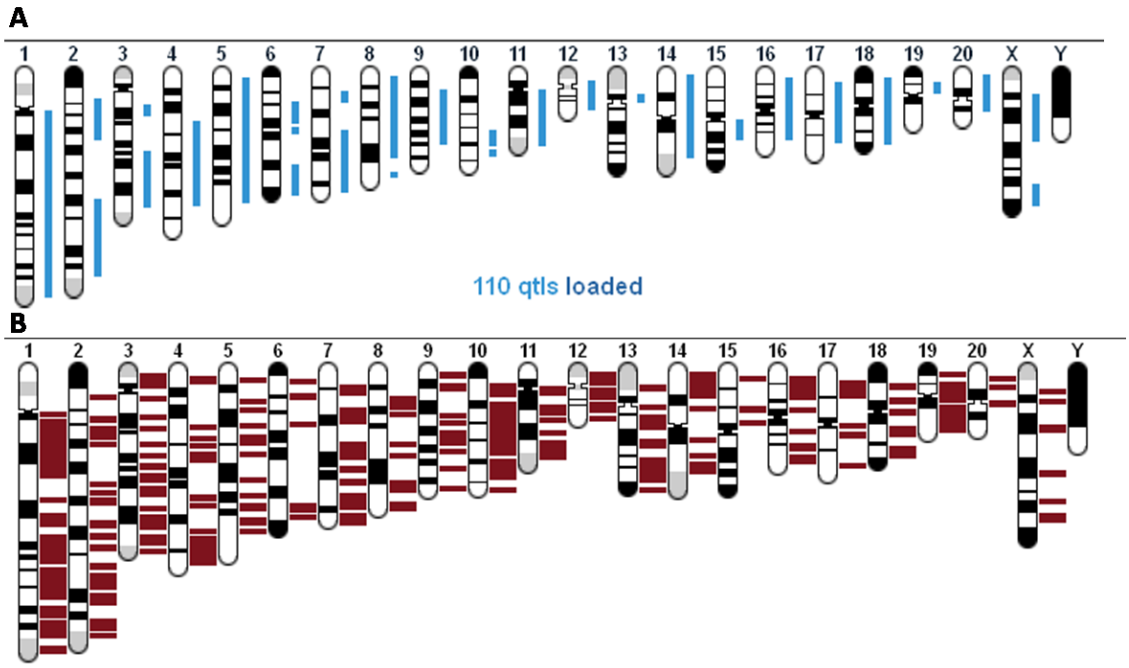

Figure 5.8 Association of differentially expressed genes in HGHF vs C to Rat diabetic QTLs. A) Localisation of 110 QTLs associated with diabetes (blue bars); B) Localisation of the top 500 differentially expressed genes in high glucose high fat in comparison to control (red bars).

Permutation statistical test showed a small but significant enrichment (1.06, $p<0.001$) of our differentially expressed genes in the QTLs, indicating that these QTLs regions include more of our glucolipotoxicity induced genes than it would be observed by chance.

Similarly, we investigated if known GWAS genes were present in our list of differentially expressed genes in glucolipotoxicity. In particular, we checked for the presence of genes associated with T2D in the NHGRI GWAS catalog (www.genome.gov/gwastudies), with a p value $<10^{-8}$. Out of 61 genes present in the catalog, 26 were differentially expressed in our experiment with statistical significance.

Considering that in our experiment we obtained 7994 differentially expressed genes in glucolipotoxicity out of 24000 rat genes (1/3), the same proportion would be expected by chance in the GWAS list (20 genes). With this calculation, there was an enrichment of our glucolipotoxicity induced genes in the GWAS list. However, the analysis with a permutation test did not give a significant enrichment.

Table 5.4 shows the list of GWAS genes differentially expressed in our experimental conditions, with the corresponding fold change and p value in conditions of high glucose/high fat compared to controls. Many of the important GWAS genes associated with diabetes are listed in this table and are differentially expressed in conditions of glucolipotoxicity with high fold change and highly significant p value. This result suggests the involvement of the specific genes identified through GWAS studies in the development of T2D.

GWAS GENE	**FOLD CHANGE**	**P VALUE**
MADD (MAP-Kinase Activating Death Domain)	1.37	0.02
TCF7L2 (Transcription factor 7-like 2)	0.46	0.05
KCNQ1 (Potassium Voltage-Gated Channel, KQT-Like Subfamily, Member 1)	0.70	0.02
PCSK1 (Proprotein Convertase Subtilisin/Kexin Type 1)	1.51	0.00557
IGF2BP2 (Insulin-Like Growth Factor 2 MRNA Binding Protein 2)	0.018	4.90 E-08
HHEX (Hematopoietically Expressed Homeobox)	0.12	0.000213
MTNR1B (Melatonin Receptor 1B)	0.01	2.17 E-05

PDE8B (Phosphodiesterase 8B)	0.31	1.35 E-08
AP3S2 (Adaptor-Related Protein Complex 3, Sigma 2 Subunit)	1.48	0.03
CAMK1D (Calcium/Calmodulin-Dependent Protein Kinase 1D)	Inf	1.65 E-06
KLF14 (Krupper-like Factor 14)	0.006	1.51 E-06
LARP6 (La Ribonucleoprotein Domain Family, Member 6)	Inf	3.19 E-05
PRC1 (Protein Regulator Of Cytokinesis 1)	1.52	0.017
HNF4A (Hepatocyte Nuclear Factor 4, Alpha)	2.09	0.0022
DUSP9 (Dual Specificity Phosphatase 9)	0.016	0.001148
LGR5 (Leucine-Rich Repeat Containing G Protein-Coupled Receptor 5)	0.13	8.74 E-05
FAH (Fumarylacetoacetate Hydrolase)	0.33	0.000213
RND3 (Rho Family GTPase 3)	1.85	0.002
ADAMTS9 (A Disintegrin And Metalloproteinase with Thrombospondin Motif 9)	0.19	0.0026
WFS1 (Wolfram Syndrome 1)	0.58	0.001454
ANK1	0.43	7.95 E-07

(Ankyrin 1)		
KCNK16 (Potassium Channel, Subfamily K, Member 16)	2.93	1.08 E-14
NOTCH2 [Notch (Drosophila) Homolog 2]	0.42	2.13 E-06
RBMS1 (RNA Binding Motif, Single Stranded Interacting Protein 1)	0.49	0.000636
RPL9P23 (Ribosomal Protein L9 Pseudogene 23)	1.47	0.006
APOB (Apolipoprotein B)	0.15	0.000449

Table 5.4 Association to known GWAS genes.

The presence of *TCF7L2*, *IGF2BP2*, *NOTCH2*, *WFS1*, *HHEX*, *ADAMTS9* is of high importance, as specified below.

- *TCF7L2* is a transcription factor involved in the Wnt signalling pathway and it is implicated in blood glucose homeostasis. Potential mechanisms by which TCF7L2 variants influence T2D include its role in adipogenesis, myogenesis and pancreatic islet development, as well as in β-cell survival and insulin secretory granules function [352]. It is also involved in the transcriptional regulation of the genes encoding for proglucagon and glucagone like peptides GLP-1 and GLP-2, which play a role in postprandial insulin secretion.
- *IGF2BP2* encodes a member of the IGF-II mRNA binding protein (IMP) family. It binds to the 5' UTR of the IGF-II mRNA and regulates IGF-II translation. In β-cells, it is important for the regulation of their function [353].
- *NOTCH2* is generally involved in development and cell fate decision, but there is increasing evidence that NOTCH2 signalling is important also for immune functions. In particular, NOTCH2 signalling pathway has been shown to suppress the TLR-induced IL-6 and TNF-α expression in macrophages. NOTCH2 genetic variants can increase the inflammatory response in T2D [354].

It has shown to be expressed in pancreatic β-cells, where it regulates pancreas development [355].

- *WFS1* is a transmembrane protein that participates in the regulation of calcium homeostasis, by modulating the filling state of the endoplasmic reticulum Ca^{2+} stores. Genetic variants of WFS1 can alter calcium dynamics involved in insulin granules secretion. In β-cells, it has been shown to be implicated in the regulation of insulin secretion [356].
- *HHEX* encodes a member of the homeobox family of transcription factors involved in hematopoietic differentiation. It is also expressed in the embryonic ventral-lateral foregut that gives rise to the ventral pancreas and the liver. This part of the pancreas is the major site of pancreatic polypeptide production. Therefore, it is possible that SNPs in this gene affect hormone's production during embryogenesis and adulthood, inducing the effects on insulin release. It has been shown that HHEX is associated with decreased β-cell sensitivity to glucose [357].
- *ADAMTS9* is a disintegrin and metalloproteinase with trombospondin motifs. It is implicated in the cleavage of proteoglycans, the control of organs shape during development and the inhibition of angiogenesis. It has also a protease-indipendent function in promoting the transport from the endoplasmic reticulum to the Golgi apparatus of a variety of secretory cargos [358].

The expression level of these genes is represented in Figure 5.9.

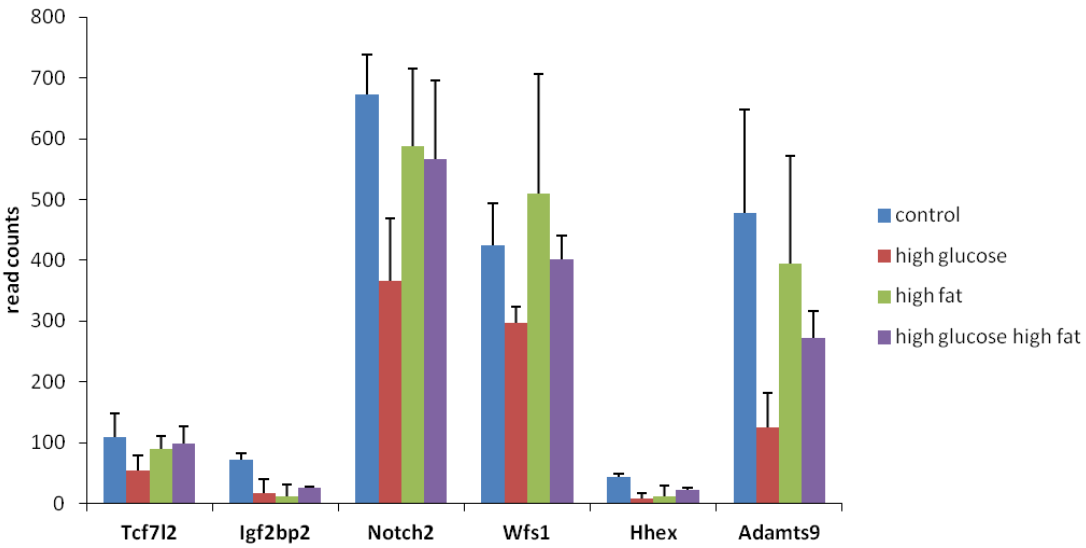

Figure 5.9 Expression level of GWAS genes. RNAseq was performed on the RNA of INS-1 cells treated with the 4 experimental conditions. Values are mean + SD of number of reads associated with a particular condition.

5.6 Identification of the top hits

We then focussed on the characterisation of the top hits genes, which are the genes differentially expressed in high glucose/high fat compared to control with the highest adjusted p value. Table 5.5 lists the top 10 hits in our list obtained from comparison between high glucose/high fat and control conditions.

GENES	FOLD CHANGE	P VALUE
SLC38A4 (Solute Carrier Family 38, Member 4)	4.9	4.67E-30
SEPP1 (Selenoprotein P, Plasma 1)	6.6	1.06E-28
PDE2A (Phosphodiesterase 2A, CGMP-Stimulated)	4.7	2.90E-27

SLC16A6 (Solute Carrier Family 16, Member 6)	0.2	7.77E-22
GPR119 (G-protein Coupled Receptor 119)	7.1	2.05E-21
ABCA4 (ATP-Binding Cassette, Sub-Family A (ABC1), Member 4)	Inf	2.63E-20
DNAJC22 (DnaJ (Hsp40) Homolog, Subfamily C, Member 22)	3,7	2.63E-20
VOM2R62 (vomeronasal 2 receptor, 62)	Inf	2.63E-20
HRSP12 (Heat-Responsive Protein 12)	3.5	1.73E-18
COL15A1 (Collagen, Type XV, Alpha 1)	Inf	3.25E-18

Table 5.5 Top hit genes in the comparison HGHF vs C p<0.05.

Most of these genes are known to be associated directly or indirectly with diabetic conditions.

- *SLC38A4* is a sodium dependent amino acids transporter. It is found predominantly in the liver. A SNP in this gene is associated with hyperglycemia [359].
- *SEPP1* is a selenoprotein responsible for some of the extracellular anti-oxidant defense properties of selenium or it might be involved in the transport of selenium. It has been shown that hepatic SEPP1 mRNA levels correlated with insulin resistance in humans and genetic variants of this gene are associated with fasting insulin [360]. In β-cells, its expression is modulated by high glucose and it is associated with the anti-oxidant protection of the β-cells [361].
- *PDE2A* is a cyclic nucleotide phosphodiesterase with a dual-specificity for the second messangers cAMP and cGMP, key regulators of many important

physiological processes. It has also a potential role in regulating calcium channel activity [362], and it may be involved in the calcium dynamics regulating insulin exocytosis in the β-cell.

- *SLC16A6* is a proton-linked monocarboxylate transporter, which catalyses the rapid transport across the plasma membrane of many monocarboxylates such as lactate and pyruvate.
- *GPR119* is a G-protein coupled receptor highly expressed in the pancreatic islets. The activation of GPR119 is associated to glucose-dependent insulin secretion in pancreatic β-cells, along with glucose-dependent insulinotropic peptide (GIP) and GLP-1 release in intestinal K cells and L cells respectively [363].
- *ABCA4* is an ATP binding cassette mainly expressed in the retina; its expression in the β-cell could be explained by the similarity in the proteome of β-cells and neurons.
- *DNAJC22* is a membrane protein associated with a rat T2D QTL.
- *VOM2R62* encodes for a vomeronasal receptor, involved in G protein coupled receptor signalling pathway. It is associated to a QTL for insulin level and diabetes.
- *HRSP12* is an endoribonuclease responsible for the inhibition of the translation by cleaving mRNA. It is associated with diabetic QTLs.
- *COL15A1* encodes the alpha chain of type XV collagen, which is mainly expressed in basement membrane zones. It may function in the adhesion of basement membranes to underlying connective tissue stroma.

The differential expression of the genes listed is represented in Figure 5.10.

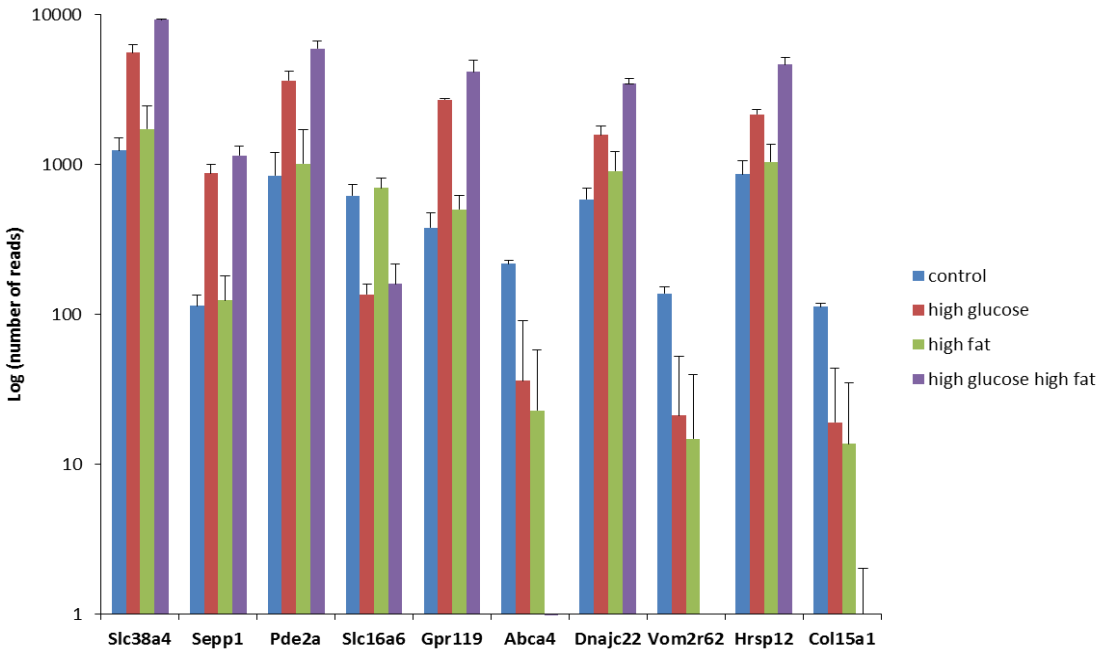

Figure 5.10 Expression level of top hit genes. RNAseq was performed on the RNA of INS-1 cells treated with the 4 experimental conditions. Values are mean + SD of number of reads associated with a particular condition.

5.7 Discussion

The study of the transcriptome allowed a deep understanding of the molecular changes implicated in the onset of many pathologic conditions and the combination with high-throughput techniques helped gaining a more complete view of all the transcriptome changes in a single experiment.

In this thesis, RNAseq technology was used to characterise the molecular changes in the β-cell after exposure to high concentrations of glucose and fatty acids. In particular, the main aim was to discover new molecules that could be involved in the impairment of β-cell function. We initially focussed our attention on the general characterisation of the experimental results, performing clustering and pathway analysis, in order to identify the principal mechanisms affected by glucolipotoxicity.

INS-1 cells were used as an experimental system and they were incubated for 72 h in four different conditions: control, high glucose (27 mM glucose), high fat (200 µM oleic

acid, 200 μM palmitic acid), high glucose/high fat (27 mM glucose, 200 μM oleic acid, 200 μM palmitic acid).

2701 genes resulted differentially expressed in high glucose, 2561 in high fat and 7994 in high glucose high fat, with an adjusted p value of $p<0.05$. Most of the genes were downregulated, suggesting that conditions of glucolipotoxicity block the expressions of numerous genes, including insulin. In addition, more than 95% of the genes differentially expressed in high glucose alone, or high fat alone, were also differentially expressed in high glucose/high fat (Figure 5.2). For this reason, the subsequent pathway analysis was performed using the combination of the two treatments. The high glucose/high fat vs control comparison contained the highest number of differentially expressed genes and this was the condition that clustered more differently from control (Figure 5.4). This result is consistent with the fact that glucose and fatty acids act together to impair β-cell function. This is consistent with our previous results on insulin secretion and content, on CD40 and TRAFs upregulation, which showed that impairment of these processes was potentiated by the combined incubation of glucose and fatty acids. Furthermore, this is also consistent with previous studies showing the synergism between fatty acids and glucose [107].

The fact that the experimental conditions used are representative of the molecular changes that affect the β-cell during the progression to diabetes was confirmed by pathways analysis (Table 5.1). Pathways involved in glucose metabolism (glycolysis), in inflammation mediated by chemokines and cytokines signalling pathways and vesicle trafficking were significantly affected by the treatments. These are all mechanisms directly involved in T2D progression, as they are connected to glucose or insulin trafficking, or to the inflammatory process generated in the β-cell under glucolipotoxic conditions [144, 154]. In addition, pathways that are indirectly involved in diabetes also resulted significantly affected. Examples of these pathways are glutamatergic neurotransmission, which may contribute to the impaired insulin secretory response in T2D and Wnt signalling pathway which is involved in cell sensitivity to insulin and in β-cell proliferation. Interestingly, another pathway that resulted affected by glucolipotoxicity involves molecules implicated in Alzheimer's disease. The pancreas is a highly innervated organ that shares a number of molecular similarities with brain at the

level of transcriptome and proteome. T2D and Alzheimer's disease are both characterised by localised amyloid deposits that progress during the course of the disease. In addition diabetes could increase the likehood of Alzheimer's disease, due to the impact of insulin abnormalities, insulin resistance and advanced glycation end products on the development of neural amyloid plaques and neurofibrillary tangles. This functional connection between pancreas and brain could be the explanation also of the presence, in the β-cell, of other molecular pathways (thyroid pathway) specific of the brain (Chapter 6).

These results are in line with the pathway analysis performed for the previous Affymetrix experiment (Chapter 3, Figure 3.9) and with microarrays studies performed by other research groups. Specifically, it has been shown differential expression of islets hormones and genes involved in metabolism, ER stress, oxidative stress, apoptosis and signalling, when rat islets and MIN6 cells were incubated to high concentrations of glucose [264-265]. Similar findings were also obtained by Cnop and coworkers, who investigated the effect of incubation of human pancreatic islets to high concentrations of palmitate [272]. However, these projects relied only on microarrays results or they only considered the effects of high glucose and fatty acids alone. Our study is novel as we used RNA sequencing, which can give more detailed information about all the transcriptome profiling, and we investigated also the effects of the combinations of high glucose and fatty acids.

Accordingly to our pathway analysis (Table 5.3), the genes that are differentially expressed under condition of glucolipotoxicity were found to be associated with several diseases including inflammation, obesity, T2D and insulin resistance, confirming that our experimental conditions influence the expression of molecules implicated in diabetes and insulin resistance. In addition, the list includes other diseases associated with diabetes, for example, cardiovascular disease and hypertension. These are generated mainly by the inflammatory process and oxidative stress characteristic of T2D.

As a further confirmation of the fact that the experimental conditions used are representative of T2D conditions, these differentially expressed genes were located in known rat diabetic QTLs loci (Figure 5.8), and contained several known GWAS genes

(Table 5.4). In particular, the top hits of the list showed the presence of TCF7L2, IGF2BP2, NOTCH2, WFS1, HHEX, ADAMTS9, whose association to diabetes has been demonstrated (Figure 5.9).

In addition, the 10 top hits of the list (the genes differentially expressed in HGHF vs C with the highest p value) were genes that are directly or indirectly connected to diabetes or its associated diseases (Table 5.5).

In conclusion, all these information confirmed that INS-1 cells respond to glucolipotoxicity in a manner similar to what is observed *in vivo* during the progression to T2D.

In conclusion, these results show all molecular changes induced by the exposure of β-cells to conditions of glucolipotoxicity. However, most of the information derived from the pathway analysis has been already studied in relation to diabetes [272, 364]. A more detailed and accurate research on the RNAseq data results is now required to discover novel mechanisms of glucolipotoxicity in T2D.

Chapter 6

Identification of novel

mechanisms of glucolipotoxicity

6.1 Introduction

As discussed in Chapter 5, using RNAseq procedures we identified several glucolipotoxicity induced differentially expressed genes, in order to discover novel mechanisms that could affect the β-cell after exposure to high concentrations of glucose and fatty acids.

Several of these differentially expressed genes and their correspondent pathways analysed so far are already known to be associated with diabetes. They overlap with, or are situated close, to rat diabetic QTLs chromosomal regions. In addition SNPs close to or within several of these genes have been reported to be associated with diabetes in many GWAS studies. Functional pathways associated with our differentially expressed genes are known to interact with insulin.

Nevertheless, after a detailed observation and analysis of our data and associated pathways, we have indentified some potential new research areas.

Consistent with our previous studies on CD40 and its role in the β-cell, we expanded the analysis to other molecules involved in the TNFR pathway, including some receptors that have not been studied previously. The TNFR pathway resulted to be highly affected by glucolipotoxicity and these findings could be useful to understand in more details the network of CD40 in glucolipotoxicity.

Supporting previous observations but highlighting a less studied pathway was the potential role of the Hypothalamic-Pituitary-Thyroid (HPT) genes in islet cells [365-368]. The thyroid is a gland located in the neck that controls the body metabolism through the hormones T3 and T4, which regulate the growth and function of other systems in the body. The connection between thyroid and β-cells is quite interesting as, not only we demonstrated that some thyroid specific molecules are expressed in the β-cell, but their expression can be also influenced by exposure to a glucolipotoxic environment.

We also identified some miRNAs, which could be interesting targets for future analysis. MiRNAs are regulatory RNAs and known to be involved in the pathogenesis and evolution of different diseases. Some of them have been associated to the pathogenesis of T2D, influencing insulin secretion through different mechanisms [295, 302-304].

Finally, with the RNAseq technology, we also identified several potentially interesting novel genes or ESTs (expressed sequence tags), encoding for proteins whose structure and functions have not been elucidated so far. Preliminary protein structural/functional bioinformatics analyses suggest that some of these novel genes could be involved in pathways regulating β-cell function.

6.2 The TNFR pathway

In previous experiments (Chapters 3 and 4), we focussed our attention on CD40, a member of TNFR superfamily, and its role in glucolipotoxicity. We also analysed the effects of glucolipotoxicity on other molecules involved in the TNFR pathway, in particular on TRAF proteins.

In this part of the project we investigated the expression changes of other molecules involved in the TNFR pathway in conditions of glucolipotoxicity.

To this end, we used the program Metacore, and we drew a pathway scheme highlighting the molecules that changed their expression in glucolipotoxicity. Figure 6.1 shows the results of the analysis. The bar on the right of the gene indicates that the gene was differentially expressed in some of the experimental conditions (1 corresponds to high glucose, 2 to high fat and 3 to high glucose/high fat). This pathway analysis shows that the TNFR pathway was highly affected by conditions of glucolipotoxicity.

Figure 6.1 shows changes in the expression of receptors (*TNFRSF1B*, *TNFRSF11A*, *TNFRSF17*), of ligands (*TNF-α*, *TNFSF4*, *CD40L*, *TNFSF11*, *TNFSF12*, *TNFSF13B*, *TNFSF13*) and of TNF inducible proteins (*IRAK1/2*, *TRAF2*, *TRAF3*, *MAP3K14*, *CAT*, *NF-κB2*, *NF-κBiB*, *BCL2A1*).

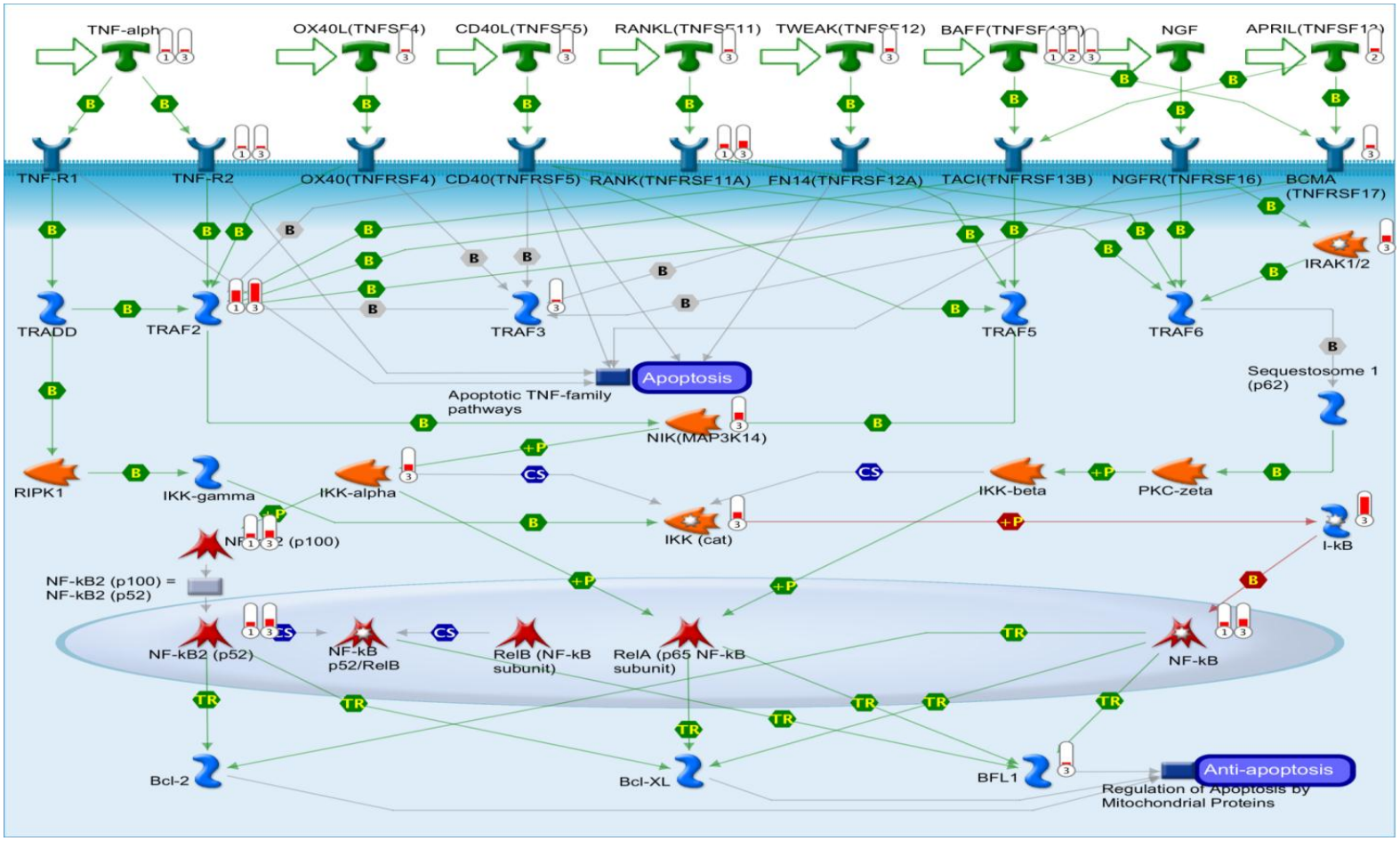

Figure 6.1 Analysis of the TNFR pathway. Representation of the TNFR pathways molecules differentially expressed in HGHF vs C with a p value $p<0.05$. The red bar at the right of the gene indicates the level of differential expression and it can indicate either upregulation or downregulation.

Figure 6.2 represents the mRNA expression changes of members of the TNFR pathway.

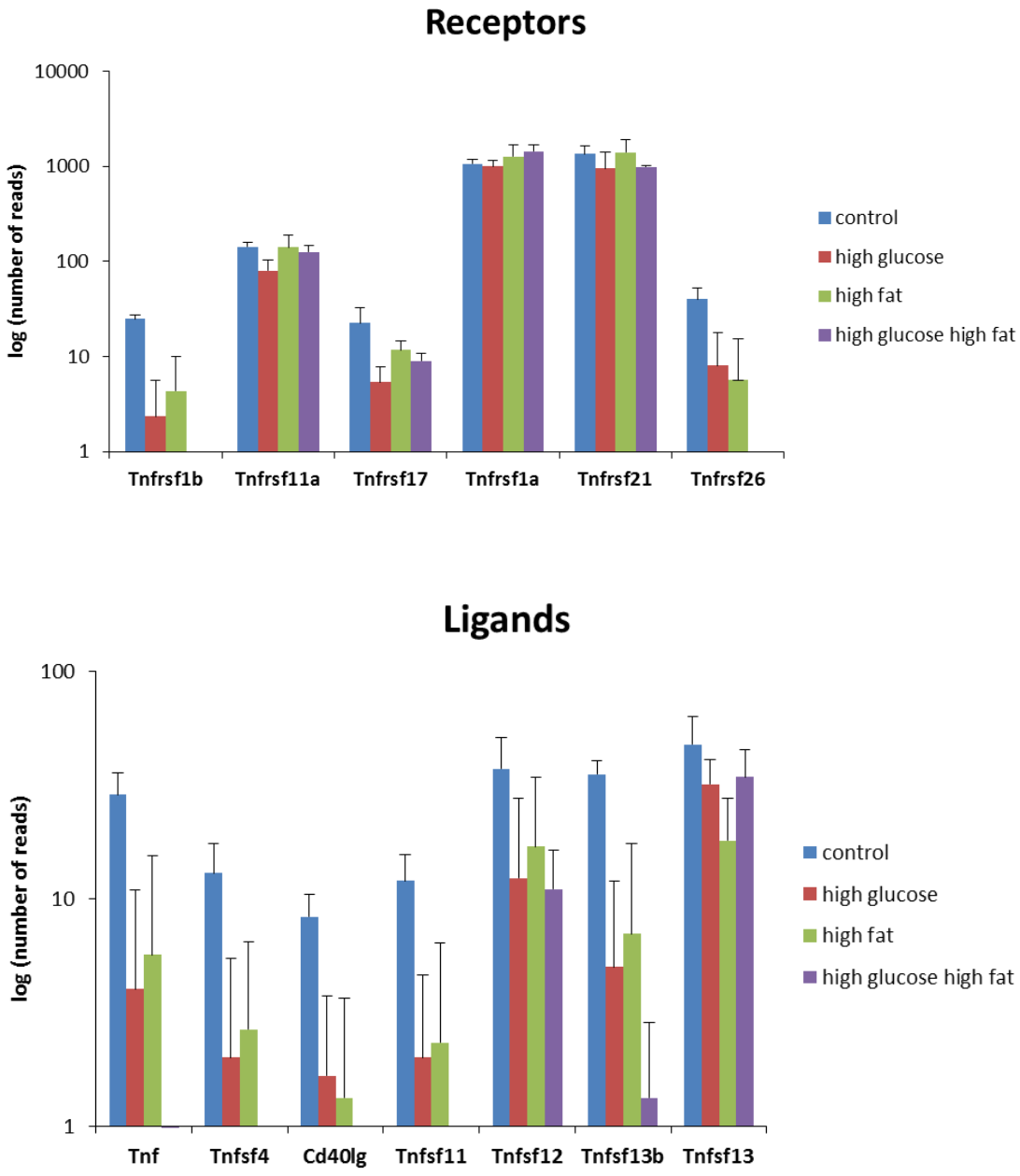

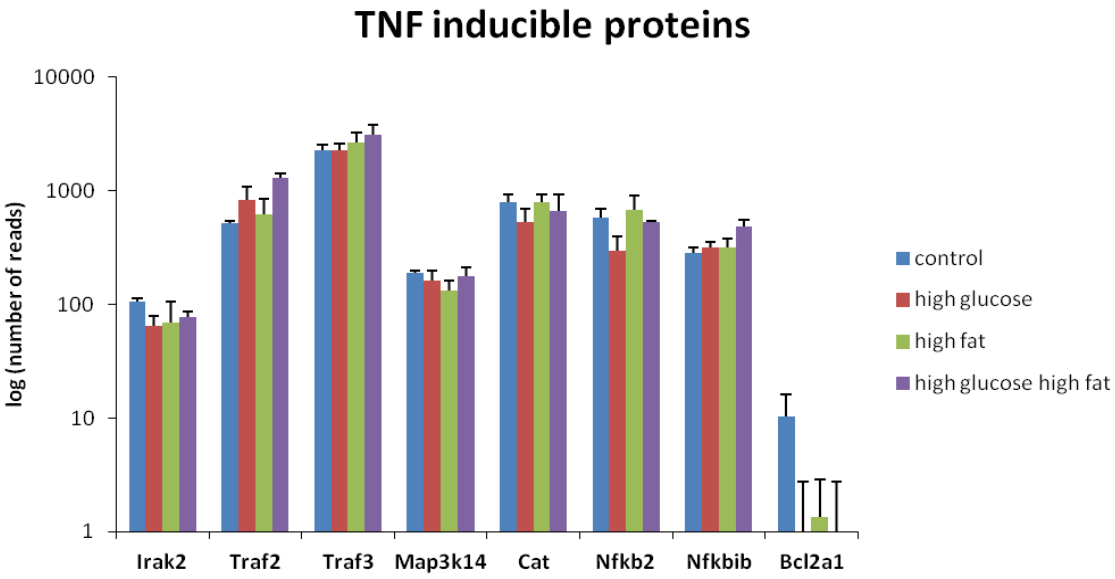

Figure 6.2 Expression levels of TNFR pathway genes. RNAseq was performed on the RNA of INS-1 cells treated with the 4 experimental conditions. Values are means + SD of number of reads associated with a particular condition.

This analysis showed that expression values for most of the receptors decreased in glucolipotoxicity (Figure 6.2), which was in contrast to the effect seen on CD40 receptor (Chapter 3), indicating that glucolipotoxicity induced specific responses on each particular TNFR. Consistent with this, TNFR1B expression decreased in glucolipotoxicity, while TNFR1A expression remained unchanged. TNFR21 and TNFR26 were considered because their expression was affected also in the previous Affymetrix experiment. TNFR21 encodes Death Receptor 6, a protein that activates NF-κB and c-Jun, inducing cell apoptosis. TNFR26 is a novel member of the TNFR family which has not been characterised so far.

Figure 6.2 shows that ligands expression decreased in glucolipotoxicity, including expression of CD40L.

These data also confirmed the increase in TRAF2 expression, and the involvement of NF-κB in glucolipotoxicity. Interestingly, data showed a reduced expression of NFKB2 in glucolipotoxicity, which would seem in contrast with our previous results showing an increased activation of NF-κB under chronic exposure to glucose and fatty acids.

However, NF-κB expression changes do not always correspond to its activation, which is determined by p65 translocation in the nucleus.

In addition, a reduced expression of IRAK2, a serine-threonine kinase associated with activated IL-1R, was also observed. IRAK is reported to be involved in the IL-1-induced upregulation of NF-kB. This can further explain why there was a decrease in the NF-κB genes expression in our experimental system.

6.2.1 TNFR pathway validation

In order to validate some of the results, we used quantitative PCR with specific primers for the genes of interest. INS-1 cells were cultured for 72h in the 4 experimental conditions, RNA was extracted, reverse transcribed and qPCR performed. Figure 6.3 shows the validation of some of the receptors.

TNFR1A did not change its expression in glucolipotoxicity, confirming the RNAseq data. TNFR21 showed a significant decrease (42%, $p<0.05$) especially in the presence of both high glucose and high fat. TNFR26 is of particular interest, as it showed a 90% decrease with high glucose or high fat alone, and a nearly 100% decrease with the combination of the conditions ($p<0.001$). Considering that TNFR26 has not been studied so far, it could be a novel and interesting subject for future studies aimed to confirm its role in glucolipotoxicity.

In addition, CD40 was validated and the RT-qPCR confirmed the results shown previously (Chapter 3). CD40 did not show statistical significant differential expression in glucolipotoxicity from the RNAseq reads count, but its expression was very low (average 30 reads for the gene), which led to difficult detection of the expression changes and consequently reduced statistical significance.

These data shows also the importance of a validation by RT-qPCR of the results obtained by RNAseq analysis, in order to confirm the differential expression.

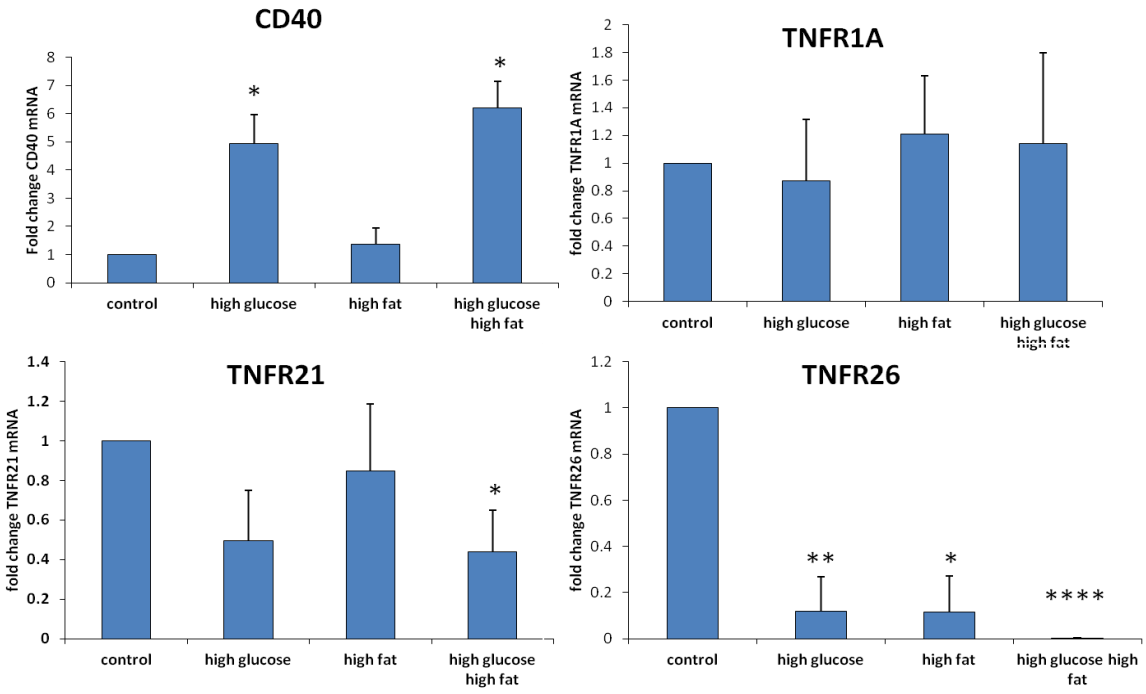

Figure 6.3 Validation of TNF receptors by RT-qPCR. INS-1 cells were cultured for 72h in the 4 experimental conditions, RNA was extracted, reverse transcribed and RT-qPCR performed using specific primers. Data represent ΔΔCt values expressed as a fold change compared to cells grown in RPMI (control). Data are expressed as means + SD of 3 independent experiments (*p<0.05; **p<0.01; ****p<0.001).

Figure 6.4 shows the validation by RT-qPCR of some of the ligands and TNF inducible proteins involved in the TNFR pathway.

TNF resulted to be downregulated in glucolipotoxicity (55% decrease, p<0.05), confirming the RNAseq data.

However, NF-κBib, NF-κB2 and IRAK did not show statistical significant differential expression in glucolipotoxicity. NF-κBib, which is NF-κB inhibitor, showed a trend towards an increased expression, while NF-κB2 had a trend towards a decreased expression in glucolipotoxicity, as shown by the RNAseq data. No change in expression was detected for IRAK by RT-qPCR.

These discrepancies between RNAseq and RT-qPCR can be explained by the fact that the fold change of some of the genes studied (NF-κBib, NF-κB2, IRAK) was not very high in the RNAseq data and the p value was at the borderline of significance. RT-qPCR

detected the variability between the samples and, as a consequence, even if data showed the same trend as the RNAseq experiment, they did not reach statistical significance.

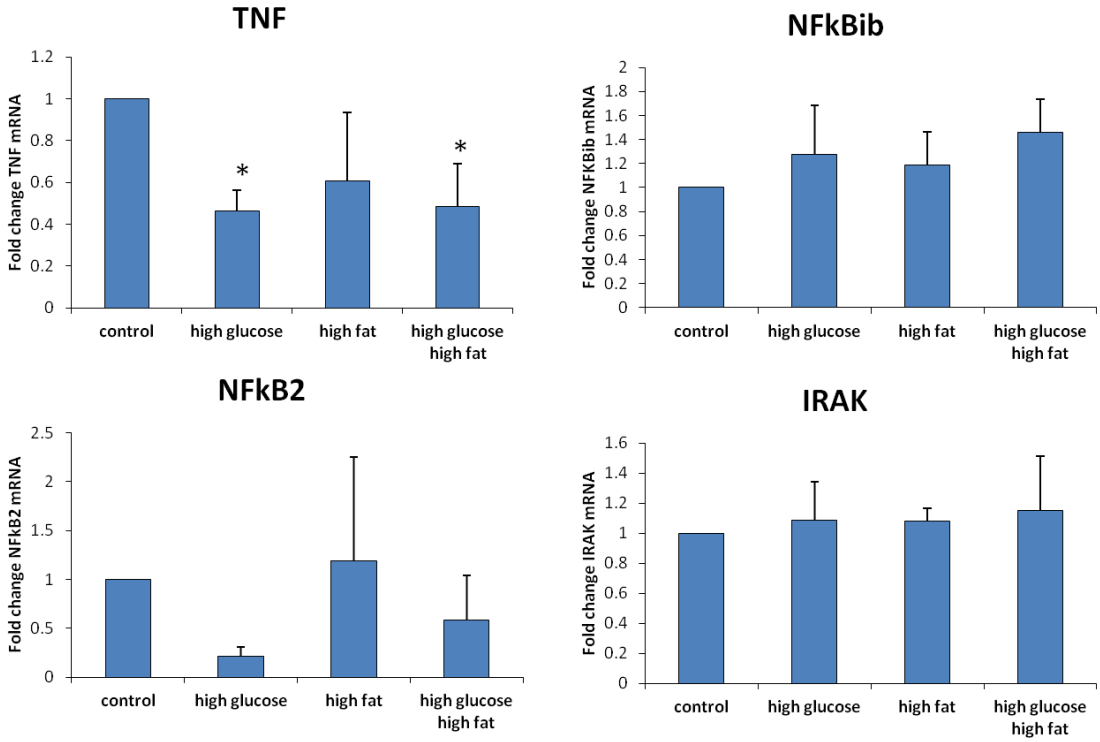

Figure 6.4 Validation of TNF ligands and inducible proteins by RT-qPCR. INS-1 cells were cultured for 72h in the 4 experimental conditions, RNA was extracted, reverse transcribed and RT-qPCR performed using specific primers. Data represent ΔΔCt values expressed as a fold change compared to cells grown in RPMI (control). Data are expressed as means + SD of 3 independent experiments (*p<0.05).

6.3 Thyroid pathway

The pathway analysis of our differentially expressed genes in glucolipotoxicity (Table 5.1) revealed changes in the Hypothalamic-Pituitary-Thyroid (HPT) pathway.

The thyroid is a gland located in the neck, which controls metabolism, how the body makes protein and it is responsive to other hormones. It produces the hormones triiodothyronine (T3) and thyroxine (T4), which regulate the growth and function of other systems in the body. The hormonal output from the thyroid is regulated by the thyroid stimulating hormone (TSH) produced by the anterior pituitary gland, which

itself is regulated by the thyrotropin stimulating hormone (TRH) produced by the hypothalamus. The hormones T3 and T4 are synthesised by follicular cells where the enzyme thyroid peroxidase (TPO) catalyses the addition of iodine to a protein called thyroglobulin (Tg). Upon stimulation by TSH, the follicular cells reabsorb Tg and cleave the iodinated tyrosines from Tg in lysosomes, forming T3 and T4 and releasing them in the blood.

There is a feedback loop regulating the release of the thyroid hormones (Figure 6.5). TRH and TSH production and secretion are suppressed when T4 levels are high. TSH production is also inhibited by somatostatin (SRIH).

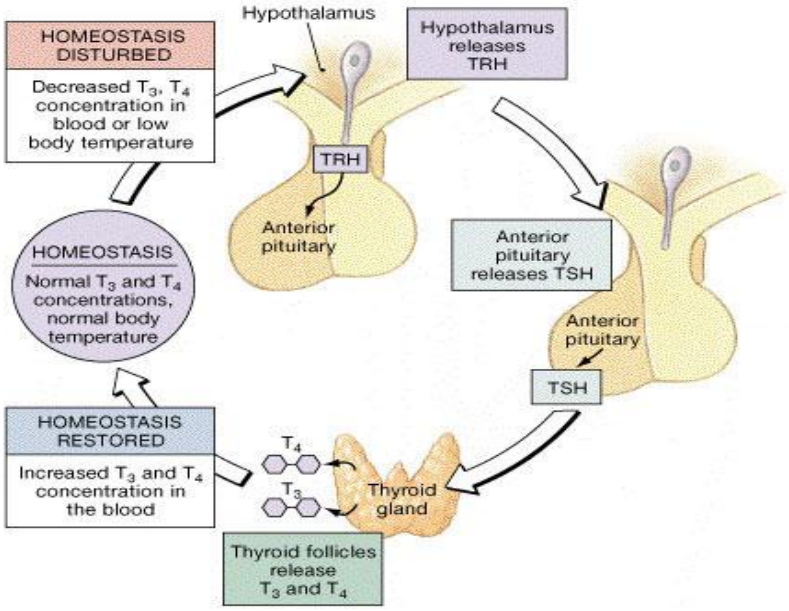

Figure 6.5 Feedback loop regulating the release of thyroid hormones. TRH and TSH productions are suppressed when the T4 levels are high. Figure adapted from "Harrison's principles of internal medicine".

As shown in Figure 6.6, several genes involved in the thyroid pathway were differentially expressed in glucolipotoxicity in our experimental system, including hormones (*TRH*), receptors (*Trhr*, *Tshr*, *Sstr*), enzymes (*Tpo*, *Dio1*), solute carriers (*Slc5ac*) and thyroid specific transcription factors (*Nkx2-1*, *Nkx2-2*).

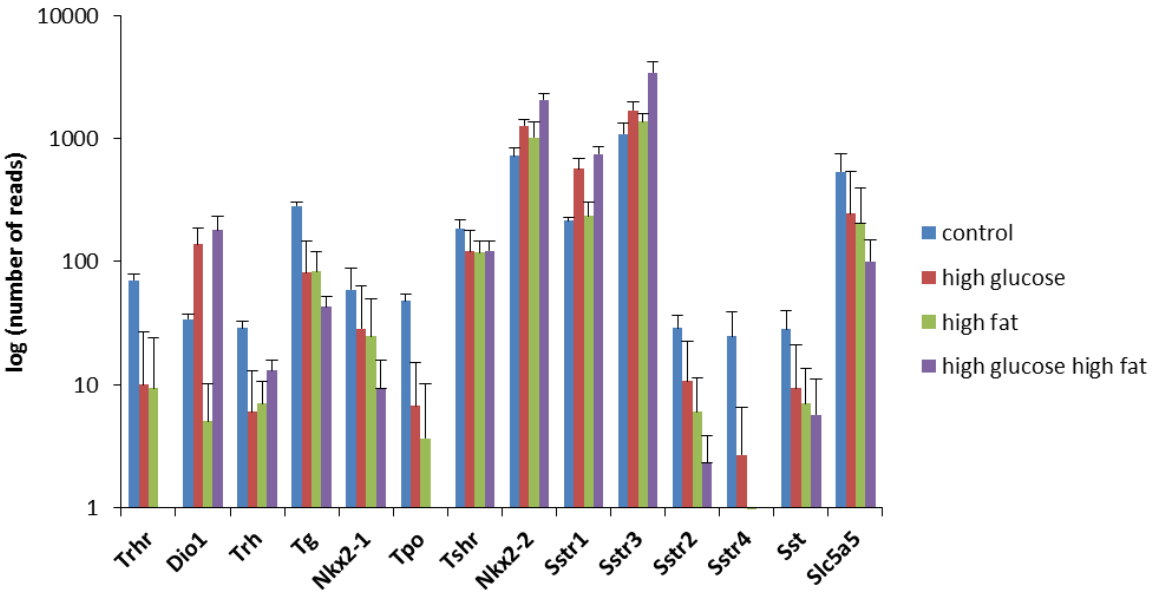

Figure 6.6 Expression levels of thyroid genes. RNAseq was performed on the RNA of INS-1 cells treated with the 4 experimental conditions. Values are mean + SD of number of reads associated with a particular condition.

Glucolipotoxicity mainly downregulates the expression of these genes, therefore we hypothesise that some of them may have a positive role in stimulating insulin secretion. For instance, it has been shown previously that TRH can promote insulin release in adult pancreatic islets and its expression can be involved in the regulation of the β-cell function [369]. The blockage of these gene expressions in glucolipotoxicity could be responsible of the impairment of β-cell function in T2D [366-367].

6.4 miRNAs

Some miRNAs have been already shown to be involved in the regulation of the pancreatic β-cell function, in particular in the development of the pancreas, as well as in the impairment of insulin secretion, or in the generation of an inflammatory status [297, 301, 303].

From our total RNAseq data, we discovered 4 miRNAs that were differentially expressed with statistical significance: Mir-3547, Mir-1949, Mir-205 and Mir-375 (Figure 6.7).

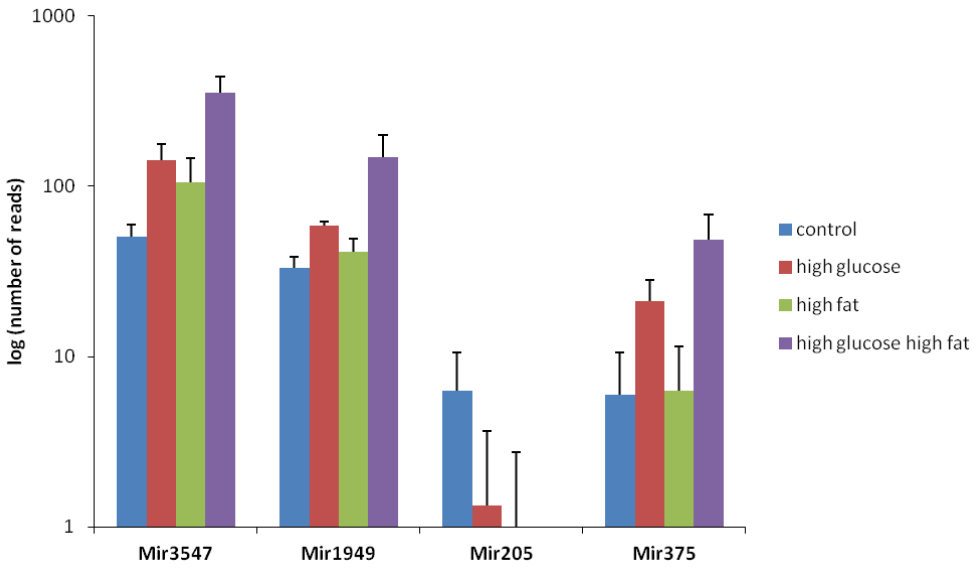

Figure 6.7 Expression levels of miRNAs. RNAseq was performed on the RNA of INS-1 cells treated with the 4 experimental conditions. Values are mean + SD of number of reads associated with a particular condition.

While Mir-1949 has not been extensively studied, it has been suggested to be associated to the progression of a leukemia [370] or to be involved in foetal lung development [371]. It is upregulated 2 times with high glucose and 5 times with high glucose/high fat (p value adjusted <0.001).

Mir-205 is a miRNA that has been associated with various cancers in several studies. It has reported to be silenced in breast cancer, prostate, bladder and lung cancer [372]. It plays also a role in regulating stem cell fate, probably regulating the expression of the tumour suppressor PTEN. Its expression is also associated with obesity [301]. While Mir-205 was downregulated by glucolipotoxicity in our experiment, its role in insulin secretion and development of T2D remains to be determined.

Mir-375 is a miRNA known to be associated to diabetes. It has a key role in β-cell development and function and it is essential for insulin secretion [295]. It has also been proposed as a biomarker for β-cell cell death [373]. Overexpression of this miRNA impairs exocytosis of insulin-containing intracellular vesicles due to aberrant regulation of its target myotropin [295]. Consistent with this, Mir-375 is upregulated 3 times with high glucose and 8 times with high glucose high fat (p value adjusted 0.0025).

The detection of these small RNAs from the RNAsequencing experiment, which should filter short transcripts, can be explained by the fact that miRNAs are transcribed as longer RNA molecules that are then processed to produce the mature miRNAs. Therefore the RNAseq system can detect the longer RNA molecule.
The presence of miRNAs associated with diabetes and obesity is a further confirmation that our experimental system is a reliable representation of the conditions of T2D.

6.4.1 Mir-3547 is overexpressed in glucolipotoxicity

Very little is known about Mir-3547. As mentioned above, our data showed that it was upregulated 3 times in conditions of high glucose, 2 times with high fat and 7 times with combination of high glucose/high fat (adjusted p value 3.10 E-11). We hyphothesised that Mir-3547 could be a novel biomarker for diabetes, and, for this reason, we decided to investigate this miRNA.
First we validated the results by quantitative RT-qPCR. INS-1 cells were cultured for 72h in RPMI-1640 supplemented with 27 mM glucose, 200 μM oleic acid, 200 μM palmitic acid. Cells were lysed, RNA extracted and miRNAs separated using mirVana miRNA isolation kit (Life Technologies, UK), following manufacturer's instructions. Small RNAs were retro-transcribed to cDNA using TaqMan® MicroRNA Reverse Transcription Kit (Applied Biosystems, Life Technologies, UK) with the specific assay for Mir-3547. Taqman microRNA assay kit (Applied Biosystems, Life Technologies, UK) was used to perform a RT-qPCR on the cDNA retro-transcribed from the small RNA.
Data confirmed that glucolipotoxicity increased Mir-3547 expression by more than 2 fold (Figure 6.8) confirming the RNAseq data.

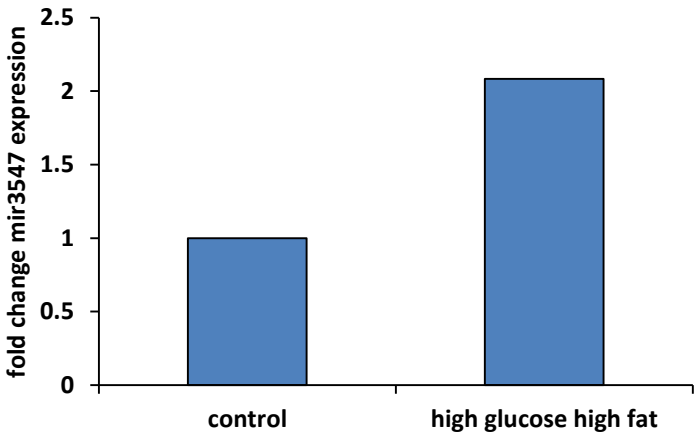

Figure 6.8 Mir-3547 expression in glucolipotoxicity. INS-1 cells were cultured for 72h in RPMI-1640 supplemented with 27 mM glucose, 200 μM oleic acid, 200 μM palmitic acid. Cells were lysed, RNA extracted and miRNAs separated using mirVana miRNA isolation kit. Small RNAs were retro-transcribed to cDNA using TaqMan® MicroRNA Reverse Transcription Kit with the specific assay for Mir-3547. Taqman microRNA assay kit was used to perform a qPCR on the cDNA retro-transcribed from the small RNA. Data represent ΔCt values expressed as a fold change compared to cells grown in RPMI (control). Data are values from 1 experiment.

6.4.2 Mir-3547 co-localises with Baiap3 locus

Mir-3547 is situated on rat chromosome 10 in the intron between exons 24/25 of another gene, Baiap3, on the rat genome (Figure 6.9). This is the same as in mouse, where the miRNA locates between exons 25/26 of Baiap3 on chromosome 17. In humans Baiap3 is located on chromosome 16, with no annotated intronic miRNA.

Baiap3 is a p53 target gene that encodes for a brain-specific angiogenesis inhibitor. The protein is a seven span transmembrane protein and a member of the secretin receptor family. It interacts with the cytoplasmic region of brain-specific angiogenesis inhibitor 1 [374]. This protein also contains two C2 domains, which are often found in proteins involved in signal transduction or membrane trafficking. Its expression pattern and similarity to other proteins suggest that it may be involved in synaptic functions and it is a member of the Munc13 protein family, which have a role in the priming step of vesicle exocytosis. It has been shown to regulate exocytosis, in particular of autocrine or paracrine growth factors by tumour cells [375].

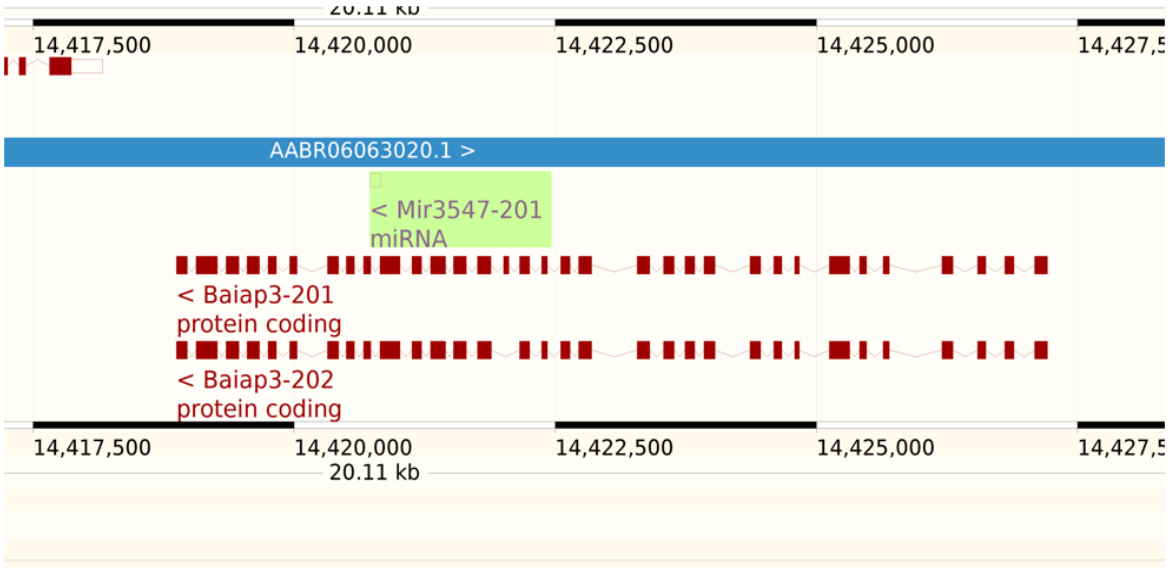

Figure 6.9 Chromosomal localisation of Mir-3547.

As Mir-3547 is located in the introns of a gene, it is one of those intronic miRNAs that can be classified as mirtrons. Mir-3547 would be co-expressed as pre-miRNA within the intron region of the host transcript using its Pol-II promoter. The intronic pre miRNA is eventually released by the host transcript after splicing machinery. However, this is not the only possible mechanism, as Mir-3547 could also be transcribed independently from Baiap3 gene using a yet unidentified promoter and following the classic miRNAs maturation processes.

In order to determine the most likely mechanism for the generation of Mir-3547, it is necessary to evaluate the rate of transcription of Baiap3, in conditions of glucolipotoxicity, as Mir-3547 is overexpressed under exposure to high concentrations of glucose and fatty acids. The RNAseq data indicated that Baiap3 is also overexpressed in glucolipotoxicity (Figure 6.10). In particular, it is overexpressed 2.5 times with high glucose and till 5/6 times with high glucose/high fat.

This suggests an important link between Baiap3 and Mir-3547, as their expressions are both affected by glucolipotoxicity. In addition, Baiap3 has been reported to be involved in secretion [375], therefore it could be implicated in the impairment of insulin secretion in glucolipotoxicity. This will need to be further explored.

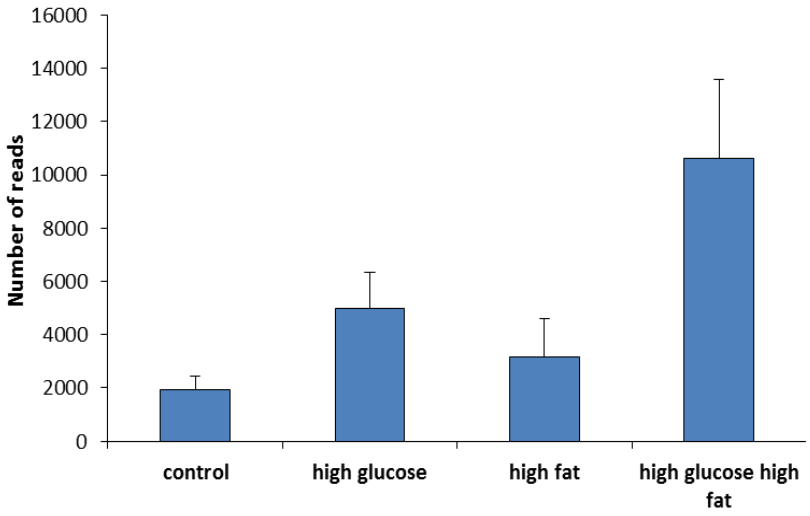

Figure 6.10 Expression level of Baiap3. RNAseq was performed on the RNA of INS-1 cells treated with the 4 experimental conditions. Values are mean + SD of number of reads associated with a particular condition.

The fact that Mir-3547 and Baiap3 are both overexpressed in glucolipotoxicity suggests that the two mRNA could be transcribed together. Preliminary experiments using quantitative RT-qPCR with primers annealing to different region of Baiap3 (as shown in Figure 6.11) could support this hypothesis. The first set of primers overlap with the junctions of exons 24 and exon 25 covering the miRNA region, the second set amplifies between exons 3 and 4, so externally to the miRNA region. These primers were used to amplify cDNA from INS-1 cells cultured for 72h in the 4 different conditions of glucolipotoxicity. In control conditions, the miRNA region shows a lower CT (more copies) in comparison to the non miRNA region. This suggests that there are more transcripts containing exon 24/25 (the region of Mir-3547) than using primers that amplify exon 3/4 region of Baiap3.

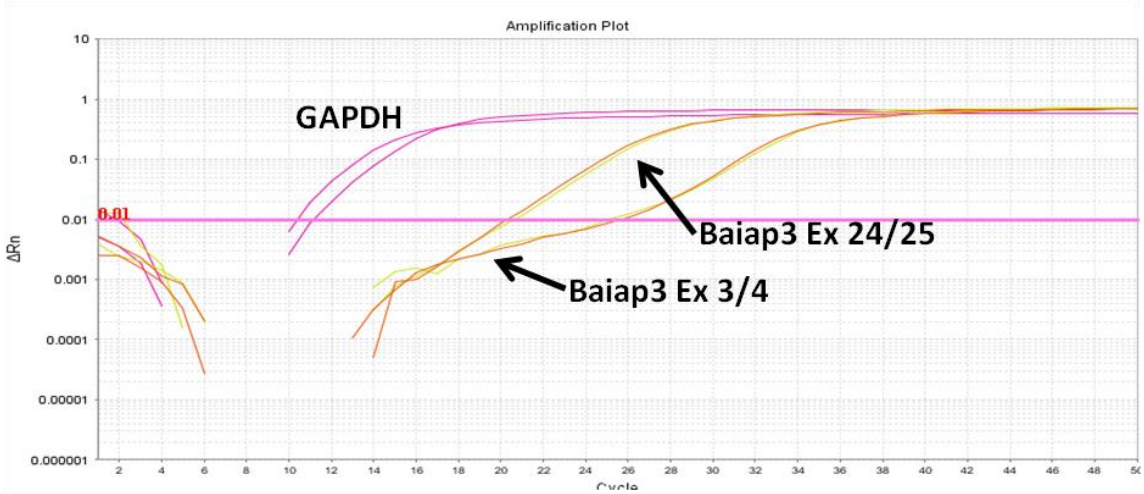

Figure 6.11 Amplification plot of Baiap3 in control conditions using different primers. The first couple of primers anneal between exon 4/5, external to the miRNA region; the second couple of primers anneals between exon 24/25, so overlapping the Mir-3547 region.

These results indicate a differential rate of transcription between Baiap3 and Mir-3547 and this could be due to the fact that:

- the different primers could have different efficiency of amplification;
- Mir-3547 could be transcribed together with Baiap3, using its promoter, and subsequently be spliced off; the differential rate of transcription could be due to alternative splicing events;
- Mir-3547 could use its own promoter, independently from Baiap3 gene;
- a combination of the above conditions.

The study of Baiap3 expression in conditions of glucolipotoxicity could help clarifying this.

6.4.3 Baiap3 is overexpressed in glucolipotoxicity

As shown in Figure 6.12 Baiap3 was overexpressed in conditions of high glucose/high fat, but the level of its overexpression changed according to the type of primers used. When primers in the miRNA region were used, we observed a nearly 3 fold increase in Baiap3 expression. Interestingly, when external primers were used we obtained a 5 fold overexpression. This result can be explained considering that the miRNA region showed a higher expression in comparison to the non miRNA region. Since we obtained more

copies of the miRNA region, we noticed a lower increase in glucolipotoxicity, because the amount was already high.

Future experiments are needed to clarify the reason of this differential expression.

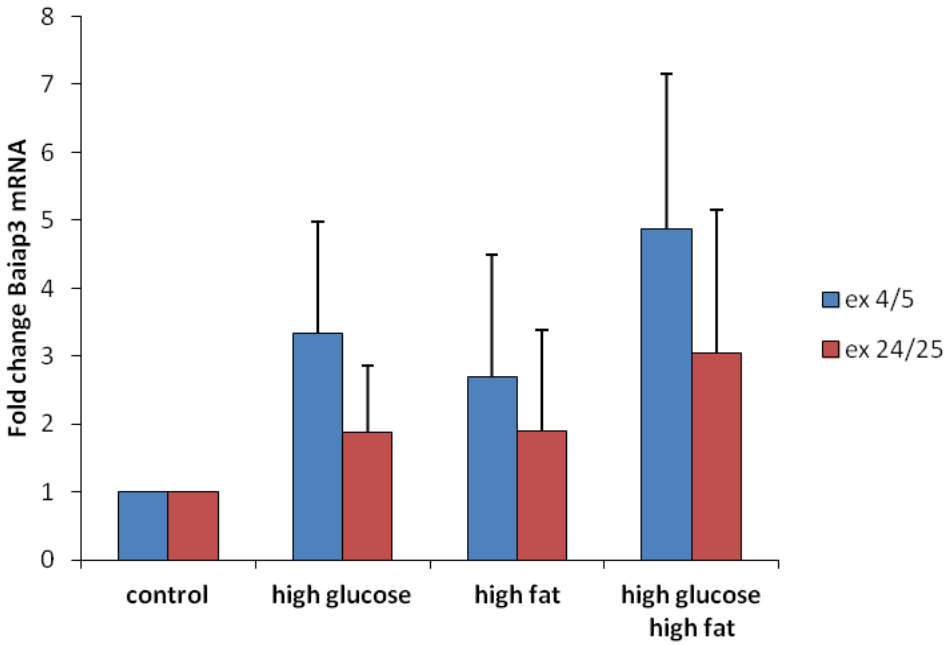

Figure 6.12 Baiap3 is differentially overexpressed in glucolipotoxicity. INS-1 cells were cultured for 72h in the 4 experimental conditions, RNA was extracted, reverse transcribed and RT-qPCR performed using 2 different couples of primers for Baiap3. The first couple of primers anneal between exon 4/5, external to the miRNA region; the second couple of primers anneals between exon 24/25, so overlapping the Mir3547 region. Data represent ΔΔCt values expressed as a fold change compared to cells grown in RPMI (control). Data are expressed as means + SD of 3 independent experiments.

6.4.4 RNAseq shows a new exon for rat Baiap3

Despite sequences for mouse and human Baiap3 genes are known and annotated, the sequence for rat Baiap3 is not annotated in November 2004 rat (*Rattus norvegicus*) genome assembly version 3.4, or in NCBI assembly/382928 (RGSC Rnor_5.0). However in Ensemble database rat BAIAP3 is annotated under ENSRNOG00000017893. Based on this sequence, Baiap3 gene is composed of 33 exons, while mouse and human Baiap3 are composed of 34 exons. Specifically, the missing exon should be exon 1, localised 4 kbases upstream of exon 2 (Figure 6.13A).

The alignment of the reads from our RNAseq data to the Baiap3 region shows a concentration of reads in a region that may correspond to the missing exon (Figure 6.13B). Nucleotide sequence blast suggests that this region of rat chromosome 10 (derived from our reads) is highly homologous (>80%) to exon 1 of the mouse Baiap3 on chromosome 17 (Figure 6.13C).

A

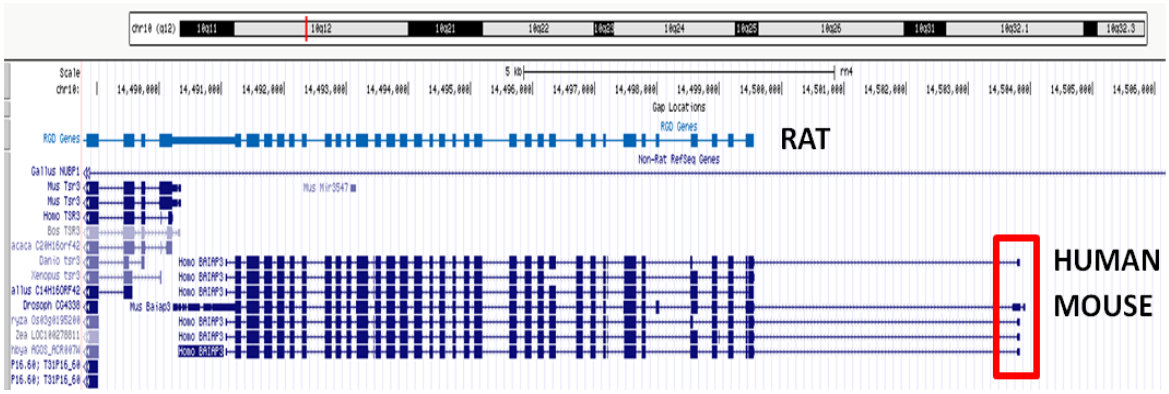

B

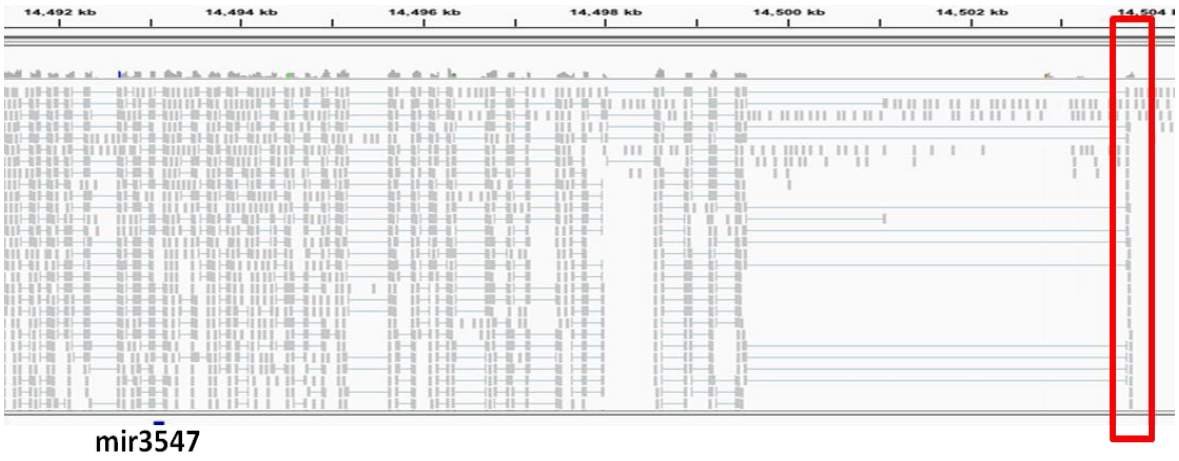

C

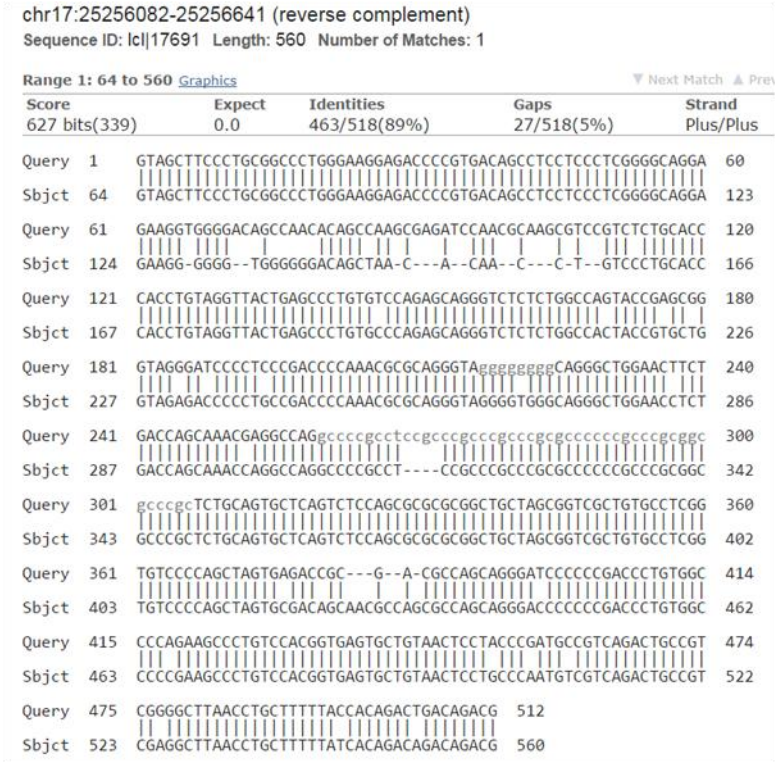

Figure 6.13 Rat Baiap3 sequence. A) Comparison of Baiap3 sequence among different species; B) RNAseq reads mapping on rat Baiap3 region C) Blast of sequence of hypothetic rat exon 1 from RNAseq to mouse exon 1.

6.4.5 Analysis of Human Baiap3 gene

No significant similarity was found between the RNAseq region studied above and exon 1 region of human Baiap3 gene on chromosome 16. In addition, there is not annotated intronic Mir-3547, but there are some shorter variants of the gene.

Analysis of the human Baiap3 genomic sequence from available methylation studies suggested that there are potentially 2 hypomethylated regions (Figure 6.14A), one upstream of exon 1 close to the start codon, which may regulate Baiap3 transcription, and the other internal between exon 10 and 15. We hypothesise that this internal hypomethylated region may be an enhancer site or a promoter for shorter proteins derived from alternative splicing of Baiap3 gene (Figure 6.14B).

Furthermore we noticed that various studies have identified two active promoters (purple regions in Figure 6.14C), one upstream of exon 1 and one internal to the gene in

different cell lines. These regions overlap with the hypomethylated sites showed in Figure 6.14A. This second active site could be regulating the variant BAIAP3-015 expression in human.

However, in rat and mouse, our data led us to propose that Mir-3547 could have its own promoter, located internally to the Baiap3 gene, which can be used for transcription independently from Baiap3 transcription. There is the possibility that the internal promoter could regulate the transcription of the miRNA but further investigations are required to understand gene regulations in this locus.

A

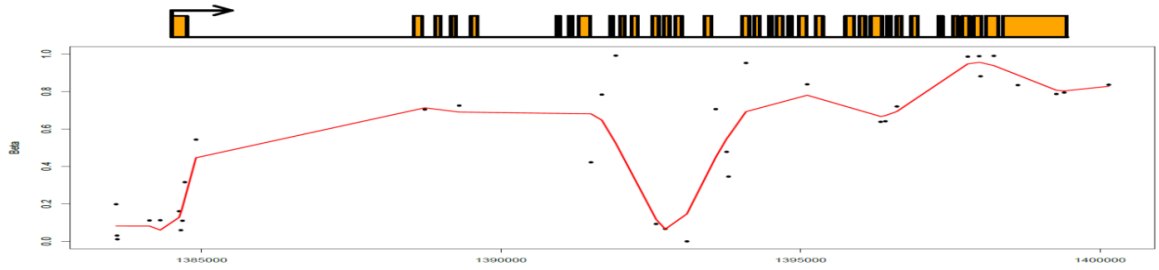

B

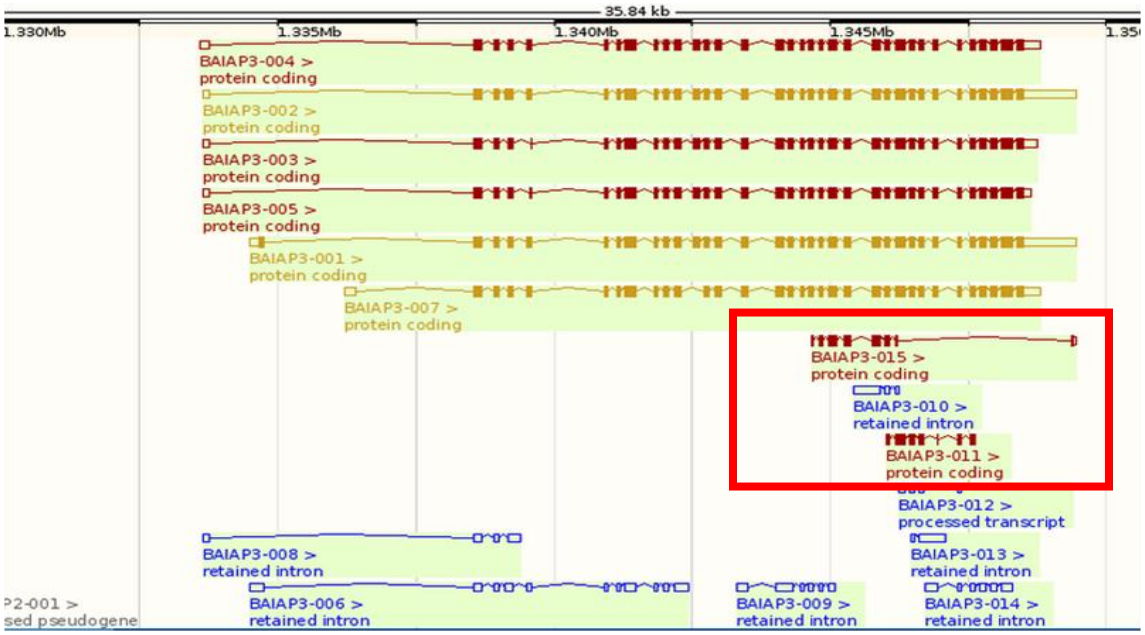

C

Figure 6.14 Promoter's regions near human Baiap3 genes. A) The graph represents the methylation pattern of the human Baiap3 area. A low value is indicative of hypomethylation. B) Different splice variants of human Baiap3 gene. C) The image represents the active promoters regions on human Baiap3 genes (indicated in purple). Each row corresponds to a different cell line.

6.5 Novel genes

As mentioned before, RNAseq technology can also detect novel genes or expressed sequence tag (ESTs) whose function and role in the cell is still unknown. In general, their name is a number indicating the chromosomal position proceeded by LOC (locus) or RGD (rat genome database).

Several of these genes are differentially expressed in condition of glucolipotoxicity, some of which are listed in Figure 6.15.

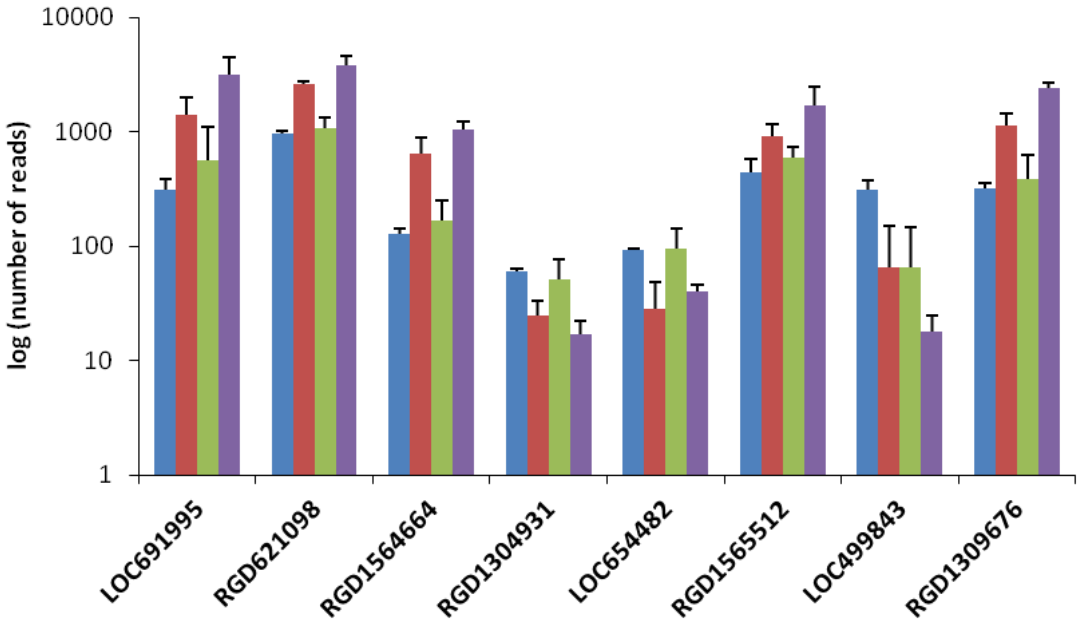

Figure 6.15 Expression levels of novel genes. RNAseq was performed on the RNA of INS-1 cells treated with the 4 experimental conditions. Values are means + SD of number of reads associated with a particular condition.

To elucidate the function of some selected novel genes we subjected them to structural analysis, using the on-line platform for protein structure and function predictions I-TASSER server (http://zhanglab.ccmb.med.umich.edu/I-TASSER/) as well as the Protein Sequence Analysis Workbench (PSIPRED (http://bioinf.cs.ucl.ac.uk/psipred/)) The following genes are of particular interest: *LOC691995*, *RGD1564664*, *RGD1304931*, *RGD621098*, *RGD1309676*. The predicted structure of these genes is represented in Figure 6.16.

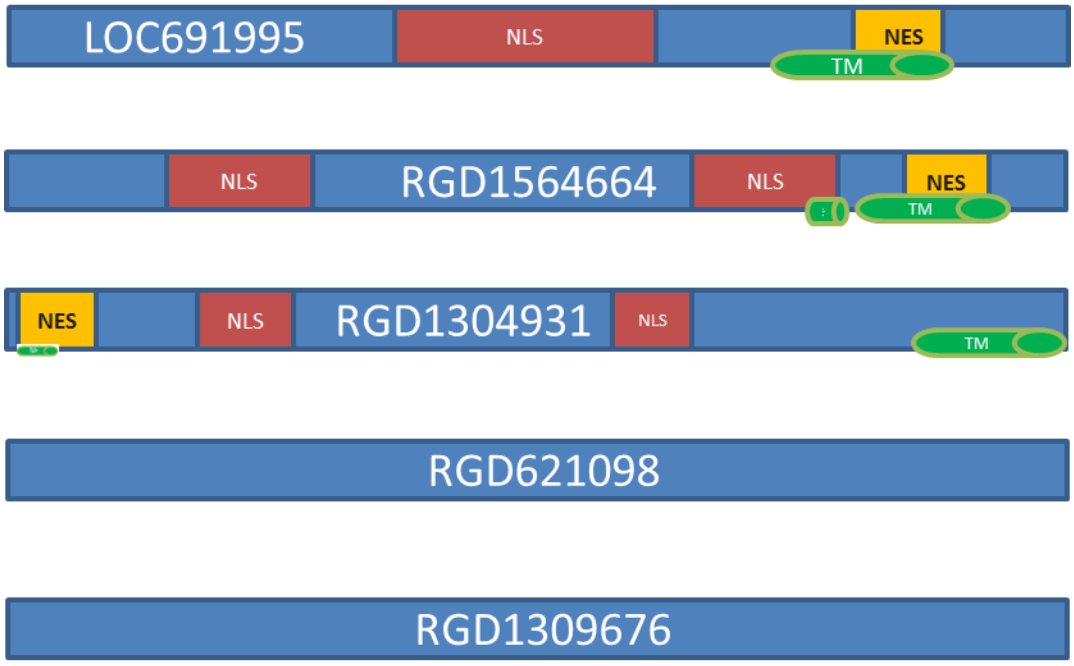

Figure 6.16 Predicted structures of novel genes. The figure shows the nuclear localization signal (NLS) in red, the nuclear export signal (NES) in yellow and the transmembrane domain (TM) in green.

LOC691995 is a predicted transporter protein containing both nuclear localisation signal (NLS), nuclear export signal (NES) and one or more transmembrane domains. It could be a shuttling protein involved in nuclear/cytoplasm transport.

RGD1564664 is also a putative transporter and it is mainly localised in the mitochondria, with a small percentage of the protein in the nucleus.

RGD1304931 is another predicted transporter, containing a NLS and a NES.

RGD621098 is a soluble cytoplasmatic protein, and no transmembrane domain was detected.

RGD1309676 is mainly extracellular with endoplasmic reticulum presence.

These listed clones are interesting as they are mainly transporter proteins and they contain nuclear localisation signals. This indicates that they could be possible transcription factors and be involved in the regulation of expression of genes implicated in insulin secretion. Future studies are necessary to define their role in the β-cell and if they can be implicated in the regulation of insulin secretion.

6.6 Discussion

As the incidence of T2D is increasing at an alarming rate worldwide, there is an urgent need to find new therapeutic strategies, especially therapies able to reverse the impaired β-cell function. In particular, it would be useful to identify novel strategies to restore insulin secretion during the progression of diabetes, but most of the mechanisms involved in β-cell dysfunction are still not known. The aim of this part of the study was to determine in more details the effect of glucolipotoxicity on the β-cell and the different molecules affected by exposure to high concentrations of glucose and fatty acids. The identification of novel targets can open the way to future studies aimed at the development of therapeutic strategies able to restore the β-cell function. This will allow the treatment of the disease at an early stage, when only impairment of function but not β-cell death occurs. The transcriptome profiling using RNAseq described in chapter 5 has identified some interesting pathways that could be further investigated to assess their role in the β-cell function.

Considering our previous studies on CD40 (Chapter 3 and 4) and its role in the β-cell function, particular attention was paid to the study of the TNFR pathway in its complex and its validation by RT-qPCR. Many of the genes involved in this pathway were differentially expressed under the experimental conditions, among which receptors (*TNFRSF1B*, *TNFRSF11A*, *TNFRSF17*), ligands (*TNF-α*, *TNFSF4*, *CD40L*, *TNFSF11*, *TNFSF12*, *TNFSF13B*, *TNFSF13*) and TNF inducible proteins (*IRAK1/2*, *TRAF2*, *TRAF3*, *MAP3K14*, *CAT*, *NF-κB2*, *NF-κBiB*, *BCL2A1*) (Figure 6.1).
There was a specific effect of the exposure of cells to high concentrations of glucose and fatty acids on this pathway, as some of the receptors resulted in downregulation in glucolipotoxicity, while others, as CD40 (studied in chapter 3 and 4) resulted upregulated. On the other hand, the expression of the ligands was generally downregulated, but their differential expression has proven to be difficult to validate by RT-qPCR because of their low expression levels. In addition, glucolipotoxicity changed the expression of genes involved in the NF-κB pathways, confirming the activation of inflammatory and apoptotic pathways generated by the involvement of TNF receptors.

Another interesting pathway identified by this RNAseq experiment is the thyroid pathway. Many genes involved in thyroid metabolism were differentially expressed in glucolipotoxicity in INS-1 cells, both hormones, receptors, enzymes and transcription factors (Figure 6.6), the expression of which are normally associated with the thryoid gland and the hypothalamus. Interestingly these genes were expressed in the β-cell and their expression was affected by glucolipotoxicity. Previous studies have reported the expression of TRH and its receptor in the pancreas and its colocalisation with insulin secretory granules, suggesting a potential involvement in insulin secretion [376]. In addition, Kulkarni et al demonstrated that TRH can promote insulin release in the adult pancreatic islet and its expression can be involved in the regulation of the β-cell function [369]. Expression of TRH has also been demonstrated in INS-1 cells, where it is able to increase insulin production in cells extracts [365]. Moreover, it has been shown that blockage of TRH synthesis can influence insulin secretion [366], which suggests that TRH is implicated in regulation of insulin secretion in β-cells. The down-regulation of this gene in condition of glucolipotoxicity could have a role in the reduction of insulin secretion and production observed in these experimental conditions. In addition, other studies showed that thyroid hormone (TH) receptor is expressed in rat β-cells and TH can regulate MAFA expression, affecting insulin secretion [367]. TH has also been positively associated to insulin secretion in people with pre-diabetes [368]. The fact that most of the thyroid genes are expressed in the β-cell and that their expression is affected by conditions of glucolipotoxicity can be due to the fact that the pancreas or pancreatic cell lines show similarities in the developmental process or gene expression to neurons, and possess variable derivative peptides and hormones. This is another mechanism that underlies the connection between brain and pancreas, suggesting the possibility of a similar regulation and control. A functional action of the thyroid hormones in the pancreas could be to oppose the effects of somatostatin (which reduces insulin and glucagon secretion) to balance the regulation of islets cell function. In addition, there could be an autocrine or paracrine effect of TRH in the pancreas, which can activate the transcription of the other genes. Future studies are necessary to define the role of this pathway in insulin secretion or production and the way it could be used to develop novel therapies to preserve insulin secretion.

Four differentially expressed miRNAs were identified in the list from the RNAsequencing (Figure 6.7). In particular, Mir-205 and Mir-375 are known to be associated with diabetes or obesity [295, 301]. Of interest is Mir-3547, which resulted overexpressed with high statistical significance in glucolipotoxicity, as also confirmed by an independent qPCR (Figure 6.8). Interestingly, Mir-3547 localises within a gene, Baiap3, on chromosome 10 (Figure 6.9). In particular, it locates in the intron between exons 24/25 of Baiap3 on the rat genome. Baiap3 is a p53 target gene that encodes for a brain-specific angiogenesis inhibitor. This protein also contains two C2 domains, which are often found in proteins involved in signal transduction or membrane trafficking. It is a member of the Munc13 protein family and it can regulate exocytosis [375], and, for this reason, it is an interesting object of study because it could be involved in insulin secretion. Baiap3 was overexpressed in glucolipotoxicity as well (Figure 6.10), but our results showed a different level of expression changes accordingly to the primers used: primers overlapping with the miRNA region generated more transcript than primers annealing externally to the miRNA region (Figure 6.11). This may suggest that alternative splicing occurs or that Mir-3547 uses an independent internal promoter to regulate its own transcription. These data are also complemented by the study of hypomethylation sites or active promoter regions on human Baiap3 region (Figure 6.14). Together with the promoter of Baiap3 gene, another region, internal to the gene, resulted active and hypomethylated. This could be an enhancer of the Baiap3 gene, a promoter of shorter transcripts of Baiap3 gene or, more interestingly, a Mir-3547 promoter. Future studies are required to define the transcriptional regulation of these genes in rodents and humans. Dysregulation of either Baiap3 or Mir-3547 has not previously reported to be implicated in β-cell function in response to glucolipotoxicity. Baiap3 is likely to be involved in vesicle exocytosis and therefore could have a role in insulin secretion. Future studies to characterise Baiap3 in the β-cell, its overexpression in human and to understand the genetic architecture in rodent and man are required to further evaluate a role in insulin secretion.

Finally, the RNAseq experiment identified some novel genes, in which the structure and function are still unknown (Figure 6.15). In particular, *LOC691995*, *RGD1564664*,

RGD1304931 are of particular interest because their predicted structure contains both a Nuclear Localization Signal and a Nuclear Export Signal (Figure 6.16). This structure suggests that they could be shuttling protein involved in nuclear/cytoplasm transport or transcription factors, regulating genes involved in insulin secretion. At the moment, experiments are ongoing in order to characterise the biological function of these molecules and their potential role in regulating insulin and β-cell function.

The four pathways analysed are only starting point for future analysis that could identify novel pathways involved in glucolipotoxicity. The fact that these molecules are differentially expressed in glucolipotoxicity is the first result but further validation is necessary, in particular to investigate a potential involvement in the regulation of insulin secretion.

Chapter 7

General discussion and conclusions

7.1 General discussion

Over the past three decades, the number of people with diabetes mellitus has more than doubled globally, making it one of the most important public health challenges to all nations. The World Health Organization states that 347 million people worldwide were suffering from diabetes in 2008, which equates to 9.5% of the adult population [63]. T2D and pre-diabetes are increasingly observed among children, adolescents and young adults and they make up 90% of the diabetes cases. The causes of the epidemic of T2D are embedded in a very complex group of genetic and epigenetic systems interacting within an equally complex framework that determines behaviour and environmental influences.

In the UK, the cost of diabetes to the NHS is over £1.5 million an hour or 10% of the NHS budget for England and Wales. In total, an estimated £14 billion per year is spent to treat diabetes and its complications, with the treatment of complications representing the much higher cost [377].

As diabetes is triggered by many genetic and environmental factors, different for each individual, treatments should also vary individually and specifically, the so called "personalised medicine". Regular and successful treatments can also decrease the risk of developing diabetes complications. The main therapeutic approaches are the following:

- *healthy lifestyle:* corrections in diet, with assumptions of high fibre, low fat foods (low carbs fruits, vegetables, whole grains) and regular aerobic physical exercise can help to ameliorate glucose levels without the need of other medications.
- *medications:* drugs are used to reduce hyperglycemia and increase insulin secretion or action or to reduce the inflammatory process. For example, metformin decreases hyperglycemia primarly by reducing glucose production by the liver, activating AMP kinase and stimulating insulin sensitivity (acting on GLUT4 to enhance peripheral glucose uptake). Sulfonylureas stimulate insulin secretion by binding to an ATP sensitive K^+ channel, leading to membrane depolarisation. Thiazolidinediones act by activating peroxisome proliferator-activated receptors (PPARs), which bind to DNA and increase the transcription

of genes implicated in glucose and fatty acids metabolism and they reduce the level of inflammatory cytokines. GLP-1 receptor agonists activate GLP-1 receptor, stimulating adenylyl cyclase pathways, which result in increased insulin release. The sodium-glucose transporter-2 (SGL2) inhibitors act by blocking the re-absorption of glucose by the kidney thereby increasing glucose secretion.

- *insulin therapy:* treatment of diabetes by administration of exogenous insulin;
- *cell based therapies:* treatment of diabetes by pancreas or islet transplantation.

Healthy lifestyle and medications are usually sufficient for the treatment of T2D, whereas patients with T1D need daily injections of insulin and, in the worst cases, islets transplantation.

With a greater understanding of the mechanisms of glucolipotoxicity on the β-cell new therapeutic approaches will be identified. A specific therapy at an early stage of the disease could restore the impaired β-cell function and avoid the development of diabetes complications, decreasing the severity and cost of the treatments.

In this thesis we aimed to identify novel molecules involved in the impairment of the β-cell function and to discover novel potential targets for therapeutic strategies. We simulated the glucolipotoxic conditions of T2D by incubating INS-1 cells in media containing 27 mM glucose, 200 μM oleic acid and 200 μM palmitic acid for 72 hours. Oleic and palmitic acid are the most abundant fatty acids in human diet, therefore these conditions are representative of the real physiology of β-cells in diabetes. In addition, the conditions of glucolipotoxicity used affected insulin secretion and production but not cell viability, therefore cells were at an early stage when cellular function is impaired but cells are still viable. In this way it was possible to investigate mechanisms implicated in the early stages of glucolipotoxicity, with the aim to develop therapeutic strategies at the onset of diabetes.

Combining transcriptome profiling using Affymetrix microarrays and RNA sequencing, we aimed to identify novel molecules differentially expressed in glucolipotoxicity. We first focussed our attention on the inflammatory process of T2D and here we showed for the first time an important role for CD40 in glucolipotoxicity-induced β-cell

dysfunction. We showed that CD40 is upregulated at the RNA and protein levels in INS-1 cells exposed to glucolipotoxic conditions. Similar data were obtained in islets of mice fed a high fat diet and in human islets exposed to fatty acids. In addition, targeted downregulation of CD40 in INS-1 cells leads to an increase in insulin secretion and production, elucidating a new direct role of this receptor in regulating β-cell function. As CD40 is able to activate NF-κB, we hypothesised that the connection between CD40 and insulin could lie in this transcription factor. We showed that there is a hypothetical NF-κB binding site upstream of the insulin promoter, which may be responsible of the effect of CD40 on insulin transcription. In addition we showed a trend of TRAF proteins (adaptor molecules that bind to the intracellular domain of CD40 and are responsible for the transduction of the signal) in mirroring CD40 expression: in conditions of CD40 downregulation we showed a trend towards decreased mRNA levels of TRAF2 and TRAF6, while in glucolipotoxicity (when CD40 is overexpressed) expression of both TRAF2 and TRAF6 increased. Increased TRAF2 mRNA levels were also observed in islets of mice fed a high fat diet. However, these results require further validation, in order to determine whether CD40 affects insulin expression through NF-κB.

In general, these experiments showed for the first time the importance of CD40 in glucolipotoxicity and the possibility of blocking its pathway as a way to improve β-cell function. In this context, the use of anti-CD40 monoclonal antibodies [334-335] may be worth of consideration for use as an adjunct therapy for people with T2D. Lucatumumab in particular would appear a strong initial candidate for this role, as not only it is reported to be well tolerated [336], at least at moderate and intermediate doses [337], but it has also previously been shown to prevent induction of NF-κB activity in multiple myeloma cells [338]. In addition, this therapy has also been used as a general immunosuppressant strategy following transplantation, so it could be used as a combined approach at a later stage of the disease to restore the function of the impaired β-cells and to favour the activity and vitality of the new transplanted cells. However, this strategy would need to be modified for the treatment of diabetes, as immune cell interactions with the Fc region of cell-bound Lucatumumab could potentially lead to either opsonisation of β-cells or antibody-dependent cell cytotoxicity. An alternative solution could be the use of phage display technology, with the generation of antibody

fragments containing heavy and light chain antigen recognition sites, whilst lacking the Fc region. This is an area that clearly warrants future research.

In order to expand the results obtained with the microarray experiment and to gain more information about the glucolipotoxicity process, we then performed a RNA sequencing experiment on INS-1 cells exposed to glucolipotoxicity. Clustering and pathway analysis confirmed the fact that the conditions used are really representative of the pathological changes observed in T2D. Most of the pathways and molecules differentially expressed in this system are already known in their association to diabetes and insulin resistance. However, a more detailed analysis allowed us to identify some new pathways that could be the objective of future studies to investigate their ability to influence β-cell function.

We identified other members of the tumour necrosis factor family (*TNFRSF21* and *TNFRSF26*), which were downregulated in response to glucolipotoxicity. These molecules have not been studied so far, therefore they could be an interesting subject to study in relation also to CD40.

Another important pathway identified in this study is the thyroid pathway. Many genes involved in the thyroid metabolism resulted differentially expressed in glucolipotoxicity in INS-1 cells, both hormones, receptors, enzymes and transcription factors. The expression of some of these genes in the β-cell and their effects on insulin secretion has already been shown previously [365, 376]. However, here we showed for the first time that the expression of these genes can be regulated by glucolipotoxity, therefore they can be possibly involved in the impairment of insulin secretion in diabetes. A clinical correlation between thyroid dysfunction and diabetes has already been elucidated, and patients with diabetes have a higher prevalence of thyroid disorders compared to the normal population [378-380]. Future studies are necessary to determine whether downregulation or overexpression of these thyroid genes in INS-1 cells could affect insulin secretion or production.

We also showed for the first time that *Mir-3547*, a novel miRNA which has not been studied so far, is upregulated in glucolipotoxicity and co-localises with a gene, *Baiap3*, encoding for a protein that could be involved in exocytosis. MiRNA deficiencies or excesses have been correlated with a number of clinically important diseases, and some

therapeutic applications aim to restore normal levels and functions of these dyregulated miRNA. A detailed study of rodent Mir-3547 in relation to insulin secretion and β-cell function, and the identification of the equivalent miRNA in humans, may reveal a potential novel mechanism by which glucolipotoxicity affects β-cells and it may define a novel target for the development of therapeutic strategies that could reduce the levels of this miRNA.

As the involvement of miRNAs in diseases is a relatively novel area of investigation and most of these miRNAs have still unknown roles, we aimed also to identify differentially expressed miRNAs in glucolipotoxicity using small RNA sequencing. The analysis of these results is still ongoing.

Finally, we showed also the involvement of some novel genes in glucolipotoxicity, whose structure and function is still unknown. In particular, *LOC691995*, *RGD1564664*, *RGD1304931* are of particular interest because their predicted structure contains both a Nuclear Localization Signal and a Nuclear Export Signal and they could be shuttling protein involved in nuclear/cytoplasm transport or transcription factors, regulating genes involved in insulin secretion.

Additional studies are now required to investigate these novel pathways of glucolipotoxicity, in order to determine whether they are involved in the impairment of insulin secretion in diabetes and, as a consequence, if they can be appropriate targets for novel therapeutic strategies.

In general, this thesis can be considered as a starting point for numerous and interesting investigations, aiming to validate and further analyse potential therapeutic targets at an early stage of the disease.

It must however be noted that the experimental system used has some limitations.

One general limitation of the system used is the fact that all the initial experiments were performed *in vitro* on INS-1 cells. INS-1 cells are good and reliable model to study expression changes on a large scale but they are not representative of the real human physiology. First of all they are rat cells and, despite rat and human genomes share high similarity, some of the molecules and pathways identified could have relevance in rat

but not in humans, an example in this thesis being Mir-3547. There are some species related differences: for example it has been shown that 24h exposure of human islets to elevated glucose and palmitate is sufficient to induce apoptosis [107], whereas we and others have not observed cell death in INS-1 cells under the same conditions for 72h [381]. Moreover, the concentration of fatty acids used in vitro varies among different studies. The key determinant is the fraction that is bound to the BSA, which is the part that can be effectively introduced in the cell.

In addition, INS-1 cells are isolated cells and therefore they do not provide information about integrative physiology and connections in the context of the human pancreas.

On the other hand, *in vitro* studies are quicker to perform and at a lower cost and they allow a strict control of the environmental conditions. This facilitates the study of conditions, like diabetes, in which there is a strong environmental counterpart. In addition, experiments using cell lines can be easier for the functional characterisation of the different targets. The use of cell lines is also preferable in whole genome sequencing experiments, as they allow reproducibility of the results and the use of set and controlled conditions.

In general, a good approach would be to perform the general screening on cell lines, like in this thesis, and then to validate the results of the interesting targets *in vivo*, in mouse or human islets, as in our characterisation of CD40 and TRAFs expressions.

Another limitation of this system is that the expression changes were only investigated after 72h of incubation. We demonstrated that the decrease in insulin expression is a gradual process, starting already after 24h of incubation. The choice of only 72h as a timepoint could miss the detection of some important mechanisms involved in the very early stages of β-cell dysfunction. However, a more detailed time-course can be investigated once the interesting targets are identified at the 72h timepoint.

7.2 Conclusions

This thesis elucidates some novel mechanisms involved in the glucolipotoxicity process associated with T2D. We identified molecular changes in the expression of molecules

involved in an early stage of glucolipotoxicity, when the function but not the viability of the β-cell is impaired. This will allow the identification of targets that can be studied to possibly define novel therapeutic approaches aiming to treat diabetes at its onset.

7.3 Future research

- **CD40 experiments:**

Confirmation of the direct role of CD40 in regulating insulin:

Since we hypothesised that CD40 can regulate insulin through NF-κB, we plan to verify, through gel shift, that NF-κB binds insulin promoter. Once verified this, we plan to investigate if there is a lower NF-κB binding in presence of CD40 downregulation.

Confirmation of decreased TRAFs expression with CD40 downregulation:

We showed a trend towards reduced expression of TRAF2 and TRAF6 upon CD40 downregulation. This needs to be confirmed.

Effect of upregulation of CD40:

The effects of CD40 on insulin and TRAFs expression could be verified by overexpressing CD40 using an expression vector. In this way we could simulate the effect of CD40 overexpression in glucolipotoxicity and confirm its direct role on insulin.

Functional analysis of other unstudied members of the TNFR pathway:

We showed that other TNF receptors (TNFRSF21 and TNFRSF26) are differentially expressed in glucolipotoxicity. It could be interesting to investigate if these genes are involved in the regulation of the β-cell function.

- **Novel pathways (Mir-3547, thyroid genes and novel genes):**

Validation of the differential expression:

We showed that Mir3547, genes of the thyroid pathways and different novel genes are differentially expressed in glucolipotoxicity. Their differential expression has to be confirmed by qPCR and Western blot (where required).

Confirmation in other systems:

Most of the data in this thesis were obtained using INS-1 cells. Results need to be validated in other systems (mouse and human islets).

Functional analysis:

In order to verify the function of these genes and pathways in the β-cells, we could downregulate or overexpress these genes and investigate the effects on cell viability and cell function.

- **Others:**

Identification of novel molecules involved in glucolipotoxicity from the RNAseq experiment:

The same validation and functional study described before can be applied to other molecules and pathways not mentioned in this thesis but differentially expressed in glucolipotoxicity.

Identification of novel miRNAs involved in glucolipotoxicity from the small RNAseq experiment:

The analysis of the data from the small RNA sequencing experiment is still ongoing. Once miRNAs significantly modulated are identified, they should be validated and analysed as before, to understand their role in the β-cell.

Bibliography

1. Fu, Z., E.R. Gilbert, and D. Liu, *Regulation of insulin synthesis and secretion and pancreatic Beta-cell dysfunction in diabetes.* Curr Diabetes Rev, 2013. **9**(1): p. 25-53.
2. Pouli, A.E., et al., *Secretory-granule dynamics visualized in vivo with a phogrin-green fluorescent protein chimaera.* Biochem J, 1998. **333 (Pt 1)**: p. 193-9.
3. Rorsman, P. and M. Braun, *Regulation of insulin secretion in human pancreatic islets.* Annu Rev Physiol, 2013. **75**: p. 155-79.
4. Matschinsky, F.M., *Regulation of pancreatic beta-cell glucokinase: from basics to therapeutics.* Diabetes, 2002. **51 Suppl 3**: p. S394-404.
5. Novak, I., *Purinergic receptors in the endocrine and exocrine pancreas.* Purinergic Signal, 2008. **4**(3): p. 237-53.
6. Henquin, J.C., *Triggering and amplifying pathways of regulation of insulin secretion by glucose.* Diabetes, 2000. **49**(11): p. 1751-60.
7. Straub, S.G., G. Shanmugam, and G.W. Sharp, *Stimulation of insulin release by glucose is associated with an increase in the number of docked granules in the beta-cells of rat pancreatic islets.* Diabetes, 2004. **53**(12): p. 3179-83.
8. Varadi, A., et al., *Involvement of conventional kinesin in glucose-stimulated secretory granule movements and exocytosis in clonal pancreatic beta-cells.* J Cell Sci, 2002. **115**(Pt 21): p. 4177-89.
9. Ivarsson, R., et al., *Temperature-sensitive random insulin granule diffusion is a prerequisite for recruiting granules for release.* Traffic, 2004. **5**(10): p. 750-62.
10. Rothman, J.E., *Mechanisms of intracellular protein transport.* Nature, 1994. **372**(6501): p. 55-63.
11. Meldolesi, J. and E. Chieregatti, *Fusion has found its calcium sensor.* Nat Cell Biol, 2004. **6**(6): p. 476-8.
12. Gauthier, B.R. and C.B. Wollheim, *Synaptotagmins bind calcium to release insulin.* Am J Physiol Endocrinol Metab, 2008. **295**(6): p. E1279-86.
13. Marshall, C., et al., *Evidence that an isoform of calpain-10 is a regulator of exocytosis in pancreatic beta-cells.* Mol Endocrinol, 2005. **19**(1): p. 213-24.
14. Evans, J.S. and M.D. Turner, *Emerging functions of the calpain superfamily of cysteine proteases in neuroendocrine secretory pathways.* J Neurochem, 2007. **103**(3): p. 849-59.
15. Barg, S., et al., *Priming of insulin granules for exocytosis by granular Cl(-) uptake and acidification.* J Cell Sci, 2001. **114**(Pt 11): p. 2145-54.
16. Melloul, D., S. Marshak, and E. Cerasi, *Regulation of insulin gene transcription.* Diabetologia, 2002. **45**(3): p. 309-26.
17. Goodison, S., S. Kenna, and S.J. Ashcroft, *Control of insulin gene expression by glucose.* Biochem J, 1992. **285 (Pt 2)**: p. 563-8.
18. German, M.S. and J. Wang, *The insulin gene contains multiple transcriptional elements that respond to glucose.* Mol Cell Biol, 1994. **14**(6): p. 4067-75.
19. Macfarlane, W.M., et al., *Glucose modulation of insulin mRNA levels is dependent on transcription factor PDX-1 and occurs independently of changes in intracellular Ca2+.* Diabetes, 2000. **49**(3): p. 418-23.

20. Peshavaria, M., et al., *The PDX-1 activation domain provides specific functions necessary for transcriptional stimulation in pancreatic beta-cells.* Mol Endocrinol, 2000. **14**(12): p. 1907-17.
21. German, M.S., L.G. Moss, and W.J. Rutter, *Regulation of insulin gene expression by glucose and calcium in transfected primary islet cultures.* J Biol Chem, 1990. **265**(36): p. 22063-6.
22. Jones, P.M. and S.J. Persaud, *Protein kinases, protein phosphorylation, and the regulation of insulin secretion from pancreatic beta-cells.* Endocr Rev, 1998. **19**(4): p. 429-61.
23. Hamilton, J.A. and F. Kamp, *How are free fatty acids transported in membranes? Is it by proteins or by free diffusion through the lipids?* Diabetes, 1999. **48**(12): p. 2255-69.
24. Newsholme, P. and M. Krause, *Nutritional regulation of insulin secretion: implications for diabetes.* Clin Biochem Rev, 2012. **33**(2): p. 35-47.
25. Keane, K. and P. Newsholme, *Metabolic regulation of insulin secretion.* Vitam Horm, 2014. **95**: p. 1-33.
26. Nolan, C.J., et al., *Fatty acid signaling in the beta-cell and insulin secretion.* Diabetes, 2006. **55 Suppl 2**: p. S16-23.
27. Haber, E.P., et al., *New insights into fatty acid modulation of pancreatic beta-cell function.* Int Rev Cytol, 2006. **248**: p. 1-41.
28. Deeney, J.T., et al., *Acute stimulation with long chain acyl-CoA enhances exocytosis in insulin-secreting cells (HIT T-15 and NMRI beta-cells).* J Biol Chem, 2000. **275**(13): p. 9363-8.
29. Wang, X., et al., *Palmitate activates AMP-activated protein kinase and regulates insulin secretion from beta cells.* Biochem Biophys Res Commun, 2007. **352**(2): p. 463-8.
30. Foufelle, F. and P. Ferre, *New perspectives in the regulation of hepatic glycolytic and lipogenic genes by insulin and glucose: a role for the transcription factor sterol regulatory element binding protein-1c.* Biochem J, 2002. **366**(Pt 2): p. 377-91.
31. Shapiro, H., et al., *Role of GPR40 in fatty acid action on the beta cell line INS-1E.* Biochem Biophys Res Commun, 2005. **335**(1): p. 97-104.
32. Floyd, J.C., Jr., et al., *Stimulation of insulin secretion by amino acids.* J Clin Invest, 1966. **45**(9): p. 1487-502.
33. Saltiel, A.R. and C.R. Kahn, *Insulin signalling and the regulation of glucose and lipid metabolism.* Nature, 2001. **414**(6865): p. 799-806.
34. Giovannone, B., et al., *Insulin receptor substrate (IRS) transduction system: distinct and overlapping signaling potential.* Diabetes Metab Res Rev, 2000. **16**(6): p. 434-41.
35. Shepherd, P.R., B.T. Nave, and K. Siddle, *Insulin stimulation of glycogen synthesis and glycogen synthase activity is blocked by wortmannin and rapamycin in 3T3-L1 adipocytes: evidence for the involvement of phosphoinositide 3-kinase and p70 ribosomal protein-S6 kinase.* Biochem J, 1995. **305 (Pt 1)**: p. 25-8.

36. Alessi, D.R., et al., *Characterization of a 3-phosphoinositide-dependent protein kinase which phosphorylates and activates protein kinase Balpha.* Curr Biol, 1997. **7**(4): p. 261-9.
37. Nakae, J., B.C. Park, and D. Accili, *Insulin stimulates phosphorylation of the forkhead transcription factor FKHR on serine 253 through a Wortmannin-sensitive pathway.* J Biol Chem, 1999. **274**(23): p. 15982-5.
38. Thomas, G. and M.N. Hall, *TOR signalling and control of cell growth.* Curr Opin Cell Biol, 1997. **9**(6): p. 782-7.
39. Ribon, V. and A.R. Saltiel, *Insulin stimulates tyrosine phosphorylation of the proto-oncogene product of c-Cbl in 3T3-L1 adipocytes.* Biochem J, 1997. **324 (Pt 3)**: p. 839-45.
40. Chiang, S.H., et al., *Insulin-stimulated GLUT4 translocation requires the CAP-dependent activation of TC10.* Nature, 2001. **410**(6831): p. 944-8.
41. Boulton, T.G., et al., *ERKs: a family of protein-serine/threonine kinases that are activated and tyrosine phosphorylated in response to insulin and NGF.* Cell, 1991. **65**(4): p. 663-75.
42. Pilkis, S.J. and D.K. Granner, *Molecular physiology of the regulation of hepatic gluconeogenesis and glycolysis.* Annu Rev Physiol, 1992. **54**: p. 885-909.
43. Shimomura, I., et al., *Insulin selectively increases SREBP-1c mRNA in the livers of rats with streptozotocin-induced diabetes.* Proc Natl Acad Sci U S A, 1999. **96**(24): p. 13656-61.
44. Bonner-Weir, S., *Life and death of the pancreatic beta cells.* Trends Endocrinol Metab, 2000. **11**(9): p. 375-8.
45. Stoffers, D.A., M.K. Thomas, and J.F. Habener, *Homeodomain protein IDX-1: a master regulator of pancreas development and insulin gene expression.* Trends Endocrinol Metab, 1997. **8**(4): p. 145-51.
46. Alonso, L.C., et al., *Glucose infusion in mice: a new model to induce beta-cell replication.* Diabetes, 2007. **56**(7): p. 1792-801.
47. Hugl, S.R., M.F. White, and C.J. Rhodes, *Insulin-like growth factor I (IGF-I)-stimulated pancreatic beta-cell growth is glucose-dependent. Synergistic activation of insulin receptor substrate-mediated signal transduction pathways by glucose and IGF-I in INS-1 cells.* J Biol Chem, 1998. **273**(28): p. 17771-9.
48. Srinivasan, S., et al., *Glucose promotes pancreatic islet beta-cell survival through a PI 3-kinase/Akt-signaling pathway.* Am J Physiol Endocrinol Metab, 2002. **283**(4): p. E784-93.
49. Fraenkel, M., et al., *mTOR inhibition by rapamycin prevents beta-cell adaptation to hyperglycemia and exacerbates the metabolic state in type 2 diabetes.* Diabetes, 2008. **57**(4): p. 945-57.
50. Heit, J.J., et al., *Calcineurin/NFAT signalling regulates pancreatic beta-cell growth and function.* Nature, 2006. **443**(7109): p. 345-9.
51. Perfetti, R., et al., *Glucagon-like peptide-1 induces cell proliferation and pancreatic-duodenum homeobox-1 expression and increases endocrine cell mass in the pancreas of old, glucose-intolerant rats.* Endocrinology, 2000. **141**(12): p. 4600-5.
52. Wang, X., et al., *Glucagon-like peptide-1 regulates the beta cell transcription factor, PDX-1, in insulinoma cells.* Endocrinology, 1999. **140**(10): p. 4904-7.

53. Habener, J.F. and D.A. Stoffers, *A newly discovered role of transcription factors involved in pancreas development and the pathogenesis of diabetes mellitus.* Proc Assoc Am Physicians, 1998. **110**(1): p. 12-21.
54. Hogg, J., et al., *Interactions of nutrients, insulin-like growth factors (IGFs) and IGF-binding proteins in the regulation of DNA synthesis by isolated fetal rat islets of Langerhans.* J Endocrinol, 1993. **138**(3): p. 401-12.
55. Benito, M., A.M. Valverde, and M. Lorenzo, *IGF-I: a mitogen also involved in differentiation processes in mammalian cells.* Int J Biochem Cell Biol, 1996. **28**(5): p. 499-510.
56. Paris, M., et al., *Specific and combined effects of insulin and glucose on functional pancreatic beta-cell mass in vivo in adult rats.* Endocrinology, 2003. **144**(6): p. 2717-27.
57. Ohsugi, M., et al., *Reduced expression of the insulin receptor in mouse insulinoma (MIN6) cells reveals multiple roles of insulin signaling in gene expression, proliferation, insulin content, and secretion.* J Biol Chem, 2005. **280**(6): p. 4992-5003.
58. Withers, D.J., et al., *Disruption of IRS-2 causes type 2 diabetes in mice.* Nature, 1998. **391**(6670): p. 900-4.
59. Brelje, T.C., et al., *Beneficial effects of lipids and prolactin on insulin secretion and beta-cell proliferation: a role for lipids in the adaptation of islets to pregnancy.* J Endocrinol, 2008. **197**(2): p. 265-76.
60. Friedrichsen, B.N., et al., *Signal transducer and activator of transcription 5 activation is sufficient to drive transcriptional induction of cyclin D2 gene and proliferation of rat pancreatic beta-cells.* Mol Endocrinol, 2003. **17**(5): p. 945-58.
61. Lingohr, M.K., R. Buettner, and C.J. Rhodes, *Pancreatic beta-cell growth and survival--a role in obesity-linked type 2 diabetes?* Trends Mol Med, 2002. **8**(8): p. 375-84.
62. *Diagnosis and classification of diabetes mellitus.* Diabetes Care, 2011. **34 Suppl 1**: p. S62-9.
63. Danaei, G., et al., *National, regional, and global trends in fasting plasma glucose and diabetes prevalence since 1980: systematic analysis of health examination surveys and epidemiological studies with 370 country-years and 2.7 million participants.* Lancet, 2011. **378**(9785): p. 31-40.
64. Murea, M., L. Ma, and B.I. Freedman, *Genetic and environmental factors associated with type 2 diabetes and diabetic vascular complications.* Rev Diabet Stud, 2012. **9**(1): p. 6-22.
65. Sladek, R., et al., *A genome-wide association study identifies novel risk loci for type 2 diabetes.* Nature, 2007. **445**(7130): p. 881-5.
66. Imamura, M. and S. Maeda, *Genetics of type 2 diabetes: the GWAS era and future perspectives [Review]*. Endocr J, 2011. **58**(9): p. 723-39.
67. Horikawa, Y., et al., *Genetic variation in the gene encoding calpain-10 is associated with type 2 diabetes mellitus.* Nat Genet, 2000. **26**(2): p. 163-75.
68. Tuomilehto, J., et al., *Prevention of type 2 diabetes mellitus by changes in lifestyle among subjects with impaired glucose tolerance.* N Engl J Med, 2001. **344**(18): p. 1343-50.

69. Shanik, M.H., et al., *Insulin resistance and hyperinsulinemia: is hyperinsulinemia the cart or the horse?* Diabetes Care, 2008. **31 Suppl 2**: p. S262-8.
70. Kim, S.H. and G.M. Reaven, *Insulin resistance and hyperinsulinemia: you can't have one without the other.* Diabetes Care, 2008. **31**(7): p. 1433-8.
71. Fonseca, V.A., *Defining and characterizing the progression of type 2 diabetes.* Diabetes Care, 2009. **32 Suppl 2**: p. S151-6.
72. Kahn, S.E., R.L. Hull, and K.M. Utzschneider, *Mechanisms linking obesity to insulin resistance and type 2 diabetes.* Nature, 2006. **444**(7121): p. 840-6.
73. LeRoith, D., *Beta-cell dysfunction and insulin resistance in type 2 diabetes: role of metabolic and genetic abnormalities.* Am J Med, 2002. **113 Suppl 6A**: p. 3S-11S.
74. Ashcroft, F.M. and P. Rorsman, *Diabetes mellitus and the beta cell: the last ten years.* Cell, 2012. **148**(6): p. 1160-71.
75. *Intensive blood-glucose control with sulphonylureas or insulin compared with conventional treatment and risk of complications in patients with type 2 diabetes (UKPDS 33). UK Prospective Diabetes Study (UKPDS) Group.* Lancet, 1998. **352**(9131): p. 837-53.
76. Butler, A.E., et al., *Beta-cell deficit and increased beta-cell apoptosis in humans with type 2 diabetes.* Diabetes, 2003. **52**(1): p. 102-10.
77. Pick, A., et al., *Role of apoptosis in failure of beta-cell mass compensation for insulin resistance and beta-cell defects in the male Zucker diabetic fatty rat.* Diabetes, 1998. **47**(3): p. 358-64.
78. Jetton, T.L., et al., *Mechanisms of compensatory beta-cell growth in insulin-resistant rats: roles of Akt kinase.* Diabetes, 2005. **54**(8): p. 2294-304.
79. Prentki, M. and C.J. Nolan, *Islet beta cell failure in type 2 diabetes.* J Clin Invest, 2006. **116**(7): p. 1802-12.
80. Liu, Y.Q., T.L. Jetton, and J.L. Leahy, *beta-Cell adaptation to insulin resistance. Increased pyruvate carboxylase and malate-pyruvate shuttle activity in islets of nondiabetic Zucker fatty rats.* J Biol Chem, 2002. **277**(42): p. 39163-8.
81. Chang-Chen, K.J., R. Mullur, and E. Bernal-Mizrachi, *Beta-cell failure as a complication of diabetes.* Rev Endocr Metab Disord, 2008. **9**(4): p. 329-43.
82. Chen, C., et al., *Mechanism of compensatory hyperinsulinemia in normoglycemic insulin-resistant spontaneously hypertensive rats. Augmented enzymatic activity of glucokinase in beta-cells.* J Clin Invest, 1994. **94**(1): p. 399-404.
83. Terauchi, Y., et al., *Glucokinase and IRS-2 are required for compensatory beta cell hyperplasia in response to high-fat diet-induced insulin resistance.* J Clin Invest, 2007. **117**(1): p. 246-57.
84. Poitout, V., et al., *Glucolipotoxicity of the pancreatic beta cell.* Biochim Biophys Acta, 2010. **1801**(3): p. 289-98.
85. Rahier, J., et al., *Pancreatic beta-cell mass in European subjects with type 2 diabetes.* Diabetes Obes Metab, 2008. **10 Suppl 4**: p. 32-42.
86. Federici, M., et al., *High glucose causes apoptosis in cultured human pancreatic islets of Langerhans: a potential role for regulation of specific Bcl family genes toward an apoptotic cell death program.* Diabetes, 2001. **50**(6): p. 1290-301.

87. Poitout, V. and R.P. Robertson, *Glucolipotoxicity: fuel excess and beta-cell dysfunction.* Endocr Rev, 2008. **29**(3): p. 351-66.
88. Fleury, C., B. Mignotte, and J.L. Vayssiere, *Mitochondrial reactive oxygen species in cell death signaling.* Biochimie, 2002. **84**(2-3): p. 131-41.
89. Maritim, A.C., R.A. Sanders, and J.B. Watkins, 3rd, *Diabetes, oxidative stress, and antioxidants: a review.* J Biochem Mol Toxicol, 2003. **17**(1): p. 24-38.
90. Lim, M., et al., *Induction of apoptosis of Beta cells of the pancreas by advanced glycation end-products, important mediators of chronic complications of diabetes mellitus.* Ann N Y Acad Sci, 2008. **1150**: p. 311-5.
91. Hou, N., et al., *Reactive oxygen species-mediated pancreatic beta-cell death is regulated by interactions between stress-activated protein kinases, p38 and c-Jun N-terminal kinase, and mitogen-activated protein kinase phosphatases.* Endocrinology, 2008. **149**(4): p. 1654-65.
92. Robertson, R.P., et al., *Beta-cell glucose toxicity, lipotoxicity, and chronic oxidative stress in type 2 diabetes.* Diabetes, 2004. **53 Suppl 1**: p. S119-24.
93. Shah, S., et al., *Oxidative stress, glucose metabolism, and the prevention of type 2 diabetes: pathophysiological insights.* Antioxid Redox Signal, 2007. **9**(7): p. 911-29.
94. Finkel, T. and N.J. Holbrook, *Oxidants, oxidative stress and the biology of ageing.* Nature, 2000. **408**(6809): p. 239-47.
95. Kaneto, H., et al., *Involvement of c-Jun N-terminal kinase in oxidative stress-mediated suppression of insulin gene expression.* J Biol Chem, 2002. **277**(33): p. 30010-8.
96. Baroja-Mazo, A., et al., *The NLRP3 inflammasome is released as a particulate danger signal that amplifies the inflammatory response.* Nat Immunol, 2014. **15**(8): p. 738-48.
97. Davis, B.K. and J.P. Ting, *NLRP3 has a sweet tooth.* Nat Immunol, 2010. **11**(2): p. 105-6.
98. Rhodes, C.J., *Type 2 diabetes-a matter of beta-cell life and death?* Science, 2005. **307**(5708): p. 380-4.
99. Kajimoto, Y. and H. Kaneto, *Role of oxidative stress in pancreatic beta-cell dysfunction.* Ann N Y Acad Sci, 2004. **1011**: p. 168-76.
100. Tanaka, Y., et al., *A role for glutathione peroxidase in protecting pancreatic beta cells against oxidative stress in a model of glucose toxicity.* Proc Natl Acad Sci U S A, 2002. **99**(19): p. 12363-8.
101. Grill, V. and A. Bjorklund, *Overstimulation and beta-cell function.* Diabetes, 2001. **50 Suppl 1**: p. S122-4.
102. Maedler, K., et al., *Glucose-induced beta cell production of IL-1beta contributes to glucotoxicity in human pancreatic islets.* J Clin Invest, 2002. **110**(6): p. 851-60.
103. Maedler, K., et al., *Glucose induces beta-cell apoptosis via upregulation of the Fas receptor in human islets.* Diabetes, 2001. **50**(8): p. 1683-90.
104. White, M.F., *IRS proteins and the common path to diabetes.* Am J Physiol Endocrinol Metab, 2002. **283**(3): p. E413-22.

105. Shah, O.J., Z. Wang, and T. Hunter, *Inappropriate activation of the TSC/Rheb/mTOR/S6K cassette induces IRS1/2 depletion, insulin resistance, and cell survival deficiencies.* Curr Biol, 2004. **14**(18): p. 1650-6.
106. Prentki, M., et al., *Malonyl-CoA signaling, lipid partitioning, and glucolipotoxicity: role in beta-cell adaptation and failure in the etiology of diabetes.* Diabetes, 2002. **51 Suppl 3**: p. S405-13.
107. El-Assaad, W., et al., *Saturated fatty acids synergize with elevated glucose to cause pancreatic beta-cell death.* Endocrinology, 2003. **144**(9): p. 4154-63.
108. Unger, R.H. and L. Orci, *Diseases of liporegulation: new perspective on obesity and related disorders.* FASEB J, 2001. **15**(2): p. 312-21.
109. Joseph, J.W., et al., *Free fatty acid-induced beta-cell defects are dependent on uncoupling protein 2 expression.* J Biol Chem, 2004. **279**(49): p. 51049-56.
110. Huang, S., et al., *Saturated fatty acids activate TLR-mediated proinflammatory signaling pathways.* J Lipid Res, 2012. **53**(9): p. 2002-13.
111. Nackiewicz, D., et al., *TLR2/6 and TLR4-activated macrophages contribute to islet inflammation and impair beta cell insulin gene expression via IL-1 and IL-6.* Diabetologia, 2014. **57**(8): p. 1645-54.
112. Gwiazda, K.S., et al., *Effects of palmitate on ER and cytosolic Ca2+ homeostasis in beta-cells.* Am J Physiol Endocrinol Metab, 2009. **296**(4): p. E690-701.
113. Izumi, T., et al., *Dominant negative pathogenesis by mutant proinsulin in the Akita diabetic mouse.* Diabetes, 2003. **52**(2): p. 409-16.
114. Eizirik, D.L., A.K. Cardozo, and M. Cnop, *The role for endoplasmic reticulum stress in diabetes mellitus.* Endocr Rev, 2008. **29**(1): p. 42-61.
115. Ozcan, U., et al., *Endoplasmic reticulum stress links obesity, insulin action, and type 2 diabetes.* Science, 2004. **306**(5695): p. 457-61.
116. Brownlee, M., *A radical explanation for glucose-induced beta cell dysfunction.* J Clin Invest, 2003. **112**(12): p. 1788-90.
117. Krauss, S., et al., *Superoxide-mediated activation of uncoupling protein 2 causes pancreatic beta cell dysfunction.* J Clin Invest, 2003. **112**(12): p. 1831-42.
118. O'Brien, T.D., et al., *Islet amyloid polypeptide: a review of its biology and potential roles in the pathogenesis of diabetes mellitus.* Vet Pathol, 1993. **30**(4): p. 317-32.
119. Mason, T.M., et al., *Prolonged elevation of plasma free fatty acids desensitizes the insulin secretory response to glucose in vivo in rats.* Diabetes, 1999. **48**(3): p. 524-30.
120. Paolisso, G., et al., *Effects of simvastatin and atorvastatin administration on insulin resistance and respiratory quotient in aged dyslipidemic non-insulin dependent diabetic patients.* Atherosclerosis, 2000. **150**(1): p. 121-7.
121. Jacqueminet, S., et al., *Inhibition of insulin gene expression by long-term exposure of pancreatic beta cells to palmitate is dependent on the presence of a stimulatory glucose concentration.* Metabolism, 2000. **49**(4): p. 532-6.
122. Briaud, I., et al., *Glucose-induced insulin mRNA accumulation is impaired in islets from neonatal streptozotocin-treated rats.* Horm Metab Res, 2000. **32**(3): p. 103-6.

123. Marshall, C., et al., *Effect of glucolipotoxicity and rosiglitazone upon insulin secretion.* Biochem Biophys Res Commun, 2007. **356**(3): p. 756-62.
124. Briaud, I., et al., *Differential effects of hyperlipidemia on insulin secretion in islets of langerhans from hyperglycemic versus normoglycemic rats.* Diabetes, 2002. **51**(3): p. 662-8.
125. Chan, C.B., et al., *Overexpression of uncoupling protein 2 inhibits glucose-stimulated insulin secretion from rat islets.* Diabetes, 1999. **48**(7): p. 1482-6.
126. Joseph, J.W., et al., *Uncoupling protein 2 knockout mice have enhanced insulin secretory capacity after a high-fat diet.* Diabetes, 2002. **51**(11): p. 3211-9.
127. Pi, J., et al., *Persistent oxidative stress due to absence of uncoupling protein 2 associated with impaired pancreatic beta-cell function.* Endocrinology, 2009. **150**(7): p. 3040-8.
128. Schmitz-Peiffer, C., et al., *Inhibition of PKCepsilon improves glucose-stimulated insulin secretion and reduces insulin clearance.* Cell Metab, 2007. **6**(4): p. 320-8.
129. Cantley, J., et al., *Deletion of PKCepsilon selectively enhances the amplifying pathways of glucose-stimulated insulin secretion via increased lipolysis in mouse beta-cells.* Diabetes, 2009. **58**(8): p. 1826-34.
130. Steneberg, P., et al., *The FFA receptor GPR40 links hyperinsulinemia, hepatic steatosis, and impaired glucose homeostasis in mouse.* Cell Metab, 2005. **1**(4): p. 245-58.
131. Kato, T., et al., *Granuphilin is activated by SREBP-1c and involved in impaired insulin secretion in diabetic mice.* Cell Metab, 2006. **4**(2): p. 143-54.
132. Takahashi, H., et al., *D-Glyceraldehyde causes production of intracellular peroxide in pancreatic islets, oxidative stress, and defective beta cell function via non-mitochondrial pathways.* J Biol Chem, 2004. **279**(36): p. 37316-23.
133. Somesh, B.P., et al., *Chronic glucolipotoxic conditions in pancreatic islets impair insulin secretion due to dysregulated calcium dynamics, glucose responsiveness and mitochondrial activity.* BMC Cell Biol, 2013. **14**: p. 31.
134. Gremlich, S., et al., *Fatty acids decrease IDX-1 expression in rat pancreatic islets and reduce GLUT2, glucokinase, insulin, and somatostatin levels.* J Biol Chem, 1997. **272**(48): p. 30261-9.
135. Kelpe, C.L., et al., *Palmitate inhibition of insulin gene expression is mediated at the transcriptional level via ceramide synthesis.* J Biol Chem, 2003. **278**(32): p. 30015-21.
136. Hagman, D.K., et al., *Palmitate inhibits insulin gene expression by altering PDX-1 nuclear localization and reducing MafA expression in isolated rat islets of Langerhans.* J Biol Chem, 2005. **280**(37): p. 32413-8.
137. Robinson, G.L., et al., *c-jun inhibits insulin control element-mediated transcription by affecting the transactivation potential of the E2A gene products.* Mol Cell Biol, 1995. **15**(3): p. 1398-404.
138. Schmitz-Peiffer, C., D.L. Craig, and T.J. Biden, *Ceramide generation is sufficient to account for the inhibition of the insulin-stimulated PKB pathway in C2C12 skeletal muscle cells pretreated with palmitate.* J Biol Chem, 1999. **274**(34): p. 24202-10.

139. Kitamura, T., et al., *The forkhead transcription factor Foxo1 links insulin signaling to Pdx1 regulation of pancreatic beta cell growth.* J Clin Invest, 2002. **110**(12): p. 1839-47.
140. Olson, L.K., et al., *Chronic exposure of HIT cells to high glucose concentrations paradoxically decreases insulin gene transcription and alters binding of insulin gene regulatory protein.* J Clin Invest, 1993. **92**(1): p. 514-9.
141. Harmon, J.S., R. Stein, and R.P. Robertson, *Oxidative stress-mediated, post-translational loss of MafA protein as a contributing mechanism to loss of insulin gene expression in glucotoxic beta cells.* J Biol Chem, 2005. **280**(12): p. 11107-13.
142. Evans-Molina, C., et al., *Peroxisome proliferator-activated receptor gamma activation restores islet function in diabetic mice through reduction of endoplasmic reticulum stress and maintenance of euchromatin structure.* Mol Cell Biol, 2009. **29**(8): p. 2053-67.
143. Pirot, P., et al., *Global profiling of genes modified by endoplasmic reticulum stress in pancreatic beta cells reveals the early degradation of insulin mRNAs.* Diabetologia, 2007. **50**(5): p. 1006-14.
144. Donath, M.Y., et al., *Islet inflammation impairs the pancreatic beta-cell in type 2 diabetes.* Physiology (Bethesda), 2009. **24**: p. 325-31.
145. Pereira, F.O., T.S. Frode, and Y.S. Medeiros, *Evaluation of tumour necrosis factor alpha, interleukin-2 soluble receptor, nitric oxide metabolites, and lipids as inflammatory markers in type 2 diabetes mellitus.* Mediators Inflamm, 2006. **2006**(1): p. 39062.
146. Targher, G., et al., *Elevated levels of interleukin-6 in young adults with type 1 diabetes without clinical evidence of microvascular and macrovascular complications.* Diabetes Care, 2001. **24**(5): p. 956-7.
147. Alexandraki, K.I., et al., *Cytokine secretion in long-standing diabetes mellitus type 1 and 2: associations with low-grade systemic inflammation.* J Clin Immunol, 2008. **28**(4): p. 314-21.
148. Ozer, G., et al., *Serum IL-1, IL-2, TNFalpha and INFgamma levels of patients with type 1 diabetes mellitus and their siblings.* J Pediatr Endocrinol Metab, 2003. **16**(2): p. 203-10.
149. Hotamisligil, G.S., N.S. Shargill, and B.M. Spiegelman, *Adipose expression of tumor necrosis factor-alpha: direct role in obesity-linked insulin resistance.* Science, 1993. **259**(5091): p. 87-91.
150. Solomon, S.S., et al., *TNF-alpha inhibits insulin action in liver and adipose tissue: A model of metabolic syndrome.* Horm Metab Res, 2010. **42**(2): p. 115-21.
151. Boni-Schnetzler, M., et al., *Increased interleukin (IL)-1beta messenger ribonucleic acid expression in beta -cells of individuals with type 2 diabetes and regulation of IL-1beta in human islets by glucose and autostimulation.* J Clin Endocrinol Metab, 2008. **93**(10): p. 4065-74.
152. Boni-Schnetzler, M., et al., *Free fatty acids induce a proinflammatory response in islets via the abundantly expressed interleukin-1 receptor I.* Endocrinology, 2009. **150**(12): p. 5218-29.

153. Donath, M.Y., et al., *Mechanisms of beta-cell death in type 2 diabetes.* Diabetes, 2005. **54 Suppl 2**: p. S108-13.
154. Donath, M.Y., et al., *Cytokine production by islets in health and diabetes: cellular origin, regulation and function.* Trends Endocrinol Metab, 2010. **21**(5): p. 261-7.
155. Dunne, A. and L.A. O'Neill, *The interleukin-1 receptor/Toll-like receptor superfamily: signal transduction during inflammation and host defense.* Sci STKE, 2003. **2003**(171): p. re3.
156. Kopp, E., et al., *ECSIT is an evolutionarily conserved intermediate in the Toll/IL-1 signal transduction pathway.* Genes Dev, 1999. **13**(16): p. 2059-71.
157. Ehses, J.A., et al., *Increased number of islet-associated macrophages in type 2 diabetes.* Diabetes, 2007. **56**(9): p. 2356-70.
158. Kristiansen, O.P. and T. Mandrup-Poulsen, *Interleukin-6 and diabetes: the good, the bad, or the indifferent?* Diabetes, 2005. **54 Suppl 2**: p. S114-24.
159. Gysemans, C.A., et al., *Disruption of the gamma-interferon signaling pathway at the level of signal transducer and activator of transcription-1 prevents immune destruction of beta-cells.* Diabetes, 2005. **54**(8): p. 2396-403.
160. Lee, M.S., *Cytokine synergism in apoptosis: its role in diabetes and cancer.* J Biochem Mol Biol, 2002. **35**(1): p. 54-60.
161. Suk, K., et al., *IFN-gamma/TNF-alpha synergism as the final effector in autoimmune diabetes: a key role for STAT1/IFN regulatory factor-1 pathway in pancreatic beta cell death.* J Immunol, 2001. **166**(7): p. 4481-9.
162. Baud, V. and M. Karin, *Signal transduction by tumor necrosis factor and its relatives.* Trends Cell Biol, 2001. **11**(9): p. 372-7.
163. Locksley, R.M., N. Killeen, and M.J. Lenardo, *The TNF and TNF receptor superfamilies: integrating mammalian biology.* Cell, 2001. **104**(4): p. 487-501.
164. Kuwano, K. and N. Hara, *Signal transduction pathways of apoptosis and inflammation induced by the tumor necrosis factor receptor family.* Am J Respir Cell Mol Biol, 2000. **22**(2): p. 147-9.
165. Naismith, J.H. and S.R. Sprang, *Modularity in the TNF-receptor family.* Trends Biochem Sci, 1998. **23**(2): p. 74-9.
166. Smith, C.A., T. Farrah, and R.G. Goodwin, *The TNF receptor superfamily of cellular and viral proteins: activation, costimulation, and death.* Cell, 1994. **76**(6): p. 959-62.
167. Fesik, S.W., *Insights into programmed cell death through structural biology.* Cell, 2000. **103**(2): p. 273-82.
168. Idriss, H.T. and J.H. Naismith, *TNF alpha and the TNF receptor superfamily: structure-function relationship(s).* Microsc Res Tech, 2000. **50**(3): p. 184-95.
169. Mukai, Y., et al., *Solution of the structure of the TNF-TNFR2 complex.* Sci Signal, 2010. **3**(148): p. ra83.
170. Hsu, H., et al., *TRADD-TRAF2 and TRADD-FADD interactions define two distinct TNF receptor 1 signal transduction pathways.* Cell, 1996. **84**(2): p. 299-308.
171. Rothe, M., et al., *A novel family of putative signal transducers associated with the cytoplasmic domain of the 75 kDa tumor necrosis factor receptor.* Cell, 1994. **78**(4): p. 681-92.

172. Turner, M.D., et al., *Cytokines and chemokines: At the crossroads of cell signalling and inflammatory disease.* Biochim Biophys Acta, 2014. **1843**(11): p. 2563-2582.
173. Micheau, O. and J. Tschopp, *Induction of TNF receptor I-mediated apoptosis via two sequential signaling complexes.* Cell, 2003. **114**(2): p. 181-90.
174. Malinin, N.L., et al., *MAP3K-related kinase involved in NF-kappaB induction by TNF, CD95 and IL-1.* Nature, 1997. **385**(6616): p. 540-4.
175. Bradley, J.R. and J.S. Pober, *Tumor necrosis factor receptor-associated factors (TRAFs).* Oncogene, 2001. **20**(44): p. 6482-91.
176. Carpentier, I. and R. Beyaert, *TRAF1 is a TNF inducible regulator of NF-kappaB activation.* FEBS Lett, 1999. **460**(2): p. 246-50.
177. Schwenzer, R., et al., *The human tumor necrosis factor (TNF) receptor-associated factor 1 gene (TRAF1) is up-regulated by cytokines of the TNF ligand family and modulates TNF-induced activation of NF-kappaB and c-Jun N-terminal kinase.* J Biol Chem, 1999. **274**(27): p. 19368-74.
178. Leo, E., et al., *TRAF1 is a substrate of caspases activated during tumor necrosis factor receptor-alpha-induced apoptosis.* J Biol Chem, 2001. **276**(11): p. 8087-93.
179. Jang, H.D., et al., *Caspase-cleaved TRAF1 negatively regulates the antiapoptotic signals of TRAF2 during TNF-induced cell death.* Biochem Biophys Res Commun, 2001. **281**(2): p. 499-505.
180. Takeuchi, M., M. Rothe, and D.V. Goeddel, *Anatomy of TRAF2. Distinct domains for nuclear factor-kappaB activation and association with tumor necrosis factor signaling proteins.* J Biol Chem, 1996. **271**(33): p. 19935-42.
181. Song, H.Y., et al., *Tumor necrosis factor (TNF)-mediated kinase cascades: bifurcation of nuclear factor-kappaB and c-jun N-terminal kinase (JNK/SAPK) pathways at TNF receptor-associated factor 2.* Proc Natl Acad Sci U S A, 1997. **94**(18): p. 9792-6.
182. Karin, M., Z. Liu, and E. Zandi, *AP-1 function and regulation.* Curr Opin Cell Biol, 1997. **9**(2): p. 240-6.
183. Baud, V., et al., *Signaling by proinflammatory cytokines: oligomerization of TRAF2 and TRAF6 is sufficient for JNK and IKK activation and target gene induction via an amino-terminal effector domain.* Genes Dev, 1999. **13**(10): p. 1297-308.
184. Nishitoh, H., et al., *ASK1 is essential for JNK/SAPK activation by TRAF2.* Mol Cell, 1998. **2**(3): p. 389-95.
185. Kuhne, M.R., et al., *Assembly and regulation of the CD40 receptor complex in human B cells.* J Exp Med, 1997. **186**(2): p. 337-42.
186. Hostager, B.S. and G.A. Bishop, *Cutting edge: contrasting roles of TNF receptor-associated factor 2 (TRAF2) and TRAF3 in CD40-activated B lymphocyte differentiation.* J Immunol, 1999. **162**(11): p. 6307-11.
187. Glauner, H., et al., *Intracellular localization and transcriptional regulation of tumor necrosis factor (TNF) receptor-associated factor 4 (TRAF4).* Eur J Biochem, 2002. **269**(19): p. 4819-29.

188. Ishida, T.K., et al., *TRAF5, a novel tumor necrosis factor receptor-associated factor family protein, mediates CD40 signaling.* Proc Natl Acad Sci U S A, 1996. **93**(18): p. 9437-42.
189. Pullen, S.S., et al., *CD40-tumor necrosis factor receptor-associated factor (TRAF) interactions: regulation of CD40 signaling through multiple TRAF binding sites and TRAF hetero-oligomerization.* Biochemistry, 1998. **37**(34): p. 11836-45.
190. Lee, S.Y., et al., *TRAF2 is essential for JNK but not NF-kappaB activation and regulates lymphocyte proliferation and survival.* Immunity, 1997. **7**(5): p. 703-13.
191. Xia, Y., et al., *JNKK1 organizes a MAP kinase module through specific and sequential interactions with upstream and downstream components mediated by its amino-terminal extension.* Genes Dev, 1998. **12**(21): p. 3369-81.
192. Lee, F.S., et al., *Activation of the IkappaB alpha kinase complex by MEKK1, a kinase of the JNK pathway.* Cell, 1997. **88**(2): p. 213-22.
193. Delhase, M., et al., *Positive and negative regulation of IkappaB kinase activity through IKKbeta subunit phosphorylation.* Science, 1999. **284**(5412): p. 309-13.
194. Yin, L., et al., *Defective lymphotoxin-beta receptor-induced NF-kappaB transcriptional activity in NIK-deficient mice.* Science, 2001. **291**(5511): p. 2162-5.
195. Zhang, S.Q., et al., *Recruitment of the IKK signalosome to the p55 TNF receptor: RIP and A20 bind to NEMO (IKKgamma) upon receptor stimulation.* Immunity, 2000. **12**(3): p. 301-11.
196. Rath, P.C. and B.B. Aggarwal, *TNF-induced signaling in apoptosis.* J Clin Immunol, 1999. **19**(6): p. 350-64.
197. Earnshaw, W.C., L.M. Martins, and S.H. Kaufmann, *Mammalian caspases: structure, activation, substrates, and functions during apoptosis.* Annu Rev Biochem, 1999. **68**: p. 383-424.
198. Deveraux, Q.L. and J.C. Reed, *IAP family proteins--suppressors of apoptosis.* Genes Dev, 1999. **13**(3): p. 239-52.
199. Balkwill, F., B. Foxwell, and F. Brennan, *TNF is here to stay!* Immunol Today, 2000. **21**(10): p. 470-1.
200. Walter, U., et al., *Monitoring gene expression of TNFR family members by beta-cells during development of autoimmune diabetes.* Eur J Immunol, 2000. **30**(4): p. 1224-32.
201. Kagi, D., et al., *TNF receptor 1-dependent beta cell toxicity as an effector pathway in autoimmune diabetes.* J Immunol, 1999. **162**(8): p. 4598-605.
202. Hotamisligil, G.S., et al., *Tumor necrosis factor alpha inhibits signaling from the insulin receptor.* Proc Natl Acad Sci U S A, 1994. **91**(11): p. 4854-8.
203. Hossain, M., et al., *Association of serum TNF-α and IL-6 with insulin secretion and insulin resistance in IFG and IGT subjects in a Bangladeshi population.* International Journal of Diabetes Mellitus, 2010. **2**(3): p. 165-168.
204. Zhang, S. and K.H. Kim, *TNF-alpha inhibits glucose-induced insulin secretion in a pancreatic beta-cell line (INS-1).* FEBS Lett, 1995. **377**(2): p. 237-9.

205. Gupta-Ganguli, M., et al., *Does therapy with anti-TNF-alpha improve glucose tolerance and control in patients with type 2 diabetes?* Diabetes Care, 2011. **34**(7): p. e121.
206. Fernandez-Real, J.M., et al., *Plasma levels of the soluble fraction of tumor necrosis factor receptor 2 and insulin resistance.* Diabetes, 1998. **47**(11): p. 1757-62.
207. Fernandez-Real, J.M., et al., *Polymorphism of the tumor necrosis factor-alpha receptor 2 gene is associated with obesity, leptin levels, and insulin resistance in young subjects and diet-treated type 2 diabetic patients.* Diabetes Care, 2000. **23**(6): p. 831-7.
208. Straczkowski, M., et al., *Increased plasma-soluble tumor necrosis factor-alpha receptor 2 level in lean nondiabetic offspring of type 2 diabetic subjects.* Diabetes Care, 2002. **25**(10): p. 1824-8.
209. Tack, C.J., et al., *Development of type 1 diabetes in a patient treated with anti-TNF-alpha therapy for active rheumatoid arthritis.* Diabetologia, 2009. **52**(7): p. 1442-4.
210. Grewal, I.S., et al., *Local expression of transgene encoded TNF alpha in islets prevents autoimmune diabetes in nonobese diabetic (NOD) mice by preventing the development of auto-reactive islet-specific T cells.* J Exp Med, 1996. **184**(5): p. 1963-74.
211. Van Hauwermeiren, F., R.E. Vandenbroucke, and C. Libert, *Treatment of TNF mediated diseases by selective inhibition of soluble TNF or TNFR1.* Cytokine Growth Factor Rev, 2011. **22**(5-6): p. 311-9.
212. Elgueta, R., et al., *Molecular mechanism and function of CD40/CD40L engagement in the immune system.* Immunol Rev, 2009. **229**(1): p. 152-72.
213. Tewari, M. and V.M. Dixit, *Recent advances in tumor necrosis factor and CD40 signaling.* Curr Opin Genet Dev, 1996. **6**(1): p. 39-44.
214. Bishop, G.A., et al., *TRAF proteins in CD40 signaling.* Adv Exp Med Biol, 2007. **597**: p. 131-51.
215. Saemann, M.D., et al., *Prevention of CD40-triggered dendritic cell maturation and induction of T-cell hyporeactivity by targeting of Janus kinase 3.* Am J Transplant, 2003. **3**(11): p. 1341-9.
216. Xie, P., et al., *Cooperation between TNF receptor-associated factors 1 and 2 in CD40 signaling.* J Immunol, 2006. **176**(9): p. 5388-400.
217. Hostager, B.S., et al., *Tumor necrosis factor receptor-associated factor 2 (TRAF2)-deficient B lymphocytes reveal novel roles for TRAF2 in CD40 signaling.* J Biol Chem, 2003. **278**(46): p. 45382-90.
218. Gallagher, E., et al., *Kinase MEKK1 is required for CD40-dependent activation of the kinases Jnk and p38, germinal center formation, B cell proliferation and antibody production.* Nat Immunol, 2007. **8**(1): p. 57-63.
219. Vallabhapurapu, S., et al., *Nonredundant and complementary functions of TRAF2 and TRAF3 in a ubiquitination cascade that activates NIK-dependent alternative NF-kappaB signaling.* Nat Immunol, 2008. **9**(12): p. 1364-70.
220. Xie, P., B.S. Hostager, and G.A. Bishop, *Requirement for TRAF3 in signaling by LMP1 but not CD40 in B lymphocytes.* J Exp Med, 2004. **199**(5): p. 661-71.

221. Propst, S.M., K. Estell, and L.M. Schwiebert, *CD40-mediated activation of NF-kappa B in airway epithelial cells.* J Biol Chem, 2002. **277**(40): p. 37054-63.
222. Peters, A.L. and G.A. Bishop, *Differential TRAF3 utilization by a variant human CD40 receptor with enhanced signaling.* J Immunol, 2010. **185**(11): p. 6555-62.
223. Lin, W.W., J.M. Hildebrand, and G.A. Bishop, *A Complex Relationship between TRAF3 and Non-Canonical NF-kappaB2 Activation in B Lymphocytes.* Front Immunol, 2013. **4**: p. 477.
224. Hauer, J., et al., *TNF receptor (TNFR)-associated factor (TRAF) 3 serves as an inhibitor of TRAF2/5-mediated activation of the noncanonical NF-kappaB pathway by TRAF-binding TNFRs.* Proc Natl Acad Sci U S A, 2005. **102**(8): p. 2874-9.
225. Rowland, S.L., et al., *A novel mechanism for TNFR-associated factor 6-dependent CD40 signaling.* J Immunol, 2007. **179**(7): p. 4645-53.
226. Barrett, T.B., G. Shu, and E.A. Clark, *CD40 signaling activates CD11a/CD18 (LFA-1)-mediated adhesion in B cells.* J Immunol, 1991. **146**(6): p. 1722-9.
227. Jabara, H.H., et al., *CD40 and IgE: synergism between anti-CD40 monoclonal antibody and interleukin 4 in the induction of IgE synthesis by highly purified human B cells.* J Exp Med, 1990. **172**(6): p. 1861-4.
228. Foy, T.M., et al., *gp39-CD40 interactions are essential for germinal center formation and the development of B cell memory.* J Exp Med, 1994. **180**(1): p. 157-63.
229. Notarangelo, L.D., et al., *CD40lbase: a database of CD40L gene mutations causing X-linked hyper-IgM syndrome.* Immunol Today, 1996. **17**(11): p. 511-6.
230. Kawabe, T., et al., *The immune responses in CD40-deficient mice: impaired immunoglobulin class switching and germinal center formation.* Immunity, 1994. **1**(3): p. 167-78.
231. Kalled, S.L., et al., *Anti-CD40 ligand antibody treatment of SNF1 mice with established nephritis: preservation of kidney function.* J Immunol, 1998. **160**(5): p. 2158-65.
232. Boon, L., et al., *Prevention of experimental autoimmune encephalomyelitis in the common marmoset (Callithrix jacchus) using a chimeric antagonist monoclonal antibody against human CD40 is associated with altered B cell responses.* J Immunol, 2001. **167**(5): p. 2942-9.
233. Gascan, H., et al., *Anti-CD40 monoclonal antibodies or CD4+ T cell clones and IL-4 induce IgG4 and IgE switching in purified human B cells via different signaling pathways.* J Immunol, 1991. **147**(1): p. 8-13.
234. Mackey, M.F., R.J. Barth, Jr., and R.J. Noelle, *The role of CD40/CD154 interactions in the priming, differentiation, and effector function of helper and cytotoxic T cells.* J Leukoc Biol, 1998. **63**(4): p. 418-28.
235. Larsen, C.P. and T.C. Pearson, *The CD40 pathway in allograft rejection, acceptance, and tolerance.* Curr Opin Immunol, 1997. **9**(5): p. 641-7.
236. Alderson, M.R., et al., *CD40 expression by human monocytes: regulation by cytokines and activation of monocytes by the ligand for CD40.* J Exp Med, 1993. **178**(2): p. 669-74.
237. Mach, F., et al., *Reduction of atherosclerosis in mice by inhibition of CD40 signalling.* Nature, 1998. **394**(6689): p. 200-3.

238. Adawi, A., et al., *Disruption of the CD40-CD40 ligand system prevents an oxygen-induced respiratory distress syndrome.* Am J Pathol, 1998. **152**(3): p. 651-7.
239. Mathur, R.K., et al., *Reciprocal CD40 signals through p38MAPK and ERK-1/2 induce counteracting immune responses.* Nat Med, 2004. **10**(5): p. 540-4.
240. Danese, S., et al., *Cutting edge: T cells trigger CD40-dependent platelet activation and granular RANTES release: a novel pathway for immune response amplification.* J Immunol, 2004. **172**(4): p. 2011-5.
241. Kaufman, J., P.J. Sime, and R.P. Phipps, *Expression of CD154 (CD40 ligand) by human lung fibroblasts: differential regulation by IFN-gamma and IL-13, and implications for fibrosis.* J Immunol, 2004. **172**(3): p. 1862-71.
242. Klein, D., et al., *A functional CD40 receptor is expressed in pancreatic beta cells.* Diabetologia, 2005. **48**(2): p. 268-76.
243. Vosters, O., et al., *CD40 expression on human pancreatic duct cells: role in nuclear factor-kappa B activation and production of pro-inflammatory cytokines.* Diabetologia, 2004. **47**(4): p. 660-8.
244. Barbe-Tuana, F.M., et al., *CD40-CD40 ligand interaction activates proinflammatory pathways in pancreatic islets.* Diabetes, 2006. **55**(9): p. 2437-45.
245. Wagner, D.H., Jr., et al., *Expression of CD40 identifies a unique pathogenic T cell population in type 1 diabetes.* Proc Natl Acad Sci U S A, 2002. **99**(6): p. 3782-7.
246. Balasa, B., et al., *CD40 ligand-CD40 interactions are necessary for the initiation of insulitis and diabetes in nonobese diabetic mice.* J Immunol, 1997. **159**(9): p. 4620-7.
247. Poggi, M., et al., *CD40L deficiency ameliorates adipose tissue inflammation and metabolic manifestations of obesity in mice.* Arterioscler Thromb Vasc Biol, 2011. **31**(10): p. 2251-60.
248. Wang, X.H., et al., *Simultaneous blockade of the CD40/CD40L and NF-kappaB pathways prolonged islet allograft survival.* Transpl Int, 2012. **25**(1): p. 118-26.
249. Kenyon, N.S., et al., *Long-term survival and function of intrahepatic islet allografts in baboons treated with humanized anti-CD154.* Diabetes, 1999. **48**(7): p. 1473-81.
250. Jinchuan, Y., et al., *Upregulation of CD40--CD40 ligand system in patients with diabetes mellitus.* Clin Chim Acta, 2004. **339**(1-2): p. 85-90.
251. Harding, S.A., et al., *Increased CD40 ligand and platelet-monocyte aggregates in patients with type 1 diabetes mellitus.* Atherosclerosis, 2004. **176**(2): p. 321-5.
252. Chatzigeorgiou, A., et al., *Blocking CD40-TRAF6 signaling is a therapeutic target in obesity-associated insulin resistance.* Proc Natl Acad Sci U S A, 2014. **111**(7): p. 2686-91.
253. Cipollone, F., et al., *Enhanced soluble CD40 ligand contributes to endothelial cell dysfunction in vitro and monocyte activation in patients with diabetes mellitus: effect of improved metabolic control.* Diabetologia, 2005. **48**(6): p. 1216-24.
254. Licatalosi, D.D. and R.B. Darnell, *RNA processing and its regulation: global insights into biological networks.* Nat Rev Genet, 2010. **11**(1): p. 75-87.

255. Lindberg, J. and J. Lundeberg, *The plasticity of the mammalian transcriptome.* Genomics, 2010. **95**(1): p. 1-6.
256. Taft, R.J., M. Pheasant, and J.S. Mattick, *The relationship between non-protein-coding DNA and eukaryotic complexity.* Bioessays, 2007. **29**(3): p. 288-99.
257. Costa, V., et al., *Uncovering the complexity of transcriptomes with RNA-Seq.* J Biomed Biotechnol, 2010. **2010**: p. 853916.
258. Malone, J.H. and B. Oliver, *Microarrays, deep sequencing and the true measure of the transcriptome.* BMC Biol, 2011. **9**: p. 34.
259. Tan, P.K., et al., *Evaluation of gene expression measurements from commercial microarray platforms.* Nucleic Acids Res, 2003. **31**(19): p. 5676-84.
260. Shi, L., et al., *The MicroArray Quality Control (MAQC) project shows inter- and intraplatform reproducibility of gene expression measurements.* Nat Biotechnol, 2006. **24**(9): p. 1151-61.
261. Clark, T.A., C.W. Sugnet, and M. Ares, Jr., *Genomewide analysis of mRNA processing in yeast using splicing-specific microarrays.* Science, 2002. **296**(5569): p. 907-10.
262. David, L., et al., *A high-resolution map of transcription in the yeast genome.* Proc Natl Acad Sci U S A, 2006. **103**(14): p. 5320-5.
263. Wada, J., et al., *Gene expression profile in streptozotocin-induced diabetic mice kidneys undergoing glomerulosclerosis.* Kidney Int, 2001. **59**(4): p. 1363-73.
264. Bensellam, M., et al., *Cluster analysis of rat pancreatic islet gene mRNA levels after culture in low-, intermediate- and high-glucose concentrations.* Diabetologia, 2009. **52**(3): p. 463-76.
265. Webb, G.C., et al., *Expression profiling of pancreatic beta-cells: glucose regulation of secretory and metabolic pathway genes.* Diabetes, 2001. **50 Suppl 1**: p. S135-6.
266. Wang, Z., M. Gerstein, and M. Snyder, *RNA-Seq: a revolutionary tool for transcriptomics.* Nat Rev Genet, 2009. **10**(1): p. 57-63.
267. Nagalakshmi, U., et al., *The transcriptional landscape of the yeast genome defined by RNA sequencing.* Science, 2008. **320**(5881): p. 1344-9.
268. Mortazavi, A., et al., *Mapping and quantifying mammalian transcriptomes by RNA-Seq.* Nat Methods, 2008. **5**(7): p. 621-8.
269. Morin, R., et al., *Profiling the HeLa S3 transcriptome using randomly primed cDNA and massively parallel short-read sequencing.* Biotechniques, 2008. **45**(1): p. 81-94.
270. Ku, G.M., et al., *Research resource: RNA-Seq reveals unique features of the pancreatic beta-cell transcriptome.* Mol Endocrinol, 2012. **26**(10): p. 1783-92.
271. Moran, I., et al., *Human beta cell transcriptome analysis uncovers lncRNAs that are tissue-specific, dynamically regulated, and abnormally expressed in type 2 diabetes.* Cell Metab, 2012. **16**(4): p. 435-48.
272. Cnop, M., et al., *RNA sequencing identifies dysregulation of the human pancreatic islet transcriptome by the saturated fatty acid palmitate.* Diabetes, 2014. **63**(6): p. 1978-93.
273. Lee, R.C., R.L. Feinbaum, and V. Ambros, *The C. elegans heterochronic gene lin-4 encodes small RNAs with antisense complementarity to lin-14.* Cell, 1993. **75**(5): p. 843-54.

274. Reinhart, B.J., et al., *The 21-nucleotide let-7 RNA regulates developmental timing in Caenorhabditis elegans.* Nature, 2000. **403**(6772): p. 901-6.
275. Griffiths-Jones, S., et al., *miRBase: tools for microRNA genomics.* Nucleic Acids Res, 2008. **36**(Database issue): p. D154-8.
276. Ardekani, A.M. and M.M. Naeini, *The Role of MicroRNAs in Human Diseases.* Avicenna J Med Biotechnol, 2010. **2**(4): p. 161-79.
277. Lagos-Quintana, M., et al., *Identification of novel genes coding for small expressed RNAs.* Science, 2001. **294**(5543): p. 853-8.
278. Lee, Y., et al., *MicroRNA genes are transcribed by RNA polymerase II.* EMBO J, 2004. **23**(20): p. 4051-60.
279. Lee, Y., et al., *The nuclear RNase III Drosha initiates microRNA processing.* Nature, 2003. **425**(6956): p. 415-9.
280. Han, J., et al., *Molecular basis for the recognition of primary microRNAs by the Drosha-DGCR8 complex.* Cell, 2006. **125**(5): p. 887-901.
281. Winter, J., et al., *Many roads to maturity: microRNA biogenesis pathways and their regulation.* Nat Cell Biol, 2009. **11**(3): p. 228-34.
282. Bohnsack, M.T., K. Czaplinski, and D. Gorlich, *Exportin 5 is a RanGTP-dependent dsRNA-binding protein that mediates nuclear export of pre-miRNAs.* RNA, 2004. **10**(2): p. 185-91.
283. Ketting, R.F., et al., *Dicer functions in RNA interference and in synthesis of small RNA involved in developmental timing in C. elegans.* Genes Dev, 2001. **15**(20): p. 2654-9.
284. MacRae, I.J., et al., *In vitro reconstitution of the human RISC-loading complex.* Proc Natl Acad Sci U S A, 2008. **105**(2): p. 512-7.
285. Preall, J.B. and E.J. Sontheimer, *RNAi: RISC gets loaded.* Cell, 2005. **123**(4): p. 543-5.
286. Peters, L. and G. Meister, *Argonaute proteins: mediators of RNA silencing.* Mol Cell, 2007. **26**(5): p. 611-23.
287. Meister, G., et al., *Human Argonaute2 mediates RNA cleavage targeted by miRNAs and siRNAs.* Mol Cell, 2004. **15**(2): p. 185-97.
288. Zeng, Y., R. Yi, and B.R. Cullen, *MicroRNAs and small interfering RNAs can inhibit mRNA expression by similar mechanisms.* Proc Natl Acad Sci U S A, 2003. **100**(17): p. 9779-84.
289. Elbashir, S.M., W. Lendeckel, and T. Tuschl, *RNA interference is mediated by 21- and 22-nucleotide RNAs.* Genes Dev, 2001. **15**(2): p. 188-200.
290. Liu, J., et al., *MicroRNA-dependent localization of targeted mRNAs to mammalian P-bodies.* Nat Cell Biol, 2005. **7**(7): p. 719-23.
291. Humphreys, D.T., et al., *MicroRNAs control translation initiation by inhibiting eukaryotic initiation factor 4E/cap and poly(A) tail function.* Proc Natl Acad Sci U S A, 2005. **102**(47): p. 16961-6.
292. Pillai, R.S., et al., *Inhibition of translational initiation by Let-7 MicroRNA in human cells.* Science, 2005. **309**(5740): p. 1573-6.
293. Cheng, C., N. Bhardwaj, and M. Gerstein, *The relationship between the evolution of microRNA targets and the length of their UTRs.* BMC Genomics, 2009. **10**: p. 431.

294. Guay, C., et al., *Diabetes mellitus, a microRNA-related disease?* Transl Res, 2011. **157**(4): p. 253-64.
295. Poy, M.N., et al., *A pancreatic islet-specific microRNA regulates insulin secretion.* Nature, 2004. **432**(7014): p. 226-30.
296. Poy, M.N., et al., *miR-375 maintains normal pancreatic alpha- and beta-cell mass.* Proc Natl Acad Sci U S A, 2009. **106**(14): p. 5813-8.
297. Joglekar, M.V., V.M. Joglekar, and A.A. Hardikar, *Expression of islet-specific microRNAs during human pancreatic development.* Gene Expr Patterns, 2009. **9**(2): p. 109-13.
298. Li, Y., et al., *miR-375 enhances palmitate-induced lipoapoptosis in insulin-secreting NIT-1 cells by repressing myotrophin (V1) protein expression.* Int J Clin Exp Pathol, 2010. **3**(3): p. 254-64.
299. El Ouaamari, A., et al., *miR-375 targets 3'-phosphoinositide-dependent protein kinase-1 and regulates glucose-induced biological responses in pancreatic beta-cells.* Diabetes, 2008. **57**(10): p. 2708-17.
300. Keller, D.M., E.A. Clark, and R.H. Goodman, *Regulation of microRNA-375 by cAMP in pancreatic beta-cells.* Mol Endocrinol, 2012. **26**(6): p. 989-99.
301. Zhao, E., et al., *Obesity and genetics regulate microRNAs in islets, liver, and adipose of diabetic mice.* Mamm Genome, 2009. **20**(8): p. 476-85.
302. Plaisance, V., et al., *MicroRNA-9 controls the expression of Granuphilin/Slp4 and the secretory response of insulin-producing cells.* J Biol Chem, 2006. **281**(37): p. 26932-42.
303. Lovis, P., S. Gattesco, and R. Regazzi, *Regulation of the expression of components of the exocytotic machinery of insulin-secreting cells by microRNAs.* Biol Chem, 2008. **389**(3): p. 305-12.
304. Tang, X., et al., *Identification of glucose-regulated miRNAs from pancreatic {beta} cells reveals a role for miR-30d in insulin transcription.* RNA, 2009. **15**(2): p. 287-93.
305. Locke, J.M., et al., *Increased expression of miR-187 in human islets from individuals with type 2 diabetes is associated with reduced glucose-stimulated insulin secretion.* Diabetologia, 2014. **57**(1): p. 122-8.
306. Lovis, P., et al., *Alterations in microRNA expression contribute to fatty acid-induced pancreatic beta-cell dysfunction.* Diabetes, 2008. **57**(10): p. 2728-36.
307. Roggli, E., et al., *Involvement of microRNAs in the cytotoxic effects exerted by proinflammatory cytokines on pancreatic beta-cells.* Diabetes, 2010. **59**(4): p. 978-86.
308. Bravo-Egana, V., et al., *Inflammation-Mediated Regulation of MicroRNA Expression in Transplanted Pancreatic Islets.* J Transplant, 2012. **2012**: p. 723614.
309. Zampetaki, A., et al., *Plasma microRNA profiling reveals loss of endothelial miR-126 and other microRNAs in type 2 diabetes.* Circ Res, 2010. **107**(6): p. 810-7.
310. Pescador, N., et al., *Serum circulating microRNA profiling for identification of potential type 2 diabetes and obesity biomarkers.* PLoS One, 2013. **8**(10): p. e77251.

311. Herrera, B.M., et al., *MicroRNA-125a is over-expressed in insulin target tissues in a spontaneous rat model of Type 2 Diabetes.* BMC Med Genomics, 2009. **2**: p. 54.
312. Ling, H.Y., et al., *CHANGES IN microRNA (miR) profile and effects of miR-320 in insulin-resistant 3T3-L1 adipocytes.* Clin Exp Pharmacol Physiol, 2009. **36**(9): p. e32-9.
313. Karbiener, M., et al., *microRNA miR-27b impairs human adipocyte differentiation and targets PPARgamma.* Biochem Biophys Res Commun, 2009. **390**(2): p. 247-51.
314. Regazzi, R., *Diabetes mellitus reveals its micro-signature.* Circ Res, 2010. **107**(6): p. 686-8.
315. Krutzfeldt, J., et al., *Silencing of microRNAs in vivo with 'antagomirs'.* Nature, 2005. **438**(7068): p. 685-9.
316. Wu, B., et al., *Octa-guanidine morpholino restores dystrophin expression in cardiac and skeletal muscles and ameliorates pathology in dystrophic mdx mice.* Mol Ther, 2009. **17**(5): p. 864-71.
317. Kota, J., et al., *Therapeutic microRNA delivery suppresses tumorigenesis in a murine liver cancer model.* Cell, 2009. **137**(6): p. 1005-17.
318. Rehman, K.K., et al., *AAV8-mediated gene transfer of interleukin-4 to endogenous beta-cells prevents the onset of diabetes in NOD mice.* Mol Ther, 2008. **16**(8): p. 1409-16.
319. Ebert, M.S., J.R. Neilson, and P.A. Sharp, *MicroRNA sponges: competitive inhibitors of small RNAs in mammalian cells.* Nat Methods, 2007. **4**(9): p. 721-6.
320. Valastyan, S., et al., *A pleiotropically acting microRNA, miR-31, inhibits breast cancer metastasis.* Cell, 2009. **137**(6): p. 1032-46.
321. Asfari, M., et al., *Establishment of 2-mercaptoethanol-dependent differentiated insulin-secreting cell lines.* Endocrinology, 1992. **130**(1): p. 167-78.
322. Karpe, F., J.R. Dickmann, and K.N. Frayn, *Fatty acids, obesity, and insulin resistance: time for a reevaluation.* Diabetes, 2011. **60**(10): p. 2441-9.
323. Peraldi, P., et al., *Tumor necrosis factor (TNF)-alpha inhibits insulin signaling through stimulation of the p55 TNF receptor and activation of sphingomyelinase.* J Biol Chem, 1996. **271**(22): p. 13018-22.
324. Nieto-Vazquez, I., et al., *Dual role of interleukin-6 in regulating insulin sensitivity in murine skeletal muscle.* Diabetes, 2008. **57**(12): p. 3211-21.
325. Wobser, H., et al., *Dominant-negative suppression of HNF-1 alpha results in mitochondrial dysfunction, INS-1 cell apoptosis, and increased sensitivity to ceramide-, but not to high glucose-induced cell death.* J Biol Chem, 2002. **277**(8): p. 6413-21.
326. Erdmann, S., et al., *Tissue-specific transcription factor HNF4alpha inhibits cell proliferation and induces apoptosis in the pancreatic INS-1 beta-cell line.* Biol Chem, 2007. **388**(1): p. 91-106.
327. Hagenfeldt, L., et al., *Uptake of individual free fatty acids by skeletal muscle and liver in man.* J Clin Invest, 1972. **51**(9): p. 2324-30.
328. Zhou, L., et al., *P38 plays an important role in glucolipotoxicity-induced apoptosis in INS-1 cells.* J Diabetes Res, 2014. **2014**: p. 834528.

329. Yuzefovych, L., G. Wilson, and L. Rachek, *Different effects of oleate vs. palmitate on mitochondrial function, apoptosis, and insulin signaling in L6 skeletal muscle cells: role of oxidative stress.* Am J Physiol Endocrinol Metab, 2010. **299**(6): p. E1096-105.
330. Gokulakrishnan, K., et al., *Soluble P-selectin and CD40L levels in subjects with prediabetes, diabetes mellitus, and metabolic syndrome--the Chennai Urban Rural Epidemiology Study.* Metabolism, 2006. **55**(2): p. 237-42.
331. Neubauer, H., et al., *Influence of glycaemic control on platelet bound CD40-CD40L system, P-selectin and soluble CD40 ligand in Type 2 diabetes.* Diabet Med, 2010. **27**(4): p. 384-90.
332. Kirk, A.D., et al., *The role of CD154 in organ transplant rejection and acceptance.* Philos Trans R Soc Lond B Biol Sci, 2001. **356**(1409): p. 691-702.
333. Sidiropoulos, P.I. and D.T. Boumpas, *Lessons learned from anti-CD40L treatment in systemic lupus erythematosus patients.* Lupus, 2004. **13**(5): p. 391-7.
334. Goldwater, R., et al., *A phase 1, randomized ascending single-dose study of antagonist anti-human CD40 ASKP1240 in healthy subjects.* Am J Transplant, 2013. **13**(4): p. 1040-6.
335. Hassan, S.B., et al., *Anti-CD40-mediated cancer immunotherapy: an update of recent and ongoing clinical trials.* Immunopharmacol Immunotoxicol, 2014. **36**(2): p. 96-104.
336. Bensinger, W., et al., *A phase 1 study of lucatumumab, a fully human anti-CD40 antagonist monoclonal antibody administered intravenously to patients with relapsed or refractory multiple myeloma.* Br J Haematol, 2012. **159**(1): p. 58-66.
337. Byrd, J.C., et al., *Phase I study of the anti-CD40 humanized monoclonal antibody lucatumumab (HCD122) in relapsed chronic lymphocytic leukemia.* Leuk Lymphoma, 2012. **53**(11): p. 2136-42.
338. Tai, Y.T., et al., *Human anti-CD40 antagonist antibody triggers significant antitumor activity against human multiple myeloma.* Cancer Res, 2005. **65**(13): p. 5898-906.
339. Beitner, R. and N. Kalant, *Stimulation of glycolysis by insulin.* J Biol Chem, 1971. **246**(2): p. 500-3.
340. Kar, S. and D. Shankar Ray, *Sustained simultaneous glycolytic and insulin oscillations in beta-cells.* J Theor Biol, 2005. **237**(1): p. 58-66.
341. Marrero, M.B., et al., *An alpha7 nicotinic acetylcholine receptor-selective agonist reduces weight gain and metabolic changes in a mouse model of diabetes.* J Pharmacol Exp Ther, 2010. **332**(1): p. 173-80.
342. Gilon, P. and J.C. Henquin, *Mechanisms and physiological significance of the cholinergic control of pancreatic beta-cell function.* Endocr Rev, 2001. **22**(5): p. 565-604.
343. Vetterli, L., et al., *Delineation of glutamate pathways and secretory responses in pancreatic islets with beta-cell-specific abrogation of the glutamate dehydrogenase.* Mol Biol Cell, 2012. **23**(19): p. 3851-62.
344. Lozovsky, D., C.F. Saller, and I.J. Kopin, *Dopamine receptor binding is increased in diabetic rats.* Science, 1981. **214**(4524): p. 1031-3.

345. Rubi, B., et al., *Dopamine D2-like receptors are expressed in pancreatic beta cells and mediate inhibition of insulin secretion.* J Biol Chem, 2005. **280**(44): p. 36824-32.
346. Akter, K., et al., *Diabetes mellitus and Alzheimer's disease: shared pathology and treatment?* Br J Clin Pharmacol, 2011. **71**(3): p. 365-76.
347. Yoon, J.C., et al., *Wnt signaling regulates mitochondrial physiology and insulin sensitivity.* Genes Dev, 2010. **24**(14): p. 1507-18.
348. Bordonaro, M., *Role of Wnt signaling in the development of type 2 diabetes.* Vitam Horm, 2009. **80**: p. 563-81.
349. Zhang, Q., et al., *Serotonin receptor 2C and insulin secretion.* PLoS One, 2013. **8**(1): p. e54250.
350. Tsugane, S. and M. Inoue, *Insulin resistance and cancer: epidemiological evidence.* Cancer Sci, 2010. **101**(5): p. 1073-9.
351. Cannata, D., et al., *Type 2 diabetes and cancer: what is the connection?* Mt Sinai J Med, 2010. **77**(2): p. 197-213.
352. Gloyn, A.L., M. Braun, and P. Rorsman, *Type 2 diabetes susceptibility gene TCF7L2 and its role in beta-cell function.* Diabetes, 2009. **58**(4): p. 800-2.
353. Magro, M.G. and M. Solimena, *Regulation of beta-cell function by RNA-binding proteins.* Mol Metab, 2013. **2**(4): p. 348-55.
354. Pan, W.C., et al., *Genetic susceptible locus in NOTCH2 interacts with arsenic in drinking water on risk of type 2 diabetes.* PLoS One, 2013. **8**(8): p. e70792.
355. Jensen, J., et al., *Independent development of pancreatic alpha- and beta-cells from neurogenin3-expressing precursors: a role for the notch pathway in repression of premature differentiation.* Diabetes, 2000. **49**(2): p. 163-76.
356. Fonseca, S.G., et al., *Wolfram syndrome 1 and adenylyl cyclase 8 interact at the plasma membrane to regulate insulin production and secretion.* Nat Cell Biol, 2012. **14**(10): p. 1105-12.
357. Pascoe, L., et al., *Common variants of the novel type 2 diabetes genes CDKAL1 and HHEX/IDE are associated with decreased pancreatic beta-cell function.* Diabetes, 2007. **56**(12): p. 3101-4.
358. Yoshina, S., et al., *Identification of a novel ADAMTS9/GON-1 function for protein transport from the ER to the Golgi.* Mol Biol Cell, 2012. **23**(9): p. 1728-41.
359. Gonzalez-Renteria, S.M., et al., *Association of the polymorphisms 292 C>T and 1304 G>A in the SLC38A4 gene with hyperglycaemia.* Diabetes Metab Res Rev, 2013. **29**(1): p. 39-43.
360. Misu, H., et al., *A liver-derived secretory protein, selenoprotein P, causes insulin resistance.* Cell Metab, 2010. **12**(5): p. 483-95.
361. Steinbrenner, H., et al., *Localization and regulation of pancreatic selenoprotein P.* J Mol Endocrinol, 2013. **50**(1): p. 31-42.
362. Verde, I., et al., *Characterization of the cyclic nucleotide phosphodiesterase subtypes involved in the regulation of the L-type Ca2+ current in rat ventricular myocytes.* Br J Pharmacol, 1999. **127**(1): p. 65-74.
363. Morgan, N.G. and S. Dhayal, *G-protein coupled receptors mediating long chain fatty acid signalling in the pancreatic beta-cell.* Biochem Pharmacol, 2009. **78**(12): p. 1419-27.

364. Sengupta, U., et al., *Expression-based network biology identifies alteration in key regulatory pathways of type 2 diabetes and associated risk/complications.* PLoS One, 2009. **4**(12): p. e8100.
365. Luo, L.G. and N. Yano, *Expression of thyrotropin-releasing hormone receptor in immortalized beta-cell lines and rat pancreas.* J Endocrinol, 2004. **181**(3): p. 401-12.
366. Najvirtova, M., et al., *A role of thyrotropin-releasing hormone in insulin secretion by isolated rat pancreatic islets.* Pflugers Arch, 2005. **449**(6): p. 547-52.
367. Aguayo-Mazzucato, C., et al., *Thyroid hormone promotes postnatal rat pancreatic beta-cell development and glucose-responsive insulin secretion through MAFA.* Diabetes, 2013. **62**(5): p. 1569-80.
368. Oda, T., et al., *Positive association of free triiodothyronine with pancreatic beta-cell function in people with prediabetes.* Diabet Med, 2014.
369. Kulkarni, R.N., et al., *Pyroglutamyl-phenylalanyl-proline amide attenuates thyrotropin-releasing hormone-stimulated insulin secretion in perifused rat islets and insulin-secreting clonal beta-cell lines.* Endocrinology, 1995. **136**(11): p. 5155-64.
370. Kuchenbauer, F., et al., *In-depth characterization of the microRNA transcriptome in a leukemia progression model.* Genome Res, 2008. **18**(11): p. 1787-97.
371. Yang, Y., et al., *Expression profile of microRNAs in fetal lung development of Sprague-Dawley rats.* Int J Mol Med, 2012. **29**(3): p. 393-402.
372. Elgamal, O.A., et al., *Tumor suppressive function of mir-205 in breast cancer is linked to HMGB3 regulation.* PLoS One, 2013. **8**(10): p. e76402.
373. Erener, S., et al., *Circulating miR-375 as a biomarker of beta-cell death and diabetes in mice.* Endocrinology, 2013. **154**(2): p. 603-8.
374. Shiratsuchi, T., et al., *Cloning and characterization of BAP3 (BAI-associated protein 3), a C2 domain-containing protein that interacts with BAI1*. Biochem Biophys Res Commun, 1998. **251**(1): p. 158-65.
375. Palmer, R.E., et al., *Induction of BAIAP3 by the EWS-WT1 chimeric fusion implicates regulated exocytosis in tumorigenesis.* Cancer Cell, 2002. **2**(6): p. 497-505.
376. Martino, E., et al., *High concentration of thyrotropin-releasing hormone in pancreatic islets.* Proc Natl Acad Sci U S A, 1978. **75**(9): p. 4265-7.
377. Alva, M.L., et al., *The impact of diabetes-related complications on healthcare costs: new results from the UKPDS (UKPDS 84).* Diabet Med, 2014.
378. Palma, C.C., et al., *Prevalence of thyroid dysfunction in patients with diabetes mellitus.* Diabetol Metab Syndr, 2013. **5**(1): p. 58.
379. Hage, M., M.S. Zantout, and S.T. Azar, *Thyroid disorders and diabetes mellitus.* J Thyroid Res, 2011. **2011**: p. 439463.
380. Wang, C., *The Relationship between Type 2 Diabetes Mellitus and Related Thyroid Diseases.* J Diabetes Res, 2013. **2013**: p. 390534.
381. Fontes, G., et al., *Involvement of Per-Arnt-Sim Kinase and extracellular-regulated kinases-1/2 in palmitate inhibition of insulin gene expression in pancreatic beta-cells.* Diabetes, 2009. **58**(9): p. 2048-58.

Appendix A: List of Primers

GENE	PRIMER FORWARD	PRIMER REVERSE
18S	TCTTCCACAGGAGGCCTACACG	GCCCCACACCCTTAATGGCAGT
INSULIN	CCCTAAGTGACCAGCTACAATCA	CCACAAAGGTGCTGTTTGAC
CD40	GTCGGATTCTTCTCCAATG	ACAGAGGGTATCAGTCTGAC
CD40 (mouse)	TGGTCATTCCTGTCGTGATG	GGCTCTGTCTTGGCTCATCT
PDX1	GAAATCCACCAAAGCTCACG	AGGCCGGGAGATGTATTTGT
MAF A	CCCGACTTCTTTCTGTGAGC	GCGGTAAGTACCTGGAGCTG
TRAF1	GAAGGTTCTCCCTGATGTGG	ACTCCTTTAGGACCCCCAGA
TRAF2	AGCCGTCTGTCCCAATGATG	CTTTACACGCAGGGCACTCAGTC
TRAF3	CCTCATAAGTGCAGCGTTCA	TGCAGCAAGGAAACCTTCTT
TRAF6	AAAGCTGTCCTCTGGCAAATATC	GTGATTCCTCTGCATCTTTTCGT
TRAF2 (mouse)	CAGCTGTCTGTCCCAATGATG	AGGCCTTTACATGCAGGACACT
TRAF6 (mouse)	TCCTCATCAGAGAACAGATGCCTA	GGTATTCTCTTGCAAGTGTCGTG
TNFR1A	GAGAAACAGAACACCGTGTG	TAGGCACAGCTTCATACATTC
TNFR21	ATTGACATCCTGAAGCTT	TGGCGTTGCAAAGAAACT

	GTA	GAT
TNFR26	CAAGAAGAAGTGTCCGAGTG	CTCCAAACAGTTTTCAGAATC
TNF	GCTCCCTCTCATCAGTTCCA	ACCACCAGTTGGTTGTCTTTG
NFkBiB	CCCTTAGTCTTTGGCTACGTCACT	GTCGTTCTGCAAGTCCAGGTACTC
NFkB2	ATTTTGAATTCAGCCCCTCCAT	TTCACAGCCATATCGAAATCTGAA
IRAK	TCCTGTGTCACCTGGAACTC	AAGGAGCATGGTTTCACAGG
BAIAP3	TAGACGACGAGGAGGTCTTGCTA	CAGAGACTTTCAGGGCATAGGTG
BAIAP3 micro	GCCCTGGATGAAGACCTTCTG	AGTCCGGAGACAGACTGATGTG

Appendix B: Agilent Bioanalyser samples analysis

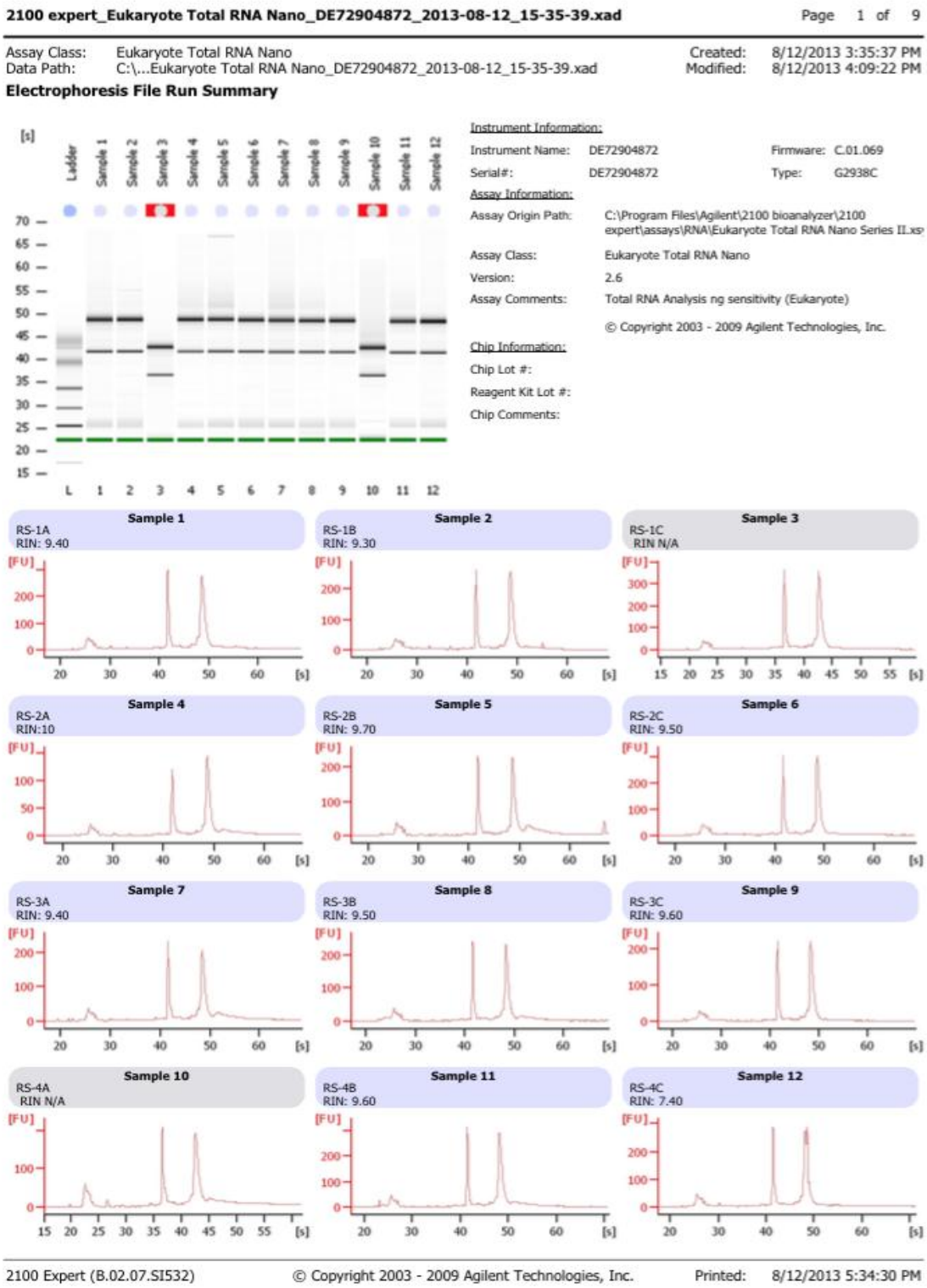

Assay Class: Eukaryote Total RNA Nano
Data Path: C:\...Eukaryote Total RNA Nano_DE72904872_2013-08-12_15-35-39.xad

Created: 8/12/2013 3:35:37 PM
Modified: 8/12/2013 4:09:22 PM

Electrophoresis File Run Summary (Chip Summary)

Sample Name	Sample Comment	Status	Result Label	Result Color
Sample 1	RS-1A	✔	RIN: 9.40	
Sample 2	RS-1B	✔	RIN: 9.30	
Sample 3	RS-1C	✔	RIN N/A	
Sample 4	RS-2A	✔	RIN:10	
Sample 5	RS-2B	✔	RIN: 9.70	
Sample 6	RS-2C	✔	RIN: 9.50	
Sample 7	RS-3A	✔	RIN: 9.40	
Sample 8	RS-3B	✔	RIN: 9.50	
Sample 9	RS-3C	✔	RIN: 9.60	
Sample 10	RS-4A	✔	RIN N/A	
Sample 11	RS-4B	✔	RIN: 9.60	
Sample 12	RS-4C	✔	RIN: 7.40	

Chip Lot # **Reagent Kit Lot #**

Chip Comments :

Assay Class: Eukaryote Total RNA Nano
Data Path: C:\...Eukaryote Total RNA Nano_DE72904872_2013-08-12_15-35-39.xad

Created: 8/12/2013 3:35:37 PM
Modified: 8/12/2013 4:09:22 PM

Electrophoresis Assay Details

General Analysis Settings

Number of Available Sample and Ladder Wells (Max.) : 13
Minimum Visible Range [s] : 17
Maximum Visible Range [s] : 70
Start Analysis Time Range [s] : 19
End Analysis Time Range [s] : 69
Ladder Concentration [ng/µl] : 150
Lower Marker Concentration [ng/µl] : 0
Upper Marker Concentration [ng/µl] : 0
Used Lower Marker for Quantitation
Standard Curve Fit is Logarithmic
Show Data Aligned to Lower Marker

Integrator Settings

Integration Start Time [s] : 19
Integration End Time [s] : 69
Slope Threshold : 0.6
Height Threshold [FU] : 0.5
Area Threshold : 0.2
Width Threshold [s] : 0.5
Baseline Plateau [s] : 6

Filter Settings

Filter Width [s] : 0.5
Polynomial Order : 4

Ladder

Ladder Peak	Size
1	25
2	200
3	500
4	1000
5	2000
6	4000

Assay Class: Eukaryote Total RNA Nano
Data Path: C:\...Eukaryote Total RNA Nano_DE72904872_2013-08-12_15-35-39.xad

Created: 8/12/2013 3:35:37 PM
Modified: 8/12/2013 4:09:22 PM

Electropherogram Summary

Ladder

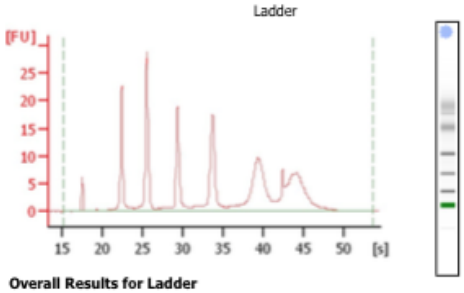

Overall Results for Ladder

RNA Area:	241.7
RNA Concentration:	150 ng/µl
Result Flagging Color:	
Result Flagging Label:	All Other Samples

Sample 1 [RS-1A]

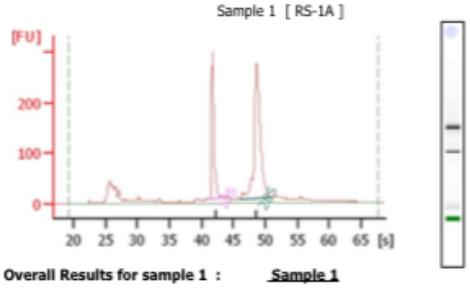

Overall Results for sample 1 : Sample 1

RNA Area:	1,718.8
RNA Concentration:	1,067 ng/µl
rRNA Ratio [28s / 18s]:	1.9
RNA Integrity Number (RIN):	9.4 (B.02.07)
Result Flagging Color:	
Result Flagging Label:	RIN: 9.40

Fragment table for sample 1 : Sample 1

Name	Start Time [s]	End Time [s]	Area	% of total Area
18S	41.32	43.38	321.8	18.7
28S	46.08	50.94	616.2	35.8

Sample 2 [RS-1B]

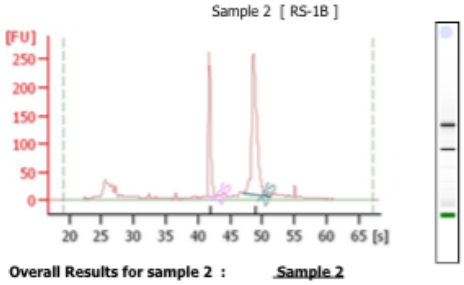

Overall Results for sample 2 : Sample 2

RNA Area:	1,439.6
RNA Concentration:	893 ng/µl
rRNA Ratio [28s / 18s]:	1.9
RNA Integrity Number (RIN):	9.3 (B.02.07)
Result Flagging Color:	
Result Flagging Label:	RIN: 9.30

Fragment table for sample 2 : Sample 2

Name	Start Time [s]	End Time [s]	Area	% of total Area
18S	41.39	42.80	259.0	18.0
28S	47.05	51.05	484.7	33.7

Sample 3 [RS-1C]

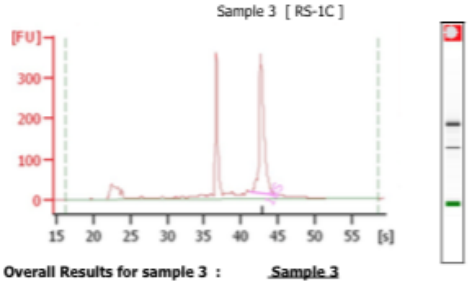

Overall Results for sample 3 : Sample 3

RNA Area:	1,615.3
RNA Concentration:	1,002 ng/µl
rRNA Ratio [28s / 18s]:	0.0
RNA Integrity Number (RIN):	N/A (B.02.07)
Result Flagging Color:	
Result Flagging Label:	RIN N/A

Fragment table for sample 3 : Sample 3

Name	Start Time [s]	End Time [s]	Area	% of total Area
18S	41.30	44.74	635.4	39.3

Assay Class: Eukaryote Total RNA Nano
Data Path: C:\...Eukaryote Total RNA Nano_DE72904872_2013-08-12_15-35-39.xad

Created: 8/12/2013 3:35:37 PM
Modified: 8/12/2013 4:09:22 PM

Electropherogram Summary Continued ...

Sample 4 [RS-2A]

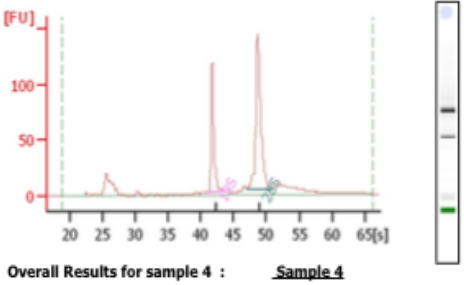

Overall Results for sample 4 : **Sample 4**

RNA Area:	691.4
RNA Concentration:	429 ng/µl
rRNA Ratio [28s / 18s]:	1.9
RNA Integrity Number (RIN):	10 (B.02.07)
Result Flagging Color:	
Result Flagging Label:	RIN:10

Fragment table for sample 4 : **Sample 4**

Name	Start Time [s]	End Time [s]	Area	% of total Area
18S	41.11	43.70	139.3	20.2
28S	47.02	50.82	259.2	37.5

Sample 5 [RS-2B]

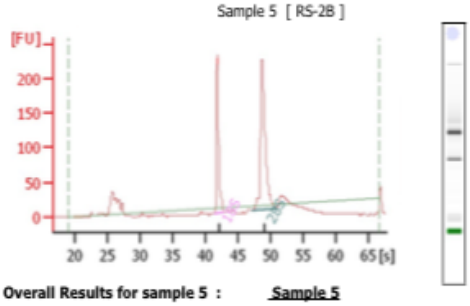

Overall Results for sample 5 : **Sample 5**

RNA Area:	734.3
RNA Concentration:	456 ng/µl
rRNA Ratio [28s / 18s]:	1.7
RNA Integrity Number (RIN):	9.7 (B.02.07)
Result Flagging Color:	
Result Flagging Label:	RIN: 9.70

Fragment table for sample 5 : **Sample 5**

Name	Start Time [s]	End Time [s]	Area	% of total Area
18S	41.42	42.92	225.6	30.7
28S	47.13	50.90	385.7	52.5

Sample 6 [RS-2C]

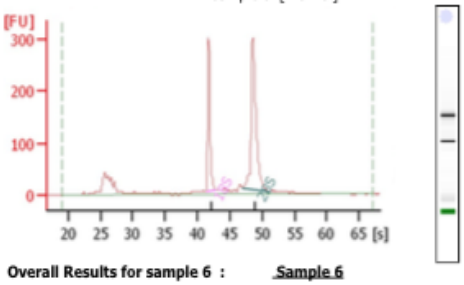

Overall Results for sample 6 : **Sample 6**

RNA Area:	1,517.5
RNA Concentration:	942 ng/µl
rRNA Ratio [28s / 18s]:	1.8
RNA Integrity Number (RIN):	9.5 (B.02.07)
Result Flagging Color:	
Result Flagging Label:	RIN: 9.50

Fragment table for sample 6 : **Sample 6**

Name	Start Time [s]	End Time [s]	Area	% of total Area
18S	41.35	42.81	293.5	19.3
28S	47.00	51.04	532.0	35.1

Sample 7 [RS-3A]

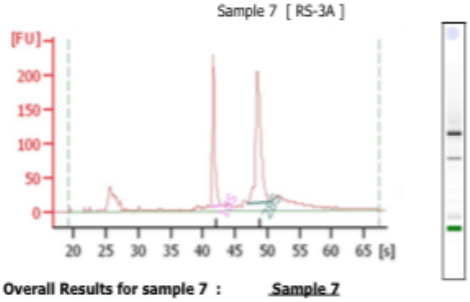

Overall Results for sample 7 : **Sample 7**

RNA Area:	1,286.8
RNA Concentration:	799 ng/µl
rRNA Ratio [28s / 18s]:	1.7
RNA Integrity Number (RIN):	9.4 (B.02.07)
Result Flagging Color:	
Result Flagging Label:	RIN: 9.40

Fragment table for sample 7 : **Sample 7**

Name	Start Time [s]	End Time [s]	Area	% of total Area
18S	41.28	42.70	226.4	17.6
28S	46.86	50.67	382.2	29.7

Assay Class: Eukaryote Total RNA Nano
Data Path: C:\...Eukaryote Total RNA Nano_DE72904872_2013-08-12_15-35-39.xad

Created: 8/12/2013 3:35:37 PM
Modified: 8/12/2013 4:09:22 PM

Electropherogram Summary Continued ...

Sample 8 [RS-3B]

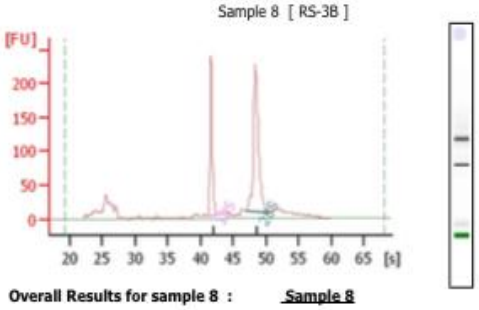

Overall Results for sample 8 : **Sample 8**

RNA Area:	1,255.6
RNA Concentration:	779 ng/µl
rRNA Ratio [28s / 18s]:	1.7
RNA Integrity Number (RIN):	9.5 (B.02.07)
Result Flagging Color:	
Result Flagging Label:	RIN: 9.50

Fragment table for sample 8 : **Sample 8**

Name	Start Time [s]	End Time [s]	Area	% of total Area
18S	41.24	42.68	228.2	18.2
28S	46.88	50.49	399.2	31.8

Sample 9 [RS-3C]

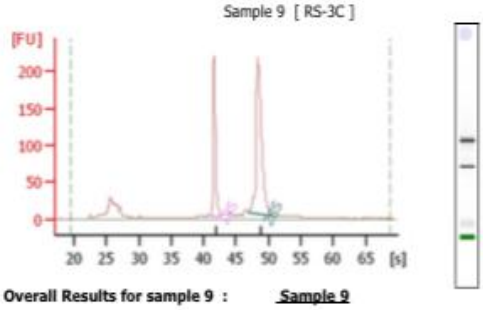

Overall Results for sample 9 : **Sample 9**

RNA Area:	1,069.2
RNA Concentration:	663 ng/µl
rRNA Ratio [28s / 18s]:	1.9
RNA Integrity Number (RIN):	9.6 (B.02.07)
Result Flagging Color:	
Result Flagging Label:	RIN: 9.60

Fragment table for sample 9 : **Sample 9**

Name	Start Time [s]	End Time [s]	Area	% of total Area
18S	41.26	42.66	211.3	19.8
28S	46.85	50.79	406.1	38.0

Sample 10 [RS-4A]

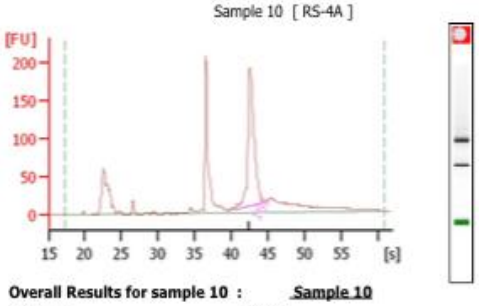

Overall Results for sample 10 : **Sample 10**

RNA Area:	1,079.0
RNA Concentration:	670 ng/µl
rRNA Ratio [28s / 18s]:	0.0
RNA Integrity Number (RIN):	N/A (B.02.07)
Result Flagging Color:	
Result Flagging Label:	RIN N/A

Fragment table for sample 10 : **Sample 10**

Name	Start Time [s]	End Time [s]	Area	% of total Area
18S	40.28	44.47	428.0	39.7

Sample 11 [RS-4B]

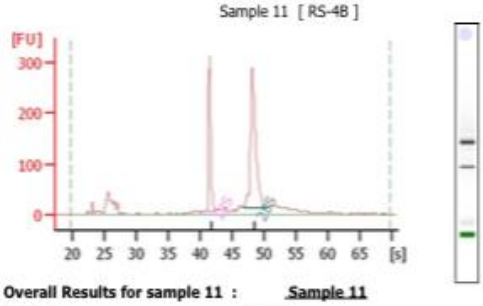

Overall Results for sample 11 : **Sample 11**

RNA Area:	1,586.7
RNA Concentration:	985 ng/µl
rRNA Ratio [28s / 18s]:	1.9
RNA Integrity Number (RIN):	9.6 (B.02.07)
Result Flagging Color:	
Result Flagging Label:	RIN: 9.60

Fragment table for sample 11 : **Sample 11**

Name	Start Time [s]	End Time [s]	Area	% of total Area
18S	41.15	42.57	295.7	18.6
28S	46.72	50.57	549.4	34.6

Assay Class: Eukaryote Total RNA Nano
Data Path: C:\...Eukaryote Total RNA Nano_DE72904872_2013-08-12_15-35-39.xad

Created: 8/12/2013 3:35:37 PM
Modified: 8/12/2013 4:09:22 PM

Electropherogram Summary Continued ...

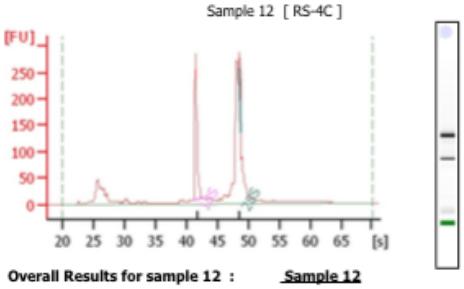

Overall Results for sample 12 : **Sample 12**

RNA Area:	1,636.6
RNA Concentration:	1,016 ng/µl
rRNA Ratio [28s / 18s]:	0.1
RNA Integrity Number (RIN):	7.4 (B.02.07)
Result Flagging Color:	
Result Flagging Label:	RIN: 7.40

Fragment table for sample 12 : **Sample 12**

Name	Start Time [s]	End Time [s]	Area	% of total Area
18S	41.13	42.61	284.2	17.4
28S	48.56	48.82	23.5	1.4

Assay Class: Eukaryote Total RNA Nano
Data Path: C:\...Eukaryote Total RNA Nano_DE72904872_2013-08-12_15-35-39.xad

Created: 8/12/2013 3:35:37 PM
Modified: 8/12/2013 4:09:22 PM

Gel Image

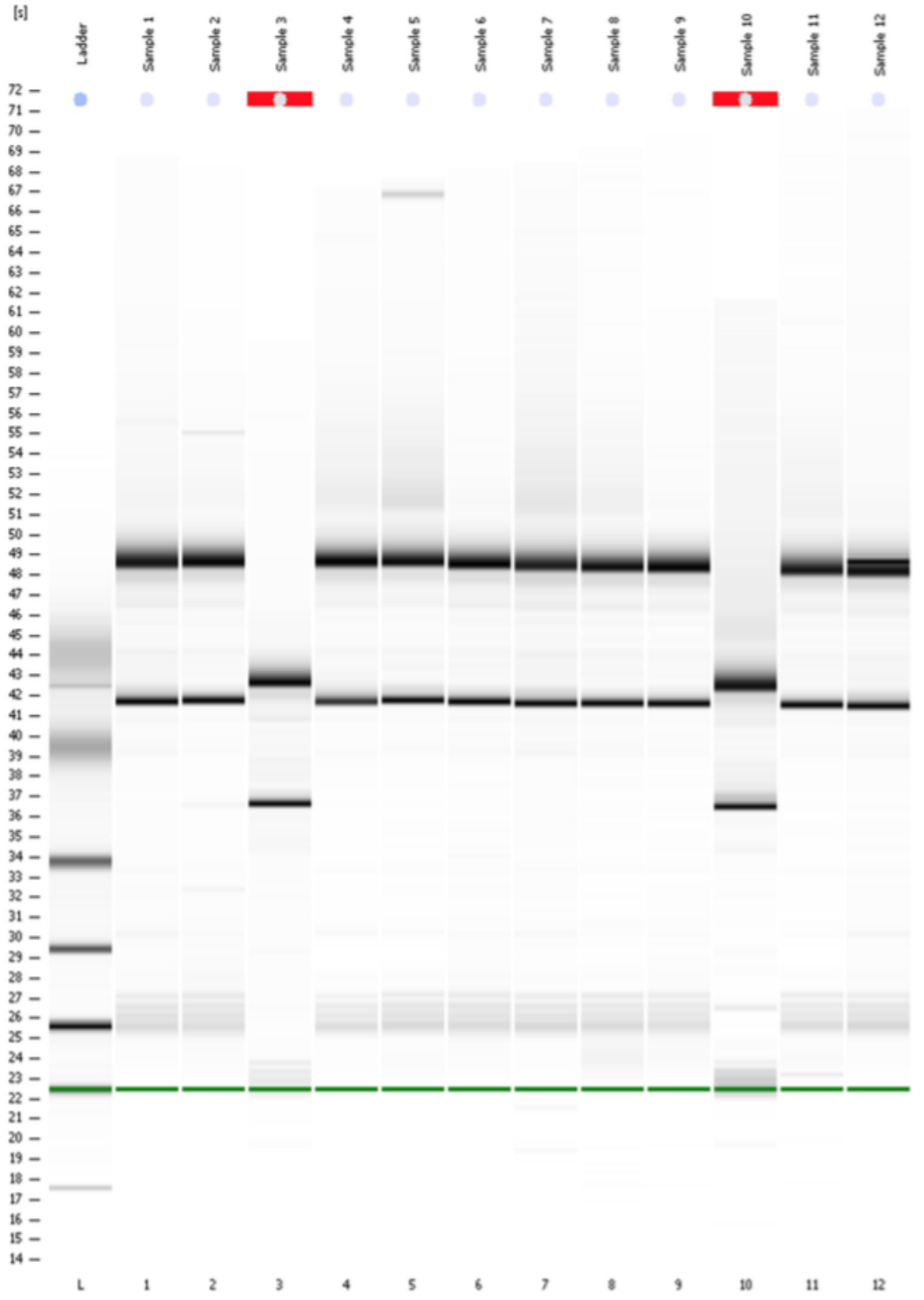

Assay Class: Eukaryote Total RNA Nano
Data Path: C:\...Eukaryote Total RNA Nano_DE72904872_2013-08-12_15-35-39.xad

Created: 8/12/2013 3:35:37 PM
Modified: 8/12/2013 4:09:22 PM

Curves

Standard Curve

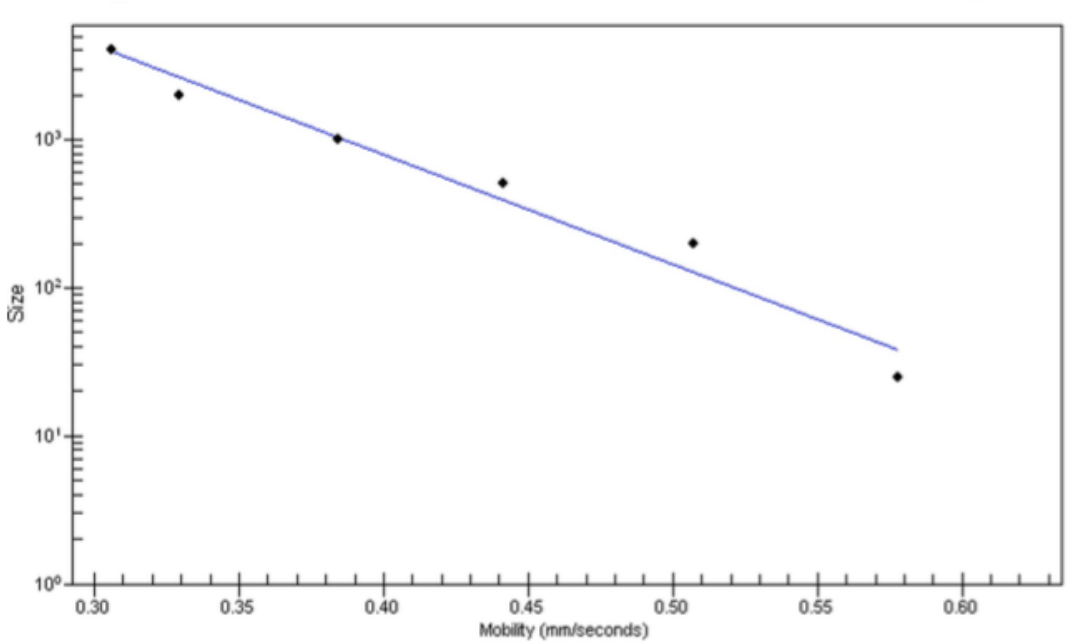

Appendix C: RNAseq statistics

Sequence Library	Total number of sequences	Concordant pair alignment	Mapping Efficency (%)
WTCHG_75162_241_1	13944504	10689061	76.7
WTCHG_75162_242_1	16013074	11900359	74.3
WTCHG_75162_243_1	15600005	11769452	75.4
WTCHG_75162_244_1	14252227	10791261	75.7
WTCHG_75162_289_1	17552825	13171860	75
WTCHG_75162_290_1	14546058	10824393	74.4
WTCHG_75162_291_1	16289889	12239908	75.1
WTCHG_75162_292_1	14613077	10697618	73.2
WTCHG_75162_293_1	15576574	11465344	73.6
WTCHG_75162_294_1	15182369	11722206	77.2
WTCHG_75162_295_1	14329846	11241417	78.4
WTCHG_75162_296_1	16283355	12541262	77
WTCHG_77933_241_1	14342859	11072772	77.2
WTCHG_77933_242_1	17097497	12792476	74.8
WTCHG_77933_243_1	13776218	10471905	76
WTCHG_77933_244_1	14979777	11377874	76
WTCHG_77933_289_1	15597258	11748738	75.3
WTCHG_77933_290_1	15392441	11547018	75
WTCHG_77933_291_1	17142410	12944205	75.5
WTCHG_77933_292_1	15435444	11383543	73.7
WTCHG_77933_293_1	16069304	11862672	73.8
WTCHG_77933_294_1	15661737	12228236	78.1
WTCHG_77933_295_1	14409691	11409584	79.2
WTCHG_77933_296_1	17285441	13360033	77.3
WTCHG_77934_241_1	14425087	11157688	77.3
WTCHG_77934_242_1	17180209	12886738	75
WTCHG_77934_243_1	13785418	10502805	76.2
WTCHG_77934_244_1	15030267	11442243	76.1
WTCHG_77934_289_1	15654339	11817744	75.5
WTCHG_77934_290_1	15382257	11566632	75.2
WTCHG_77934_291_1	17151179	12987439	75.7
WTCHG_77934_292_1	15484674	11446560	73.9
WTCHG_77934_293_1	16117244	11916366	73.9

WTCHG_77934_294_1	15727561	12324882	78.4
WTCHG_77934_295_1	14342245	11397557	79.5
WTCHG_77934_296_1	17326810	13429144	77.5
WTCHG_77935_241_1	14545807	11293450	77.6
WTCHG_77935_242_1	17405016	13101915	75.3
WTCHG_77935_243_1	13854689	10597867	76.5
WTCHG_77935_244_1	15286750	11692435	76.5
WTCHG_77935_289_1	15762445	11941010	75.8
WTCHG_77935_290_1	15694464	11852530	75.5
WTCHG_77935_291_1	17465250	13287170	76.1
WTCHG_77935_292_1	15797844	11729239	74.2
WTCHG_77935_293_1	16393651	12164830	74.2
WTCHG_77935_294_1	15946883	12547687	78.7
WTCHG_77935_295_1	14772818	11780727	79.7
WTCHG_77935_296_1	17648078	13738852	77.8
WTCHG_77936_241_1	14503410	11199468	77.2
WTCHG_77936_242_1	17383619	13006095	74.8
WTCHG_77936_243_1	13738928	10444723	76
WTCHG_77936_244_1	15217015	11556476	75.9
WTCHG_77936_289_1	15496067	11678805	75.4
WTCHG_77936_290_1	15717523	11795334	75
WTCHG_77936_291_1	17480462	13212245	75.6
WTCHG_77936_292_1	15782125	11640670	73.8
WTCHG_77936_293_1	16370522	12082381	73.8
WTCHG_77936_294_1	15851026	12394702	78.2
WTCHG_77936_295_1	14759613	11701161	79.3
WTCHG_77936_296_1	17624904	13622488	77.3
WTCHG_77937_241_1	14373087	11152438	77.6
WTCHG_77937_242_1	17225161	12957733	75.2
WTCHG_77937_243_1	13704178	10479698	76.5
WTCHG_77937_244_1	15070776	11524984	76.5
WTCHG_77937_289_1	15478860	11725487	75.8
WTCHG_77937_290_1	15589026	11770001	75.5
WTCHG_77937_291_1	17340328	13186893	76
WTCHG_77937_292_1	15626789	11602000	74.2
WTCHG_77937_293_1	16246554	12054223	74.2
WTCHG_77937_294_1	15740739	12376164	78.6
WTCHG_77937_295_1	14635521	11671636	79.7
WTCHG_77937_296_1	17496235	13616899	77.8